Water, a Unique Medium for Organic Reactions

Kinetic Studies of Intermolecular Interactions in Aqueous Solutions

Niklaas Jan Buurma

The research described in this thesis was financially supported by the University of Groningen

RIJKSUNIVERSITEIT GRONINGEN

Water, a Unique Medium for Organic Reactions

Kinetic Studies of Intermolecular Interactions in Aqueous Solutions

Proefschrift

ter verkrijging van het doctoraat in de
Wiskunde en Natuurwetenschappen
aan de Rijksuniversiteit Groningen
op gezag van de
Rector Magnificus, dr. F. Zwarts,
in het openbaar te verdedigen op
vrijdag 7 februari 2003
om 16.00 uur

door

Niklaas Jan Buurma

geboren op 28 oktober 1975
te Groningen

Promotor:
Prof. dr. J.B.F.N. Engberts

Beoordelingscommissie:
Prof. dr. M.J. Blandamer
Prof. dr. B.L. Feringa
Prof. dr. A.J. Kirby

ISBN 90-367-1769-8

WOORD VOORAF

Een woord vooraf schrijven is een hachelijke bezigheid. Voor velen is het woord vooraf, of voorwoord zoals het vaak genoemd wordt,[*] *het* te lezen gedeelte van een proefschrift. In een woord vooraf mag niemand vergeten worden en zinnen moeten bij voorkeur slechts op een enkele, positieve en vriendelijke manier te interpreteren zijn. Laat me een poging wagen...

Ten eerste wil ik Jan bedanken voor een lange lijst dingen. Voor het bieden van de mogelijkheid om mijn promotieonderzoek in de 'engbertsgroep' te doen, voor alle steun, adviezen, hulp, vertrouwen maar ook voor de gezelligheid en het laten opleven van menig gesprek met een grap of komische noot. Jan, als wetenschapper wist je op de een of andere manier eigenlijk altijd welke begeleiding ik nodig had. Als mens ben je de keus voor de engbertsgroep meer dan waard gebleken.

De beoordelingscommissie, bestaande uit prof. dr. M.J. Blandamer (University of Leicester), prof. dr. B.L. Feringa (Rijksuniversiteit Groningen) en prof. dr. A.J. Kirby (University of Cambridge) wil ik bedanken voor het lezen en corrigeren van het manuscript van dit proefschrift. In addition, I would like to thank Mike for tolerating my stubborness (in wanting to discuss single molecules instead of a mole of them), his patience and the corrections and comments on the drafts of this thesis. You have taught me a lot, thanks! Professor Teuben wil ik bedanken voor het mogelijk maken van mijn langere verblijf in Groningen.

Anno wil ik bedanken voor de hulp bij syntheses, maar ook voor zijn luisterend oor en het zijn van een constante, rust brengende factor. Dr. Van Duijnen wil ik bedanken voor alles wat ik van hem heb mogen leren over moleculaire interacties. Dat ik Theo en Sijbren samen zou noemen stond al vast vanaf de eerste dag van mij promotie-onderzoek. Hartelijk dank voor de vele nuttige discussies, o.a. over hydrofobe interacties! Theo wil ik verder nog bedanken voor de nuttige discussies over theoretische computerproblemen. Samen met Rixt heb ik met veel plezier de werkweek naar Scheveningen georganiseerd, maar ook daarbuiten was je een fantastische collega. Vorrei ringraziare Paola e Laura, senza di voi, i capitoli 2 e 5 sarebbero meno ampi o forse non esistenti. Avete portato l'entusiasmo e il sole italiano nel lab. Ma, ancora piu importante, sono contento che siamo amici. Verder wil ik ook Marie Jetta bedanken voor haar bijdrage aan hoofdstuk 5. Het 'kraken' van de additiviteit in G(c)-waarden was aan Michel goed besteed, het heeft vele

[*] Het woord *voorwoord* is een germanisme.

hoofdbrekens gekost, maar het kan toch echt! Toch vraag ik me af waar je nu het dartbord met mijn foto erop bewaart.

Een bijzondere collega was Jan Kevelam, niet alleen vanwege het fantastische 'toeval' dat wij reeds de derde generatie in de reeks Kevelam-Buurma contacten vormen. Marco Scarzello non e' solamente stato molto importante come 'insegnante' di Italiano ma anche come amico. Prima di andare in Italia insieme, non avevo mai saputo come fosse bella la montagna. Jaap's enthousiasme en wilde plannen kunnen een labzaal een heel plezierige omgeving maken. There's no escaping Paul Bell, he shows up everywhere, including in this woord vooraf. Nabil and Markus have been great company during the writing of my thesis. Nabil, thank you for the nitpicking in Chapter 3 and for being a splendid advertisement for englishness. I would like to thank Markus for reading the manuscript of Chapter 5. Gerben kan ik hier natuurlijk niet vergeten. Hoe jij mij in mijn eerste weken op het waterlab met een waar engelengeduld alles uitlegde en aanwees...

Dan zijn er nog vele anderen met wie ik gedurende kortere of langere tijd op het waterlab heb mogen samenwerken. Arjan, Bart-Jan, Dick, Dirk, Egid, Evert, Fausto, Frans, Holger, Inge, Jaap, Jan-Willem 'Vestje', Jesse, Jessica K., Jessica J., Joachim, Jorge 'the real Sinterklaas', Lisette, Luca, Luigi, Mahthild, Marc, Marco W., Marjon, Mark, Matt "time flies when you're confused", Peter, Reinskje, Roberto, Thorsten en Uwe, bedankt voor alles … Op zaal 14.0223 (en nog lang nadat we daar weg waren) heb ik genoten van het gezelschap van Franck, Richard & Minze. Roos dank ik voor het toelaten van verstekelingen in Siberië.

Marc van Gelder wil ik bedanken voor de hulp bij het opzetten van de 'kinetiek in water GC'. Hij werkt, maar wordt helaas niet gebruikt. Verder zijn er vele anderen die het werk op het lab een stuk eenvoudiger maken: de analyse-afdeling, het loket, de bibliotheek, de schoonmakers, de portiers. Een aantal mensen wil ik in het bijzonder noemen. Willem Kuil, vele jaren lang kwamen we elkaar vooral 's avonds tegen, bedankt voor de gezelligheid! Marten de Rapper, bedankt voor het talloze malen repareren van zo ongeveer elk willekeurig apparaat in het lab en de geduldige uitleg daarbij. Hilda Biemold en Yvonne van der Weerd voor alle hulp bij het 'geregel' van mijn promotie. Voor de integratie binnen OMAC is het vaak goed gebleken mee te doen aan het tourspel, de super-11 en het F1-spel. Organisatoren, bedankt!

Many thanks go out to everyone of the Reference Manager mailing list. If we keep solving problems together and Tech Support keeps listening, we'll get there in the end. I was pleasantly surprised by all the help from Edwin Straver of Frontsys in

setting up least-squares optimisation methods in Microsoft Excel. It is not often that one gets help of this quality directly from a company creating software.

Veel van mijn vrije tijd is de afgelopen jaren opgegaan aan het volleyballen bij Donitas. Met vele teamgenoten heb ik vele wedstrijden gespeeld en nog veel vaker getraind. Al mijn oud-teamgenoten (uit H9, H8, H6 en H5) hier noemen zou onbegonnen werk zijn, enkele noemen zou oneerlijk zijn. Ik noem er dus geen. Dit neemt niet weg dat ik vele fantastische herinneringen heb overgehouden aan al die jaren!

I would like to thank Anne, Cristina and Erika for being good friends, despite the distance. There is no doubt in my mind that we will remain friends for much longer. Hetzelfde geldt voor Paul en Frank, maar dan in het Nederlands.

Ondanks het feit dat we allemaal scheikunde hebben gestudeerd gingen de gesprekken met Menno, Gerard en Thomas vrijwel altijd over andere zaken. Gerard en Thomas, succes met schrijven… en Menno, jij kan altijd blijven zeggen dat je gelijk had. Gaan we binnenkort weer eens *gamen*? Deze uitnodiging geldt wanneer jullie dit voorwoord ook lezen, al is het in 2050. Verder wil ik Gerard bedanken voor het uitvinden van de 'partynimf'.

Albert, op het moment dat ik dit schrijf, lijkt het te gaan lukken, je bent er nog! Wie had dat durven hopen?! Samen met Ernst, Johan en Kirsten heb ik me altijd uitstekend vermaakt, leukere broers en zussen zijn er niet. Pap en mam hebben me altijd overal in gesteund en geloofden in mij, zelfs wanneer ik dat zelf niet meer deed. Zonder jullie was dit proefschrift er nooit geweest. Bedankt voor alles! Tot slot, de persoon die het meest het 'slachtoffer' is geworden van mijn promotieonderzoek: Marleen, ik ben soms verbaasd maar vooral blij dat jij het óók hebt volgehouden, bedankt!

Voor pap en mam, voor Albert.

TABLE OF CONTENTS

CHAPTER 3: GENERAL-BASE CATALYSED HYDROLYSIS AND NUCLEOPHILIC SUBSTITUTION OF ACTIVATED AMIDES IN AQUEOUS SOLUTIONS

CHAPTER 4: HYDROLYSIS IN AQUEOUS SOLUTIONS CONTAINING HYDROTROPES

CHAPTER 5: HYDROLYSIS IN AQUEOUS SOLUTIONS CONTAINING MICELLE FORMING SURFACTANTS

Water, the Unique Reaction Medium

1.1 INTRODUCTION

1.1.1 WATER[1,2]

1.1.1.1 WATER AS THE SOLVENT OF LIFE

Water is the "matrix of life",[3] arguably with good reason. There is no other solvent offering such a wealth of possibilities for the processes sustaining life as we know it. No wonder that finding water on the moon, on other planets and generally in space has high priority for space agencies. Apart from its stability in oxidation processes, of obvious importance in aerobic life-forms, water provides an excellent reaction medium for many types of reaction. Water plays an important role as a mediator in interactions in proteins,[4,5] a concept that has also recently been used in supramolecular chemistry.[6] In addition, water meets the demand for a solvent of life to support reversible processes, especially reversible aggregation processes. In fact, in comparison with other solvents, aqueous solutions in principle support the same types of interactions, albeit with different strength,[7] and one additional interaction, *viz.* the hydrophobic interaction. In the following, only water-specific hydrophobic interactions will be discussed.

Because of its high heat capacity, water moderates changes in temperature. In addition, strong enthalpy-entropy compensation frequently found for hydrophobic interactions moderates changes in Gibbs energy when the temperature changes.[8] In a way, water is medium, mediator and moderator of processes occurring in solution, and it can play the role of solvent, reactant and/or catalyst.[9]

Being the solvent of life, water is necessarily a non-toxic solvent. As such, it has frequently been promoted as an ideal solvent in green chemistry. In essence, water is an interesting and useful solvent in organic chemistry, but the ability of liquid water to drive apolar molecules together, as expressed in the low solubility of apolar substances, is often seen as a disadvantage. Yet, it is precisely this property that can be used with advantage for bimolecular (catalytic) reactions, as the coming together of reactants and/or catalysts is a prerequisite for those processes. Further, solvent water itself may also act as a catalyst by, for example, hydrogen-bond stabilisation of an activated complex.[10] If necessary, apolar compounds can also be solubilised by addition of amphiphiles, *e.g.* hydrotropes or surfactants. Currently,

numerous synthetic organic reactions not only have been found to proceed in aqueous solution but are sometimes accelerated and are more (stereo)selective (relative to organic solvents) in water-rich environments.[11-15] This is obviously true for hydrolysis reactions, but also for other organic reactions that are less expected to show rate enhancements in aqueous media, the Diels–Alder reaction[16] and Claisen rearrangement[17,18] being well known examples.

1.1.1.2 SOME PROPERTIES OF WATER

Water is a small molecule that can form a strong 3-dimensional hydrogen-bond network resulting from its 2 hydrogen-bond donating and 2 hydrogen-bond accepting sites. This strong hydrogen-bond network largely dictates water's intriguing properties, *e.g.* the high boiling point (*i.e.* the high cohesive energy density), the fact that ice floats on water, and the (related) existence of a temperature of maximum density. The relatively high molar heat capacity of water is also related to the characteristics of hydrogen bonding. Polarisation effects accompanying hydrogen bonding cause the dipole moment of water to be very different in the gas and solution phases; the gas phase dipole moment is 1.86 D ($6.20\ 10^{-30}$ C m) whereas the dipole moment in the liquid is 2.9±0.6 D ($9.67±2.0\ 10^{-30}$ C m) at 24.45±0.05°C[19] (from X-ray structure factors),[20] a value still under debate.

1.1.1.3 WATER, THE DISPUTED SOLVENT

Water chemistry is a field of extensive debate. To some extent, the debate arises from different approaches, different thermodynamic schemes,[21] different standard states[22,23] as well as different computational methods. As a result, different research groups sometimes fail to see that they essentially agree on the essential features of aqueous chemistry. The situation is worsened by the fact that water forms a very popular research topic, resulting in an extraordinarily large number of publications. A striking point in this respect is that titles of articles on hydrophobicity or hydrophobic effects tend to contain words indicating that the article presents a somewhat personalised view of aqueous chemistry.[24-28] Similarly, the present chapter offers a slightly biased view, based on recent literature. Generally, reference will not be made to articles older than 10 years; for a review up to 1993, see reference 24. An extensive collection of studies of water, including many of the first experimental studies of aqueous systems is available in reference 29.

1.1.1.4 EXPERIMENTAL STUDIES OF WATER AT THE MOLECULAR LEVEL

The macroscopic properties of water discussed above (Section 1.1.1.2) are a result of the molecular properties of water. Several experimental techniques are used to study these molecular properties. The most direct way of investigating the molecular structure of water is probably provided by X-ray and neutron scattering experiments. Using scattering experiments, two-body correlations (*e.g.* $g_{oo}(r)$) can be obtained. At present, radial distribution functions (RDFs) obtained from X-ray scattering and neutron scattering are in good agreement and they could become a reliable source of quantitative structural information for water.[30] Oxygen-oxygen radial distribution functions, $g_{oo}(r)$, peak at 2.73Å, 4.44Å and 6.66Å. From integration of the first peak in the radial distribution function, a coordination number of 4.7 has been found; for purely tetrahedral water a value of 4 is expected. This number indicates the presence of "interstitial water" or a "fifth neighbouring molecule".[31] In relation to this, it is intriguing that upon increasing pressure, a shoulder develops in the RDF at 3.2Å.[32]

The electronic structure of water in the liquid is significantly different from that in ice and in water vapour as indicated by X-ray absorption spectroscopy.[33] The liquid differs from ice as a result of considerable number of broken H-bonds on the H-donating site of the water molecule.[34] In agreement with this observed change in electronic structure upon hydrogen-bond formation, a gradual change of hydrogen-bonding structure and strength towards that of bulk water was observed for clusters of water molecules going from dimers up to nonamers.[35] Notably, the hydrogen bonds in the trimer are significantly shorter than those in the dimer as a result of the hydrogen bond being strengthened by the cooperative effect of three-body forces.[35] However, even within the liquid, not all hydrogen bonds are the same; a range of hydrogen-bonded structures with different hydrogen-bond lengths and hence different hydrogen-bond strengths exists.[36] Further, the vibrational potential of the O-H stretching vibrations in water shows extreme anharmonicity resulting in the delocalisation energy of the proton in water to be less than 20% of the dissociation energy of the O-H bond of the water molecule in the gas phase.[37]

The fraction of broken hydrogen bonds[38] in water has been studied using vibrational spectroscopy techniques such as Raman spectroscopy and near infrared spectroscopy. The near-infrared spectra of water, arising from a combination of symmetric and antisymmetric O-H vibrations, has been investigated and is accounted for by hydrogen bonding and non-hydrogen bonding OH groups, 75% and 25%, respectively, at 25°C.[39] Earlier, temperature dependent Raman[40] and

^{1}H-NMR spectra[41,42] had already been interpreted using a two-state model. However, in both cases, estimates of the fraction of free hydroxyl groups at (at least) two of the studied temperatures were necessary. Spectral deconvolution of the Raman spectra at different temperatures assuming a hydrogen-bond energy of 11.7 kJ mol^{-1} also shows a considerable uncertainty in calculated fractions of intact and broken hydrogen bonds.[43] In a different study, Raman spectra together with heat capacity data were accurately reproduced and the Gibbs energy, the enthalpy and the entropy of breaking a hydrogen bond in water were found to be 2.0 kJ mol^{-1}, 7.9 kJ mol^{-1} and 20 J K^{-1} mol^{-1}, respectively.[44] Apart from this description of water as a mixture of intact and broken hydrogen bonds, water has also been described as a mixture of clusters.[45]

The dynamics of water molecules in the liquid and their hydrogen-bond dynamics have also been studied. The lifetime of the hydrogen bond is commonly taken to be *ca.* 1 ps. Hydrogen-bond breaking in the water trimer is accelerated a thousand fold upon excitation of a single quantum in the librational mode,[35] indicating the importance of librational motion in hydrogen-bond breaking processes. Femtosecond mid-infrared pump-probe studies indicate that the reorientational lifetime of water molecules is longer for stronger hydrogen bonds. In fact, lengthening of the O-H···O bond is a prerequisite for reorientation.[36] These fast dynamics indicate a highly dynamic liquid whereas the relatively strong directionally-sensitive hydrogen bonds provide a certain extent of structuring. According to Luzar: "For water to be a fluid, it is essential that bonds break and form all the time. The frequency of these events, rather than the equilibrium fraction of broken bonds, is responsible for the fluidity of water."[46] In summary, at ambient temperatures and pressures, water cooperatively forms a highly dynamic yet structured condensed phase. Dynamics, liquid structure, molecular and electronic structure are all strongly variable making water a liquid of rather unusual properties.

1.1.1.5 COMPUTATIONAL STUDIES OF WATER

As in many subject areas in chemistry, computational chemistry has rapidly acquired an important place in the study of water. *Ab initio* methods are traditionally regarded as the ultimate in computational chemistry, but their drawback so far has been the computational demand. Pure *ab initio* calculations of both liquids and solutions are as yet not feasible.[47] The Car-Parrinello (CP) method is presently closest to a pure *ab initio* calculation.[48] The results of the most

extensive *ab initio* molecular dynamics simulation (using the CP method) of water involving 64 water molecules indicate that the electronic structure is markedly different in the bulk liquid phase compared to the gas phase.[49] The electronic charge becomes more spherically distributed around the oxygen atoms and the intramolecular O–H distance is significantly increased. This increases the dipole moment and the magnitude of the eigenvalues of the quadrupole moment tensor. It is clear from the preceding that valuable information can be obtained from CP/*ab initio* methods. However, apart from a few other *ab initio* MD simulations, *ab initio* methods are primarily used for the development of better classical models.[50]

In simulations employing classical force fields describing the interactions between molecules, the line between experiment and computation is sometimes thin, as many force fields have been optimised to reproduce certain experimental properties of water. These experimental properties could include the temperature of maximum density, the density vs. temperature profile but also the experimentally determined $g_{oo}(r)$. For example, correlation functions from scattering experiments have been used to improve and check molecular force fields in an approach called empirical potential structure refinement (EPSR). However, deriving reliable sets of site-site pair potentials *only* from scattering data seems impossible.[51] In addition to the use of experimental properties for force field development, the results of *ab initio* studies of water have been parameterised. As a result of all these different ways of force-field development, a number of force fields is available for water. The most commonly used force fields include CF1 or CFM, TIP4P, SPC/E and the two-dimensional MB model.[52,53] Many of these models do not *explicitly* include polarisation effects but include them indirectly, parameterised as normal charges. These models are therefore rather limited in use at different pressures and temperatures. The most direct example of this limitation is provided by calculations of the vapour-liquid coexistence curve in which polarisable models perform far better than non-polarisable models.[54] A model employing diffuse charges on the oxygen and hydrogen atoms provides far better transferability from the liquid to the gas phase and it accurately reproduces the relative permittivity “for virtually any state point”.[55] Similarly, polarisable models were found to be superior for simulations of the viscosity[56] and the microstructure of water.[57]

The parameterisation of polarisation effects into effective charges and dipoles has prompted a strong debate about the importance of these effects in classical simulations and whether they have been included properly. Despite all concern, most models have been optimised for ambient conditions and accordingly, a

comparison of classical and QM methods shows that the average electrostatic properties at room temperature and ambient pressure are described quite well by standard rigid models.[58] Including intramolecular flexibility, electronic polarisation or quantum effects "does not immediately lead to better reproduction of the thermodynamic properties of bulk water at a range of thermodynamic state points."[59] It should be noted, however, that *some* properties of water are reproduced well by the non-polarisable models, whereas other properties are not.[60]

Despite these controversies, simulations have led to an increased understanding of water at the molecular level; *e.g.* of the importance of interstitial water molecules in the dynamics of water.[61] At the same time, an understanding of the possibilities of simulation techniques has developed.

1.1.1.6 SCALED PARTICLE THEORY

A rather different description of liquids and solutions involves scaled particle theory (SPT). Somewhat similar to the fitting procedures used to construct the classical models describing water discussed above, in SPT the properties of hard spheres representing water molecules are adjusted in order to reproduce properties of water. These properties can be chosen to be, for example, isothermal compressibility or surface tension. Unlike the classical models describing water for which simulations are required to obtain results, for SPT analytical equations have been derived for calculation of properties depending on the water structure, *e.g.* the Gibbs energy of cavity formation (*vide infra*). Remarkably, in one of the first reviews of SPT, referring to water (and liquid metals near their melting points) Reiss[62] concluded that "the theory fails where it should". Despite this pessimistic view, SPT has played an important role in many studies of water, and has been successfully used in many studies, especially of aqueous solubility and hydrophobic hydration (*vide infra*). The remarkable success of SPT in the description of water may originate from the fact that effects such as hampered rotational averaging of solvent molecules resulting from hydrogen bonding end up in the size of the water molecules. Similarly, the strength and directional sensitivity of hydrogen bonds are included in the density and the temperature dependence of the density of water.

1.1.2 HYDROPHOBIC HYDRATION

1.1.2.1 AQUEOUS SOLUBILITY OF APOLAR COMPOUNDS

Many decades of research have been devoted to the low solubility (unfavourable, positive Gibbs energy of transfer) of apolar compounds in water. This low solubility is essentially caused by the apolar solute being unable to compete with water itself for "positions" in the liquid phase.[63] However, the directional sensitivity of interactions between water molecules provides a way of hydrating apolar molecules, called hydrophobic hydration, that minimises the (unfavourable) Gibbs energy change of solvation in water,[64] and causes a pronounced thermodynamic signature. Typically, the enthalpy of transfer is negative, but this is more than cancelled by a strongly negative entropy of transfer. The heat capacity of transfer is positive making both the enthalpy and entropy of transfer positive at higher temperatures. However, not all apolar solutes show the same transfer parameters. The size and shape of solutes proves to be important as well. For example, increasing the size of noble gases decreases the Gibbs energy of transfer into water for Ben-Naim standard conditions.[65] However, increasing the size of alkanes, the Gibbs energy of transfer into water for Ben Naim standard conditions first decreases but then increases again (resulting in a V-shaped plot). Also the nature (aliphatic or aromatic) of the apolar compounds has a pronounced influence on the observed transfer parameters as obvious from the fact that transfer of aromatic solutes to water is spontaneous ($\Delta_{transfer}G < 0$ J mol^{-1}) at room temperature for Ben-Naim standard conditions.[66-68]

Central questions in studies of hydrophobic hydration are whether hydrogen bonds are stronger in the hydrophobic hydration shell and whether it is the size of the water molecule, the high directionality of the hydrogen bond or the particular strength of the hydrogen bonds that causes the unfavourable Gibbs energy of transfer. A recent example of this debate still being very much alive is given by Kodaka and Graziano.[69-71]

1.1.2.2 EXPERIMENTAL STUDIES OF HYDROPHOBIC HYDRATION AT THE MOLECULAR LEVEL

An important part of the unique behaviour of many solutes in aqueous solutions is directly related to the special way in which water solvates small apolar solutes. As described above, the hydrogen-bond network of water is relatively strong and results from highly cooperative interactions. Hence, small apolar solutes not

offering sites for comparably strong interactions with water are not able to compete for hydrogen bonds. As a result, at ambient temperatures, water molecules tend to keep their hydrogen-bond network intact and the solute is surrounded by water molecules hydrogen bonded to each other. As a result of this tendency to maintain the water hydrogen-bond network, there is a preference for a tangential (with respect to the solute surface) orientation of the O-H bonds as observed in neutron diffraction studies.[72,73] The hydration shell thus formed around apolar solutes is called the "hydrophobic hydration shell" (Figure 1.1).

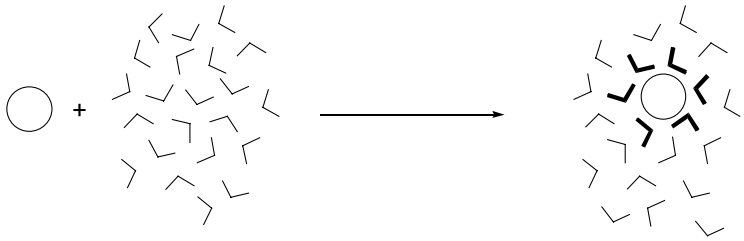

Figure 1.1: The hydrophobic hydration shell in which water molecules hydrating an apolar solute (highlighted) retain their hydrogen-bond structure.

The concept of tangential solvation is almost generally accepted and is supported by computational studies (*vide infra*). As with every other restriction, this preference for tangential orientation (or the exclusion of directions in which hydrogen bonds can be formed) is accompanied by an unfavourable entropy. In fact, entropies of hydration have been calculated using only the space angle in which hydrogen bonds cannot be formed.[74] Rotational and possibly vibrational motion of water molecules are probably assisted by neighbouring water molecules. In agreement with this, the rotational correlation times of water molecules in the hydration shell are longer.[75] This decreased mobility also corresponds to a lower entropy.

In an alternative thermodynamic scheme, transfer of a solute into water is divided into cavity formation and solute insertion. A cavity term is determined from either the particle insertion method or from SPT. This cavity term opposes the insertion of solutes in water. Next, a solute is "inserted" into the cavity and the solute-solvent interactions are "switched on", which is a favourable process. In water, the excluded volume term accompanying cavity formation is dominant, causing the low solubility of nonpolar compounds in water. The purely structural reorganisation of H-bonds around the nonpolar solute is a compensating process that does not affect the Gibbs energy change,[76] but contributes to the enthalpy and entropy changes as well as to the large positive molar heat capacity change.[77]

A strong debate remains on the strength of hydrogen bonds in the hydrophobic hydration shell. This discussion is partly inspired by the surprisingly favourable enthalpy of transfer of apolar solutes into water, which might be caused by the hydrogen bonds in the hydrophobic hydration shell being lower in enthalpy than in bulk water. But it could also indicate exceptionally favourable solute-solvent interactions. Enthalpically-favourable solute-solvent interactions can be caused by the dipole-induced dipole interactions between water and solute. A unique feature of water in this respect is that it has a relatively low coordination number, which causes water to lose relatively few water-water interactions, whereas other dipolar solvents are expected to lose more solvent-solvent interactions by accommodating the apolar solute. Alternatively, or maybe even additionally, "proton hopping" has been proposed[24] as the cause of an additional favourable interaction. Proton hopping may introduce an additional term in the interaction energy as a result of the bulk polarisability of water.[24] Despite the fact that simulations (*vide infra*) have been suggested[24] to clarify this matter, this proton hopping term will be rather difficult to calculate from simulations, as it is related to the relative movement, and not the relative orientation of the solute and solvent molecules.

From the temperature dependence of the proton chemical shift and the heat capacity change upon hydration together with a two-state model in which hydrogen bonds in bulk water and in the hydration shell are either intact or broken, it was suggested that in the hydration shell hydrogen bonds are enthalpically stronger but fewer than in the bulk.[78] Similarly, from Raman and $\Delta_{transfer}C_p$, the thermodynamic parameters for breaking a hydrogen bond in the hydration shell of noble gases were determined. Taking neon as an example, breaking a hydrogen bond takes a Gibbs energy of 2.1 kJ mol^{-1}, an enthalpy of 10.0 kJ mol^{-1} and an entropy change of 26.6 J K^{-1} mol^{-1}.[44] Comparing these numbers with the numbers for bulk water (*vide supra*) suggests an increase in hydrogen bond strength upon transferring a hydrogen bond from bulk water to the hydrophobic hydration shell of argon. The enthalpy of hydrogen-bond breaking in the hydration shell is higher, but entropically, it is more favourable to break a hydrogen bond in the hydration shell. Similar results were obtained from computational studies (Section 1.1.2.3).

The origin of the different plots of the size dependence of the transfer Gibbs energies of noble gases and alkanes from the gas phase into water was determined using SPT and the experimentally determined transfer parameters. For noble gases, the energy of the van der Waals interactions between solute and water increases more rapidly than the cavity formation term. For alkanes however, this is not the

case.[79] This difference is "determined by the larger number of weakly bound electrons of the former [the noble gases], which strengthen the van der Waals interactions with water."[79] The remarkable behaviour of aromatic solutes is caused by the favourable enthalpy of transfer as a result of aromatic ring - water H-bonding.[66-68] With the exception of the stronger solute-solvent interactions, the transfer process is qualitatively the same as the transfer process of aliphatic apolar compounds.[68]

The hydration of large apolar solutes is different from the hydration of small solutes. For certain sizes of solutes, water molecules in the hydration shell are increasingly unable to retain their hydrogen-bond network. The difference in hydration structure is clear from the behaviour of water at hydrophobic surfaces, including the air-water interface. At such interfaces, each water molecule gives up one of its hydrogen bonds and points it at the apolar surface, creating a "dangling hydrogen bond".[80-82]

1.1.2.3 COMPUTATIONAL STUDIES OF HYDROPHOBIC HYDRATION AT THE MOLECULAR LEVEL

Computer simulations of hydrophobic hydration use the techniques already mentioned for simulations of water itself. Hence, also in the computational study of hydrophobic hydration, the inclusion of polarisation is under debate. Nymand claimed that "it is expected that many-body contributions [in which polarisation effects are important] are even more important when the solvation of molecules and the properties of liquids at surfaces are examined."[60]

Different approaches towards the study of hydrophobic hydration are possible. Most straightforward is a simulation (either classical or *ab initio*[83]) of the solute in water. However, there are other, more efficient, ways. A time-saving technique involves simulation of water followed by particle insertion. In this method, water configurations generated in an MD or MC run are searched for cavities big enough to hold a solute. This can be done for several solutes of different sizes and shapes using only a single computational study of water. Scaled particle theory, on the contrary, uses analytical equations describing particle insertion. For these calculations, the effect of solvent reorganisation after particle insertion (after "switching on" the solute-solvent interactions) is calculated independently.

The preference for tangential orientation of the O-H bonds as observed in experiment is also found in computational studies.[84-87] The potential energy surface (PES) of the 1:1 neon-water interaction shows only a slight preference for tangential solvation, indicating that the preference for tangential solvation is caused by

cooperative effects.[88,89] The importance of cooperative effects is also clear from the observation that the two-body approximation for the calculation of the entropy in cold water is not sufficient. This approach overestimates the degree of ordering, and so the higher terms add an additional disorder.[90] The calculated dipole moments of water molecules near a methane molecule are not significantly different from their average values in bulk water.[58,91] On the other hand, polarisability makes the rate of forming and breaking hydrogen bonds more dependent on the local environment.[92]

The surprisingly favourable enthalpy of transfer has been attributed to several possible causes. It has been attributed to a decrease in the number of repulsive non-hydrogen bonding interactions between water molecules, while the negative hydration entropy is caused by a subtle enhancement of the structure of water.[93] An alternative explanation by Sharp *et al.*[94] involves the interstitial water molecules: nonpolar solutes tend "to occupy the same positions with respect to the quasi-tetrahedral lattice that the more weakly interacting water would, in effect competing for this mismatch site." This effectively reduces the fraction of interstitial water molecules resulting in an additional favourable enthalpy and an additional unfavourable entropy. The same model also accounts for the isobaric molar heat capacity of hydration. Another study suggesting the importance of taking more than just the first hydration shell into account, discusses the thermodynamic effects as an expansion of water around an apolar solute.[95]

According to the Muller model applied to a simulation of MB (Mercedes Benz) water (Figure 1.2), inserting a nonpolar solute into cold water causes ordering (as indicated by the lower enthalpy and entropy of *intact* hydrogen bonds in the hydration shell) and strengthening of the H-bonds in the first hydration shell. However, the reverse applies for hot water (as indicated by the higher enthalpy and entropy of *broken* hydrogen bonds in the hydration shell).[96] Significantly, transferring intact hydrogen bonds from bulk water into the hydrophobic hydration shell causes an additional favourable enthalpy term.[96]

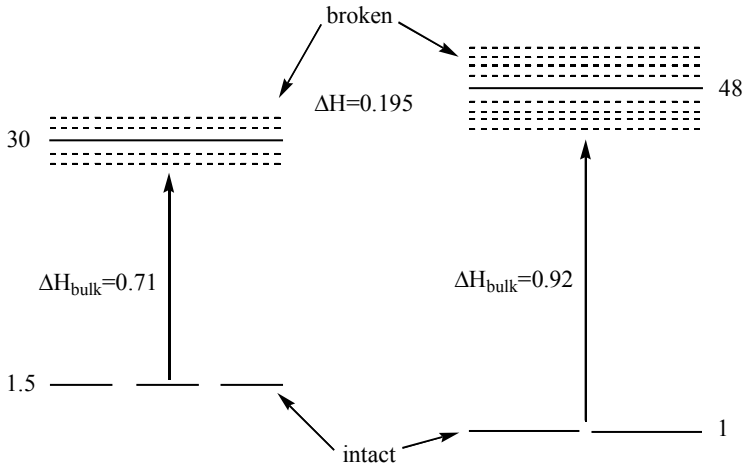

Figure 1.2: Energy diagram of hydrogen bonds according to the extended Muller model. *Left:* Hydrogen bond in bulk water. *Right:* Hydrogen bond in the hydrophobic hydration shell. Enthalpies are in units of "the energy of an idealised hydrogen bond configuration in which one arm of molecule *i* aligns with an arm of molecule *j*, and the two molecules' centers are separated by a distance r_{HB}" The numbers next to each energy level indicate the relative degeneracy. Picture taken from reference 96.

Comparison of TIP4P water and Lennard-Jones (LJ) water (the latter having the same size and density as TIP4P water but without hydrogen bonds) solvating hydrophobic solutes shows that the thermodynamic signature of hydrophobic hydration is caused by both the small size of water molecules and the hydrogen bonding pattern.[26,97] Lazaridis[98] also found that the (Ben-Naim standard) enthalpy and entropy of solvation are almost identical to the solute-solvent enthalpy and entropy and that the solvent reorganisation energy and entropy are small as a result of almost cancelling contributions (a positive contribution from the solvent exclusion and a negative contribution from the orientational arrangement of water next to the solute). The large isobaric heat capacity of hydrophobic hydration is caused by the fact that the preference for orientations in the hydrophobic hydration shell is lost upon increasing the temperature leading to an increasing loss of hydrogen bonds between water molecules (in agreement with Figure 1.2). Hence, an increase in the hydration energy with respect to the solute is found with increasing temperature.[98]

The importance of size and curvature of the solute for the way in which it is solvated (see also Section 1.1.2.1) has been studied by several authors using computational methods.[86] An increase in solute size causes an increase in Gibbs energy (total Gibbs energies of solutions were calculated).[99] From an MB model simulation of the effect of the cosolute's size, it is concluded that large hydrophobic particles are not hydrophobic in the classical sense; if the hydrophobic surface is

not curved enough to be straddled by the hydrating water molecules, water points its hydrogen bonds at the hydrophobic surface[87] and the hydrating water molecules are less strongly hydrogen bonded.[100] This is similar to the hydration behaviour at high temperatures indicating once more the delicate balance between enthalpy and entropy in the hydrophobic hydration shell. That this balance is truly delicate is also shown by the fact that the calculated hydration shell structure for solutes of intermediate size is model sensitive.[101] Similarly, water inside a hydrophobic cavity forms fewer hydrogen bonds and has fewer near neighbours and reorientational dynamics are accelerated.[102] These different solvation modes also lead to different values for the ΔC_p per unit surface of hydration of curved and (relatively) flat hydrophobic surfaces.

1.1.3 HYDROPHOBIC INTERACTION

Hydrophobic interactions are important non-covalent driving forces for inter- and intramolecular binding and assembly processes in aqueous chemistry in general and in biochemistry in particular.[24,103-105] Hydrophobic interactions are thought to be one of the major factors providing protein stability. However, hydrophobic interactions are often not necessarily the sole driving force, but rather one of the driving forces, a fact that is most obvious for protein stability and binding to proteins.[104-106]

Justifiably, the origin of hydrophobic interaction has been sought in the special mode of water in hydrating hydrophobic moieties, forming a hydrophobic hydration shell. In a pairwise hydrophobic interaction, less water molecules are needed to encompass the hydrophobic moieties, leading to a favourable entropy term accompanying association, which, together with a negative heat capacity change, is one of the key indications of hydrophobic interactions (Figure 1.3).

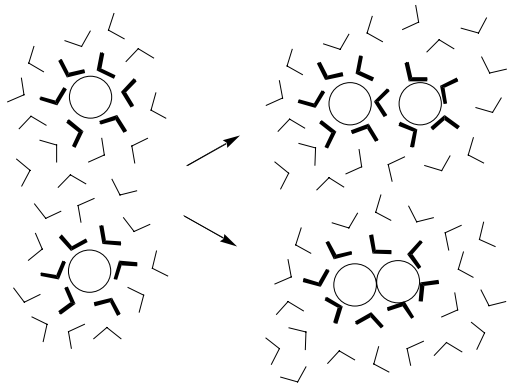

Figure 1.3: Hydrophobic interactions can take place in the form of solvent separated pairs (above) and contact pairs (bottom). Water molecules are released from hydrophobic hydration shells upon hydrophobic interaction.

Hydrophobic interactions vary from relatively weak pairwise intermolecular contacts (*e.g.* coming together of two apolar reactants in aqueous solution) to cooperative bulk association processes (*e.g.* phase separation, micellisation or formation of bilayer vesicles).

1.1.3.1 EXPERIMENTAL STUDIES OF (PAIRWISE) HYDROPHOBIC INTERACTION AT THE MOLECULAR LEVEL

According to mass-spectrometry, hydrophobic compounds cluster in aqueous solution.[107] Intermolecular ^{1}H-NOESY NMR spectroscopy shows that in mixed aqueous solvents, hydrophobic solutes are preferentially solvated by the organic component of the solvent mixture.[108] The relative enrichment of the solvation shell is stronger in more water-rich solvent mixtures, indicating the importance of bulk water for hydrophobic interactions.[109] Similarly, the relative self-association (the concentration of the alcohol in the solvation shell of alcohol molecules relative to the bulk concentration) determined using intermolecular proton relaxation rates and quantified by the A_{22}-parameter[110] monotonically increases with decreasing concentration[111] of alcohols,[112-114] except for 2-methylpropan-2-ol, for which it decreases again at low concentration.[115,116] The break in self-association pattern observed for 2-methylpropan-2-ol was also found using Kirkwood-Buff Integral calculations[117-119] of aqueous solutions containing 2-methylpropan-2-ol and 1-propanol.[120] Ethanol in water shows a far less tendency to self-associate.[121] These results support those from X-ray scattering.[120,121] The enthalpy of interaction between apolar groups in different alcohols is rather dependent on the distance of these apolar groups from hydrophilic group.[122,123] Neutron diffraction studies have also provided RDFs of apolar molecules in aqueous solution. However, these RDFs have been determined at rather high concentrations of solute. As a result, the measured intermolecular distances are not significantly different from the "statistical distances" between molecules.[124-126]

This last point introduces an intrinsic problem with most experimental studies of hydrophobic interactions. A certain minimum concentration of the apolar solute is essential in order to obtain accurate results. However, at these concentrations, solutes are necessarily in contact and hence there is no direct link between hydrophobic interaction and hydrophobic hydration as it occurs in dilute solutions. This difference in behaviour of dilute and concentrated solutions is obvious from low frequency Raman studies showing a threshold mole fraction for clustering of 2-methylpropan-2-ol at x=0.05.[127] Similarly, from the excess molar enthalpies of

alkanols in aqueous solution, different “mixing schemes” were identified.[128] The transition between a mixing scheme describing the most dilute solutions and one describing more concentrated solutions takes place at higher mole fractions for smaller hydrophobic alcohols, as expected for a change of mixing scheme caused by molecular size. Notably, for aqueous solutions of 2-methylpropan-2-ol the mixing scheme describing the most dilute solution ends at a mole fraction of 0.045,[129] below the mole fraction at which most experimental studies of hydrophobic interactions involving 2-methylpropan-2-ol are performed. This indicates that the relation between the studied interactions and hydrophobic hydration as it occurs in dilute solutions is rather ambiguous.

Hydrophobic interactions are often invoked, relevant or not, to explain interactions in aqueous solution between molecules bearing one or more of a multitude of apolar moieties. As a result alkyl chains and phenyl rings are often thought to be comparable hydrophobic moieties even though there are distinctions in behaviour of these two[66,68] in aqueous solutions. An even more striking change in thermodynamic behaviour occurs upon binding of hydrophobic guests to hosts inside a “hydrophobic” cavity, a process commonly assumed to be driven by hydrophobic interactions.[130,131] Contrary to “classical hydrophobic interactions”, these binding processes are often enthalpy driven, whereas binding is entropically unfavourable.[131] The reason for the peculiar enthalpy and entropy contributions has been claimed to be the release of “high energy water” from inside the cavity. Water molecules inside the cavity cannot take part in a hydrogen-bond network, as indicated above. Hence, their liberation is expected to be enthalpically favourable and entropically unfavourable.[132] The driving force of such an association is not a hydrophobic interaction.

1.1.3.2 COMPUTATIONAL STUDIES OF HYDROPHOBIC INTERACTION AT THE MOLECULAR LEVEL

With experimental studies at the disadvantage of requiring high concentrations, computational methods have been employed in the study of hydrophobic interactions. However, considering the lack of agreement over computational studies of hydrophobic hydration and the lack of experimental data (apart from that derived from the A_{22} parameter and Kirkwood Buff Integral (KBI) studies), results from simulations must be interpreted with care.

In agreement with expectation, an MD simulation shows that the aggregation of methane is slightly unfavourable, but driven by entropy.[133] The aggregation tendency of methane increases with increasing temperature. The increase in

tendency to aggregate is at the expense of solvent separated contact pairs (see Figure 1.3).[134]

A clear example of the difficulties in obtaining results from simulations is provided by calculations of the potential of mean force (PMF) between apolar molecules. When the interaction potential between 2 methane molecules is calculated using non-polarisable models, both the contact pair and the solvent separated pair are local minima on the potential energy surface (PES). However, using a polarisable water model, the solvent separated minimum disappeares[24] Recently, however, the inclusion of polarisability has been shown not to lead to a change in potential of mean force between methane molecules compared to the non-polarisable models and the solvent-separated minimum is found again.[135] Even worse, calculating the effects of pressure on contact pair and the solvent separated pair using three different simulations[136-138] yields totally different results.

1.1.4 WATER, HYDROPHOBIC HYDRATION AND HYDROPHOBIC INTERACTION - SUMMARY

In summary, the peculiar properties of water lead to the characteristic and peculiar thermodynamic transfer parameters and eventually to hydrophobic interactions. We contend, however, that this causality-chain is only valid in sufficiently dilute aqueous solutions and that care has to be taken when different solutes are compared since size, curvature and type (aliphatic, aromatic, noble gas) of solute are all important parameters in the observed effects. At present, there seem to be no indications of increased hydrogen-bond interaction between water molecules hydrating small apolar solutes, apart from effects expected for the exclusion of space angles in which hydrogen bonds can be formed. If hydrogen bonds in the hydrophobic hydration shell are broken, apolar solutes present less favourable interactions than neighbouring water molecules and hence, both enthalpy and entropy of a broken hydrogen bond in a hydrophobic hydration shell are higher than in bulk water. Considering both increasing temperature but also lack of (convex) curvature of the hydrophobic binding site or surface lead to breaking of hydrogen bonds in the hydration shell, the actual structure of the hydrophobic hydration shell is the result of a very delicate balance of enthalpy and entropy.

1.1.5 HYDROPHOBIC INTERACTION AND REACTIVITY

In the previous sections, hydrophobic hydration and hydrophobic interactions were discussed from an association/aggregation or equilibrium point of view. In addition to these chemical equilibria, hydrophobic interactions often play a key role in chemical reactions[11-15] and catalytic processes[139] since coming together of reactants is a prerequisite for bimolecular reactions.

The study of the thermodynamics and kinetics of the formation of encounter complexes in aqueous solutions has immediate relevance for a mechanistic understanding of reactions in aqueous media. Often, the formation of an encounter complex is driven (or made less unfavourable) by hydrophobic interactions and constitutes the first step in the activation process of a bimolecular reaction. Insight into factors governing encounter complex formation aids in a quantitative analysis of second-order rate constants for such chemical transformations. Furthermore, reactant-catalyst interaction is an important topic in current research and better insights into such interactions should lead to an improved rational design of catalysts.

The advantage of using reaction kinetics as a means of studying hydrophobic interactions stems from the fact that rate constants can normally be measured accurately, with errors in rate constant typically less than 2%. Therefore, if hydrophobic effects cause rate constants to change, the concomitant changes in Gibbs energy can often be calculated with higher precision than in the case of equilibrium processes. This provides the opportunity to measure carefully hydrophobic effects, even when they are small. This leads to the added advantage that measurements can be done at low concentrations, eliminating the conceptual problems of hydrophobic interactions at higher concentrations. However, the approach has a disadvantage as well in that it gives *differences in the stabilisation* of initial state and transition state.

1.2 A THERMODYNAMIC FRAMEWORK

1.2.1 THE HYDROLYSIS OF ACTIVATED ESTERS AND ACTIVATED AMIDES

As a model system for the study of effects of hydrophobic (and other) interactions on chemical reactions, the hydrolysis of activated amides and esters was chosen. These reactions, in general, are water-catalysed between pH 2.0 and 5.5. The reactions proceed *via* a dipolar activated complex in which two water molecules, one acting as a general base, are involved *with three protons in flight* (Scheme 1.1).[140-142] Rates of hydrolysis of such esters and amides in aqueous solution are reported in this thesis and are characterised by (pseudo-) first-order rate constants. The molecularity of these reactions with respect to water is at least two but this information does not emerge from analysis of the kinetic data reported here because the water concentration remains essentially constant. In order to recognise this complexity, the term '(pseudo-) first-order rate constant' is used.

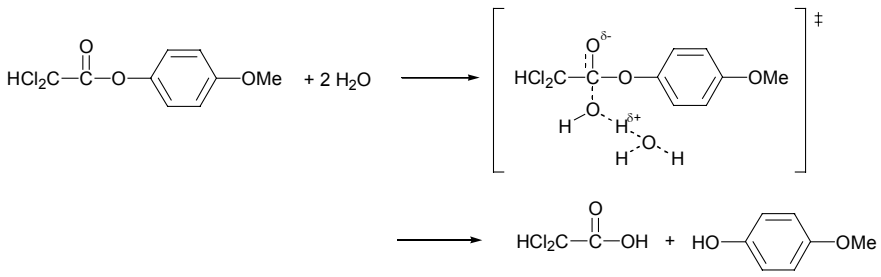

Scheme 1.1

These hydrolysis reactions are retarded by added hydrophobic cosolutes, as will be discussed in more detail in Chapter 2. The advantage of using these water-catalysed reactions is that there is a fairly large pH-range in which the reaction is water-catalysed, so there is no need to use buffers that could interfere with interactions, in particular with hydrophobic interactions. The hydrophobicity of the hydrolytic probes can be changed through variation of substituents enabling the study of the effects of hydrophobicity of both the hydrolytic probe and of the cosolute. In addition, the reactivity of the probes can be manipulated by the introduction of electron-donating and/or electron-withdrawing groups. The rate constants of these hydrolysis reactions are sensitive to hydrophobic interactions as hydrophobic interactions change or remove the hydration shell around the hydrolytic probe.

1.2.2 COMPUTER SIMULATIONS

The hydrolysis reaction of *p*-methoxyphenyl dichloroethanoate has been investigated by detailed computer simulations, using both quantum and classical dynamics. The simulations revealed that proton tunnelling is involved in the rate-determining step.[143] As the likeliness of proton tunnelling is critically dependent on the shape of the potential energy surface around the activated complex,[144] the water molecules involved in the activated complex are subject to severe orientational requirements. Consistent with these views, strongly negative entropies of activation have been found for this reaction.[142] The configurations from which proton tunnelling, leading to the product, could occur were called "active configurations".[145] In a subsequent molecular dynamics simulation, it was shown that added cosolutes can effectively decrease the average frequency with which these active configurations occur.[146] This lower number of occurrences of active configurations logically leads to a decrease in rate constant. Notably, this decrease in active configurations is stronger than expected on the basis of a totally random distribution of the added cosolute molecules over the available (solution), indicating a preferential interaction. The tendency for this preferential interaction was stronger for more hydrophobic hydrolytic probes and more hydrophobic cosolutes.

1.2.3 ANALYSIS OF KINETIC SOLVENT EFFECTS IN DILUTE MIXED AQUEOUS SOLUTIONS IN TERMS OF PAIRWISE GIBBS ENERGY INTERACTION PARAMETERS

The thermodynamic model for interactions between a reacting molecule and an inert hydrophobic cosolute was developed several years ago.[147,148] This model interprets the rate retardations in terms of the effect of added cosolute on activity coefficients of initial and transition states of the ester or amide undergoing hydrolysis. Here, only key equations are given. For a full derivation, see reference 148. In the following, c denotes the cosolute whereas i denotes the hydrolytic probe, as either reactant or activated complex.

The Gibbs energy of interaction stems from the non-ideal part of the Gibbs energy of the total solution, the excess Gibbs energy G^E. For a dilute solution containing two solutes; hydrolytic probe i and cosolute c, G^E is given by Equation 1.1.[149,150]

$$G^{\mathrm{E}}(\mathrm{aq}) = g_{\mathrm{ii}} \cdot \left(\frac{m_{\mathrm{i}}}{m^0}\right)^2 + 2 \cdot g_{\mathrm{ic}} \cdot m_{\mathrm{i}} \cdot m_{\mathrm{c}} \cdot \left(\frac{1}{m^0}\right)^2 + g_{\mathrm{cc}} \cdot \left(\frac{m_{\mathrm{c}}}{m^0}\right)^2 \qquad (1.1)$$

Here, g_{ii}, g_{ic} and g_{cc} are Gibbs energy interaction parameters quantifying the interactions between the solutes, m and m^o are molalities. The latter the reference state of 1 mol kg^{-1}. From the excess Gibbs energy given by Equation 1.1, the osmotic coefficient ϕ (Equation 1.2) and the activity coefficient of solute-i (γ_i) (Equation 1.3) can be calculated (both derived using the Gibbs-Duhem equation).

$$\frac{(1-\phi)}{m_i} = -\left(\frac{1}{R \cdot T}\right) \cdot \left\{ \frac{\mathrm{d}\left[G^{\mathrm{E}}(\mathrm{aq}) / m_i \right]}{\mathrm{d}m_i} \right\} \tag{1.2}$$

$$\ln \gamma_{\mathrm{i}} = \left(\frac{1}{R \cdot T}\right) \cdot \left(\frac{\mathrm{d}G^{\mathrm{E}}(\mathrm{aq})}{\mathrm{d}m_{\mathrm{i}}}\right) \tag{1.3}$$

Here, T is the temperature and R is the gas constant. As the solutions contain low molalities of kinetic probes, the terms in m_i are negligible, resulting in Equation 1.4 for the osmotic coefficient and Equation 1.5 for the activity coefficient of solute-i.

$$1-\phi = -\left(\frac{1}{R \cdot T}\right) \cdot m_{\mathrm{c}} \cdot \left(\frac{1}{m_{\mathrm{o}}}\right)^2 \tag{1.4}$$

$$\ln \gamma_{\mathrm{i}} = \left(\frac{2}{R \cdot T}\right) \cdot g_{\mathrm{ic}} \cdot m_{\mathrm{c}} \tag{1.5}$$

In the transition state theory description of chemical reactions,[151] the reactants are assumed to be in equilibrium with the activated complex. For the present hydrolysis reaction in which two water molecules are involved in the activated complex, this equilibrium is given by Equation 1.6.

$$\mu_{\mathrm{R}}^{\mathrm{eq}}(\mathrm{aq}) + N \cdot \mu_{\mathrm{S}}^{\mathrm{eq}} = \mu_{\neq}^{\mathrm{eq}}(\mathrm{aq}) \tag{1.6}$$

Here, $\mu_{\mathrm{R}}^{\mathrm{eq}}$ and $\mu_{\mathrm{S}}^{\mathrm{eq}}$ are the chemical potentials of the reactant and the solvent (involved in the reaction) in equilibrium with the activated complex, with chemical potential $\mu_{\neq}^{\mathrm{eq}}$. Using Equation 1.6, rewriting the chemical potentials as products of molalities and activity coefficients and combining with Equation 1.4 leads to Equation 1.7 for the molality of activated complex.

$$m_{\neq}^{\mathrm{eq}} = m_{\mathrm{R}}^{\mathrm{eq}} \cdot \left(\gamma_{\mathrm{R}} / \gamma_{\neq}\right) \cdot {}^{\neq}K^{\mathrm{o}}(\mathrm{aq}) \cdot \exp\left(-N \cdot \phi \cdot m_{\mathrm{j}} \cdot M_1\right) \tag{1.7}$$

Here, ${}^{\neq}K^{\circ}(\mathrm{aq})$ is the equilibrium constant for formation of the activated complex in the (hypothetical) solution in the reference state, M_l is the molar mass of water, N is the number of water molecules involved in the rate-determining step, and ϕ is the practical osmotic coefficient for the aqueous solution where the molality of added solute is m_c. In the present study, N equals 2 (*vide supra*). For dilute solutions, $m_{\neq}^{\mathrm{eq}} / m_{\mathrm{R}}^{\mathrm{eq}} = c_{\neq}^{\mathrm{eq}} / c_{\mathrm{R}}^{\mathrm{eq}}$ and combination with transition state theory[151] eventually leads to a rate constant given by Equation 1.8

$$k(\mathrm{aq}) = \left(\frac{k_{\mathrm{B}} \cdot T}{h}\right) \cdot \left(\gamma_{\mathrm{R}} / \gamma_{\neq}\right) \cdot {}^{\neq}K^{\circ}(\mathrm{aq}) \cdot \exp\left(-N \cdot \phi \cdot m_{\mathrm{j}} \cdot M_1\right) \tag{1.8}$$

Here, k_{B} and h are the Boltzmann and Planck constants, respectively. Rewriting Equation 1.8 gives $\ln(k(\mathrm{aq})/k(\mathrm{aq,ideal}) = \ln \gamma_{\mathrm{R}} - \ln \gamma_{\neq} - N \cdot \phi \cdot M_1 \cdot m_{\mathrm{j}}$ which, using Equation 1.5 for the activity coefficients, gives Equation 1.9.

$$\ln\left[\frac{k(m_c)}{k(m_c = 0)}\right] = \frac{2}{R \cdot T \cdot m_o^2} \cdot \left[g_{cx} - g_{c\neq}\right] \cdot m_c - N \cdot \phi \cdot M_l \cdot m_c \tag{1.9}$$

Here $k(m_c)$ is the (pseudo-)first-order rate constant in an m_c molal aqueous solution of cosolute c, $k(m_c=0)$ the rate constant in the absence of added cosolute. Significantly, $[g_{cx}\text{-}g_{c\neq}]$ is the difference in interaction Gibbs energies between the cosolute c and the reactants x on one hand and the activated complex ≠ on the other hand. Further, the solutions are very dilute and hence, ϕ can be taken as unity; m_o is the (hypothetical) ideal reference state and corresponds to 1 mol kg^{-1}. The term $[g_{cx} - g_{c\neq}]$ is denoted as G(c). Apart from being used in the analysis of rate-retarding effects on the hydrolysis of activated esters and amides (which will be discussed in more detail in Chapter 2), this analysis of kinetic results, which involves a direct link between thermodynamics and transition state theory, has also been employed for completely different reactions, including keto-enol tautomerisation,[152] rate-determining electron transfer reactions[153] and aquation of iron(II) complexes in aqueous solutions.[154] These G(c)-values can be re-expressed using the procedures described by Wood[155] in terms of pairwise solute-solute interaction parameters. This results in group contributions to the observed rate retarding effects.

Equation 1.1 is valid for dilute solutions of two solutes. In the present case, one of the solutes is undergoing a reaction that is monitored. Depending on concentration, Equation 1.1 may contain non-negligible higher order terms as well,

resulting in a situation where Equation 1.9 is no longer linear in m_c. It should be noted that "dilute" has a slightly ambiguous meaning in this context, as the presence of higher order terms is also dependent on the interaction parameters *g*. Similarly, introduction of a third solute introduces additional terms in Equation 1.1, though for dilute solutions, these terms indicate additivity of the rate-retarding effects.

1.3 AGGREGATION AND AGGREGATE MORPHOLOGY IN AQUEOUS SOLUTION

As already indicated in Section 1.2.4, apart from interacting with the hydrolytic probes, cosolute-cosolute interactions are important. As the concentration/molality of added cosolutes is typically several orders of magnitude higher than that of the hydrolytic probe, self-interaction of the cosolute could be important. If the self-interactions of cosolutes are strong enough, thermodynamically stable aggregates will be formed. These aggregates can range from dimers to rather complex structured aggregates, containing hundreds of monomers. In particular, surfactants form a range of structured aggregates comprising spherical micelles, wormlike micelles, bilayers, vesicles and inverted micelles (Figure 1.4).

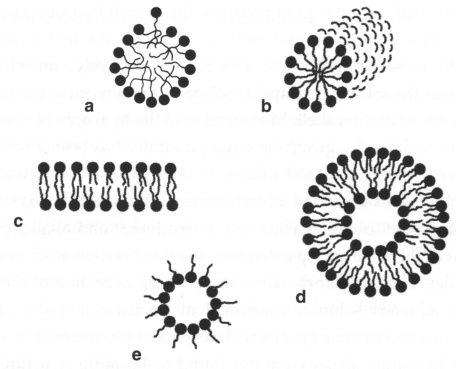

Figure 1.4: Aggregate morphologies of surfactants self-assemblies in aqueous solution; spherical micelle (a), wormlike micelle (b), bilayer fragment (c), vesicle (d) and inverted micelle (e). Picture taken from reference 156.

As a *guideline* to the shape of the aggregates formed by surfactants, Ninham and Israelachvili developed the concept of the packing parameter.[157] The packing parameter *P* is calculated using Equation 1.10

$$P = \frac{V}{a_o \cdot l} \tag{1.10}$$

in which V is the volume of the hydrocarbon chain(s) of the surfactant, a_o the mean cross-sectional (effective) headgroup surface area and l the length of the hydrocarbon chain in the all-trans configuration. The predicted morphologies of the aggregate are given in Table 1.1.

Table 1.1: Relationship between aggregate morphology and shape of the surfactant as given by the packing parameter P.

surfactant shape		P	aggregate morphology
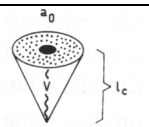	cone	<1/3	spherical micelles
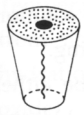	truncated cone	1/3-1/2	wormlike micelles
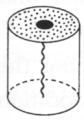	cylinder	1/2-1	flat bilayers or vesicles
	inverted (truncated) cone	>1	inverted micelles

Pictures taken from reference 156.

1.4 AIM AND SURVEY OF CONTENTS

In the previous sections, several aspects of water and aqueous solutions have been (briefly) discussed. The properties of water are unique and hence as a solvent, water provides an interesting alternative to organic solvents. In order to take full advantage of the possibilities that aqueous solutions have to offer as a reaction medium, it is crucially important that the solvent properties of water are well understood. The research described in this thesis was inspired by the need for an overview and a quantification of the patterns governing reactivity in aqueous solutions containing different hydrophobic cosolutes. Pairwise hydrophobic interactions, of interest for bimolecular reactions and substrate catalyst interactions (in homogeneous catalysis), were investigated as well as the effect of self-association of the added cosolute. Apart from inert cosolutes, reactive (either as a catalyst or as a reactant) cosolutes were also added. The nature of the micellar pseudophase as a reaction medium was investigated. In addition, kinetics of

hydrolysis in a temperature range around the temperature of maximum density was studied and the relevance of such studies in the determination of activation parameters under isochoric conditions was tested.

The nature of the rate-retarding effects on the hydrolysis of activated esters and activated amides is discussed in Chapter 2. This Chapter also provides a quantification of the Gibbs energy, enthalpy and entropy of encounter complex formation and the stabilisation of encounter complexes by hydrophobic interactions. Changes in reactivity of activated amides in aqueous solution in the presence of general bases are the topic of Chapter 3. The changes in reactivity of activated amides with basicity of added general-base are investigated and compared with the reactivity of *p*-nitrophenyl ethanoate. The effect of hydrophobicity on the reactivity is discussed briefly. Self-aggregation of hydrotropes and the effect of self-aggregation of added cosolutes on the rate-retardation of the hydrolysis of activated amides is discussed in Chapter 4. An attempt is made to explain the solubilising potential of compounds of which the hydrophobic group is not large enough to induce cooperative association by itself. The nature of the micellar Stern region as a reaction medium is studied in Chapter 5. Model solutions for the micellar Stern region are constructed and their use in the understanding of micellar rate effects is discussed. Chapter 6 describes the kinetics of hydrolysis of an activated amide around the temperature of maximum density of water. Rate constants around the temperature of maximum density are used to calculate isochoric activation parameters. The usefulness of isochoric activation parameters is discussed.

1.5 ACKNOWLEDGEMENT

Dr. Sijbren Otto and Theo Rispens are most gratefully acknowledged for many enlightening discussions on many aspects of hydrophobicity.

1.6 REFERENCES AND NOTES

(1) The word "water" in this thesis indicates water in its liquid phase under standard pressure or the molecule water. We trust no confusion will result from this.

(2) For a survey of many aspects of water, see reference 3.

(3) Ball, P. "H_2O A Biography of Water" Phoenix, London, **2000**.

(4) Fischer, S., Verma, C. S. and Hubbard, R. E. *J. Phys. Chem. B* **1998**, *102*, 1797-1805.

(5) Chaplin, M. F. *Biochem. Mol. Biol. Edu.* **2001**, *29*, 54-59. This author also maintains a detailed description of water structure and behaviour, presently available at http://www.sbu.ac.uk/water/ (keywords "water" "chaplin")

(6) Browne, V., Haq, I., and Hunter, C. A., Personal Communication.

(7) The best example of interactions in water having different strength is provided by ionic interactions. Whereas ions of opposite charge in organic solvents are often not individually solvated as a result of strong electrostatic interactions, in water, often they are since ion-water interactions can compete with electrostatic interactions. However, ion pairing in water can still occur at high concentration and when enforced by other interactions. For an example of ion pairing occurring as a result of the inhibition of hydration of an ionic group by the presence of a nearby hydrophobic group, see Thompson, S. E. and Smithrud, D. B. *J. Am. Chem. Soc.* **2002**, *124*, 442-449.

(8) Liu, L., Yang, C. and Guo, Q. X. *Biophys. Chem.* **2000**, *84*, 239-251.

(9) The properties of water inside the living cell may be entirely different from the properties of bulk water. See, *e.g.*, Mentre, P. *Cell. Mol. Biol.* **2001**, *47*, 709-715, Ball, P. *Cell. Mol. Biol.* **2001**, *47*, 717-720 and Asaad, N., den Otter, M. J., and Engberts, J. B. F. N., personal communication.

(10) van der Wel, G. K., Wijnen, J. W. and Engberts, J. B. F. N. *J. Org. Chem.* **1996**, *61*, 9001-9005.

(11) "Organic Synthesis in Water", (Grieco, P. A., ed.). Blackie, London, **1998**.

(12) A special double issue of Advanced Synthesis & Catalysis (*Adv. Synth. Catal.* **2002**, *344*, issue 3-4) was devoted to chemistry in water.

(13) Lindström, U. M. *Chem. Rev.* **2002**, *102*, 2751-2772.

(14) Lubineau, A., Augé, J. and Queneau, Y. *Synthesis* **1994**, 741-760.

(15) Li, C. *Chem. Rev.* **1993**, *93*, 2023-2035.

(16) Rideout, D. C. and Breslow, R. *J. Am. Chem. Soc.* **1980**, *102*, 7816-7817.

(17) Gajewski, J. J., Jurayj, J., Kimbrough, D. R., Gande, M. E., Ganem, B. and Carpenter, B. K. *J. Am. Chem. Soc.* **1987**, *109*, 1170-1186.

(18) Copley, S. D. and Knowles, J. R. *J. Am. Chem. Soc.* **1987**, *109*, 5008-5013.

(19) The dipole moment in the liquid is not constant with temperature. In addition, as a result of the effect of (cooperative) hydrogen bonding on the dipole moment and the range of hydrogen bonding strengths, the quoted dipole moment is an average, possibly of a rather wide distribution.

(20) Badyal, Y. S., Saboungi, M. L., Price, D. L., Shastri, S. D., Haeffner, D. R. and Soper, A. K. *J. Chem. Phys.* **2000**, *112*, 9206-9208.

(21) The expression "thermodynamic scheme" is used here to describe the splitting of Gibbs energies, enthalpies and entropies into different contributions.

(22) See, for example, reference 68.

(23) Ben-Naim, A. and Mazo, R. *J. Phys. Chem. B* **1997**, *101*, 11221-11225.

(24) Blokzijl, W. and Engberts, J. B. F. N. *Angew. Chem. , Int. Ed. Engl.* **1993**, *32*, 1545-1579.

(25) Hvidt, A. and Westh, P. *J. Solution Chem.* **1998**, *27*, 395-402.

(26) Lazaridis, T. *Acc. Chem. Res.* **2001**, *34*, 931-937.

(27) Ruelle, P. *J. Phys. Org. Chem.* **1999**, *12*, 769-786.

(28) Southall, N. T., Dill, K. A. and Haymet, A. D. J. *J. Phys. Chem. B* **2002**, *106*, 521-533.

(29) "Water: A Comprehensive Treatise", Vol. 1-7, (Franks, F., ed.). Plenum, New York, **1972-1982**.

(30) Head-Gordon, T. and Hura, G. *Chem. Rev.* **2002**, *102*, 2651-2670.

(31) Sorenson, J. M., Hura, G., Glaeser, R. M. and Head-Gordon, T. *J. Chem. Phys.* **2000**, *113*, 9149-9161.

(32) Okhulkov, A. V., Demianets, Y. N. and Gorbaty, Y. E. *J. Chem. Phys.* **1994**, *100*, 1578-1588.

(33) In this case, X-ray absorption spectroscopy measures the excitation from the oxygen 1s orbital into the antibonding O-H 4a1 and 2b1 molecular orbitals. The characteristics of these antibonding orbitals strongly depend on the electronic structure of the molecule.

(34) Myneni, S., Luo, Y., Naslund, L. A., Cavalleri, M., Ojamae, L., Ogasawara, H., Pelmenschikov, A., Wernet, P., Vaterlein, P., Heske, C., Hussain, Z., Pettersson, L. G. M. and Nilsson, A. *J. Phys. : Condens. Matter* **2002**, *14*, L213-L219.

(35) Keutsch, F. N. and Saykally, R. J. *Proc. Natl. Acad. Sci. U. S. A.* **2001**, *98*, 10533-10540.

(36) Bakker, H. J., Woutersen, S. and Nienhuys, H. K. *Chem. Phys.* **2000**, *258*, 233-245.

(37) Bakker, H. J. and Nienhuys, H. K. *Science* **2002**, *297*, 587-590.

(38) Šašic (reference 39) defined "non-hydrogen-bonded" as "species of which the hydrogen bonds are stretched or bent but not literally broken". Related to this, Agmon (Agmon, N. *J. Phys. Chem.* **1996**, *100*, 1072-1080) calculated that a "broken hydrogen bond" is still energetically favourable compared to the total loss of

interactions as it occurs on vapourisation. He further claimed the following about broken hydrogen bonds: "An additional enthalpy of about 2.7 kcal/mol [11.3 kJ/mol] should then be ascribed to isotropic electrostatic interactions with the remaining "bulk" water molecules. Loosely speaking, these are "rotational" and "translational" components of the hydrogen bond."

(39) Sasic, S., Segtnan, V. H. and Ozaki, Y. *J. Phys. Chem. A* **2002**, *106*, 760-766.

(40) Walrafen, G. E., Fisher, M. R., Hokmabadi, M. S. and Yang, W.-H. *J. Chem. Phys.* **1986**, *85*, 6970-6982.

(41) Muller, N. *J. Chem. Phys.* **1965**, *43*, 2555-2556.

(42) Muller, N. *Acc. Chem. Res.* **1990**, *23*, 23-28.

(43) Hare, D. E. and Sorensen, C. M. *J. Chem. Phys.* **1990**, *93*, 6954-6961.

(44) Silverstein, K. A. T., Haymet, A. D. J. and Dill, K. A. *J. Am. Chem. Soc.* **2000**, *122*, 8037-8041.

(45) Combining heat capacity, spectra, density, and other properties, Dougherty *et al.* (Dougherty, R. C. and Howard, L. N. *J. Chem. Phys.* **1998**, *109*, 7379-7393) developed an equilibrium structural model for liquid water which uses four structural components (tetrahedral, pentagonal, ''planar''-hexagonal and square water molecules) to describe water from the extrapolated-homogeneous nucleation temperature of 221 K up to the temperature of the maximum dissociation constant for water, 513K. Structural components are monomeric water molecules that are part of a random structural network. These structural components form the local definition of the structure.

(46) Luzar, A. *Farad. Discuss.* **1996**, *103*, 105.

(47) Pure *ab initio* methods normally use the "supermolecule" approach in which the whole system is optimised using "supermolecular orbitals". The advantage of this approach is that it provides accurate answers for the total energy. The disadvantages are that the interaction terms are determined by subtraction of large numbers (the total energy minus the energy of the individual molecules), making the final answer rather sensitive to small errors and the fact that dynamics is not included. Still, the method is successfully used for the determination of intermolecular potentials.

(48) The Car-Parrinello method uses the local density approximation in a DFT calculation.

(49) Silvestrelli, P. L. and Parrinello, M. *J. Chem. Phys.* **1999**, *111*, 3572-3580.

(50) Classical models describe interactions between (water) molecules in a non-quantum chemical way. These models typically employ Lennard-Jones potentials and fixed charges.

(51) Soper, A. K. *Mol. Phys.* **2001**, *99*, 1503-1516.

(52) CF1 or CFM (central force model) treats water as a mixture of oxygen and hydrogen species that interact with each other through central potentials. In the TIP4P

(Transferable Intermolecular Potential 4 Point) model, water is parameterised as 4 point charges. SPC/E (Simple Point Charge / Extended) uses 3 charges, the extended SPC/E model is an effective pair potential to which a polarisation energy correction must be applied. The Mercedes Benz model is the most surprising of these models as it describes water using a 2-dimensional parameterisation; *viz.* as "two-dimensional Lennard-Jones disks, with three orientation-dependent hydrogen-bonding arms arranged as in the Mercedes Benz (MB) logo" (see reference 53). The advantage of this model lies in the fact that phase space can be explored (using NPT Monte-Carlo simulations) more effectively resulting in better convergence of the results. The MB model, despite its two-dimensionality, predicts the experimental trends with temperature of the Gibbs energy, entropy, enthalpy, molar volume, and heat capacity correctly (see reference 53).

(53) Silverstein, K. A. T., Haymet, A. D. J. and Dill, K. A. *J. Am. Chem. Soc.* **1998**, *120*, 3166-3175.

(54) Chen, B., Xing, J. H. and Siepmann, J. I. *J. Phys. Chem. B* **2000**, *104*, 2391-2401.

(55) Guillot, B. and Guissani, Y. *J. Chem. Phys.* **2001**, *114*, 6720-6733.

(56) Balucani, U., Brodholt, J. P., Jedlovszky, P. and Vallauri, R. *Phys. Rev. E* **2000**, *62*, 2971-2973.

(57) Chialvo, A. A., Yezdimer, E., Driesner, T., Cummings, P. T. and Simonson, J. M. *Chem. Phys.* **2000**, *258*, 109-120.

(58) Delle Site, L., Lynden-Bell, R. M. and Alavi, A. *J. Mol. Liq.* **2002**, *98-9*, 79-86.

(59) Mahoney, M. W. and Jorgensen, W. L. *J. Chem. Phys.* **2001**, *115*, 10758-10768.

(60) Nymand, T. M., Linse, P. and Astrand, P. O. *Mol. Phys.* **2001**, *99*, 335-348.

(61) Interstitial water (or the "fifth neighbouring molecule") accounts for the different rotational relaxation times in water (Yeh, Y. K. and Mou, C. Y. *J. Phys. Chem. B* **1999**, *103*, 3699-3705). The reorientational relaxation time is related to hydrogen-bond strength (reference 36) and hydrogen-bond breaking is related to librational motion (reference 35). Hence, one might conclude that the interstitional water molecule changes the local potential in such a way that the librational potential is less steep.

(62) Reiss, H. *Adv. Chem. Phys.* **1966**, *9*, 1-84.

(63) Lazaridis (reference 26) uses the term "lipophobic" for water instead of hydrophobic for the solute (referring to Hildebrand, J.H. *J. Phys. Chem.*, **1968**, *72*, 1841-1842) indicating that water "is afraid of [interacting with] apolar solutes" whereas the apolar solute is not "afraid of water".

(64) The directional sensitivity of the strong intermolecular interactions of water probably cause the exceptionally high solubility of apolar solutes. A liquid with strong isotropic interactions could well be more "lipophobic" than water as breaking of

strong interactions would be unavoidable upon dissolution of apolar solutes (see reference 26 and relevant references therein).

(65) Ben-Naim standard conditions for the determination of solvation parameters imply transfer between an ideal gas phase and a liquid. In both the ideal gas phase and the liquid, the number density (or molarity) of the solute is the same. See Ben-Naim, A. "Solvation Thermodynamics" Plenum, New York, **1987**.

(66) Makhatadze, G. I. and Privalov, P. L. *Biophys. Chem.* **1994**, *50*, 285-291.

(67) Graziano, G. and Lee, B. *J. Phys. Chem. B* **2001**, *105*, 10367-10372.

(68) Costas, M. and Kronberg, B. *Biophys. Chem.* **1998**, *74*, 83-87.

(69) Kodaka, M. *J. Phys. Chem. B* **2001**, *105*, 5592-5594.

(70) Graziano, G. *J. Phys. Chem. B* **2002**, *106*, 7713-7716.

(71) Kodaka, M. *J. Phys. Chem. B* **2002**, *106*, 7717.

(72) Bowron, D. T., Filipponi, A., Lobban, C. and Finney, J. L. *Chem. Phys. Lett.* **1998**, *293*, 33-37.

(73) Finney, J. L. and Soper, A. K. *Chem. Soc. Rev.* **1994**, *23*, 1-10.

(74) DeMaeyer, L., Trachimow, C. and Kaatze, U. *J. Phys. Chem. B* **1998**, *102*, 8480-8491.

(75) Yoshida, K., Ibuki, K. and Ueno, M. *J. Chem. Phys.* **1998**, *108*, 1360-1367.

(76) Lee, B. *Biophys. Chem.* **1994**, *51*, 271-278.

(77) Graziano, G. and Barone, G. *J. Am. Chem. Soc.* **1996**, *118*, 1831-1835.

(78) Lee, B. and Graziano, G. *J. Am. Chem. Soc.* **1996**, *118*, 5163-5168.

(79) Graziano, G. *J. Chem. Soc. , Faraday Trans.* **1998**, *94*, 3345-3352.

(80) Du, Q., Freysz, E. and Shen, Y. R. *Science* **1994**, *264*, 826-828.

(81) Du, Q., Superfine, R., Freysz, E. and Shen, Y. R. *Phys. Rev. Lett.* **1993**, *70*, 2313-2316.

(82) This difference in structure of water hydrating large apolar solutes and bulk water could well be the cause of surface charging effects observed for dispersions of uncharged compounds in water (Marinova, K. G., Alargova, R. G., Denkov, N. D., Velev, O. D., Petsev, D. N., Ivanov, I. B. and Borwankar, R. P. *Langmuir* **1996**, *12*, 2045-2051) by, for example, stabilising hydroxide ions compared to bulk solution.

(83) The computational method refers to the way water is modelled. For example, a treatment in which only the solute is treated in an *ab initio* fashion, the solvent is treated as a polarisable continuum (PCM) and the cavity term is obtained from SPT (an approach described in *Phys. Chem. Chem. Phys.*, **2001**, *3*, 4001-4009) is not considered an *ab initio* method in the present Chapter.

(84) Cheng, Y. K. and Rossky, P. J. *Nature* **1998**, *392*, 696-699.

(85) Guillot, B., Guissani, Y. and Bratos, S. *J. Chem. Phys.* **1991**, *95*, 3643-3648.

(86) Chau, P. L., Forester, T. R. and Smith, W. *Mol. Phys.* **1996**, *89*, 1033-1055.

(87) Southall, N. T. and Dill, K. A. *J. Phys. Chem. B* **2000**, *104*, 1326-1331.

(88) Bagno, A. *J. Chem. Soc. , Faraday Trans.* **1998**, *94*, 2501-2504.

(89) Hodges, M. P., Wheatley, R. J. and Harvey, A. H. *J. Chem. Phys.* **2002**, *117*, 7169-7179.

(90) Silverstein, K. A. T., Dill, K. A. and Haymet, A. D. J. *J. Chem. Phys.* **2001**, *114*, 6303-6314.

(91) Delle Site, L. *Mol. Simul.* **2001**, *26*, 353-365.

(92) Xu, H. F., Stern, H. A. and Berne, B. J. *J. Phys. Chem. B* **2002**, *106*, 2054-2060.

(93) Besseling, N. A. M. and Lyklema, J. *J. Phys. Chem. B* **1997**, *101*, 7604-7611.

(94) Sharp, K. A. and Madan, B. *J. Phys. Chem. B* **1997**, *101*, 4343-4348.

(95) Wiggins, P. M. *Physica A* **1997**, *238*, 113-128.

(96) Silverstein, K. A. T., Haymet, A. D. J. and Dill, K. A. *J. Chem. Phys.* **1999**, *111*, 8000-8009.

(97) Ikeguchi, M., Shimizu, S., Nakamura, S. and Shimizu, K. *J. Phys. Chem. B* **1998**, *102*, 5891-5898.

(98) Lazaridis, T. *J. Phys. Chem. B* **2000**, *104*, 4964-4979.

(99) Arthur, J. W. and Haymet, A. D. J. *J. Chem. Phys.* **1998**, *109*, 7991-8002.

(100) Scatena, L. F., Brown, M. G. and Richmond, G. L. *Science* **2001**, *292*, 908-912.

(101) Vlcek, L. and Nezbeda, I. *Phys. Chem. Chem. Phys.* **2002**, *4*, 3704-3711.

(102) Chau, P. L. *Mol. Phys.* **2001**, *99*, 1289-1298.

(103) Kauzmann, W. *Nature* **1987**, *325*, 763-764.

(104) Ben-Naim, A. *Biopolymers* **1990**, *29*, 567-596.

(105) Ben-Naim, A. *J. Chem. Phys.* **1989**, *90*, 7412-7425.

(106) Graziano, G., Catanzano, F., Riccio, A. and Barone, G. *J. Biochem. (Tokyo)* **1997**, *122*, 395-401.

(107) Mochizuki, S., Usui, Y. and Wakisaka, A. *J. Chem. Soc. , Faraday Trans.* **1998**, *94*, 547-552.

(108) Bagno, A., Scorrano, G. and Stiz, S. *J. Am. Chem. Soc.* **1997**, *119* , 2299-2300.

(109) Bagno, A., Campulla, M., Pirana, M., Scorrano, G. and Stiz, S. *Chem. Eur. J.* **1999**, *5*, 1291-1300.

(110) Capparelli, A. L., Hertz, H. G. and Tutsch, R. *J. Phys. Chem.* **1978**, *82*, 2023-2029.

(111) Incomprehensible aggregation upon dilution has been observed for a variety of compounds and is discussed in: Samal, S. and Geckeler, K. E. *Chem. Commun.* **2001**, 2224-2225. A recent study, however, failed to find comparable results: Hallwass, F., Engelsberg, M. and Simas, A.M. *Chem. Commun.* **2002**, 2530-2531.

(112) Sacco, A., Asciolla, A., Matteoli, E. and Holz, M. *J. Chem. Soc. , Faraday Trans.* **1996**, *92*, 35-40.

(113) Sacco, A. and Holz, M. *J. Chem. Soc. , Faraday Trans.* **1997**, *93*, 1101-1104.

(114) Sacco, A., DeCillis, F. M. and Holz, M. *J. Chem. Soc. , Faraday Trans.* **1998**, *94*, 2089-2092.

(115) Mayele, M., Holz, M. and Sacco, A. *Phys. Chem. Chem. Phys.* **1999**, *1*, 4615-4618.
(116) Mayele, M. and Holz, M. *Phys. Chem. Chem. Phys.* **2000**, *2*, 2429-2434.
(117) Kirkwood, J. G. and Buff, F. P. *J. Chem. Phys.* **1951**, *19*, 774-777.
(118) Newman, K. E. *Chem. Soc. Rev.* **1994**, *1994*, 31-40.
(119) Ben-Naim, A. *J. Chem. Phys.* **1977**, *67*, 4884-4890.
(120) Shulgin, I. and Ruckenstein, E. *J. Phys. Chem. B* **1999**, *103*, 872-877.
(121) Shulgin, I. and Ruckenstein, E. *J. Phys. Chem. B* **1999**, *103*, 2496-2503.
(122) Castronuovo, G., Elia, V., Moniello, V., Velleca, F. and Perez, C. S. *Phys. Chem. Chem. Phys.* **1999**, *1*, 1887-1892.
(123) Castronuovo, G., Elia, V. and Velleca, F. *J. Solution Chem.* **1996**, *25*, 971-982.
(124) Ansell, S., Cser, L., Grosz, T., Jancso, G., Jovari, P. and Soper, A. K. *Physica B* **1997**, *234*, 347-348.
(125) Finney, J. L., Bowron, D. T. and Soper, A. K. *J. Phys. : Condens. Matter* **2000**, *12*, A123-A128.
(126) Bowron, D. T., Finney, J. L. and Soper, A. K. *J. Phys. Chem. B* **1998**, *102*, 3551-3563.
(127) Yoshida, K. and Yamaguchi, T. *Z. Naturforsch. , A: Phys. Sci.* **2001**, *56*, 529-536.
(128) Tanaka, S. H., Yoshihara, H. I., Ho, A. W. C., Lau, F. W., Westh, P. and Koga, Y. *Can. J. Chem.* **1996**, *74*, 713-721.
(129) Koga, Y., Siu, W. W. Y. and Wong, T. Y. H. *J. Phys. Chem.* **1990**, *94*, 7700-7706.
(130) Martinez, N., Junquera, E. and Aicart, E. *Phys. Chem. Chem. Phys.* **1999**, *1*, 4811-4817.
(131) Piatnitski, E. L., Flowers, R. A. and Deshayes, K. *Chem. Eur. J.* **2000**, *6*, 999-1006.
(132) Smithrud, D. B., Sanford, E. M., Chao, I., Ferguson, S. B., Carcanague, D. R., Evanseck, J. D., Houk, K. N. and Diederich, F. *Pure Appl. Chem.* **1990**, *62*, 2227-2236.
(133) Smith, D. E., Zhang, L. and Haymet, A. D. J. *J. Am. Chem. Soc.* **1992**, *114*, 5875-5876.
(134) Mancera, R. L., Buckingham, A. D. and Skipper, N. T. *J. Chem. Soc. , Faraday Trans.* **1997** , *93*, 2263-2267.
(135) Rick, S. W. and Berne, B. J. *J. Phys. Chem. B* **1997**, *101*, 10488-10493.
(136) Ghosh, T., Garcia, A. E. and Garde, S. *J. Am. Chem. Soc.* **2001**, *123*, 10997-11003.
(137) Ghosh, T., Garcia, A. E. and Garde, S. *J. Chem. Phys.* **2002**, *116*, 2480-2486.
(138) Rick, S. W. *J. Phys. Chem. B* **2000**, *104*, 6884-6888.
(139) Otto, S. and Engberts, J. B. F. N. *J. Am. Chem. Soc.* **1999**, *121*, 6798-6806.
(140) Fife, T. H. and McMahon, D. M. *J. Am. Chem. Soc.* **1969**, *91*, 7481-7485.
(141) Karzijn, W. and Engberts, J. B. F. N. *Tetrahedron Lett.* **1978**, 1787-1790.
(142) Engbersen, J. F. J. and Engberts, J. B. F. N. *J. Am. Chem. Soc.* **1975**, *97*, 1563-1568.

(143) Lensink, M. F., Mavri, J. and Berendsen, H. J. C. *J. Comput. Chem.* **1999**, *20*, 886-895.

(144) Note that the activated complex is rather peculiar in the present case, as it incorporates an imaginary wavefunction corresponding to the tunnelling proton.

(145) Intriguingly, the hydrolysis reactions under study here provide a nice example of Marcus Theory (Marcus, R.A. *J. Phys. Chem.* **1968**, *72*, 891-899). The proton tunnelling in the activated complex will only occur provided an 'active configuration' has been preformed (reference 143). The formation of the active configuration is thereby identified as the work function, whereas the proton tunnelling is the intrinsic barrier. Hydrophobic interactions can change the work function by interacting differently with inactive and active configurations (reference 146).

(146) Rispens, T., Lensink, M.F., Berendsen, H.J.C. and Engberts, J.B.F.N., submitted for publication.

(147) Blokzijl, W., Engberts, J. B. F. N. and Blandamer, M. J. *J. Phys. Chem.* **1987**, *91*, 6022-6027.

(148) Blandamer, M. J., Burgess, J., Engberts, J. B. F. N. and Blokzijl, W. *Annu. Rep. R. Soc. Chem. ,Sect. C* **1990**, 45-74.

(149) Garrod, J. E. and Herrington, T. M. *J. Phys. Chem.* **1969**, *73*, 1877-1884.

(150) Perron, G. and Desnoyers, J. E. *J. Chem. Thermodyn.* **1981**, *13*, 1105-1121.

(151) Eyring, H. *J. Chem. Phys.* **1935**, *3*, 107-115.

(152) Blokzijl, W., Engberts, J. B. F. N. and Blandamer, M. J. *J. Chem. Soc. , Perkin Trans. 2* **1994**, 455-458.

(153) Bietti, M., Baciocchi, E. and Engberts, J. B. F. N. *Chem. Commun.* **1996**, 1307-1308.

(154) Blandamer, M. J., Burgess, J., Cowles, H. J., De Young, A. J., Engberts, J. B. F. N., Galema, S. A., Hill, S. J. and Horn, I. M. *J. Chem. Soc. , Chem. Commun.* **1988**, 1141-1142.

(155) Savage, J. J. and Wood, R. H. *J. Solution Chem.* **1976**, *5*, 733-750.

(156) Buwalda, R. T., *Molecular Aggregation in Water. The Interplay of Hydrophobic and Electrostatic Interactions.*, PhD Thesis, University of Groningen, **2001**. Available online: http://www.ub.rug.nl/eldoc/dis/science/r.t.buwalda/

(157) Israelachvili, J. N., Mitchell, D. J. and Ninham, B. W. *J. Chem. Soc. , Faraday Trans. 2* **1976**, 1525-1568.

Kinetic evidence for hydrophobically-stabilised encounter complexes formed by hydrophobic esters and amides in aqueous solutions containing monohydric alcohols[1]

*The pH-independent hydrolyses of four activated esters, p-methoxyphenyl 2,2-dichloroethanoate (**2.1a**), p-methoxyphenyl 2,2-dichloropropanoate (**2.1b**), p-methoxyphenyl 2,2-dichlorobutanoate (**2.1c**) and p-methoxyphenyl 2,2-dichloropentanoate (**2.1d**), and two activated amides, 1-(4-methylbenzoyl)-1,2,4-triazole (**2.2a**) and 1-(4-n-butylbenzoyl)-1,2,4-triazole (**2.2b**), in dilute aqueous solution have been studied as a function of the molality of added cosolutes ethanol, 1-propanol and 1-butanol. Rate constants for the neutral hydrolysis decrease with increasing cosolute molality. These kinetic medium effects respond to both the hydrophobicity of the ester and of the monohydric alcohol. The observed rate effects are analysed using both a thermodynamic and a kinetic model. According to the kinetic model a hydrophobically-stabilised encounter complex is formed with equilibrium constants K_{ec} often smaller than unity, in which the cosolute blocks the reaction center of the hydrolytic ester or amide from attack by water. Formation of these encounter complexes leads to a dominant initial-state stabilisation as described by the thermodynamic model set out in Chapter 1. Decreases in both apparent enthalpies and entropies of activation for these hydrolysis reactions correspond to unfavourable enthalpies and favourable entropies of complexation, which confirms that the encounter complexes are stabilised by hydrophobic interactions*

2.1 INTRODUCTION

2.1.1 THERMODYNAMIC ANALYSIS OF 1:1 HYDROPHOBIC INTERACTIONS

Weak hydrophobic interactions between reacting molecules and inert added cosolutes in aqueous solutions have been investigated for over a decade using the thermodynamic analysis presented in Chapter 1.

As mentioned in Chapter 1, previous studies[2] showed that hydrolysis of activated esters structurally similar to **2.1a-d**, but also of similar activated amides structurally similar to **2.2a,b**[3] is retarded by many hydrophobic cosolutes, except α-amino acids. In the past, a variety of cosolutes has been examined in combination with several hydrolytic probes. An overview of previous studies is given in Table 2.1.

Table 2.1: Kinetic solvent effect studies on the hydrolysis of activated amides and activated esters in dilute aqueous media, which have been analysed using Equation 1.9, excluding studies in this thesis.

Cosolute	References	
	Amides	Esters
mono-, di- and polyhydric alcohols	4,5	
(alkyl substituted) urea(s)	6	6,7
carboxamides	8	8,9
sulfonamides/sulfones/sulfoxides	6	6,10
carbohydrates	8,9	
N-alkyl-2-pyrrolidinones	11	11
sodium alkylsulfates	12	
N-alkylated ammonium bromides	13	
α-amino acids	14,15	

Rate retardations caused by added cosolutes often follow an additivity scheme[16] in which each methylene unit or functional group makes a common contribution to $G(c)$, the SWAG-approach (Savage-Wood additivity of group interactions).[17] The observed changes in standard Gibbs energy of activation were found to be mainly caused by a stabilisation of the initial state by hydrophobic interactions.[18] Hence, $G(c)$ has been interpreted in terms of stabilisation of the initial state by (hydrophobic) interactions with added cosolutes.

In the analysis of previously reported kinetic data for this class of system, emphasis was placed mainly on varying the structure of the cosolute (see Table 2.1) and in particular on varying the hydrophobicity of the cosolutes.[2]

2.1.2 TOWARDS A COMBINED THERMODYNAMIC AND MOLECULAR MODEL

In the present study, both the hydrophobicity of cosolute molecules and of reacting esters or amides were varied (Scheme 2.1).

2.1 a R=H, **b** R=Me, **c** R=Et, **d** R=n-Pr

2.2 a R=Me, **b** R=n-Bu

Scheme 2.1

The activated esters and amides hydrolyse according to the mechanism described in Chapter 1. Results of the analysis based on both a thermodynamic analysis and a molecular model using Equations 1.9 and 2.1, respectively, are reported.[19] Furthermore, isobaric activation enthalpies and entropies for hydrolysis of **2.1c** in the presence of hydrophobic cosolutes were determined in order to obtain more information on the thermodynamics of encounter complex formation (*vide infra*) and to understand the relationship between the thermodynamic description and the molecular picture of rate inhibition. We show that both approaches account for the kinetic data.

2.1.3 ANALYSIS OF KINETIC SOLVENT EFFECTS IN TERMS OF ENCOUNTER COMPLEX FORMATION

The severe orientational requirements on water molecules in the activated complex as described in Chapter 1 prompt the idea of formation of an encounter complex between ester or amide and added solute, in which the cosolute blocks the reaction center from attack by water.[20] Such a model, assuming that the encounter complex is inert, is strongly supported by computer simulations[21,22] of the hydrolysis reaction described in Chapter 1.

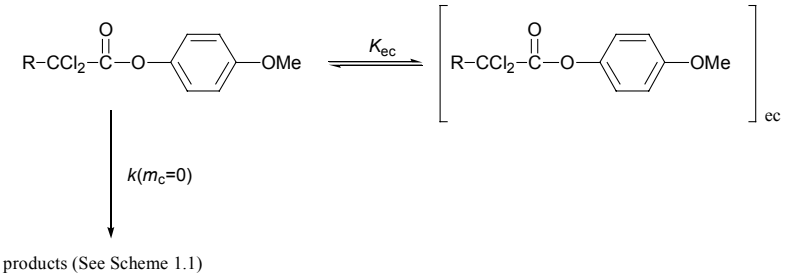

Scheme 2.2

A kinetic scheme based on this molecular picture (Scheme 2.2) emerges in which ester molecules that are not solvated by cosolute molecules react with a rate constant $k(m_c=0)$. Since a kinetically observable hydrophobic interaction with cosolute occurs close to the reaction center, the critical orientation of the water molecules for attack at the ester carbonyl group is disturbed and hydrolysis is (largely) inhibited. The hydrolysis rate constant for ester in an encounter complex is therefore assumed to be zero, leading to the following expression for the observed rate constant (Equation 2.1)

$$k(m_c) = \frac{k(m_c = 0)}{1 + K_{ec} \cdot m_c} \tag{2.1}$$

Here K_{ec} is the equilibrium constant for encounter complex formation in kg mole^{-1}, m_c the molality of added cosolute, $k(m_c)$ the observed (pseudo-) first-order rate constant in an m_c molal solution.

The rate constant of hydrolysis in the encounter complex is assumed to be zero, as the largest rate effect will be caused by the direct blocking of the reaction center from attack by water. The influence of encounter complexes in which the cosolute molecule does not directly block attack by water will be more complex, possibly only partially inhibiting reaction. However, incorporating this further complexity in Equation 2.1 is not warranted, as the number of data points does not permit the introduction of more variables (*vide infra*).

Two examples of encounter complexes expected to show more complex behaviour deserve discussion. If the cosolute molecule binds to the hydrolytic probe far (relative to the size of the cosolute molecule) from the reaction centre, it will not block attack by water. Obviously, the rate of hydrolysis in these encounter complexes cannot be assumed to be zero and these encounter complexes will not be observed as a consequence of the absence of a rate effect (*vide infra*). In addition, the effect of cosolutes binding on the side of the carbonyl opposite that on which a water molecule is attacking, is unclear from this molecular picture. Because of the induced change in solvation shell around the amide group, it may have a rate effect. Consequently, the equilibrium constant for encounter complex formation is a minimum value. In the case of a small hydrolytic probe, however, it is expected that essentially all encounter complexes will inhibit reaction as binding can only take place close to the reaction center.

The assumptions described above are summarised in Figure 2.1.

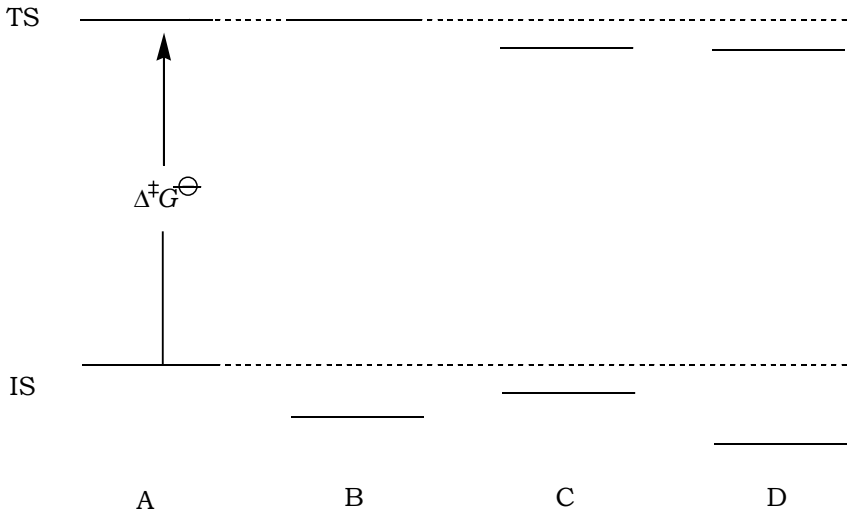

Figure 2.1: The chemical potential of the reactant and activated complex as influenced by the cosolute. For a discussion of the different possible effects of encounter complex formation (A-D), see page 39.

In Figure 2.1, the chemical potential of the hydrolytic probe in "different solutions" is sketched. On the left hand side of the figure (A), the Gibbs energy of activation of the hydrolysis reaction in water without added cosolute is depicted. The Gibbs energy of activation of the hydrolysis reaction in the presence of 1 mol kg^{-1} of a cosolute binding close to the reactive centre is shown (B). The weak interaction between hydrolytic probe and cosolute (equilibrium constants up to 1.21 kg mol^{-1}, *vide infra*) leads to a lowering of the chemical potential of the hydrolytic probe. The activated complex cannot form an encounter complex as the water molecules involved in the activated complex cannot be removed without destroying the activated complex. In other words, the activated complex has lost its hydrophobicity.

The third, hypothetical, case would occur if a cosolute molecule interacts only far away from the reactive centre. In this case, both reactant state and transition state are lowered, both to exactly the same extent (C). The right hand side of Figure 2.1 (D) depicts the situation in which binding to the hydrolytic probe is possible both close to and remote from the reaction centre. In this case, both the initial and the transition state will be stabilised, but the effect is larger for the initial state, leading to a decrease in the rate of reaction.

It will be clear from the above that there exists a strong link between the molecular picture and the thermodynamic model. This includes the "kinetic invisibility" of encounter complexes involving cosolutes complexing far from the reaction center as, typically, the chemical potential of the transition state is

assumed to remain unchanged (*vide supra*). This assumption results in encounters occurring remote from the reaction centre to go unnoticed in the thermodynamical description as well.

2.2. RESULTS AND DISCUSSION

2.2.1 HYDROLYSIS OF HYDROPHOBICALLY MODIFIED ACTIVATED ESTERS AND ACTIVATED AMIDES IN THE ABSENCE OF COSOLUTES

(Pseudo-)first-order rate constants at 298.2K for the hydrolysis of **2.1a-d** and **2.2a,b** in water are summarised in Table 2.2.

Table 2.2: (Pseudo-)first-order rate constants for the water-catalysed hydrolysis of **2.1a-d** and **2.2a,b** in water at 298.2K.

Compound	$10^4 \times k(m_c=0)/s^{-1}$
2.1a	30.9
2.1b	11.7
2.1c	3.06
2.1d	2.73
2.2a	9.44
2.2b	8.99

Increasing hydrophobicity of the alkyl chain in the alkanoate moiety of the ester retards the rate of hydrolysis. Previously, the influence of alkyl groups on the water-catalysed hydrolysis of activated amides was studied using Charton's expanded branching equation.[23,24] The size of the data set in Table 2.2 does not allow a similar analysis. Unfortunately, the data set cannot be expanded due to the severe solubility problems encountered with more hydrophobic esters.

Electronic effects are expected to play only a minor role in the observed rate retardation. Substitution of H by Me in going from **2.1a** to **2.1b** could cause a small rate inhibition resulting from electronic effects on the basis of the Taft substituent parameters σ_i being 0.00 and –0.06, respectively (σ_i for Et equals -0.07).[25]

Apart from the electronic effect, a decrease in reaction rate will also be caused by the increased intramolecular steric hindrance by the alkyl tail. Upon elongation of the alkyl chain, it is increasingly able to fold back towards the reaction centre. This effect is levelling off between **2.1c** and **2.1d**, attributed to the fact that there is

hardly any difference in the ability of the alkyl chain to fold back in the direction of the reaction center. A similar effect was found for 1-acyl-(3-substituted)-1,2,4-triazoles when the alkyl chain of the acyl moiety was elongated or branched at the β-position.[26]

Rates of hydrolysis of the two activated amides **2.2a,b** are almost identical (*i.e.* within 5%). For these probes the alkyl tail was introduced further away from the reaction center. As a result, there is no additional interaction between the alkyl chain and the reaction center introduced upon increasing hydrophobicity. Interpretation of the results of the experiments with added cosolutes is therefore not complicated by this additional interaction.

2.2.2 THE THERMODYNAMIC MODEL

Rate constants for the hydrolysis of the esters **2.1a**-**d** and amides **2.2a-b** decrease upon increasing cosolute molality (*e.g.* Figure 2.2). The decrease in rate constant is more pronounced for the more hydrophobic cosolutes, in accord with previous observations.[2]

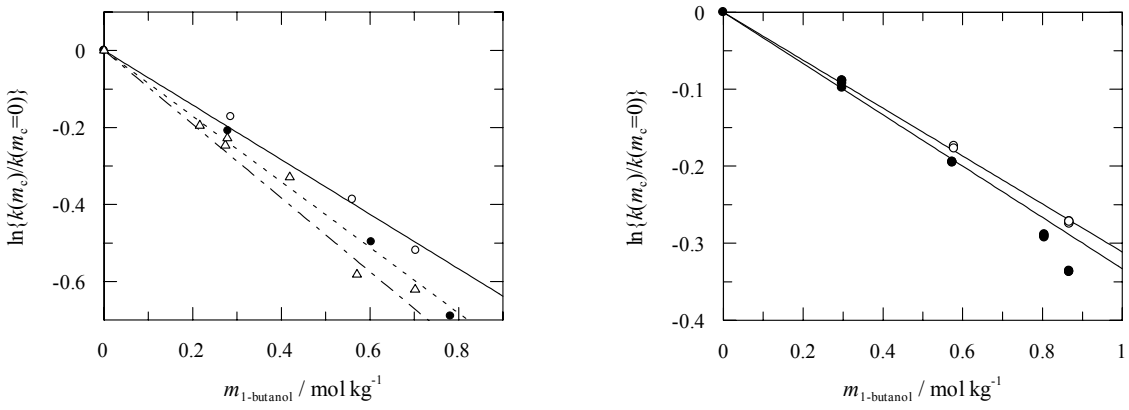

Figure 2.2: *Left:* Hydrolysis of **2.1b** (o), **2.1c** (•) and **2.1d** (Δ) as a function of molality of 1-butanol. *Right:* Hydrolysis of **2.2a** (o) and **2.2b** (•) as a function of molality of 1-butanol. The lines are the best fits using Equation 1.9. In the fit for **2.2b**, only data for molalities up to 0.57 mol kg^{-1} have been used.

Analysis of the kinetic data using Equation 1.9, as described in Chapter 1, yields the *G*(c)-values summarised in Table 2.3.

Table 2.3: *G*(c)-values for the hydrolysis of esters **2.1a-d** and amides **2.2a,b** in aqueous solution at 298.2 K in the presence of short-chain alcohols.[a]

Ester	Cosolute		
	EtOH	*n*-PrOH	*n*-BuOH
	G(c) / J kg mol^{-2}	*G*(c) / J kg mol^{-2}	*G*(c) / J kg mol^{-2}
2.1a	-304±5	-474±8	-709±10
2.1b	-338±9	-555±22	-833±29
2.1c	-400±4	-592±22	-1044±54
2.1d	-466±22	-634±52	-1213±70
2.2a	n.d.	-210±3	-341±3
2.2b	n.d.	-224±2	-374±10[b]

[(a)] Numbers in brackets are standard errors based on a least-squares fit of the kinetic data using Equation 1.9. [(b)] Data fitted up to 0.57 mol kg^{-1}.

Assuming the (standard) chemical potential of the transition state to be largely unaffected by the cosolute as mentioned before, a negative *G*(c) signifies a lowering of the standard chemical potential of the initial state. *G*(c) decreases upon increasing the hydrophobicity of both added cosolute and ester, indicating increasing stabilisation of the initial state ester.

The results are summarised in Figure 2.3 (Please note that minus *G*(c) is plotted in Figure 2.3).

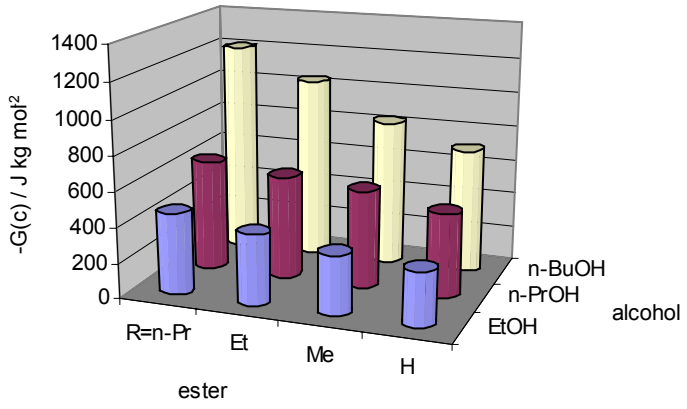

Figure 2.3: Absolute values of *G*(c) in J kg mol^{-2} for different probe-cosolute combinations.

In Figure 2.3, the *x*- and *y*-axes show scales having constant increments for one methylene unit. The *z*-axis records *G*(c)-values which follow an approximate additivity scheme in accord with the SWAG theory, leading to nearly constant decreases in *G*(c) upon lengthening the alkyl moiety in the ester with one methylene unit (*i.e.* stepping either down in Table 2.3, or sideways in Figure 2.3).

For the small range of cosolutes studied, definite conclusions about additivity cannot be drawn. The effects of longer-chain alcohols were not examined because their solubility ranges are small. As was observed for similar hydrolytic probe and cosolute systems, the methylene units closest to the hydrophilic group are partially shielded by the hydrophilic hydration shell of the polar moiety, reducing their hydrophobic effect. Similar shielding effects by nonionic hydrophilic groups have been found by other authors.[27]

The more hydrophobic the ester the more slowly it hydrolyses. It might therefore seem as if the rate retarding effect of the alkyl chain is amplified by the added cosolute. However, from Table 2.3 and Figure 2.3, it is clear that for all three cosolutes, the increments in *G*(c) per methylene unit are constant. This pattern indicates that even when the rate of hydrolysis in the absence of cosolute levels off from decreases by 70% to decreases of only 11%, the effect of the cosolute remains the same. In addition, it is very likely that the origin of the rate retardation changes from an electronic effect (going from **2.1a** to **2.1b**) to a steric effect (upon further elongation of the alkyl chain). It is unlikely that both types of effect will be amplified to the same extent, yet the observed increments remain the same.

In order to verify the conclusion that the rate retardations are solely caused by hydrophobic interactions, the cosolute effects on the hydrolysis reactions of **2.2a** and **2.2b** were studied. Apart from an increased hydrophobicity of **2.2b** compared to **2.2a**, both probes have identical reactivity, rate constants of hydrolysis being equal within 5% (*vide supra*). For these activated amides, there are no differences in intramolecular steric interactions or electronic effects that can be amplified by the cosolute. From Table 2.3, it can be seen that also for these probes the rate retarding effect is dependent on hydrophobicity of both the alcohol and the amide. This pattern clearly shows that hydrophobicity of the hydrolytic probe governs the observed rate retardation. A similar correlation between hydrophobicity of the substrate and the observed rate decrease was found previously for the hydrolysis of 1-acyl-(3-substituted)-1,2,4-triazoles,[26] while a correlation between cosolute-induced rate decrease and reactivity in pure water was not observed.

2.2.3 A MULTIPLICATIVE SCHEME

In order to further investigate the conclusion that hydrophobically-enhanced 1:1 interactions are the origin of the observed rate decreases, the observed *G*(c)-values (Table 2.2) were written as a matrix that can be written as a matrix product (Equation 2.2 is a least squares analysis).

$$\begin{pmatrix} -304 & -474 & -709 \\ -338 & -555 & -833 \\ -400 & -592 & -1044 \\ -466 & -634 & -1213 \end{pmatrix} = -301.1 \cdot \begin{pmatrix} 1 \\ 1.15 \\ 1.34 \\ 1.51 \end{pmatrix} \begin{pmatrix} 1 & 1.50 & 2.49 \end{pmatrix} \tag{2.2}$$

Or, in matrix notation:

$$\mathbf{G}(c) = a \cdot \mathbf{ec} \tag{2.3}$$

Here a is a constant denoting the interaction between *p*-methoxyphenyl 2,2-dichloroethanoate and ethanol. The vectors **e** and **c** identify the increment in interaction upon increasing the hydrophobicity of ester and cosolute, respectively, as a multiplication factor. In this matrix notation, the SWAG theory should lead to constant increments in both **e** and **c**. Indeed, this pattern is effectively followed in **e**, the differences being 0.15, 0.19 and 0.17 (0.17±0.02) indicating that the interactions between probe and cosolute are additive with respect to the probe. However, interactions between probe and cosolute do not seem to be additive with respect to the cosolutes. In this case, additivity is most probably not observed as a result of the small range of cosolutes used.

2.2.4 MOLECULAR DESCRIPTION

In the molecular description leading to Equation 2.1, the observed decrease in rate constant upon increasing the molality of cosolute is accounted for in terms of the formation of an encounter complex by hydrophobic probe and cosolute. Encounter complexes are formed in solution as a result of random movements of molecules and (de)solvation processes. The chances of encounter complex formation increase with increasing size and molality of the solutes. In fact, the formation of encounter complexes is necessary for any bimolecular reaction to occur and the concept of encounter complexes is commonly used in bimolecular photochemical reactions.[28-31] Based on typical sizes of solvents and solutes, equilibrium constants for formation of these randomly formed complexes are commonly estimated to range from

0.2 dm^3 mol^{-1} to values slightly larger than unity.[32] In aqueous solution, encounter complexes formed from apolar components will be stabilised by hydrophobic interactions and the stabilisation will increase with an increased hydrophobicity of the encounter complexes constituents.

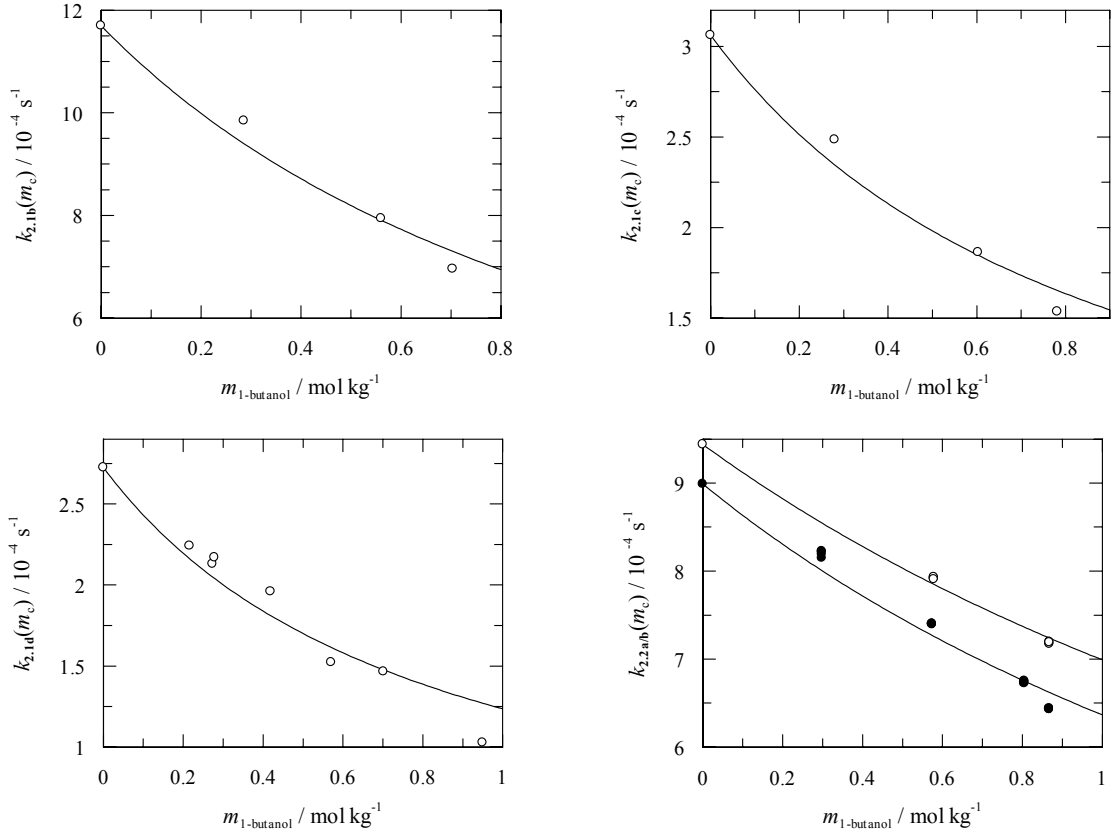

Figure 2.4: Hydrolysis of **2.1b**, **2.1c**, **2.1d**, **2.2a** (o) and **2.2b** (•) as a function of molality of 1-butanol. The lines are the best fits using Equation (2.1).

Non-linear least-squares fitting of the observed rate data to Equation 2.1 results in the equilibrium constants and standard Gibbs energies of encounter complex formation, $\Delta_{ec}G^o$, given in Table 2.4. Typical examples of the fits are shown in Figure 2.4[33]

Table 2.4: Thermodynamic parameters for encounter complex formation of **2.1b-d** and **2.2a,b** in the presence of short-chain alcohols.

ester	Cosolute					
	EtOH		n-PrOH		n-BuOH	
	K_{ec} / kg mol^{-1}	$\Delta_{ec}G^o$ / kJ mol^{-1}	K_{ec} / kg mol^{-1}	$\Delta_{ec}G^o$ / kJ mol^{-1}	K_{ec} / kg mol^{-1}	$\Delta_{ec}G^o$ / kJ mol^{-1}
2.1b	0.34±0.02	2.67±0.15	0.56±0.05	1.44±0.22	0.86±0.07	0.37±0.20
2.1c	0.45±0.02	1.98±0.11	0.64±0.01	1.11±0.08	1.09±0.10	-0.21±0.23
2.1d	0.51±0.03	1.67±0.15	0.71±0.04	0.85±0.14	1.21±0.12	-0.47±0.25
2.2a	n.d.[a]	n.d.[a]	0.24±0.01	3.59±0.11	0.35±0.02	2.60±0.15
2.2b	n.d.[a]	n.d.[a]	0.25±0.01	3.41±0.10	0.41±0.06	2.21±0.36

[(a)] n.d.: not determined

The equilibrium constants for formation of pairwise encounter complexes are in general smaller than unity. The equilibrium constants increase upon increasing the hydrophobicity of the ester and/or the hydrophobic cosolute.

Rewriting $\Delta_{ec}G^o$ in a matrix expression similar to Equation 2.2 leads to Equation 2.4 as determined using a weighted least squares fit.

$$\begin{pmatrix} 2.67 & 1.44 & 0.37 \\ 1.98 & 1.11 & -0.21 \\ 1.67 & 0.85 & -0.47 \end{pmatrix} = 10.0 - 7.5 \begin{pmatrix} 1 \\ 1.07 \\ 1.10 \end{pmatrix} \begin{pmatrix} 1 & 1.11 & 1.28 \end{pmatrix} \tag{2.4}$$

Or, in matrix notation:

$$\Delta_{ec}G^0 = \Delta_{ec}G(\text{noninteract}) - G \cdot \mathbf{G}_{\mathbf{ec}}^{\mathbf{e}} \mathbf{G}_{\mathbf{ec}}^{\mathbf{c}} \tag{2.5}$$

Here, $\Delta_{ec}G$(noninteract) is the unfavourable standard Gibbs energy term associated with bringing ester and cosolute together if there were no favourable interactions between the two. In the present analysis, $\Delta_{ec}G$(noninteract) has been set to 10.0 (RTln(0.018)), corresponding to the chance (based on mole fractions) of finding a cosolute molecule near the reaction center in the cosolute reference state of 1 mol kg^{-1}.[34] $\Delta_{ec}G$(noninteract) was restricted as the size of the data set does not allow independent determination of all variables.[35] G is the favourable interaction between *p*-methoxyphenyl 2,2-dichloropropanoate and ethanol. $\mathbf{G}_{\mathbf{ec}}^{\mathbf{e}}$ and $\mathbf{G}_{\mathbf{ec}}^{\mathbf{c}}$ are vectors describing the relative increments in interaction upon increasing the hydrophobicity of ester and cosolute by subsequent additions of one methylene

unit, respectively. Again, the increment is given as a multiplication by a number >1. The interaction becomes more favourable upon increasing the hydrophobicity of ester and cosolute, in accord with the encounter complex being increasingly stabilised by hydrophobic interactions.

The numbers in Equation 2.5 form the essence of pairwise hydrophobic interactions. They quantify stabilisation of 1:1 interaction complexes in water by hydrophobic effects compared to random interaction in non-aqueous solvents.

2.2.5 MOLECULAR DESCRIPTION – DISTANCE DEPENDENCE

Rate retardations observed for **2.2a,b** in the presence of 1-propanol and 1-butanol show an interesting pattern. The effect of the relatively small 1-propanol molecule is moderate for both **2.2a** and **2.2b**. Increasing the hydrophobicity of the hydrolytic probe to **2.2b** induces a small increase in the observed rate retardation. This pattern can be attributed to the increase in binding mainly occurring remote from the reaction center so that the 1-propanol molecule does not substantially affect the hydration shell around the reaction center. As indicated in Figure 2.1 (*vide supra*), encounter complexes in which the cosolute complexes in a remote position from the reaction center are not expected to inhibit the reaction. These encounter complexes cannot be observed using kinetics alone. They can only be identified using Gibbs energy of transfer studies as they lower the transition state to the same extent as the initial state. With 1-butanol as a cosolute, however, the rate effect on the hydrolysis of **2.2a** is already larger than the rate effect of 1-propanol. In addition, the effect of increasing the hydrophobicity of the hydrolytic probe is larger. There are two causes for this effect. First, 1-butanol will form more stable encounter complexes because of its more hydrophobic nature. Second, the 1-butanol molecule is larger than 1-propanol, meaning that the chances of disturbing the hydration shell around the reaction center are also larger.

2.2.6 ACTIVATION PARAMETERS

Enthalpies and entropies of activation for the hydrolysis of **2.1c** as a function of the molality of ethanol, 1-propanol and 1-butanol are summarised in Figure 2.5.

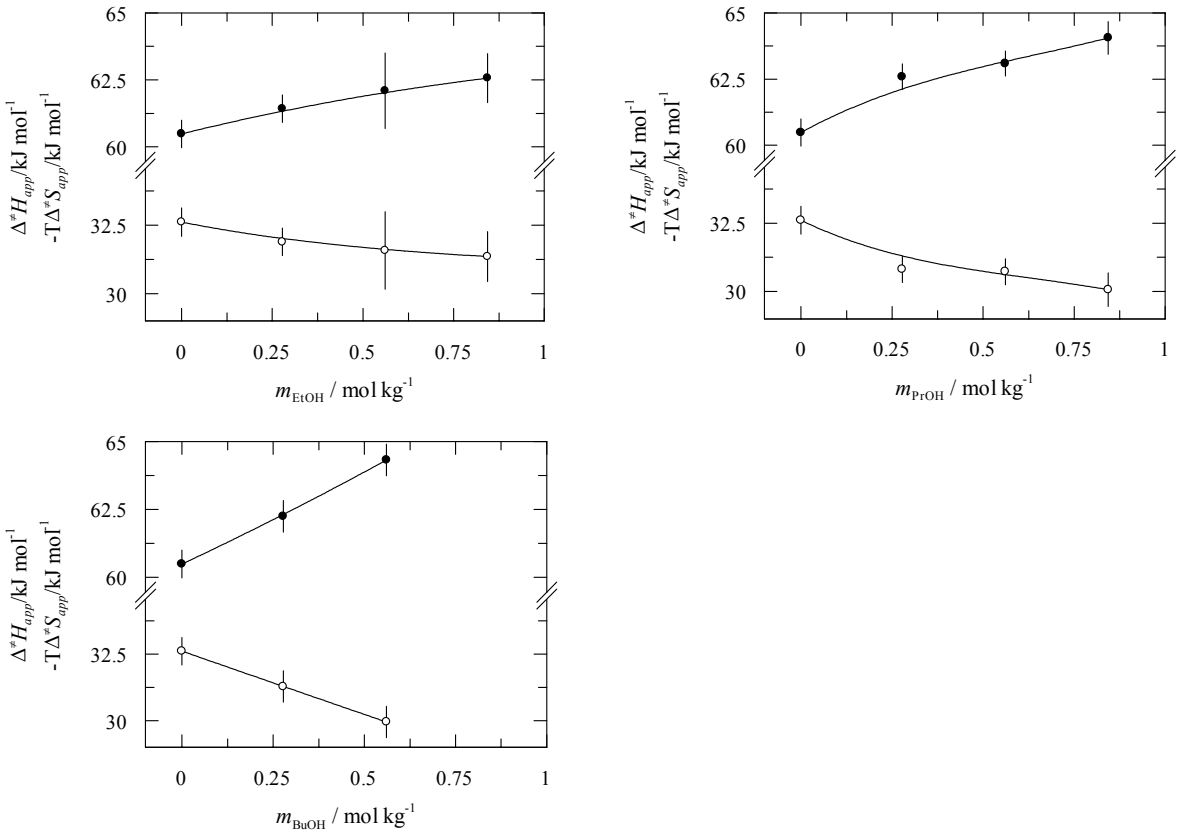

Figure 2.5: Activation parameters, $\Delta^{\neq}H^{o}_{app}$ (o) and -T $\Delta^{\neq}S^{o}_{app}$ (•), at 25°C of the hydrolysis of **2.1c** in the presence of ethanol, 1-propanol and 1-butanol.

Apparent enthalpies of activation $\Delta^{\neq}H^{o}_{app}$ for the hydrolysis reaction according to Scheme 2.2 are given by Equation 2.6.

$$\Delta^{\neq}H^{o}_{app} = \Delta^{\neq}H^{o}_{w} - \frac{K_{ec}\cdot[R'Y]}{1+K_{ec}\cdot[R'Y]}\cdot\Delta_{ec}H^{o} \qquad (2.6)$$

Here, $\Delta_{ec}H^{o}$ is the enthalpy of formation of the encounter complex and $\Delta^{\neq}H_{w}{}^{o}$ is the enthalpy of activation for the hydrolysis reaction in the absence of cosolute.

Using a non-linear least squares analysis based on Equation 2.6 using K_{ec} values obtained from fitting the kinetic data to Equation 2.1, the enthalpies of encounter complex formation were calculated. Using the standard Gibbs energies of encounter complex formation, standard entropies of encounter complex formation were obtained; Table 2.5.

Table 2.5: Thermodynamics of encounter complex formation of **2.1c** with short-chain alcohols.

	$\Delta_{ec}G^{o}$ / kJ mol^{-1}	$\Delta_{ec}H^{o}$ / kJ mol^{-1}	$T\Delta_{ec}S^{o}$ / kJ mol^{-1}
ethanol	1.98±0.11	4.95±0.50	2.97±0.52
1-propanol	1.11±0.08	7.71±0.92	6.60±0.93
1-butanol	-0.21±0.23	6.68±0.82	6.89±0.85

Formation of encounter complexes is enthalpically opposed and entropically favoured, as expected for hydrophobic interactions[36] in which water molecules are liberated from their orientationally restricted positions in the hydration shells of the ester and cosolute.[37] Increasing the hydrophobicity of the cosolute results in a more favourable entropic term, while the changes in the enthalpy are less pronounced. The entropic effect is most pronounced, leading to a lowering of the standard Gibbs energy of encounter complex formation and eventually even to a favourable standard Gibbs energy of encounter complex formation (K_{ec}>1). $\Delta_{ec}G$(noninteract) (Equation 2.5) is purely entropic and $T\Delta_{ec}S^{o}$(noninteract) equals -10.0 kJ mol^{-1} whereas $\Delta_{ec}H^{o}$(noninteract) is zero. Hence, the stabilising effect on encounter complex formation by hydrophobic interactions is brought about by the larger favourable increase in $T\Delta_{ec}S^{o}$ compared to the unfavourable increase in $\Delta_{ec}H^{o}$.

Moreover, from the standard entropy and enthalpy of encounter complex formation, it is anticipated that both the entropy and the enthalpy of the initial state are increased. This, assuming no change in the standard Gibbs energy of the activated complex, is in accord with the observation that with increasing molality of added alcohol, the decrease in apparent entropy of activation is more pronounced than the decrease in apparent enthalpy of activation.

2.2.7 THE VALIDITY OF THE ASSUMPTION OF PAIRWISE INTERACTIONS

Both Equation 1.9 and 2.1 assume the dominance of 1:1 interactions causing the observed rate decreases. According to Figure 2.4, the fitted rate constants tend to deviate from the observed rate constants at higher cosolute molalities. We attribute this trend to higher order interactions. Interestingly, deviation from linearity is not observed in the analysis using Equation 1.9. Traditionally, absence of deviation from linearity has been used as evidence for 1:1 interactions.

In order to assess the possibility of higher-order interactions, estimates were made about the tendency for self-association of the cosolutes and the self-association behaviour of the cosolutes was calculated. Based on the equilibrium constants given in Table 2.4, we contend that the equilibrium constants for self-association K_{ass} of the alcohols used as cosolutes will be in the order of 0.2 kg mol^{-1} to 0.5 kg mol^{-1}.[32] In the following, the self-association of the cosolute molecules is assumed to occur stepwise and in a non-cooperative fashion as shown in Scheme 2.3.

Scheme 2.3

Based on the above assumptions, it is possible to calculate the molalities of monomer, dimers, trimers, etc. as a function of the total molality of cosolute. Typical examples are given in Figure 2.6

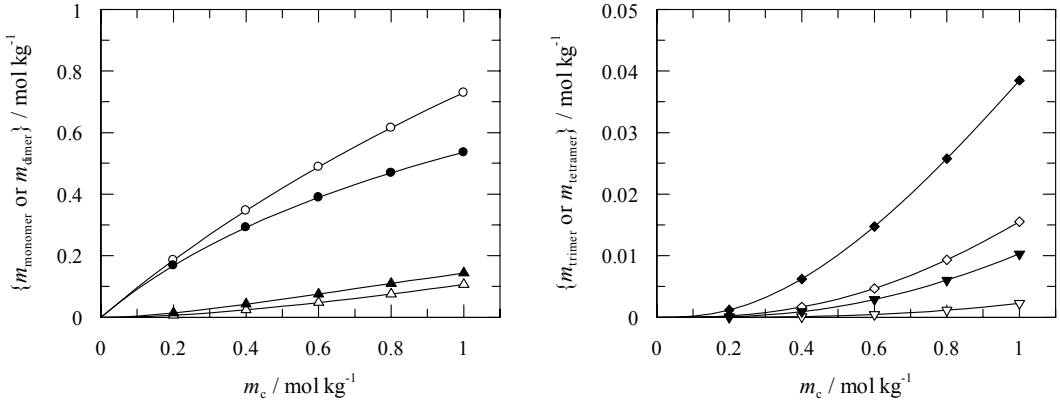

Figure 2.6: Molalities of monomers up to tetramers as a function of the molality of cosolute. *Left:* Monomers (o) and dimers (Δ), *Right:* trimers (◊) and tetramers (∇) for K_{ass}=0.2 kg mol^{-1} (open symbols) and 0.5 kg mol^{-1} (closed symbols). Only 1 out of 4 calculated data points are shown, curves are based on all data points.

As can be seen from Figure 2.6, the molality of cosolute molecules present in solution as monomers is lower than the total molality of cosolute. Extending equations 1.9 or 2.1 to include terms describing all the possible higher-order interactions is possible. However, this would lead to equations that will not yield significant results when used in the curve fitting procedures, as they would over interpret the available data.

In order to make an estimate of the effect of self-association of the cosolute on the observed kinetics, different quantities were calculated. Considering that 1:1 interaction is still possible with (at least some of) the cosolute molecules constituting the dimer, trimer, etc., the cosolute molality available for 1:1 interactions will be somewhere in between the total molality of cosolute clusters (including monomers) and the total cosolute molality. The results summarised in Figure 2.7 show that the total molality of cosolute clusters (including monomers) varies nearly linearly with total cosolute molality. We therefore contend that the possibility of engaging in 1:1 interactions increases essentially linearly with total cosolute molality.

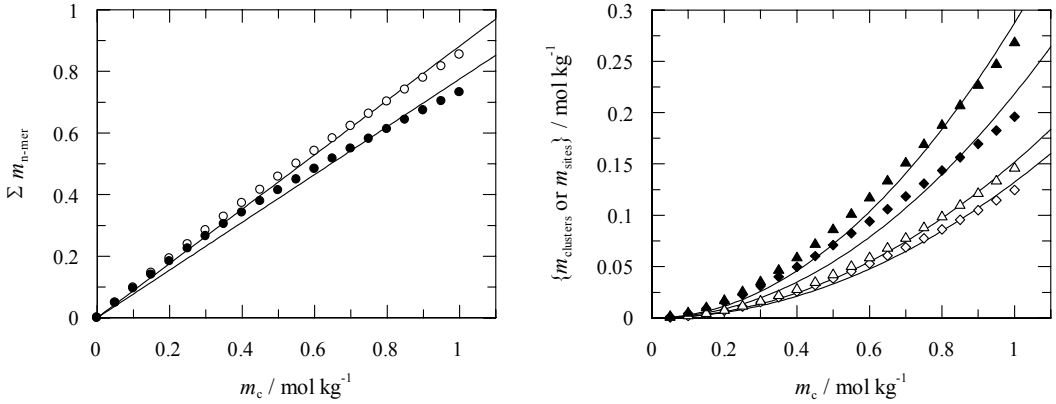

Figure 2.7: Molalities of cosolute clusters (including monomers), of clusters (n>1) up to decamers and "molalities of binding sites" (as described in the text) as a function of the molality of cosolute. *Left:* Clusters including monomers (o), curves are linear fits and *Right:* clusters n>1 (◊) and "binding sites" (Δ), curves are quadratic fits for K_{ass}=0.2 kg mol^{-1} (open symbols) and 0.5 kg mol^{-1} (closed symbols).

We assume that higher-order interactions will mainly occur as a result of 1:1 interaction with the clusters present in solution. The possibility to engage in 1:2 and higher order interactions will correlate with (i) the molality of clusters or (ii) the number of higher-order binding sites present in solution. The molality of clusters is given by $\sum_{n>1}\{[\text{n-mer}]\}$ whereas the number of higher-order binding sites will correlate roughly with $\sum_{n>1}\{(n-1)\cdot[\text{n-mer}]\}$, which provides an estimate of the molality of binding sites in between any two cosolute molecules that are part of a cluster. According to Figure 2.7, for small values of K_{ass}, both terms increase approximately quadratically with cosolute molality. Introducing an additional term into Equation 2.1 to account for the binding to clusters in which 1:2 interaction can take place,

the molality of which is approximated by a quadratic term $q \cdot m_c^2$, leads to Equation 2.7.

$$k(m_c) = \frac{k(m_c = 0)}{1 + K_{ec} \cdot m_c + K_{ecc} \cdot q \cdot m_c^{\,2}} \tag{2.7}$$

With K_{ecc} the equilibrium constant for encounter complex formation with clusters, q the constant obtained in the quadratic approximation described above. This constant is mainly influenced by K_{ass} (q=0.13-0.15 for K_{ass}=0.2 kg mol^{-1} and q=0.22-0.29 for K_{ass}=0.5 kg mol^{-1}). All other variables are defined as in Equation 2.1.

Using Equation 2.7, combining K_{ecc} and q in K'_{ecc}, a consistent set of values for K_{ec} and K'_{ecc} can be obtained and fitted curves are better than in Figure 2.4; Table 2.6.

Table 2.6: Binding constants K_{ec} and K_{ecc}.

ester	Cosolute					
	EtOH		n-PrOH		n-BuOH	
	K_{ec}[a] / kg mol^{-1}	K'_{ecc} / kg mol^{-1}	K_{ec}[a] / kg mol^{-1}	K'_{ecc} / kg mol^{-1}	K_{ec}[a] / kg mol^{-1}	K'_{ecc} / kg mol^{-1}
2.1b	0.30	0.055	0.47	0.130	0.71	0.290
2.1c	0.36	0.080	0.53	0.154	0.85	0.440
2.1d	0.41	0.099	0.57	0.191	0.96	0.530

[a] K_{ec} has been set to – d [ln {$k(m_c)/k(m_c=0)$}] / d m_c (*vide infra*).

2.2.8 COMPARISON OF THE MODELS

Both thermodynamic model and molecular description account for the observed rate decreases. A link between the two descriptions can be derived for $K_{ec} \cdot m_c < 1$,

$$\ln\left\{\frac{k(m_c)}{k(m_c = 0)}\right\} = -\ln\left\{1 + K_{ec} \cdot m_c\right\} \approx -K_{ec} \cdot m_c \tag{2.8}$$

Comparison of Equation 2.8 and Equation 1.9 shows that the terms in Equation 1.9 describing the interaction between ester and alcohol and the term for the lowering of the water activity in Equation 2.8 are replaced by an equilibrium constant. Hence, the lowering of the standard Gibbs energy of encounter complex formation, as given by the increasing equilibrium constants, is equivalent to a stabilisation of the initial state, as revealed by the negative G(c).

The inclusion of higher-order terms in Equation 2.1 leading to Equation 2.7 shows a peculiar difference between the thermodynamic model and the molecular picture. 1:1-Interactions are still sufficient for the thermodynamic model to give a reasonable fit, but the fit based on the molecular picture improves quite strongly upon adding a term describing higher-order interactions. The fact that $\ln\{k(m_c)/k(m_c=0)\}$ changes linearly with m_c in the molality range studied suggests that $k(m_c)/k(m_c=0)$ varies approximately exponentially with m_c.

$$\frac{k\left(m_c\right)}{k\left(m_c=0\right)} \approx e^{-a\cdot m_c} = \left[e^{a\cdot m_c}\right]^{-1} \approx \left[1 + a\cdot m_c + \tfrac{1}{2}\cdot a^2\cdot {m_c}^2 + \ldots\right]^{-1} \tag{2.9}$$

Comparing Equation 2.9 and Equation 2.7 suggest that K'_{ecc} should equal $\frac{1}{2}\cdot K_{ec}^2$, which is indeed observed (Figure 2.8).

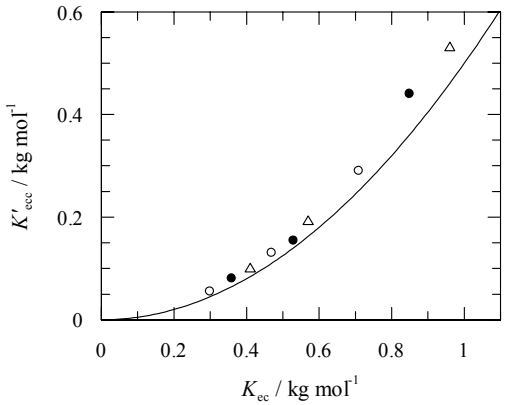

Figure 2.8: K'_{ecc} as a function of K_{ec} for cosolutes ethanol (o), *n*-propanol (•) and *n*-butanol (Δ). The curve indicates $\frac{1}{2}\cdot K_{ec}^2$.

As can be concluded from the above, the significance of K'_{ecc} is rather ambiguous. In one explanation, it reflects just another term of the Taylor series approximating an exponential function correctly describing the observed kinetics. Alternatively, the fact that K'_{ecc} happens to be close to $\frac{1}{2}\cdot K_{ec}^2$ causes $\ln\{k(m_c)/k(m_c=0)\}$ to vary almost linearly with m_c. In fact, comparable factors in the thermodynamic description could also lead to an overestimate of the molality range in which 1:1 interactions are dominant. This, in turn, could explain the non-additivity of the G(c)s of some combinations of cosolutes.[5,38]

The entropy and the enthalpy of the initial state both are increased by the encounter complex formation between ester and cosolute, as described before. Therefore, the molecular description explains previous observations[2] of the negative G(c), signifying initial state stabilisation, being accompanied by a strong enthalpic

destabilisation of the initial state, directly in terms of the thermodynamics of encounter complex formation.

Using the molecular model of encounter complex formation, the observed thermodynamics, including the G(c)-values, can be fully accounted for.

The inherent advantage of the molecular description is its possibility to link the observed kinetics and thermodynamics to a molecular picture of two interacting molecules. However, one has to keep in mind that an important contribution to the thermodynamics of interaction is caused by water molecules being released from restricted positions in the hydration shells of those molecules.

2.3 CONCLUSION

Inert cosolutes can influence reactions in solution by forming encounter complexes. In aqueous solution, these encounter complexes can be stabilised by hydrophobic interactions. This results in larger cosolute effects on chemical reactions as the unfavourable entropy term associated with bringing the molecules together is partially or completely (depending on molality) compensated by the release of water molecules from the hydration shell. For the water-catalysed hydrolysis of the activated esters used in the present study, the formation of encounter complexes, with equilibrium constants K_{ec} often smaller than unity, leads to an initial state stabilisation as given by G(c). The stabilisation of the encounter complex by hydrophobic interactions results in a decrease in both apparent enthalpy and apparent entropy of activation.

2.4 EXPERIMENTAL

2.4.1 KINETIC EXPERIMENTS

Aqueous solutions were prepared by weight immediately before use. Water was distilled twice in an all-quartz distillation unit. All reactions were monitored at 288 nm and at 25.0±0.1°C (in the determination of the *G*(c)-values) and at least 6 different temperatures in the interval between 20.0±0.1°C and 50.0±0.1°C (except for the 1.5mol% 1-propanol and the 0.5mol% 1-butanol solutions for which measurements were performed at 4 and 5 temperatures, respectively, in the interval between 20.0±0.1°C and 50.0±0.1°C). Reactions were followed for at least six half-lives using a Perkin-Elmer lambda 2, lambda 5 or lambda 12 spectrophotometer. Good to excellent first-order kinetics were obtained, the error in the rate constants being 2% or less. Esters were injected as 20-30 μl of stock solutions containing **2.1a-d** in cyanomethane into about 15 ml of an aqueous solution of cosolute in the concentration range of 0-2mol% (up to 1.68 mol% for 1-butanol, below the solubility limit of 1.92mol%) followed by sonication of the solution for 5 min. The sonicated solutions were centrifuged, decanted and diluted to about 20 ml. Of the resulting solution, 6-7 ml aliquots were transferred into a 2.000 cm path length stoppered quartz cuvette. The resulting concentrations of hydrolytic probe were about 10^{-5} mol dm^{-3} or less. All these precautions were taken in order to prevent problems due to the low solubility of the more hydrophobic esters. Amides were injected as 5-7 μl of stock solutions containing **2.2a,b** in cyanomethane into about 2.8 ml of an aqueous solution of cosolute in the molality range of 0-1.15 mol kg^{-1} for *n*-propanol and 0-0.87 mol kg^{-1} for *n*-butanol in a stoppered 1.000 cm quartz cuvette. The resulting concentrations were about 10^{-5} mol dm^{-3} or less. The pH of all solutions was adjusted to 3.6±0.3 using aqueous HCl. The pH was checked again at the end of each kinetic experiment and was found to be 3.6±0.3, well within the pH-range in which solely water-catalysed hydrolysis takes place.

2.4.2 MATERIALS

Cosolutes were of analytical grade and were purchased from Merck. The esters were synthesised using the route shown in Scheme 2.4.

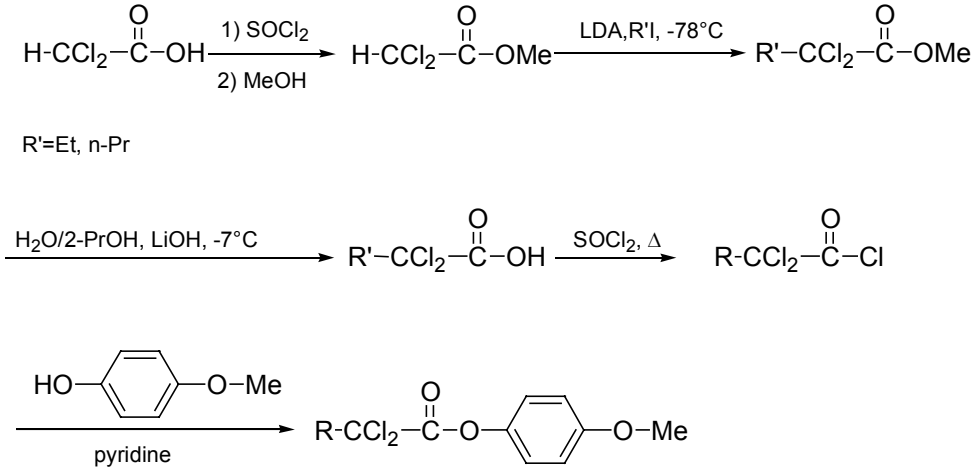

2.1 a R=H, **b** R=Me, **c** R=Et, **d** R=n-Pr

Scheme 2.4

The starting materials for the syntheses were purchased from Aldrich and were used as received. NMR spectra were recorded on Varian Gemini 200 (^{1}H: 200MHz) and VRX 300 (^{1}H: 300MHz) spectrometers. IR-spectra were recorded using a Perkin Elmer 841 infrared spectrophotometer. Methyl dichloroethanoate was obtained by reacting dichloroethanoic acid with methanol in the presence of sulfuric acid.[39] ^{1}H-NMR ($CDCl_3$, ppm): 3.92 (3H, OC*H*$_3$, s), 5.97 (1H, *H*CCl_2, s), IR (CCl_4, cm^{-1}): 1773, 1753. 1-(4-Methylbenzoyl)-1,2,4-triazole **2.2b** and 1-(4-n-butylbenzoyl)-1,2,4-triazole **2.2b** were synthesised according to literature procedures.[40]

Methyl 2,2-dichlorobutanoate. An adapted literature procedure[41] was used. To a solution of 5.8 ml (40 mmol) of anhydrous diisopropylamine 20 ml of sodium-dried THF, 14.4 ml of a 2.5M solution of BuLi in hexane (36 mmol) was added slowly at -78°C. After stirring for 5 min, 4.0 grams (28 mmol) of methyl 2,2-dichloroethanoate were added and stirring continued for another 15 min. Next, 2.9 ml (28 mmol) of ethyl iodide was added. The mixture was stirred for another 15 min and then allowed to reach room temperature. The reaction mixture was poured out into a saturated NH_4Cl solution and 60 ml of ether was added. The ether layer was separated from the aqueous layer and washed with water and brine. The ether layer was dried over sodium sulfate, filtered and ether was removed by evaporation. Distillation in a Kugelrohr apparatus (120°C, circa 10 mm Hg) gave 4.153 g (24 mmol, 60%) of product. ^{1}H-NMR ($CDCl_3$): δ (ppm): 1.16 (3H, CH_2CH_3, t), 2.46 (2H, $CH_3CH_2CCl_2$, m), 3.89 (3H, OC*H*$_3$, s). ^{13}C-NMR ($CDCl_3$, ppm): 8.0, 37.1, 52.8.

Methyl 2,2-dichloropentanoate was synthesised analogously using *n*-propyl iodide. ^{1}H-NMR ($CDCl_3$): δ (ppm): 1.00 (3H, CH_2CH_3, t), 1.59 (2H, $CH_3CH_2CH_2$, sextet), 2.40 (2H, $CH_2CH_2CCl_2$, m), 3.89 (3H, OCH_3, s). ^{13}C-NMR ($CDCl_3$, ppm): 11.9, 17.0, 45.6, 52.8, 84.3, 166.6, IR (CCl_4, cm^{-1}): 1748, 1768.

2,2-Dichlorobutanoic acid was synthesised from methyl 2,2-dichlorobutanoate according to a literature procedure.[42] ^{1}H-NMR ($CDCl_3$): δ (ppm): 1.19 (3H, CH_3CH_2, t), 2.47 (2H, $CH_3CH_2CCl_2$, q), ^{13}C-NMR ($CDCl_3$, ppm): 7.0, 36.1, 83.4, 165.3, IR (CCl_4, cm^{-1}): 1732.

2,2-Dichloropentanoic acid was synthesised analogously using methyl 2,2-dichloropentanoate. ^{1}H-NMR ($CDCl_3$): δ (ppm): 1.00 (3H, CH_2CH_3, t), 1.65 (2H, $CH_3CH_2CH_2$, sextet), 2.41 (2H, $CH_2CH_2CCl_2$, m). ^{13}C-NMR ($CDCl_3$, ppm): 11.9, 17.1, 45.5, 84.3, 166.6, IR (CCl_4, cm^{-1}): 1734.

2,2-Dichloropentanoyl chloride. A mixture of 1.94 g (11.4 mmol) of 2,2-dichloropentanoic acid and 2.74 g (23 mmol) of $SOCl_2$ was refluxed for 3 h. Distillation of the reaction mixture under reduced pressure gave 1.13 g (6 mmol, 53%) of 2,2-dichloropentanoyl chloride. ^{13}C-NMR ($CDCl_3$, ppm): 13.1, 18.3, 46.6, IR (CCl_4, cm^{-1}): 1779, 1799.

2,2-Dichlorobutanoyl chloride was synthesised analogously from 2,2-dichlorobutanoic acid. 2,2-Dichlorobutanoyl chloride: ^{1}H-NMR ($CDCl_3$): δ (ppm): 1.20 (3H, CH_3CH_2, t), 2.53 (2H, $CH_3CH_2CCl_2$, q), ^{13}C-NMR ($CDCl_3$, ppm): 7.0, 36.0, 88.5, 165.5, IR (CCl_4, cm^{-1}): 1773, 1802.

2,2-Dichloropropanoyl chloride was synthesised analogously from 2,2-dichloropropanoic acid. 2,2-Dichloropropanoyl chloride: ^{1}H-NMR ($CDCl_3$): δ (ppm): 2.36 (3H, CH_3CCl_2, t), IR (CCl_4, cm^{-1}): 1778, 1795.

***p*-Methoxyphenyl 2,2-dichloroethanoate 2.1a** was synthesised according to a literature procedure.[43]

***p*-Methoxyphenyl 2,2-dichloropentanoate 2.1d**. To 3 ml of absolute ether, equimolar amounts (6 mmol) of 2,2-dichloropentanoyl chloride and *p*-methoxyphenol and pyridine were added. The mixture was stirred for 3h at room temperature. Pyridine salts were filtered off and the solvent was evaporated. The crude ester was dissolved in petroleum ether 40/60. On cooling, a two-phase system was formed. The upper colourless layer was separated and the solvent was removed by evaporation, yielding the crude ester. The ester was further purified by

column chromatography over silica, using 1:1 CH_2Cl_2/n-hexane as the eluent. ^{1}H-NMR ($CDCl_3$, ppm): 1.07 (3H, C*H*$_3$CH$_2$, t), 1.82 (2H, CH$_3$C*H*$_2$CH$_2$, sextet), 2.53 (2H, CH$_2$C*H*$_2$CCl$_2$, m), 3.81 (3H, CH_3O, s), 7.00 (4H, phenyl, AB-system).

***p*-Methoxyphenyl 2,2-dichlorobutanoate 2.1c** was synthesised analogously. *p*-Methoxyphenyl 2,2-dichlorobutanoate: ^{1}H-NMR ($CDCl_3$, ppm): 1.36 (3H, C*H*$_3$CH$_2$, t), 2.58 (2H, CH$_3$C*H*$_2$CCl$_2$, q), 3.81 (3H, CH_3O, s), 7.00 (4H, phenyl, AB-system).

***p*-Methoxyphenyl 2,2-dichloropropanoate 2.1b** was synthesised analogously. *p*-Methoxyphenyl 2,2-dichloropropanoate: ^{1}H-NMR ($CDCl_3$, ppm): 2.43 (3H, C*H*$_3$CCl$_2$, s), 3.85 (3H, CH_3O, s), 7.00 (4H, phenyl, AB-system).

1-(4-n-Butylbenzoyl)-1,2,4-triazole 2.2b. To a suspension of 0.71 g (10.3 mmol) of freshly recrystallised 1,2,4-triazole in 50 ml of dry (distilled from P_2O_5) ether, a solution of 1.00 g (5.09 mmol) of 4-(n-butyl)benzoyl chloride was added. The suspension was stirred overnight at room temperature. The liquid was removed via a cannula. The ether was evaporated under reduced pressure and petroleum-ether 40-60 was added. The liquid fraction was removed via a cannula again, after which the petroleum-ether was evaporated under reduced pressure. Yield 1.01 g (4.39 mmol, 86%) ^{1}H-NMR ($CDCl_3$, ppm): 0.89 (3H, C*H*$_3$CH$_2$, t), 1.32 (2H, CH$_3$C*H*$_2$CH$_2$, sextet), 1.59 (2H, CH$_3$CH$_2$C*H*$_2$CH$_2$, pentet), 2.66 (2H, CH$_2$C*H*$_2$Ph, t), 7.30 and 8.11 (4H, phenyl, AB-system), 8.06 (1H, triazole-H, s), 9.02 (1H, triazole-H, s).

2.5 ACKNOWLEDGEMENT

Laura Pastorello is gratefully acknowledged for performing the synthesis of some of the compounds used in this chapter and for performing the initial kinetic experiments. Marten de Rapper is thanked for excellent technical support. Theo Rispens and Sijbren Otto contributed to the chapter by countless enlightening discussions.

2.6 REFERENCES AND NOTES

(1) Part of this chapter has been published: Buurma, N. J., Pastorello, L., Blandamer, M. J. and Engberts, J. B. F. N. *J.Am.Chem.Soc.* **2001**, *123*, 11848-11853.

(2) Engberts, J. B. F. N. and Blandamer, M. J. *J. Phys. Org. Chem.* **1998**, *11*, 841-846.

(3) Karzijn, W. and Engberts, J. B. F. N. *Tetrahedron Lett.* **1978**, 1787-1790.

(4) Blokzijl, W., Jager, J., Engberts, J. B. F. N. and Blandamer, M. J. *J. Am. Chem. Soc.* **1986**, *108*, 6411-6413.

(5) Blokzijl, W., Engberts, J. B. F. N. and Blandamer, M. J. *J. Am. Chem. Soc.* **1990**, *112*, 1197-1201.

(6) Kerstholt, R. P. V., Engberts, J. B. F. N. and Blandamer, M. J. *J. Chem. Soc. , Perkin Trans. 2* **1993**, 49-51.

(7) Blokzijl, W., Engberts, J. B. F. N. and Blandamer, M. J. *J. Phys. Chem.* **1987**, *91*, 6022-6027.

(8) Galema, S. A., Blandamer, M. J. and Engberts, J. B. F. N. *J. Am. Chem. Soc.* **1990**, *112*, 9665-9666.

(9) Galema, S. A., Blandamer, M. J. and Engberts, J. B. F. N. *J. Org. Chem.* **1992**, *57*, 1995-2001.

(10) Engberts, J. B. F. N., Kerstholt, R. P. V. and Blandamer, M. J. *J. Chem. Soc. , Chem. Commun.* **1991**, 1230-1231.

(11) Apperloo, J. J., Streefland, L., Engberts, J. B. F. N. and Blandamer, M. J. *J. Org. Chem.* **2000**, *65*, 411-418.

(12) Noordman, W. H., Blokzijl, W., Engberts, J. B. F. N. and Blandamer, M. J. *J. Org. Chem.* **1993**, *58*, 7111-7114.

(13) Hol, P., Streefland, L., Blandamer, M. J. and Engberts, J. B. F. N. *J. Chem. Soc. , Perkin Trans. 2* **1997**, 485-488.

(14) Streefland, L., Blandamer, M. J. and Engberts, J. B. F. N. *J. Phys. Chem.* **1995**, *99*, 5769-5771.

(15) Streefland, L., Blandamer, M. J. and Engberts, J. B. F. N. *J. Am. Chem. Soc.* **1996**, *118*, 9539-9544.

(16) Apart from additivity within series of compounds, promising results are obtained in the attempt to determine an additivity scheme describing all cosolutes used in combination with one particular probe. M. Wijnhold, personal communication.

(17) Savage, J. J. and Wood, R. H. *J. Solution Chem.* **1976**, *5*, 733-750.

(18) Karzijn, W. and Engberts, J. B. F. N. *Recl. Trav. Chim. Pays-Bas* **1983**, *102*, 513-515.

(19) Correlations between ln(k) and several solvent parameters yield less satisfactory results than the analyses using Equations 1.9 and 2.1 as presented in this Chapter. For example, ln(k) for individual probes correlates reasonably well with the relative

permittivity ε for aqueous solutions within a series of concentrations using only one cosolute. Plotting ln(*k*) vs relative permittivity for solutions of different alcohols, however, results in different correlations for different alcohols.

(20) In terms of the Marcus Theory description in Chapter 1, this corresponds to an increase in the work function.

(21) Lensink, M. F., Mavri, J. and Berendsen, H. J. C. *J. Comput. Chem.* **1999**, *20*, 886-895.

(22) Rispens, T.; Lensink, M.F.; Berendsen, H.J.C.; Engberts, J.B.F.N., submitted for publication.

(23) Charton, M. *J. Chem. Soc. , Perkin Trans. 2* **1983**, 97-104.

(24) Mooij, H. J., Engberts, J. B. F. N. and Charton, M. *Recl. Trav. Chim. Pays-Bas* **1988** , *107*, 185-189.

(25) Maskill, H. "The Physical Basis of Organic Chemistry" first edition Oxford University Press, Oxford, **1993**.

(26) Blokzijl, W., Blandamer, M. J. and Engberts, J. B. F. N. *J. Org. Chem.* **1991**, *56*, 1832-1837.

(27) Cheng, Y. K. and Rossky, P. J. *Biopolymers* **1999**, *50*, 742-750.

(28) Kavarnos, G. J. and Turro, N. J. *Chem. Rev.* **1986**, *86*, 401-449.

(29) Hubig, S. M. and Kochi, J. K. *J. Am. Chem. Soc.* **1999**, *121* , 1688-1694.

(30) Weng, H. X. and Roth, H. D. *J. Phys. Org. Chem.* **1998**, *11*, 101-108.

(31) Rathore, R., Hubig, S. M. and Kochi, J. K. *J. Am. Chem. Soc.* **1997**, *119*, 11468-11480.

(32) North, A. M. "The Collision Theory of Chemical Reactions in Liquids" first edition, (Emeleus, H. J., Style, D. W. G., and Bell, R. P., eds.). Methuen, London, **1964**.

(33) The rate decrease cannot be caused by the decreased water concentration alone. Based on known densities of aqueous solutions (see *e.g.*: Jolicoeur, C.; Lacroix, G., *Can. J. Chem.* **1976**, *54*, 624), the water concentration in dilute aqueous solutions used in the present study can be calculated. Considering that the hydrolysis reactions are second-order in water, the decreased water concentration in, for example, a 0.57 m solution of 1-propanol would result in a rate decrease of 6.5%, whereas experimentally rate effects around 25% are found for the different probes.

(34) This is one of the possible choices for ΔG(noninteract). The advantage of this choice is that it is the same for all different cosolutes. Other possible choices include values based on the molar volume of the cosolute.

(35) ΔG(noninteract) and G are not independent. For a rather wide range of ΔG(noninteract), a good fit is possible with a different value for G.

(36) Blokzijl, W. and Engberts, J. B. F. N. *Angew. Chem. , Int. Ed. Engl.* **1993**, *32*, 1545-1579.

(37) The changes in $\Delta^{\neq}H^{o}$ and $\Delta^{\neq}S^{o}$ as a function of cosolute concentration are consistent with recent computer simulations, which show a favourable entropy of association of

two methane molecules in water, provided a sufficiently close approach in the aqueous medium. See: Smith, D. E.; Zhang, L.; Haymet, A. D. J. *J.Am.Chem.Soc.* **1992**, *114*, 5875-5876.

(38) Rispens, T. *et al.*, to be published.

(39) Urry, W. H., Eiszner, J. R. and Wilt, J. W. *J. Am. Chem. Soc.* **1957**, *79*, 918-922.

(40) a) Staab, H. A., Lüking, M. and Dürr, F. H. *Chem. Ber.* **1962**, *95*, 1275-1283. b) Karzijn, W., *The water- and hydroxide-ion catalyzed hydrolysis of 1-acyl-1,2,4-triazoles*, Ph.D. Thesis, University of Groningen, **1979**. c) Mooij, H. J., Engberts, J. B. F. N. and Charton, M. *Recl.Trav.Chim.Pays-Bas* **1988**, *107*, 185-189.

(41) Villieras, J., Disnar, J. R., Perriot, P. and Normant, J.-F. *Synthesis* **1975**, 524-525.

(42) Benedetti, M., Forti, L., Ghelfi, F., Pagnoni, U. M. and Ronzoni, R. *Tetrahedron* **1997**, *53*, 14031-14042.

(43) Fife, T. H. and McMahon, D. M. *J. Am. Chem. Soc.* **1969**, *91* , 7481-7485.

General-Base Catalysed Hydrolysis and Nucleophilic Substitution of Activated Amides in Aqueous Solutions[1]

*The reactivity of 1-benzoyl-3-phenyl-1,2,4-triazole (**3.1a**) has been studied in the presence of a range of weak bases in aqueous solution. A change in mechanism is observed from general-base catalysed hydrolysis to nucleophilic substitution and general-base catalysed nucleophilic substitution. A slight tendency is also observed for the more hydrophobic general bases to show higher reactivity towards **3.1a**. Aspartame is an effective nucleophile possibly because nucleophilic substitution is subject to intramolecular general-base catalysis. A general conclusion derived from the present results is that unexpected rate effects can only be rationalised provided that the detailed reaction mechanisms are well understood.*

3.1 INTRODUCTION

3.1.1 REACTIONS OF 1-BENZOYL-3-PHENYL-1,2,4-TRIAZOLE IN THE PRESENCE OF GENERAL BASES

The analyses as described in Chapters 1 and 2 are valid for non-reacting and non-catalytically active cosolutes. However, most cosolutes contain one or more functional groups that could introduce changes in reactivity. In order to take account of changes in reactivity, possible changing reaction pathways must be explored.

The hydrolysis reaction of the activated amide 1-benzoyl-3-phenyl-1,2,4-triazole (**3.1a**) is general-base catalysed (Scheme 3.1).[2]

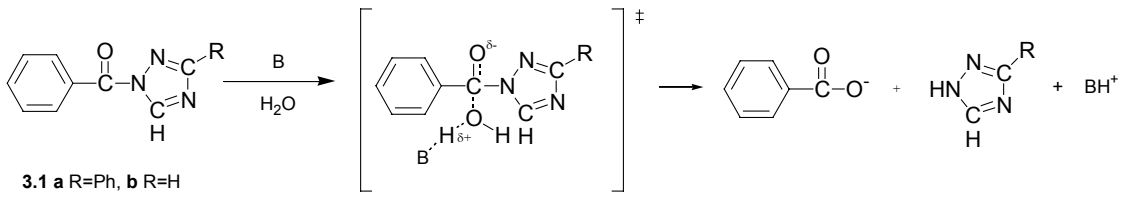

Scheme 3.1

In highly aqueous solutions, the concentration of water is sufficiently high for water to (detectably) act as a general base as well as a nucleophile. Hence, in the

absence of other general bases, the water-catalysed pH-independent hydrolysis discussed in Chapter 1 is the sole reaction. In the presence of sufficiently basic cosolutes, the water-catalysed reaction is unimportant. More basic cosolutes are much more effective catalysts for hydrolysis than water. Consequently, despite the relatively low molality of added general bases,[3] the general-base catalysed hydrolysis pathway competes with the water-catalysed pathway. It is stressed that even though in the water-catalysed reaction the second water molecule in the activated complex (*i.e.* B=H_2O, Scheme 3.1) acts as a general base, a distinction is drawn between water-catalysed reaction and general-base catalysed reaction.

Increased basicity of cosolutes usually leads to a concomitant increase in nucleophilicity. This increase in nucleophilicity provides an alternative reaction pathway: nucleophilic attack on the carbonyl functionality, followed by loss of the (substituted) 1,2,4-triazole leaving group (Scheme 3.2).

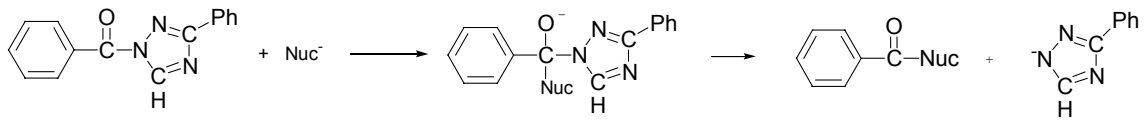

Scheme 3.2

This reaction is related to the water-catalysed hydrolysis described in Chapter 1, but the nucleophilic water molecule is replaced by a stronger nucleophile. The similarity with the water-catalysed hydrolysis goes even further, as the nucleophilic substitution reaction can also be catalysed by general acids and bases. Some of the possible catalysed reaction pathways for nucleophilic substitution[4-7] are illustrated in Scheme 3.3.

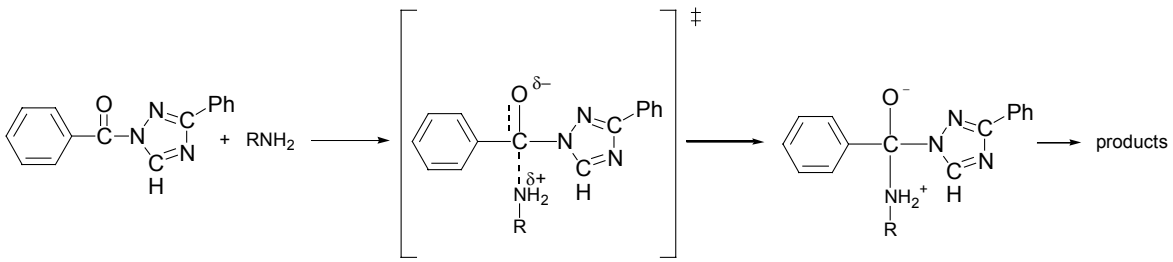

Scheme 3.3

If nucleophilic attack is the rate-determining step, the reaction can be catalysed by a general base or by hydroxide, deprotonating the nucleophile. Similarly, the

negative charge developing on the amide carbonyl can be stabilised by general acids, resulting in general-acid catalysis. However, if expulsion of the 3-phenyl-1,2,4-triazole from a protonated tetrahedral intermediate is rate determining, the reaction could be general-base catalysed. Further, departure of the leaving group may be general-acid catalysed.

In this intricate play of reactivity, reactants can assume many different roles, resulting in a series of related but different reaction pathways. It is therefore of paramount importance to have a detailed understanding of these reaction pathways if we are to fully understand the observed rate effects induced by cosolutes. We have therefore studied the effect of a range of general bases on the reactivity of **3.1a** in order to identify possible competing reaction pathways. The results are used in a reinterpretation of the previously[8] reported rate-accelerating effects of α-amino acids on the hydrolysis of **3.1a**.

3.1.2 Effects of hydrophobicity on reactions of 1-benzoyl-3-phenyl-1,2,4-triazole in the presence of general bases

Encounter complexes between reactive probes and added inert cosolutes can be stabilised by hydrophobic interactions. However, if the cosolute is not inert, formation of an encounter complex constitutes the first step for bimolecular (or higher molecularity) reactions. Hence, if a cosolute reacts with the reactive probe, or catalyses the reaction of the reactive probe, more *hydrophobic* cosolutes are expected to show slightly more effective catalysis or slightly higher reactivity than *hydrophilic* cosolutes with identical functional groups. Similarly, in a linear free energy relationship, more hydrophobic reactive cosolutes are expected to show deviations towards higher reactivity provided hydrophobic interactions are not of similar importance in both processes.

The molecular picture of an unreactive cosolute blocking the reactive centre of the activated amide from attack by water as described in Chapter 2 is expected to be equally valid in general-base catalysed hydrolysis and (catalysed) nucleophilic substitution. In buffer solutions of general bases in which the conjugate general acid is present as well, intriguing compensating effects are possible. Increasing the hydrophobicity of the general base will lead to an increased efficiency in general-base catalysis (*vide supra*) and to a concomitant increase in the rate-retarding effect of the conjugate general base.

3.2. RESULTS AND DISCUSSION

3.2.1 GENERAL-BASE CATALYSIS BY CARBOXYLATE IONS AND WATER

The effect was determined of different general bases on the (pseudo-) first-order rate constant of hydrolysis of **3.1**. In all cases, at low molality and constant buffer ratio, the increase in rate constants was linear with increasing molality of added general base (Figure 3.1).

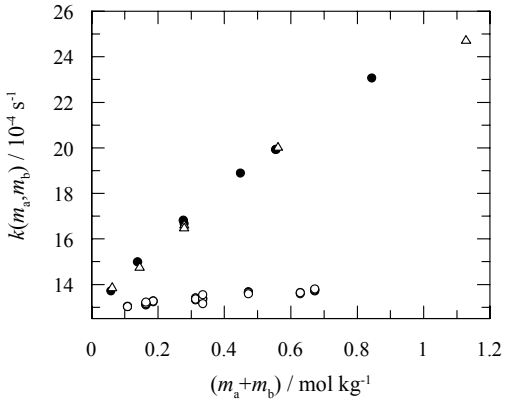

Figure 3.1: Effect of added ethanoate/ethanoic acid (Δ), butanoate/butanoic acid (•) and chloroethanoate/chloroethanoic acid (o) buffers (all buffer ratios 3:1 and pH-values of 5.15±0.10, 5.20±0.10 and 3.20±0.10, respectively, m_a and m_b are the molalities of acid and base, respectively) on the hydrolysis of **3.1a**.

In order to obtain the sole effect by the general bases, the effect of the conjugate general acid on the observed rate has to be calculated. In the absence of general base, the general acids were found to decrease the rate of the water-catalysed reaction with G(c)-values of -331 and -715 J kg mol^{-2} for ethanoic acid and butanoic acid, respectively. As described in Chapter 2, we attribute this decrease to blocking by the cosolute of the reaction centre from attack by water. We contend that a similar inhibition of reaction occurs for the general-base catalysed hydrolysis.

Hypothetically, in the absence of inhibition by cosolute and in the pH-range in which the reaction without added general bases is only water-catalysed, the rate constant is described by Equation 3.1.

$$k(m_b) = k(m_c = 0) + m_b \cdot k_b \qquad (3.1)$$

Here, m_b is the molality of general base, k_b is the (pseudo-) second-order rate constant[3] for catalysis by the general base and $k(m_c=0)$ is the (pseudo-) first-order rate constant in the absence of cosolute. Equation 1.9 describes the effects of inert

cosolutes on the hydrolysis reactions. Equation 3.2 is a simpler form of Equation 1.9.

$$\ln\left\{\frac{k(m_c)}{k(m_c=0)}\right\} = a \cdot m_c \tag{3.2}$$

Here, m_c is the molality of inert cosolute c and a quantifies the rate effect induced by cosolute c.[9] Equation 3.2 can be rewritten as shown in Equation 3.3.

$$k(m_c) = k(m_c=0) \cdot e^{a \cdot m_c} \tag{3.3}$$

The conjugate acid of the general-base catalyst is the only inert cosolute. Hence, for the present case, m_c is the molality of conjugate acid m_a. If Equation 3.1, describing the kinetics of reaction without inhibition, is substituted into Equation 3.3, describing the inhibiting effect of added unreactive cosolutes, we obtain Equation 3.4.

$$k(m_a, m_b) = \{k(m_c=0) + m_b \cdot k_b\} \cdot e^{m_a \cdot a} \tag{3.4}$$

Now, a is the (rate-retarding) effect of the acidic form of the cosolute on both the water-catalysed and general-base catalysed reaction. The kinetic data were fitted to Equation 3.4. The results together with pK_a-values[10] are summarised in Table 3.1.

Table 3.1: General-base catalysed hydrolysis of **3.1a** at 298.2 K.[a]

	ethanoate	chloroethanoate	butanoate
pK_a	4.76[11]	2.86[12]	4.82[11]
k_b / 10^{-4} s^{-1} mol^{-1} kg	16.63±0.47	2.08±0.09	20.61±0.22
a / kg mol^{-1}	-0.30±0.03	-0.11±0.02	-0.56±0.01
$k(m_c=0)$ / 10^{-4} s^{-1}	13.2±0.2	13.0±0.1	13.0±0.1

(a) Numbers in brackets are standard errors based on a least-squares fit of kinetic data using Equation 3.4.

G(c)-values were calculated using Equation 3.5 (*cf.* Equations 3.2 and 1.9).

$$a = \frac{2}{R \cdot T \cdot m_0^2} \cdot G(c) - N \cdot \phi \cdot M_w \tag{3.5}$$

Here, m_0, N, ϕ and M_w are defined as described in Chapter 1. N was set to 2, despite the fact that only one water molecule is involved in the rate-determining step for the

general-base catalysed reaction. The error introduced in this way is small as the term $N\phi M_w$ is small and the contribution of general-base catalysis to the overall rate constant is generally less than 50%. The G(c)-values for ethanoate and butanoate of -327±37 and -649±13 J kg mol^{-2}, respectively, correspond with the corresponding values for the water-catalysed reaction. This correspondence supports the hypothesis that rate-retarding effects are similar for water-catalysed and for general-base catalysed hydrolysis and is consistent with the notion that the rate-retarding effects are (largely) caused by blocking of the reaction center.

Using the results given in Table 3.1, a Brønsted plot was constructed[13] for carboxylate general bases and water (Figure 3.2, Equation 3.6).

$$\log(k_b) = 0.29 \cdot pK_a - 4.24 \qquad (3.6)$$

The Brønsted β is 0.29±0.05, slightly lower than the value for activated amides without the phenyl substituent in the triazole ring.[2,14,15]

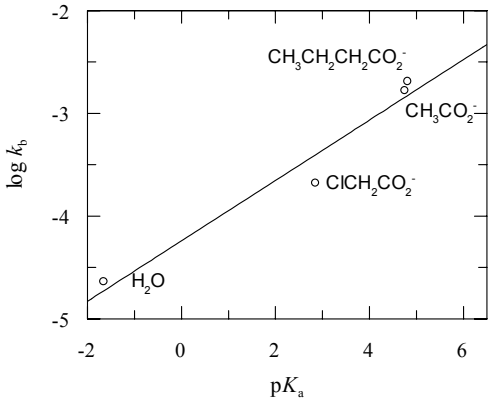

Figure 3.2: Brønsted plot for general-base catalysed hydrolysis of **3.1a**.

Interestingly, in terms of general-base catalysis, comparison of ethanoate and butanoate shows that the latter is slightly more effective. The observed difference cannot be explained on the basis of its slightly higher pK_a. This pattern could be caused by the more hydrophobic nature of butanoate, resulting in additional hydrophobic stabilisation of the encounter complexes formed between **3.1a** and butanoate in the initial stage of the activation process.

3.2.2 FROM BASE-CATALYSED HYDROLYSIS TO NUCLEOPHILIC SUBSTITUTION

Phenylalaninamide hydrochloride and alaninamide hydrochloride are both rate retarding in their fully protonated form; G(c) equals –1869 and –234 J kg mol^{-2}, respectively.[8,16] In their deprotonated forms, they can function as general bases. It was expected that especially phenylalaninamide, being strongly rate-retarding in the protonated state and hence forming rather stable encounter complexes, would be an effective catalyst for hydrolysis.

Indeed, the reactivity of **3.1a** in the presence of unprotonated alaninamide and phenylalaninamide is high. The pH-dependence of the reactivity of **3.1a** in the presence of alaninamide and phenylalaninamide (Figure 3.3) indicates that high reactivity is indeed associated with deprotonation of the general base.

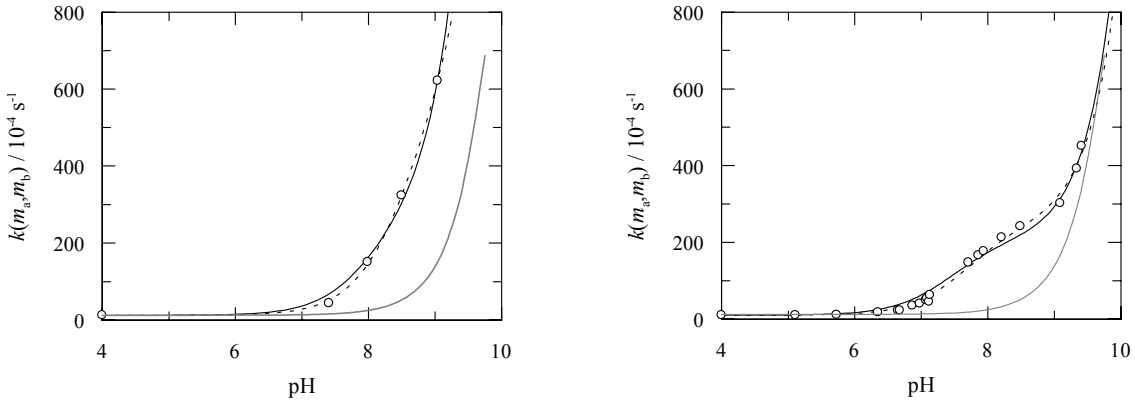

Figure 3.3: pH-Dependence of the reactivity of **3.1a** in the presence of α-amino acid derivatives. *Left:* 0.11 mol kg^{-1} alaninamide with pK_a set to 8.02 (solid line) and pKa 8.58 (dotted line) and *Right:* 0.11 mol kg^{-1} phenylalaninamide, pK_a set to 7.45 (solid line) and pKa 7.69 (dotted line). Gray lines indicate hydroxide-catalysed hydrolysis.

The results for alaninamide and phenylalaninamide have been fitted to Equation 3.7, using a non-linear least squares procedure.

$$k(m_c, pH) = k(m_c) + k_{\mathrm{OH}} \cdot 10^{pH-14} + \frac{k_{3.1a} \cdot m_c}{1+10^{pK_a - pH}} \qquad (3.7)$$

The first term on the right hand side, $k(m_c)$ is the rate constant for hydrolysis at pH 4 in the presence of m_c molal of protonated cosolute c. The second term on the right hand side yields the rate of hydroxide-ion catalysed hydrolysis with k_{OH} the second-order rate constant for hydroxide-catalysed hydrolysis and 10^{pH-14} the concentration of hydroxide.[3] The third term on the right hand side represents the rate of reaction with the cosolute, where $k_{\mathbf{3.1a}}$ is the rate constant of reaction of the cosolute with

3.1a, m_c is the total molality of cosolute and $(1+10^{pK_a-pH})^{-1}$ is the fraction of cosolute in the deprotonated form. The results are summarised in Table 3.2.

Table 3.2: Reactivity of **3.1a** in the presence of alaninamide and phenylalaninamide at 298.2 K.

	alaninamide	phenylalaninamide
pK_a	8.58 (lit.: 8.02[17])	7.69 (lit.: 7.45[17])
$k_{\mathbf{3.1a}}$ / s^{-1} mol^{-1} kg	0.51±0.17[a]	0.22±0.02
$k(m_c)$ / 10^{-4} s^{-1}	12.3	10.3
k_{OH} / s^{-1} mol^{-1} dm^3	n.s.[b]	7.3±0.8

[(a)] Errors are standard errors based on a least-squares fit of kinetic data using Equation 3.7. [(b)] The value of 1720±930 s^{-1} mol^{-1} dm^3 obtained from the curve-fitting procedure cannot be regarded as significant considering the error margin.

The rate constants, 51±17 10^{-2} s^{-1} mol^{-1} kg and 22±2 10^{-2} s^{-1} mol^{-1} kg for alaninamide and phenylalaninamide, respectively, are significantly higher than the values 12.2 10^{-3} and 8.33 10^{-3} s^{-1} mol^{-1} kg predicted on the basis of the Brønsted plot for general-base catalysed hydrolysis and their literature pK_a's of 8.02 and 7.45, respectively.[17] (The pK_a-values obtained from fitting to Equation 3.7 lead to only marginally higher predicted values). We attribute this marked difference in reactivity of **3.1a** for these general bases to a change in reactivity from general-base catalysed hydrolysis to nucleophilic substitution.[18] The structurally-related activated amide 1-ethanoyl-1,2,4-triazole also has been shown to undergo general-base catalysed hydrolysis and substitution by a variety of nucleophiles.[19]

The rate constant for hydroxide-catalysed hydrolysis of **3.1a** in the presence of phenylalaninamide is considerably lower than the rate constant of 1130 s^{-1} mol^{-1} dm^3 for hydroxide-catalysed hydrolysis of **3.1a** without cosolute.[15] Previously,[14] the effect of 2-methylpropan-2-ol on the hydroxide-ion catalysed hydrolysis of **3.1a** has been studied. At low mole fractions of added 2-methylpropan-2-ol, the second-order rate constants (k_{OH}) showed a maximum when plotted against the mole fraction of 2-methylpropan-2-ol. This maximum was attributed to a destabilisation of the initial state of the hydroxide-ion catalysed hydrolysis. This destabilisation of the initial state has been shown to originate from the unfavourable Gibbs energy of transfer of the hydroxide anion from water to water with cosolute, more than cancelling the corresponding favourable Gibbs energy of transfer of **3.1a**. For neutral hydrolysis of **3.1a** in aqueous solutions containing 2-methylpropan-2-ol,[20]

G(c) equals –392 J kg mol^{-2}. G(c) for the same reaction in the presence of phenylalaninamide hydrochloride[16] is –1869 J kg mol^{-2}. Compared to solutions with added 2-methylpropan-2-ol, this pattern indicates that the standard chemical potential of **3.1a** is lowered more in solutions with added phenylalaninamide. Therefore, added phenylalaninamide could lead to a rate decrease if the stabilising effect of phenylalaninamide more than cancels the expected destabilising effect of phenylalaninamide on the hydroxide anion. However, the effect of phenylalaninamide on the standard chemical potential of hydroxide anion is unknown. Hence, reliable estimates of k_{OH} cannot be made.[21]

The values for pK_a obtained using Equation 3.7 as given in Table 3.2 are both higher than literature values. Together with the observed pattern in the deviation between the experimental and calculated values (Figure 3.3, right hand side), this trend indicates that Equation 3.7 underestimates the rate constants at higher pH. As nucleophilic substitution can be general-base catalysed, the increasing molalities of unprotonated amine not only increase nucleophile molalities, but also increase catalyst molalities. In addition, at lower pH, the rate constants might be underestimated as a result of inhibition of reaction by the protonated amine. In order to test the hypothesis of general-base catalysed nucleophilic substitution, the effect of both ethanoate/ethanoic acid and butanoate/butanoic acid buffers on the rate of reaction of **3.1a** with phenylalaninamide was determined (Figure 3.4).

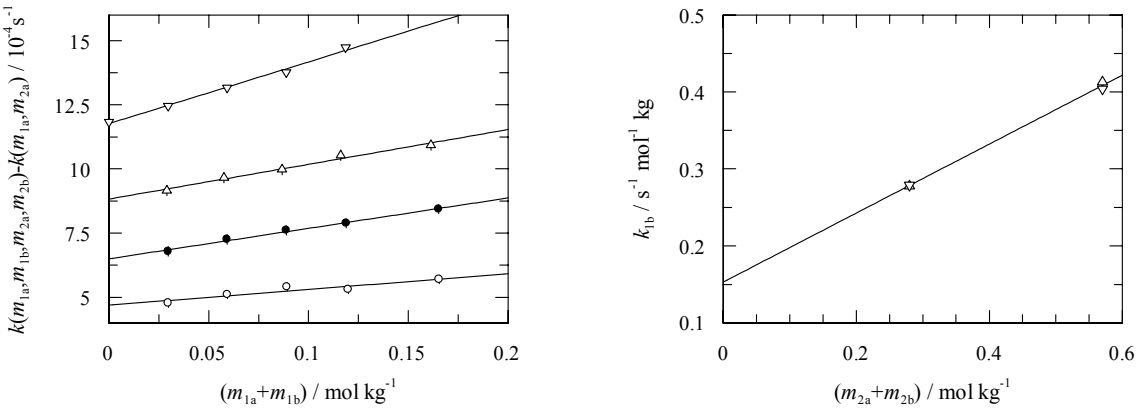

Figure 3.4: Reactivity of **3.1a** with alaninamide and phenylalaninamide in the presence of ethanoate/ethanoic acid and butanoate/butanoic acid buffers. *Left:* The contributions of general-base catalysed hydrolysis and nucleophilic substitution to the observed rates as a function of total molality of protonated alaninamide and alaninamide (m_{1a} + m_{1b}) at total concentrations of ethanoate/ethanoic acid (3:1) buffers (m_{2b}+m_{2a}) of 0.27 (o), 0.44 (•), 0.56(Δ) and 0.75 (∇) mol kg^{-1}. *Right*: Second-order rate constant k_{1b} for nucleophilic substitution by phenylalaninamide as a function of total molality (m_{2a}+m_{2b}) of ethanoate/ethanoic acid (Δ) and butanoate/butanoic acid (∇) molality.

According to the plot on the left hand side of Figure 3.4, the rate of reaction between **3.1a** and alaninamide increases with increasing buffer concentration.[22] A similar pattern is found for the reaction of phenylalaninamide with **3.1a**. This pattern suggests that general-base catalysed nucleophilic substitution is indeed occurring,[23] which explains the deviating pK_a-values from the curve fits. From a plot of the corresponding second-order rate constants as a function of total buffer molality $m_{2a}+m_{2b}$ (Figure 3.4, right hand side), the rate constant for uncatalysed nucleophilic substitution k_{nuc} can be determined. For phenylalaninamide, a value of 0.153±0.007 s^{-1} mol^{-1} kg is obtained (*cf.* Table 3.2). Unfortunately, based on the available data, a value for k_{nuc} for alaninamide cannot be determined.

Using hydroxylamine, an even higher reactivity than that observed for alaninamide and phenylalaninamide was found, despite its lower pK_a (Figure 3.5).

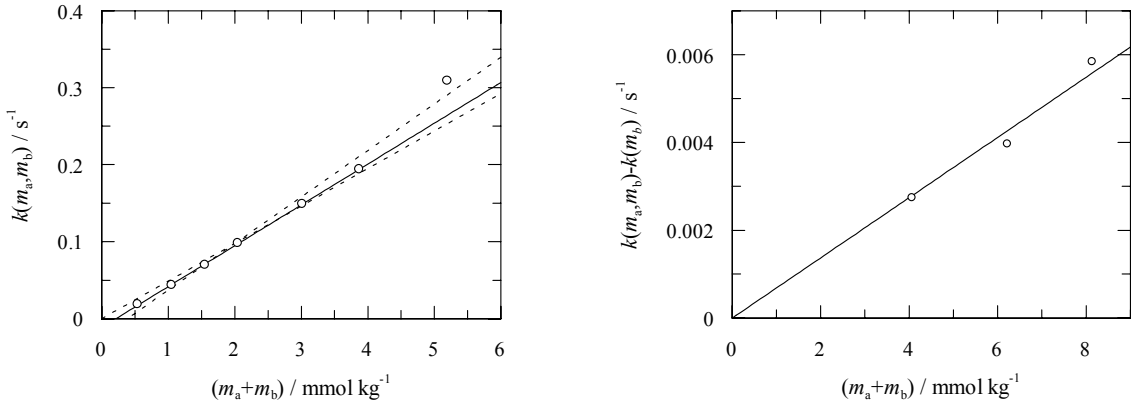

Figure 3.5: Reactivity of **3.1a** in the presence of hydroxylamine and protonated hydroxylamine. Concentrations are total concentrations. *Left*: hydroxylamine and protonated hydroxylamine in 1:1 ratio, pH=5.91±0.06. Dotted lines indicate error margins (see reference 24). *Right*: protonated hydroxylamine (hydroxylamine hydrochloride), pH=3.76±0.03.

The observed rate constant[24] of 53.1±7.4 s^{-1} mol^{-1} kg (104.9±14.8 s^{-1} mol^{-1} kg based on only neutral hydroxylamine, whereas for the protonated hydroxylamine $k_{HONH2.HCl}$=0.69±0.03 s^{-1} mol^{-1} kg) is exceptionally high. Based on the pK_a of 5.96[25] and Equation 3.6, the expected rate constant is 40.1 10^{-4} s^{-1} mol^{-1} kg for general-base catalysis. This large discrepancy between the predicted value for general-base catalysed hydrolysis and the observed value again strongly suggests that the reaction pathway that is followed is not general-base catalysed hydrolysis. The high reactivity of hydroxylamine is often accounted for in terms of the α-effect,[26] therefore the results are indicative of nucleophilic attack on **3.1a**. Hydroxylamine

has two nucleophilic centers (of different reactivity), further enhancing reactivity. Nucleophilic attack by hydroxylamine will occur on the amide functionality of **3.1a**, eventually leading to *N*-hydroxybenzamide.[27]

Using *n*-propyl- and *n*-pentylamine as well as benzylamine, again high reactivities were found but the observed rate constants were not linear with concentration of general base (Figure 3.6). We attribute this pattern to general-base catalysed nucleophilic substitution,[7] but general-acid catalysis (by the conjugate acids) cannot be excluded.[6,28,29]

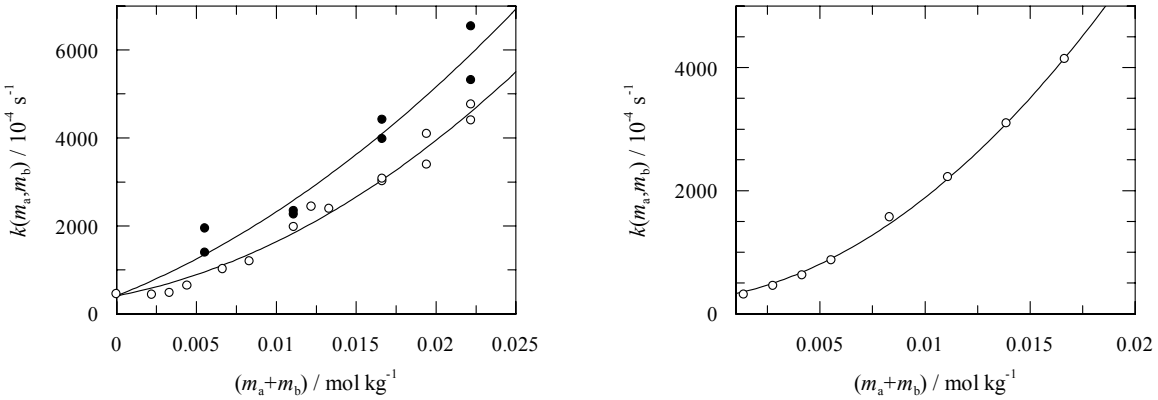

Figure 3.6: Observed rates of reaction for **3.1a** in the presence of *Left*: *n*-propylamine (o) and *n*-pentylamine (•). Buffer ratios are 1:9 (base:acid), pH=9.54±0.07 for *n*-propylamine and 9.53±0.03 for *n*-pentylamine. *Right*: benzylamine (o). Buffer ratio is 1:1 (base:acid) and pH=9.34±0.04.

The observed rate constants were fitted to Equation 3.8

$$k(m_c) = k_{\mathrm{pH}} + k_{\mathrm{2nd}} \cdot m_c + k_{\mathrm{3rd}} \cdot m_c^2 \qquad (3.8)$$

Here, k_{pH} is the (pseudo-) first-order rate constant for reaction in the absence of added general base at the experimental pH; k_{2nd} is the second-order rate constant based on total buffer concentration for nucleophilic substitution (and a minor fraction general-base catalysed hydrolysis) by cosolute c, m_{c} is the molality of cosolute c and k_{3rd} is the third-order rate constant for the general-base catalysed nucleophilic substitution. Assuming that general-base catalysed hydrolysis makes a negligible contribution to the observed rate, k_{nuc} can be calculated (Table 3.3) from k_{2nd}.[30]

Table 3.3: Nucleophilic substitution of **3.1a** in aqueous solution at 298.2 K in the presence of amine/ammonium HCl buffers.[a,b]

	n-propylamine	*n*-pentylamine	benzylamine
pK_a	10.66[31]	10.64[32]	9.36[33]
k_{2nd} / s^{-1} kg mol^{-1}	6.9±1.8	14.5±4.6	5.5±0.8
k_{nuc} / s^{-1} kg mol^{-1}	69±18	145±46	11.1±1.6
k_{3rd} / s^{-1} kg^2 mol^{-2}	5.4±1.0	4.6±2.4	10.7±0.6

[(a)] Errors are standard errors based on a least-squares fit of the kinetic data using Equation 3.8. [(b)] $k_{nuc}=10 \cdot k_{2nd}$, the rate effect of the protonated amine in this concentration range is expected to be negligible.[34]

According to Table 3.3, *n*-pentylamine provides the most effective non-catalysed (by general base) nucleophilic substitution. However, the increase in reactivity appears to be too large to be solely caused by the difference in pK_a and different steric effects. This increase in reactivity points towards more favourable interactions between *n*-pentylamine and **3.1a** compared to those between *n*-propylamine and **3.1a**. The second-order terms (in amine), however, are comparable (though care has to be taken in interpreting the value for *n*-pentylamine) suggesting that self-association of *n*-pentylamine is comparable to self-association of *n*-propylamine. Previously, for nucleophilic substitution of sufficiently hydrophobic *p*-nitrophenyl esters by hydrophobic amines, the second-order (in nucleophile) process was found to be more effective because the reactants tend to cluster.[35,36]

The reactivity of benzylamine in comparison with that of the alkylamines is surprisingly high taking into account its lower pK_a. Given the present data set, the second-order term (in amine) cannot be compared to second-order terms for the alkylamines. The buffer ratio is different and the influence of basicity (or acidity) on general-base (or general-acid) catalysis of nucleophilic substitution is unknown, because Brønsted plots for general-base catalysis and general-acid catalysis of nucleophilic substitution have not been determined.[19]

An experiment, conducted under the conditions of the kinetic runs, was performed on a mg (of substrate) scale. Benzylamine was used as nucleophile and **3.1b** instead of **3.1a** was used as substrate. Both ^{1}H-NMR and ^{13}C-NMR spectra of the product correspond to literature spectra of *N*-benzyl benzamide,[37-39] corroborating the view that nucleophilic substitution did indeed take place. Reaction between **3.1b** and phenylamine in benzene was shown to yield *N*-phenyl benzamide.[40] Moreover, **3.1b** has been used as benzoylation reagent in dry

cyanomethane,[41] both consistent with the possibility of nucleophilic substitution of **3.1b** and the related **3.1a**.

An overall Brønsted plot of rate constants for general-base catalysed hydrolysis k_b and uncatalysed nucleophilic substitution k_{nuc} of **3.1a** (both indicated by $k_{\mathbf{3.1a}}$) shows considerable scattering (Figure 3.7).[42]

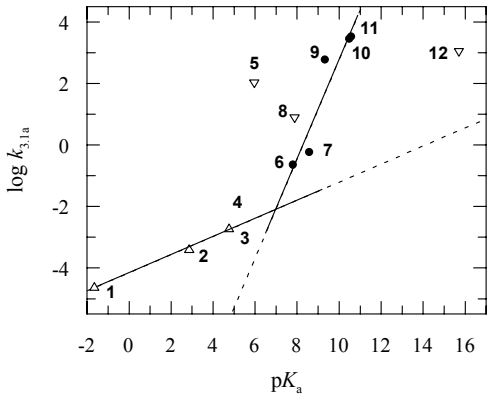

Figure 3.7: Plots of k_b and k_{nuc} (indicated by $k_{\mathbf{3.1a}}$) vs. pK_a for **3.1a**. General-base catalysis (Δ) by: water (1), chloroethanoate (2), ethanoate (3) and butanoate (4). Nucleophilic substitution by amines (•) *viz.*: phenylalaninamide (6), alaninamide (7), benzylamine (9), propylamine (10) and pentylamine (11). Nucleophilic substitution by other compounds (∇) *viz.*: hydroxylamine (5), aspartame (8) and hydroxide (12). Line through the data for amines was drawn to guide the eye.

For general bases with comparable nucleophilic groups, a correlation is obtained between observed rate constant and pK_a. However, the correlation does not extend over different groups of bases, in agreement with extensive literature data.[43,44] Remarkably, observed rate constants for aromatic amines acting as a nucleophile seem to be consistently higher than those for nonaromatic amines would have been, *i.e.*, the data points for aromatic amines lie above and to the left of a line through the nonaromatic amines.

An interesting case is presented by aspartame (AspPheOMe), Scheme 3.4.

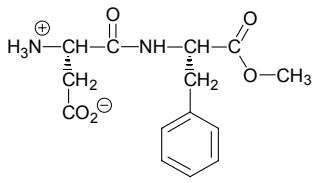

Scheme 3.4

Aspartame offers a number of functional groups, the carboxylic acid and the amine being the most important for the present study. The carboxylate group is expected

to be a general-base catalyst in the hydrolysis reaction of **3.1a**. The amine group will act as nucleophile, the relative importance of both reactions being dependent on the degree of protonation of both groups. From the pK_a of the carboxylic acid functionality[45,46] of 3.2, we conclude that in the molality range up to 0.044 mol kg^{-1} of aspartame, the contribution of the carboxylate group to the observed rate of reaction is negligible. The pH – rate profile for reaction of **3.1a** with aspartame at 3 different concentrations of aspartame is given in Figure 3.8.

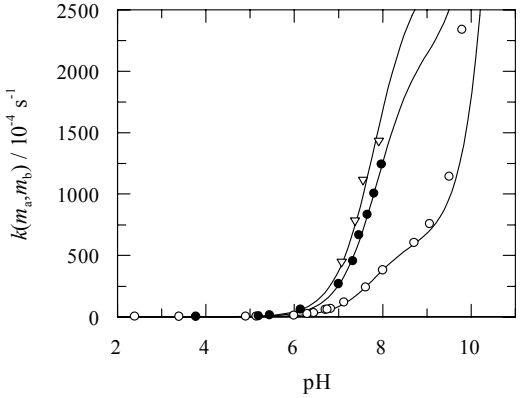

Figure 3.8: pH - rate profile for **3.1a** in the presence of different total molalities m_a+m_b of aspartame;[47] 0.007 mol kg^{-1} (o), 0.028 mol kg^{-1} (•) and 0.044 mol kg^{-1} (∇). Lines are fits to Equation 3.7 with k_{OH} set to 1200 dm^3 mol^{-1} s^{-1}.

From the nonlinear least-squares fits of the observed rate profiles to Equation 3.7 with k_{OH} set to 1200 dm^3 mol^{-1} s^{-1},[15] the second-order rate constant for nucleophilic substitution on **3.1a** by aspartame is 7.8±0.2 s^{-1} mol^{-1} kg. As can be seen from Figure 3.7, this rate constant for nucleophilic substitution is clearly much higher than anticipated. We attribute this increase to two factors. First, aspartame is a rather hydrophobic molecule, which could form hydrophobically-stabilised encounter complexes, *cf.* the effect of benzylamine. Second, the nucleophilic substitution by aspartame can be general-base catalysed by the carboxylate functionality, thereby greatly enhancing the nucleophilicity of aspartame (Scheme 3.5).[48]

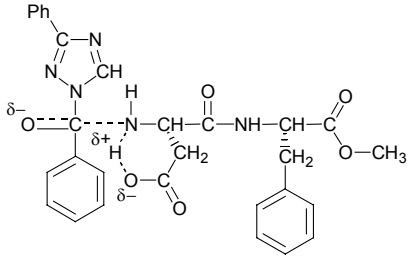

Scheme 3.5

3.2.3 GENERAL-BASE CATALYSED HYDROLYSIS AND UNCATALYSED NUCLEOPHILIC SUBSTITUTION ON 1-BENZOYL-3-PHENYL-1,2,4-TRIAZOLE; A LINEAR FREE ENERGY RELATIONSHIP

Reactivity of general bases in nucleophilic substitution is roughly correlated with their basicity.[49] However, there are many factors influencing reactivity other than basicity,[50] the most important being the elusive α-effect[26] and steric factors. Often, nucleophilicity varies with basicity within a series of compounds, which can be attributed to differences in solvation of different nucleophilic groups and a difference in hardness/softness of the nucleophile. In view of the failure of basicity as an indicator of nucleophilicity, alternative scales of nucleophilicity have been developed, most importantly Ritchie's N_+[51] (for nucleophilic addition on sp^2 carbon) and the Swain and Scott[52] n-parameter (for nucleophilic substitution on sp^3 carbon). There are links between the two scales,[53] but a unifying scale for nucleophilicity does not exist.

We compare rate constants for uncatalysed nucleophilic substitution and general-base catalysed hydrolysis of **3.1a** with the rate constants for the same reactions of *p*-nitrophenyl ethanoate (*p*-NPA). There is ample[54] experimental data on nucleophilic substitution on *p*-NPA[5,55-58] and the available data for *p*-NPA form a reliable basis for linear free energy relationships (LFERs).[59] Most importantly, however, the change in reaction pathway from general-base catalysed hydrolysis to nucleophilic substitution of **3.1a** is mirrored by *p*-NPA. Both are carbonyl compounds showing approximately the same reactions with added general bases. Also, the anions of both 3-phenyl-1,2,4-triazole and 4-nitrophenol are reasonably good leaving groups based on the pK_a-values of the parent compounds of 9.58[60] and 7.15,[61] respectively.

When log $k_{\mathbf{3.1a}}$ is plotted as a function of log $k_{p\text{-NPA}}$ for different bases/nucleophiles, a linear correlation is found (Figure 3.9) with a slope of 0.91. The correlation includes data points for hydroxylamine (an α-effect nucleophile) and hydroxide anion (a charged nucleophile).

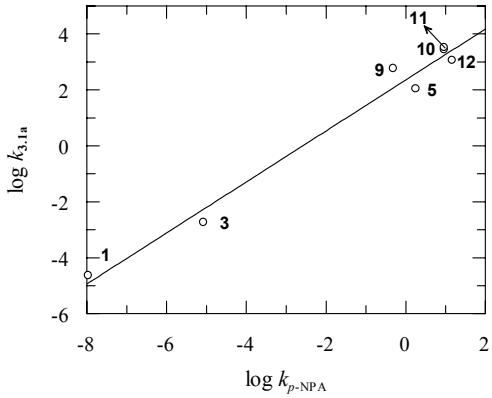

Figure 3.9: Linear free energy relationship between nucleophilic substitution on **3.1a** and nucleophilic substitution on *p*-NPA by different bases/nucleophiles. Numbering as in Figure 3.7.

Interestingly, the LFER spans regions of different reactivity; general-base catalysed hydrolysis for both **3.1a** and *p*-NPA by water (1) and ethanoate (3)[62] and nucleophilic substitution by hydroxylamine (5) benzylamine (9), propylamine (10), pentylamine (11) and hydroxide (12). This pattern is in line with the argument formulated by Jencks[63] that "such a correlation shows only that the two compounds being compared have similar transition states for each individual reaction under consideration; if there is a change in the nature of the transition state with changing nucleophile … the correlation shows that this change takes place in a similar manner for both compounds."

We conclude that the enhanced reactivity compared to what would be expected on the basis of general-base catalysis alone is indeed caused by a change in mechanism to nucleophilic substitution. The linear free energy relationship also allows reliable estimates to be made of the rates of uncatalysed nucleophilic substitution on **3.1a**.

3.2.4 GENERAL-BASE CATALYSIS, NUCLEOPHILIC SUBSTITUTION AND INHIBITION

As described above, a range of possible interactions between cosolute and hydrolytic probe sometimes results in rather complex reactivity patterns. For example, phenylalaninamide and alaninamide show rate decreasing effects in their protonated forms, but are strong nucleophiles in their deprotonated forms. Similarly, the effect of the carboxylate buffers is a composite effect of the rate retardation by the protonated form and catalysis by the carboxylate.

Previously,[64] rate effects induced by α-amino acids have been studied at a pH of 4.0, at which the α-amino acids are present mainly in their zwitterionic forms. Rate-

enhancing effects were found for a range of α-amino acids and even for some of their derivatives. Rate enhancing effects were not found to correlate with the pK_a of the carboxylic acid moiety. Furthermore, the kinetic solvent isotope effect did not change significantly and no linearity of the slope of k_{obsd} versus molality of cosolute was observed. Hence, the kinetic effects were "not governed by general-base catalysis of the α-amino acid carboxylate group, but involve medium effects instead."[64] The kinetic analyses presented here, however, indicate that apart from general-base catalysis by the α-amino acid carboxylate group, nucleophilic substitution by the α-amino acid amine group is also a possible reaction pathway. Consequently, the observed rate effects are rather difficult to interpret, as a linear Brønsted plot is not to be expected. In addition, given the observed *G*(c)-values and the data in Figure 4.1 of reference 64, it is difficult to draw conclusions about the linearity of the observed rate effects with molality of cosolute. This is especially the case since possible general-base or general-acid catalysis will produce deviations from linearity in plots of $k(m_c)$ *versus* molality. The deviation is towards higher $k(m_c)$ at higher molalities, which can coincidentally produce good linear plots of $\ln(k(m_c)/k(m_c=0)$ against cosolute molality m_c. Finally, the observed kinetic solvent isotope effect of 2.49 for the hydrolysis of **3.1a** in 0.5 mol kg^{-1} glycine at pH 4 is very similar to 2.69 observed for the reaction in water at pH 4 without cosolute. Unfortunately, however, this value will be influenced by the increase in pK_a of both the α-amino acid carboxylate and the α-amino acid amine functionality upon changing the solvent from H_2O to D_2O. The increase in pK_a for the glycine carboxylate group[65] of 0.39 results in a larger fraction of the α-amino acid carboxylate group becoming neutralised. Together with the expected kinetic solvent isotope effect, this leads to a decrease in rate constant. Consequently, the observed rate of the nucleophilic substitution reaction will be decreased, even though no proton transfer takes place in the uncatalysed nucleophilic substitution reaction. The increase in pK_a of the α-amino acid amine functionality[65] of 0.63 results in fewer free amine groups available for reaction, also leading to a decrease in observed rate constant. Hence, the similarity in kinetic solvent isotope effects could be merely coincidental, which interfered with the interpretation of the result obtained for α-amino acids.

We contend that for the least hydrophobic α-amino acids, rate-retarding effects are negligible and only rate enhancements are observed caused by general-base catalysed hydrolysis and nucleophilic substitution.[64] The effect of general-base

catalysis of hydrolysis can be calculated using Equation 3.6, pK_a-values of the α-mino acids[66] and pH (Table 3.4).

Table 3.4: Reactivity of **3.1a** in aqueous solution at 298.2 K in the presence of α-amino acids.

α-amino acid	pK_a[a]	G(c) / J kg mol^{-2}	$k(m_c=m_o)$ / 10^{-4} s^{-1}	$m_b \cdot k_b$[b] / 10^{-4} s^{-1}	k_{nuc} / 10^2 kg mol^{-1} s^{-1}
glycine	2.35, 9.78	875±21	24.5±0.5	2.8±1.3	5.8±1.5
alanine	2.34, 9.69	558±16	19.0±0.3	2.7±1.2	2.0±0.8
valine	2.32, 9.62	467±9	17.6±0.2	2.7±1.2	1.2±0.6
leucine	2.36, 9.60	518±21	18.4±0.4	2.8±1.3	1.4±0.6

[a] In the calculation of the errors in G(c), $m_b \cdot k_b$ and k_{nuc}, the errors in the pK_a-values have been set to 0.05 and 0.1 for the first and second pK_a, respectively. [b] Calculated using Equation 3.6

If the residual observed rate enhancements are attributed to uncatalysed nucleophilic substitution by free amine, excellent correlation is again observed (Figure 3.10) with data for *p*-NPA.

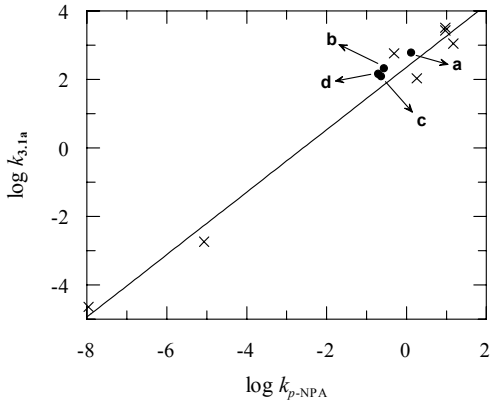

Figure 3.10: Data for nucleophilic substitution on **3.1a** by α-amino acids (•) glycine (a), alanine (b), valine (c) and leucine (d) compared to the LFER as described in Figure 3.9 (x).

Hence, even though the fraction of unprotonated amine functionalities is of the order of ppm, the unprotonated amine functionality of α-amino acids is strongly nucleophilic, rendering nucleophilic substitution kinetically detectable at a pH as low as 4.0 for hydrophilic α-amino acids. More hydrophobic α-amino acids, however, show rate retardation as the main effect at a pH of 4.0. However, the observed rate retardations will be a combined effect of inhibition by the hydrophobic α-amino acid, general-base catalysis and nucleophilic substitution.

3.3 CONCLUSIONS

In aqueous solutions containing general bases, activated amide **3.1a** is subject to water-catalysed hydrolysis, general-base catalysed hydrolysis with a Brønsted β of 0.29 and nucleophilic substitution with a Brønsted β of approximately 0.91 for amine nucleophiles. In certain cases, nucleophilic substitution is general-base and/or general-acid catalysed. Reactivities of more hydrophobic general bases seem to be consistently higher than reactivities of hydrophilic general bases supporting an explanation based on the formation of hydrophobically-stabilised encounter complexes. In future studies, rate effects of cosolutes, in particular rate-enhancing effects, should be scrutinised for unexpected catalytic effects or changes in mechanism. In the present study we have shown that small fractions of compounds present in, *e.g.*, a deprotonated state, albeit in ppm, can induce large rate effects.

3.4 EXPERIMENTAL

3.4.1 KINETIC EXPERIMENTS

Aqueous solutions were prepared by weight immediately before use. Buffers were prepared by partially (to the desired buffer ratio) neutralising the corresponding acid by adding the appropriate amount of 1.000 mol l^{-1} aqueous NaOH by volume or by weight. Buffer ratios were routinely accurate to within 1%. Buffer solutions containing *n*-propylamine and *n*-pentylamine were prepared by addition of the appropriate amount of 1.000 M aqueous HCl within 2 minutes prior to monitoring the reaction of **3.1a** in order to prevent evaporation of the volatile amines from the solutions. Water was distilled twice in an all-quartz distillation unit. All reactions were monitored at 273 nm (or the lowest possible wavelength above 273 nm if a given cosolute had absorption bands at that wavelength) and at 25.0±0.1°C. Amide **3.1a** was injected as 5-7 μl of a stock solution containing **3.1a** in cyanomethane into about 2.8 ml of an aqueous solution of cosolute in a concentration range in which the reaction could be followed in a stoppered 1.000 cm quartz cuvette. The resulting concentrations were about 10^{-5} mol dm^{-3} or less. The pH of all solutions was checked at the end of each kinetic experiment using either a ROSS Semi-micro combination pH electrode or a SENTRON ISFET pH probe and was found to correspond well (not more than 0.2 pK_a units below) with the predicted pH from the

pK_a and the buffer ratio. NMR spectra were recorded on Varian Gemini 200 (^{1}H: 200 MHz) and VXR 300 (^{1}H: 300 MHz) spectrometers.

3.4.2 MATERIALS

All buffers were made from commercially available acids, alkylamines or benzylamine (from Acros or Aldrich) using aqueous NaOH or aqueous HCl of known concentration (Titrisol®). Aspartame was kindly provided by Prof. Dr. H.E. Schoemaker (DSM / University of Amsterdam), 1-benzoyl-3-phenyl-1,2,4-triazole (**3.1a**) and 1-benzoyl-1,2,4-triazole were synthesised according to literature procedures.[15,67]

3.5 ACKNOWLEDGEMENTS

Dr. Matt Fielden is thanked for helpful mechanistic discussion.

3.6 REFERENCES AND NOTES

(1) Part of this chapter is to be published: Buurma, N. J., Blandamer, M. J. and Engberts, J. B. F. N. in press.

(2) Karzijn, W. and Engberts, J. B. F. N. *Tetrahedron Lett.* **1978**, 1787-1790.

(3) Second-order and third-order rate constants in this chapter are given with units s^{-1} mol^{-1} kg and s^{-1} mol^{-2} kg^2, respectively. These unconventional units facilitate comparison with and introduction of *G*(c)-values. The exceptions are rate constants for hydroxide-catalysed hydrolysis, given in s^{-1} mol^{-1} dm^3, as hydroxide concentrations were calculated from the pH of the solutions.

(4) There are many different pathways for reactions of nucleophiles with amides and esters. The exact pathway depends on factors such as leaving group ability, nucleophilicity and solvent. In this chapter, we will only discuss those reactions pathways, that, we contend, are relevant for the system under study.

(5) Johnson, S. L. *Adv. Phys. Org. Chem.* **1967**, *5*, 237-330.

(6) Bruice, T. C., Donzel, A., Huffman, R. W. and Butler, A. R. *J. Am. Chem. Soc.* **1967**, *89*, 2106-2121.

(7) Bruice, T. C., Hegarty, A. F., Felton, S. M., Donzel, A. and Kundu, N. G. *J. Am. Chem. Soc.* **1970**, *92*, 1370-1378.

(8) Streefland, L., Blandamer, M. J. and Engberts, J. B. F. N. *J. Am. Chem. Soc.* **1996**, *118*, 9539-9544.

(9) The basic form of the added cosolute was assumed to exert only a catalysing effect. Fitting data to an equation related to Equation 3.3, in which the acidic form is assumed to inhibit only the water-catalysed reaction, leads to less satisfactory fits. Introducing an additional parameter to distinguish between rate-retarding effects on the water-catalysed and on the base-catalysed hydrolysis seems unjustifiable.

(10) All pK_a-values, except those for the α-amino acids and hydroxylamine, were obtained from a literature search using the Beilstein Crossfire system. Available values were collected, assessed and averaged. Only one, representative, reference is given for every pK_a.

(11) Headley, A. D., Starnes, S. D., Wilson, L. Y. and Famini, G. R. *J. Org. Chem.* **1994**, *59*, 8040-8046.

(12) Niazi, M. S. K. *J. Chem. Eng. Data* **1993**, *38*, 527-530.

(13) Admittedly, the number of data points used to contruct the Brønsted plot is low. However, as the Brønsted plot constructed here resembles the plot for structurally similar **3.1b** (see reference 15), we trust that additional data does not lead to a dramatic change in the derived Equation 3.6.

(14) Karzijn, W. and Engberts, J. B. F. N. *Recl. Trav. Chim. Pays-Bas* **1983**, *102*, 513-515.

(15) Karzijn, W., *The water- and hydroxide-ion catalyzed hydrolysis of 1-acyl-1,2,4-triazoles*, PhD Thesis, Rijksuniversiteit Groningen, **1979**

(16) Streefland, L., Blandamer, M. J. and Engberts, J. B. F. N. *J. Phys. Chem.* **1995**, *99*, 5769-5771.

(17) Chambers, R. W. and Carpenter, F. H. *J. Am. Chem. Soc.* **1955**, *77*, 1522-1526.

(18) The UV/Vis properties of amides, the expected products of nucleophilic substitution reactions, are only slightly different from those of the products of hydrolysis. Hence the spectral changes upon reaction (followed at a single wavelength) give no information about the actual reaction occurring, other than that the amide functionality is reacting. However, comparison with literature (see Ley, H.; Specker, H. *Chem. Ber.* **1939**, *72*, 192-202 and Moser, C. M.; Kohlenberg, A. I. *J. Chem. Soc.* **1951**, 804-809) reveals that the difference spectrum upon reaction is in accord with formation of an amide instead of a carboxylate.

(19) Fox, J. P. and Jencks, W. P. *J. Am. Chem. Soc.* **1974**, *96*, 1436-1449.

(20) Blokzijl, W., Engberts, J. B. F. N. and Blandamer, M. J. *J. Am. Chem. Soc.* **1990**, *112*, 1197-1201.

(21) Related to the unknown effect of the added cosolute on the standard chemical potential of the hydroxide anion, the effect of added cosolute on the water self-ionisation constant is unknown. Hence, using $[OH^-]$ based on the observed pH should be done with caution.

(22) The contribution of general-base catalysed hydrolysis and (general-base catalysed) nucleophilic substitution is calculated from the observed rate constant $k(m_{1a},m_{1b},m_{2a},m_{2b})$ and the calculated rate constant of the water-catalysed reaction in the presence of only the rate retarding protonated cosolutes $k(m_{1a},m_{2a})$. The values obtained in this way were not corrected for rate retarding effects.

(23) Unfortunately, using the present data, a salt effect on (instead of general-base catalysis of) nucleophilic substitution cannot be excluded because the experiments were not done under conditions of constant ionic strength. The reason for not using conditions of constant ionic strength is that our initial interest was in hydrophobic interactions instead of the (unexpected) changes in mechanism.

(24) Error margins are based on inclusion of the apparent outlier at 5.2 mmol kg^{-1} and the notion that a negative intercept is physically unrealistic. The negative intercept could be caused by two factors. First, a small change in protonation (pH decreases slightly) upon dilution of the hydroxylamine buffer stock solution. Second, a second-order (in total hydroxylamine molality) term corresponding to general-base or general-acid catalysed nucleophilic substitution. Both effects would lead to an overestimate of the second-order rate constant of reaction.

(25) Kallies, B. and Mitzner, R. *J. Phys. Chem. B* **1997**, *101*, 2959-2967.

(26) Edwards, J. O. and Pearson, R. G. *J. Am. Chem. Soc.* **1961**, *84*, 16-24.

(27) Surprisingly, the hydroxyl moiety is most nucleophilic in hydroxylamine in case p-nitrophenyl ethanoate is the substrate undergoing nucleophilic attack, resulting in an initial excess of the product from nucleophilic attack by the hydroxyl moiety. However, this initial unstable product can react further to *N*-hydroxybenzamide (see *e.g.* Jencks, W. P. *J.Am.Chem.Soc.* **1958**, *80*, 4581-4584 and 4585-4588 and reference 56). The zwitterionic form of hydroxylamine is not present in detectable amounts (see *e.g.* references 56 and 25), practically excluding the O-deprotonated hydroxylamine as the nucleophile.

(28) Jencks, W. P. and Carriuolo, J. *J. Am. Chem. Soc.* **1960**, *82*, 675-681.

(29) Bruice, T. C. and Mayahi, M. F. *J. Am. Chem. Soc.* **1960**, *82*, 3067-3071.

(30) A solvent kinetic isotope effect of 1.6 was found for the reaction. However, many factors influence this isotope effect, including the shift in pK_a of the amine upon changing from H_2O to D_2O as the solvent.

(31) Lin, B., Islam, N., Friedman, S., Yagi, H., Jerina, D. M. and Whalen, D. L. *J. Am. Chem. Soc.* **1998**, *120*, 4327-4333.

(32) Hoerr, C. W., McCorkle, M. R. and Ralston, A. W. *J. Am. Chem. Soc.* **1943**, *65*, 328-329.

(33) Arrowsmith, C. H., Guo, H. X. and Kresge, A. J. *J. Am. Chem. Soc.* **1994**, *116*, 8890-8894.

(34) Hol, P., Streefland, L., Blandamer, M. J. and Engberts, J. B. F. N. *J. Chem. Soc. , Perkin Trans. 2* **1997**, 485-488.

(35) Oakenfull, D. *J. Chem. Soc. , Perkin Trans. 2* **1973**, 1006-1012.

(36) Oakenfull, D. *J. Chem. Soc. , Chem. Commun.* **1970**, 1655-1656.

(37) Keck, G. E., Wager, T. T. and McHardy, S. F. *Tetrahedron* **1999**, *55*, 11755-11772.

(38) Darbeau, R. W. and White, E. H. *J. Org. Chem.* **1997**, *62*, 8091-8094.

(39) Knowles, H. S., Parsons, A. F., Pettifer, R. M. and Rickling, S. *Tetrahedron* **2000**, *56*, 979-988.

(40) Purygin, P. P. and Pankov, S. V. *Russ. J. Org. Chem.* **1996**, *32*, 871-873.

(41) Humpf, H. U., Berova, N., Nakanishi, K., Jarstfer, M. B. and Poulter, C. D. *J. Org. Chem.* **1995**, *60*, 3539-3542.

(42) In the LFERs, only the linear terms describing the bimolecular (uncatalysed) nucleophilic substitution reaction have been used.

(43) Heo, C. K. M. and Bunting, J. W. *J. Chem. Soc. , Perkin Trans. 2* **1994**, 2279-2290.

(44) Bruice, T. C. and Lapinski, R. *J. Am. Chem. Soc.* **1958**, *80* , 2265-2267.

(45) Maheswaran, M. M. and Divakar, S. *Indian J. Chem. , Sect. A* **1991**, *30*, 30-34.

(46) Skwierczynski, R. D. and Connors, K. A. *Pharm. Res.* **1993**, *10*, 1174-1180.

(47) The stability of aspartame under these conditions is reasonable in comparison with the reaction under study, see reference 46. The pH of aspartame solutions was adjusted (from a pH in the range of 4-7) immediately before performing the measurement.

(48) Aspartame can be cyclised, rendering the molecule nonnucleophilic. It is interesting to think of this molecule as a general-base catalyst of hydrolysis. The molecule consists of two α-amino acids, has a hydrophobic "binding site" and a "catalytic center".

(49) Comparing basicities of nucleophiles with kinetic nucleophilic reactivities towards carbon compounds is not a proper rate-equilibrium comparison, Parker and Hine developed the concept of "carbon basicity". See Parker, A. J. *Proc.Chem.Soc.* **1961**, 371 and Hine, J.; Weimar Jr, R. D. *J.Am.Chem.Soc.* **1965**, *87*, 3387-3396.

(50) Bunnett, J. F. *Ann. Rev. Phys. Chem.* **1963**, *14*, 271-290.

(51) Ritchie, C. D. *Can. J. Chem.* **1986**, *64*, 2239-2250.

(52) Swain, C. G. and Scott, C. B. *J. Am. Chem. Soc.* **1953**, *75*, 141-147.

(53) Bunting, J. W., Mason, J. M. and Heo, C. K. M. *J. Chem. Soc. , Perkin Trans. 2* **1994**, 2291-2300.

(54) Only references to literature used for the present study are given.

(55) Acher, F. and Wakselman, M. *J. Org. Chem.* **1984**, *49*, 4133-4138.

(56) Jencks, W. P. and Carriuolo, J. *J. Am. Chem. Soc.* **1960**, *82*, 1778-1786.

(57) Jencks, W. P. and Gilchrist, M. *J. Am. Chem. Soc.* **1968**, *90*, 2622-2637.

(58) Tee, O. S., Gadosy, T. A. and Giorgi, J. B. *Can. J. Chem* **1997**, *75*, 83-91.

(59) Gregory, M. J. and Bruice, T. C. *J. Am. Chem. Soc.* **1967**, *89*, 2121-2125.

(60) Kröger, C.-F. and Freiberg, W. *Z. Chem.* **1965**, *5*, 381-382.

(61) Mock, W. L. and Morsch, L. A. *Tetrahedron* **2001**, *57*, 2957-2964.

(62) Butler, A. R. and Gold, V. *J. Chem. Soc.* **1962**, 1334-1339.

(63) Fersht, A. R. and Jencks, W. P. *J. Am. Chem. Soc.* **1970**, *92*, 5442-5452.

(64) Streefland, L., *Effects of overlap of hydration shells on noncovalent interactions in aqueous solution*, PhD Thesis, University of Groningen, **2000**. Available online: http://www.ub.rug.nl/eldoc/dis/science/e.streefland/

(65) Li, N. C., Tang, P. and Mathur, R. *J. Phys. Chem.* **1961**, *65*, 1074-1076.

(66) "Handbook of Biochemistry and Molecular Biology, Proteins" 3rd edition, (Fasman, G. D., ed.). CRC Press, Cleveland, Ohio, **1976**.

(67) a) Staab, H. A., Lüking, M. and Dürr, F. H. *Chem. Ber.* **1962**, *95*, 1275-1283. b) Mooij, H. J., Engberts, J. B. F. N. and Charton, M. *Recl.Trav.Chim.Pays-Bas* **1988**, *107*, 185-189.

Hydrolysis in Aqueous Solutions Containing Hydrotropes[1]

The effect of added hydrotropes on the rates of neutral hydrolysis of 1-benzoyl-3-phenyl-1,2,4-triazole ***4.1*** *has been studied, together with the molality dependence of the* ^{1}*H-NMR spectra of the hydrotropes in aqueous solution. Hydrotropes include sodium 4-alkylbenzenesulfonates* ***4.2a-e****, sodium 4-methoxybenzenesulfonate* ***4.2f****, sodium 4-hydroxybenzene-sulfonate* ***4.2g****, caesium benzenesulfonate* ***4.3****, benzamidinium chloride* ***4.4****, phenyltrimethylammonium bromide* ***4.5a*** *and benzyltrimethyl-ammonium bromide* ***4.5b****. All hydrotropes, except* ***4.2g****, induce strong rate retarding effects, indicative of strong interactions with* ***4.1*** *and of remarkably strong hydrophobic interactions between aromatic moieties. Most hydrotropes show neither spectroscopic nor kinetic evidence for cooperative aggregation in the molality range studied, i.e. from 0 to 1.4 mol* kg^{-1}*. Cooperative aggregation is absent because the hydrophobic moieties are too small for hydrophobic interactions to overcome electrostatic repulsion. Lack of aggregation results in high availability of hydrophobic binding sites, thereby accounting for the high solubilising power characteristic for hydrotropes. However, sodium 4-*n*-propylbenzene-sulfonate* ***4.2d*** *and sodium 4-*n*-butylbenzenesulfonate* ***4.2e*** *show cooperative self-association forming highly dynamic, loose micellar-type structures.*

4.1 Introduction

4.1.1 Hydrolysis of 1-benzoyl-3-phenyl-1,2,4-triazole in the presence of self-associating cosolutes

The procedures as set up in Chapters 1 and 2 are valid for non-reacting and non-catalytically active cosolutes and are normally used for dilute cosolutes so that only pairwise (1:1) interactions have to be considered. As described in Chapter 3, a range of basic cosolutes either catalyse hydrolysis or react with the activated amides and the basic pattern underlying the reactivity of basic compounds has been explored.

The next topic under study is the effect of self-association of cosolutes. Equation 1.9, describing the rate-retarding effects resulting from 1:1-interactions, is derived from general equations which include the possibility of higher than 1:1-interactions.[2] Further quantities related to G(c)-values can be defined incorporating these higher-order interactions. Normally,[3] however, molalities are intentionally kept low and cosolute hydrophobicity is kept within limits in order to prevent higher than 1:1-interactions.

Many organic cosolutes, however, are rather hydrophobic which can lead to a higher propensity to self-associate. This tendency to self-associate is expected to show up in deviations from linearity in plots of $\ln[k(m_c)/k(m_c=0]$ as a function of cosolute molality m_c.

4.1.2 HYDROTROPES

In the present study of the effect of self-association of cosolute molecules, we used hydrotropes as cosolutes.[4,5] Hydrotropes normally comprise hydrophilic and hydrophobic moieties, with the hydrophobic moiety being typically too small to induce micelle formation. The extent and mechanism of self-association are under debate with both non-cooperative step-wise self-aggregation[4,6-8] and cooperative self aggregation[9] (*vide infra*) being suggested.

Hydrotropes induce a characteristic steep increase in aqueous solubilities of sparingly soluble hydrophobic compounds around a certain hydrotrope concentration, after which solubilities remain unchanged.[9] The sudden increase in solubilisation by hydrotropes after a certain threshold concentration, called the minimum hydrotrope concentration (MHC), has been attributed to a cooperative process. This involves cooperative self-aggregation of the hydrotropes since the threshold concentration for solubilisation appears to be rather solubilisate insensitive.[9] This cooperativity is disputed,[10] however, as is the exact mechanism of solubilisation by hydrotropes.[11]

Solubilisation by hydrotropes differs from that of typical salting-in compounds and cosolvents in that the increase in solubility is sigmoidally dependent on hydrotrope concentration. Salting-in cosolutes and cosolvents usually cause a monotonic increase in solubility without a levelling off at higher concentrations.[9] Compared to micelle-forming surfactants, hydrotropes are more effective in solubilising organic solutes and can be more selective.[9,12,13] Further, self-aggregation of hydrotropes most probably differs from that for micelles (Chapter 5).[12] A crucial difference between micelle-forming surfactants and hydrotropes

becomes clear from phase diagrams of their respective aqueous solutions. Aqueous solutions of hydrotropes lack the lamellar liquid crystal region found in solutions of micelle-forming surfactants. This lamellar region separates the normal micellar solution from the inverse micellar one. Instead, the phase diagrams of aqueous solutions of hydrotropes display a single continuous isotropic liquid phase.[5,14,15]

The solubilising power of hydrotropes was recognised as early as 1916 by Neuberg.[16] The potential use of hydrotropes in industry was stressed in 1946 by McKee.[17] However, hydrotropes have received much less attention in the chemical literature than micelle-forming surfactants (Chapter 5). Despite this lack of attention, hydrotropes have been applied in liquid household detergents, shampoos, degreasing compounds and printing pastes, as well as used to extract pentosans and lignins in the paper industry and as an additive for glues used in the leather industry.[18] Arguably, there are numerous areas that could benefit from the use of hydrotropes.[4,5]

For organic synthesis in aqueous solutions, the use of hydrotropes can be beneficial, as for example, in the microwave-enhanced Hantzsch dihydropyridine ester synthesis,[19] and the Claisen-Schmidt reaction[20] in aqueous solution. In addition, hydrotropes enhance rates of reactions in multiphase transformations,[21] which can lead to autocatalysis in the biphasic alkaline hydrolysis of aromatic esters.[22]

Apart from their use as solubilising agents for organic synthesis in aqueous solutions, hydrotropes could also find application in formulations of pharmaceuticals[23-27] (a number of pharmaceuticals turned out to be hydrotropes themselves[28,29]) and in extraction and separation processes.[13,30,31] In fact, most of the recent research into the action of hydrotropes has been performed in the latter two subjects. In addition, the effect of hydrotropes on micelle-forming[32,33] and vesicle-forming[34-36] surfactants and copolymers[37-40] in aqueous solution has been investigated, as well as the influence on oil-in-water (OW) microemulsions[41,42] and related cleaning and washing processes. Their biological action has also received attention.[5]

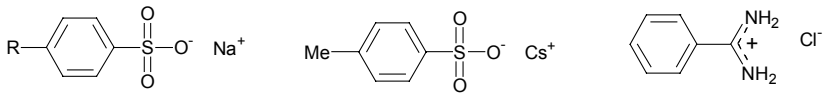

4.2 **a** R=H, **b** R=Me, **c** R=Et, **d** R=n-Pr, **e** R=n-Bu, **f** R=MeO, **g** R=HO

4.3

4.4

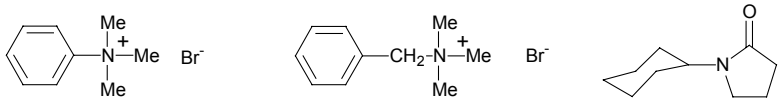

4.5a

4.5b

4.6

Scheme 4.1

In order to probe noncovalent interactions between hydrophobic solutes, we have studied the effects of sodium 4-alkylbenzenesulfonates **4.2a-e**, 4-methoxybenzene-sulfonate **4.2f**, 4-hydroxybenzenesulfonate **4.2g**, caesium 4-methylbenzene-sulfonate **4.3**, benzamidinium chloride **4.4**, aromatic ammonium bromides **4.5a-b** and *N*-cyclohexyl-2-pyrrolidinone **4.6** (Scheme 4.1) on the water-catalysed hydrolysis (Chapter 1) of 1-benzoyl-3-phenyl-1,2,4-triazole **4.1** (Scheme 4.2).

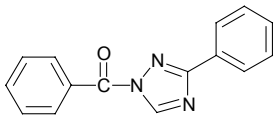

4.1

Scheme 4.2

These hydrotropes are not sufficiently basic to act as general bases in the hydrolysis of **4.1**, nor are they nucleophilic enough to act as nucleophiles (with the possible exception of **4.2g**) in the nucleophilic substitution of **4.1** (Chapter 3). Furthermore, we determined the molality dependence of the ^{1}H-NMR-spectra of benzenesulfonates **4.2b**,**d** and **e** in D_2O in order to examine the self-association of the hydrotropic cosolutes in a probe-independent way.

4.2 RESULTS AND DISCUSSION

4.2.1 AN OVERVIEW OF RATE EFFECTS OF HYDROTROPES ON HYDROLYSIS OF 1-BENZOYL-3-PHENYL-1,2,4-TRIAZOLE

All tested hydrotropes, except **4.2g**, induce strong rate retardations (Figure 4.1). The hydrotropes **4.2d** and **4.2e**, bearing longer alkyl chains, show sigmoidal dependence of $\ln[k(m_c)/k(m_c=0)]$ on molality of added hydrotrope, indicative of cooperative self-association.

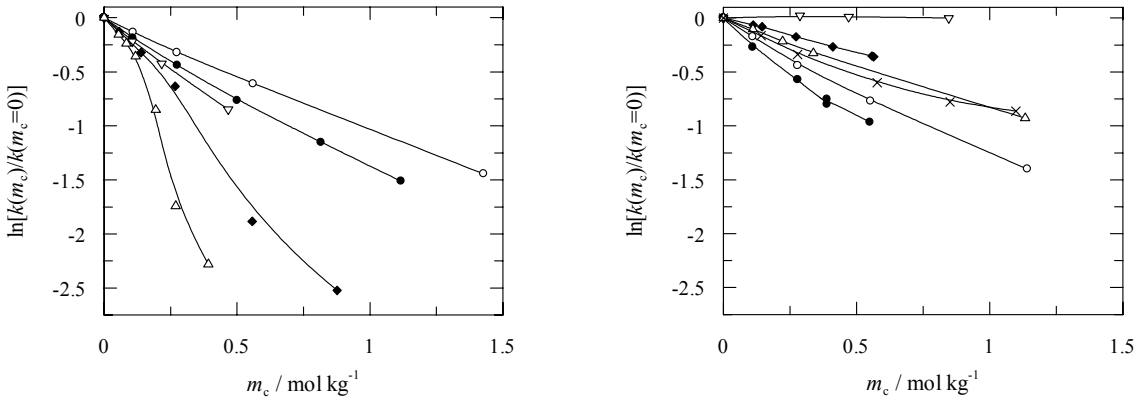

Figure 4.1: The effect of different hydrotropes on the hydrolysis of **4.1**. *Left*: alkylated benzenesulfonates **4.2a** (o), **4.2b** (•),**4.2c** (▽),**4.2d** (♦),**4.2e** (Δ). *Right:* **4.2f** (•),**4.2g** (▽),**4.3** (o), **4.4** (x), **4.5a** (♦) and **4.5b** (Δ).

4.2.2 KINETICS OF REACTIONS IN DILUTE SOLUTIONS OF HYDROTROPES

For all hydrotropes, plots of $\ln[k(m_c)/k(m_c=0)]$ against molality of hydrotrope (Equation 1.9) were constructed for the molality range up to 0.3 mol kg^{-1} (0.1 mol kg^{-1} for **4.2e**). This molality range was chosen in order to avoid possible complexities in the data due to 2:1 and higher order interactions. All plots show a linear dependence of $\ln[k(m_c)/k(m_c=0)]$ on molality of hydrotrope (Figure 4.2).

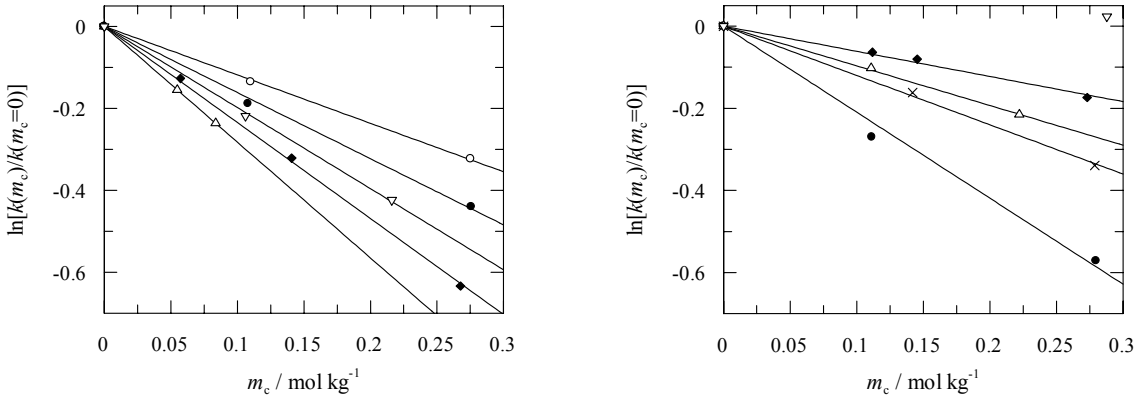

Figure 4.2: The effect of different hydrotropes on the hydrolysis of **4.1** at low molality. *Left:* the alkylated benzenesulfonates **4.2a** (o), **4.2b** (•),**4.2c** (∇),**4.2d** (♦),**4.2e** (Δ). *Right:* **4.2f** (•),**4.2g** (∇),**4.3** (o), **4.4** (x), **4.5a** (♦) and **4.5b** (Δ).

This pattern accords with the results of Friberg *et al.*[43] who showed that the vapour pressure of phenylethyl alcohol decreases linearly with the mole fraction of added sodium xylenesulfonate up to mole fractions of the latter of at least 0.5 mol% (0.25 mol kg^{-1}). The slopes of the plots of $\ln[k(m_c)/k(m_c=0)]$ vs. m_c for the dilute region yield the G(c)-values given in Table 4.1.

Table 4.1: G(c) values of hydrotropes **4.2a-g**, **4.3**, **4.4** and **4.5a-b** at 298K.[a]

Hydrotrope	G(c) / J kg mol^{-2}
4.2a	-1475±25
4.2b	-1950±50
4.2c	-2408±37
4.2d	-2858±30
4.2e	-3456±6
4.2f	-2551±116
4.2g	~0
4.3	-1909±6
4.4	-1443±27
4.5a	-715±26
4.5b	-1153±8

[(a)] Errors are standard errors based on a least-squares fit of kinetic data using Equation (1.9).

All G(c)-values are large and negative (apart from that for **4.2g**), indicating strong inhibition of hydrolysis by substrate-solute interactions involving added

hydrotropes. In terms of the model leading to Equation 2.1, the observed pattern is consistent with the formation of relatively stable encounter complexes with equilibrium constants of formation K_{ec} larger than unity, except in the cases of **4.5a** and **4.5b**. The values for K_{ec} are comparable to those found by Ueda.[44] For encounter complexes between **4.1** and **4.5a** and **4.5b**, ΔG_{ec} is larger than 0 kJ mol^{-1} (K_{ec}<1 kg mol^{-1}) with respect to the individually solvated molecules. Previously, significantly negative G(c)-values were also reported for the effects of added aromatic α-amino acids and derivatives of aromatic α-amino acids on rate constants for hydrolysis of **4.1**,[45-47] despite the possibility of nucleophilic substitution (Chapter 3). In combination with the present results, we suggest that hydrophobic interactions involving aromatic molecules are particularly strong.

Thermodynamics of solution of aromatic molecules in aqueous solutions are different from that of aliphatic molecules in that standard Gibbs energies of transfer from the gas to the aqueous phase are negative for aromatic molecules, whereas they are positive for aliphatic molecules. This is an enthalpic effect, attributed to the aromatic ring being able to accept hydrogen bonds from hydration-shell water molecules.[48,49] In addition, interactions between aromatic molecules themselves are more favourable than those between comparable aliphatic molecules.[48]

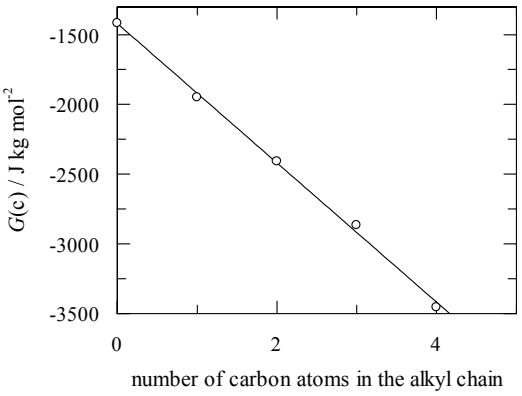

Figure 4.3: G(c) as a function of the number of methylene units in the alkyl-chain of hydrotropic cosolutes **4.2a-e**.

For hydrotropes **4.2a-e**, G(c) varies linearly with the number of methylene groups in the alkyl chain (Figure 4.3), in accord with the Savage Wood Additivity of Group interactions (SWAG) theory.[50] The decrease in G(c) per methylene unit, viz. -500±131 J kg mol^{-2}, is large when compared with previously reported estimates. Typically, increments for undisturbed methylene units are in the order of -100 J kg mol^{-2},[51,52] although values up to -340 J kg mol^{-2} have been observed for the less hydrophobic substrate 1-benzoyl-1,2,4-triazole.[53]

The remarkably high group contribution of the methylene group to the present *G*(c)-values is attributed to a synergistic effect of the aromatic benzenesulfonate moiety and of the methylene groups. Sodium benzenesulfonate itself is a potent inhibitor of the reaction, as can be seen from the *G*(c) for **4.2a**. In terms of the analysis leading to Equation 2.1, the observed strongly negative *G*(c) corresponds to a rather stable encounter complex which inhibits the reaction (Chapter 2).[54] Further hydrophobic stabilisation of this encounter complex by elongating the alkyl chains of the added hydrotropes increases the rate retarding effect.

Surprisingly, the rather polar **4.2f** induces rather a strong rate retardation, comparable to that of **4.2c**. Apparently, the methylene unit or oxygen is "invisible" to hydrophobically interacting species. Previously, shielding of hydrophobicity by hydrophilic groups has been attributed to the prevention of the formation of a hydrophobic hydration shell.[3] We contend that the methyl and phenyl moieties prevent formation of a hydrophilic hydration shell around the oxygen, resulting in the oxygen's hydration shell becoming part of a slightly disturbed hydrophobic hydration shell of its neighbouring groups. Hence the oxygen is masked as a hydrophilic moiety in 1:1 hydrophobic interactions.

For the hydroxy-substituted benzenesulfonate **4.2g**, *G*(c) is positive but small. General-base catalysis by the deprotonated phenol is expected to be negligible as the pK_a of **4.2g** was found to be 8.6 by titration of a 0.5mol% solution. Using the LFER as derived in Chapter 3, Figure 3.9, kinetic data for nucleophilic substitution by phenolates of *p*-NPA[55] and the pK_a, we estimate the second-order rate constant for nucleophilic attack of **4.2g** on **4.1** to be 5 kg mol^{-1} s^{-1}. At pH 4.0 and unit cosolute molality, 25 μmol kg^{-1} of phenol is deprotonated leading to a rate increase of approximately 1.3×10^{-4} s^{-1}, which corresponds to a *G*(c) of +162 J kg mol^{-2}. This accounts for the observed small positive *G*(c). However, it also indicates that (the remaining) protonated **4.2g** has a negligible rate-retarding effect. The lack of hydrophobic interaction between **4.2g** and **4.1** is opposite to that of **4.2f**. Here, the hydrophobic nature of the phenyl ring is masked by the hydration shells of the hydrophilic sulfonate and hydroxy group, making the phenyl ring unavailable for hydrophobic interactions. Similar behaviour has been found for L-proline, where 4-hydroxylation results in a total loss of hydrotropic behaviour.[56] The mole fraction solubilities of phenol and methoxybenzene, being 1.78×10^{-2} and 1.75×10^{-3}, respectively,[57] show that the phenolic compound is far more hydrophilic than the methoxy-substituted benzene.

To investigate the effect of the relative electron density in the aromatic ring, non-alkylated hydrotropes **4.2a**, **4.4**, **4.5a** and **4.5b** were studied. Aromatic interactions are strongest for donor-acceptor systems, followed by acceptor-acceptor systems whereas electron-rich aromatic species do not stack well because the aromatic π-electron clouds repel each other.[58] Kinetically, at low molality, non-alkylated cationic hydrotrope **4.4** strongly resembles non-alkylated anionic hydrotrope **4.2a**. The average chemical shifts of the aromatic protons show that the electron density in the aryl rings of **4.2a** and **4.4** is similar (Table 4.2).

Based on the higher average NMR chemical shift, the aromatic ring of the non-alkylated cationic hydrotrope **4.5a** is more electron deficient than that of **4.2a** and **4.4**. Considering that both aromatic rings in **4.1** are relatively electron deficient, **4.5a** is expected to interact more weakly with **4.1**, leading to a less negative *G*(c), as borne out in practice.

Table 4.2: ^{1}H-NMR chemical shifts of aromatic protons of hydrotropes **4.2a-f**, **4.4** and **4.5a-b**.

	δ / ppm
Hydrotrope	Average
4.2a	7.68
4.2b	7.52
4.2c	7.55
4.2d	7.54
4.2e	7.55
4.2f	7.41
4.2g	n.d.[a]
4.3	n.d.[a]
4.4	7.68
4.5a	7.72
4.5b	7.55

[(a)] n.d.: not determined

Structurally related **4.5b**, having a lower average chemical shift, is intermediate in *G*(c). Even though *G*(c) shows no correlation with the average chemical shift of the aromatic protons, the lack of correlation with average chemical shifts alone is caused by the fact that the trimethylammonium moiety of **4.5b** is not directly attached to the aromatic ring. The hydrophilic hydration shell around the ionic

moiety will therefore not overlap as strongly with the hydration shell of the aromatic ring as is the case for **4.2a**, **4.5a** and **4.4**. Consequently, the hydrophobicity of the aromatic ring is less attenuated for **4.5b**, causing *G*(c) to be more strongly negative than expected on the basis of electron density in the aromatic ring alone, which is indeed observed.

As noted above, the dilute molality range in which the *G*(c)-values have been determined was chosen to avoid 2:1 and higher order interactions. To check the validity of this assumption, the molality dependence of the ^{1}H-NMR spectrum of **4.2b** was examined. The short-chain benzenesulfonate **4.2b** shows an almost linear dependence of the chemical shift of the meta hydrogen on molality in aqueous solution indicating the absence of cooperative aggregation. The decrease in chemical shift of the meta hydrogen is caused by the decrease in interhydrotrope distances upon increasing cosolute molalities and the accompanying weak non-cooperative interaction between the individual hydrotrope molecules. As a result of the increasing molality, both intermolecular aromatic ring current effects[59] and the decreasing polarity of the solution[60] cause an upfield shift.

In addition, aggregation into loose micellar-type aggregates would have been associated with a difference in *G*(c) between **4.2b** and **4.3**. Larger aggregates will bind counterions as a result of the increasing charge density with increasing aggregation number. Replacing sodium counterions by caesium counterions is known to enhance association: a less unfavourable dehydration of the caesium cations leads to more efficient stabilisation of the double (or higher) positive charge in the dimer (or higher aggregates). In the dilute solutions for which *G*(c) have been determined, this is not observed.

The equilibrium constants for hydrotrope self-association also indicate the prevalence of 1:1 interactions. The equilibrium constant for encounter complex formation (Chapter 2) between **4.1** and any of the investigated hydrotropes does not exceed 3 kg mol^{-1}. We therefore contend that the equilibrium constant of association between individual hydrotropic molecules does not exceed 1 kg mol^{-1} for the investigated systems, since binding between the hydrolytic probe and hydrotropic cosolute is only governed by favourable hydrophobic interactions, whereas binding between two hydrotropic cosolute molecules is counteracted by electrostatic interactions. We assume the equilibrium constants for formation (K_{ass}) of the (n+1)-mer from the n-mer to be less than 1 kg mol^{-1}, assuming non-cooperative association (Scheme 4.3, *cf*. Section 2.2.7).

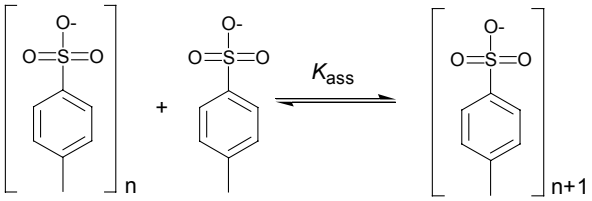

Scheme 4.3

Using an upper value of 1 kg mol^{-1} for K_{ass}, we calculated the compositions, in terms of monomer and oligomer molalities,[61] of solutions in which the total hydrotrope molality ranges between 0 and 0.3 mol kg^{-1} (Figure 4.4).

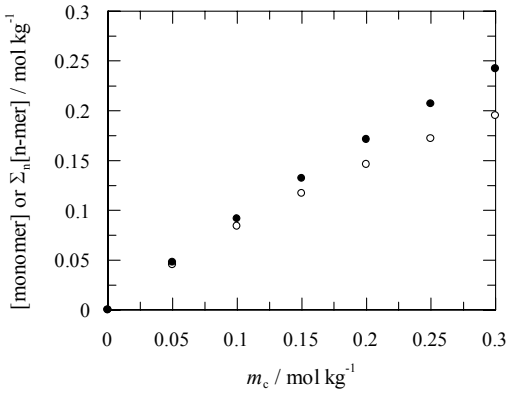

Figure 4.4: Molalities of monomers (o) and of oligomers (•) as a function of the molality of a weakly self-associating solute.

At all total hydrotrope molalities m_c, the molality of monomeric hydrotropic cosolute ([monomer]) is smaller than the total molality of hydrotropic cosolute. However, in the range between 0 and 0.3 mol kg^{-1}, the total molalities of monomers and oligomers combined, Σ_n[n-mer] is only about 20% less than the total hydrotrope molality and it varies almost linearly with total hydrotrope molality. Therefore, 1:1-interactions still prevail. For the expected values of K_{ass} smaller than 1 kg mol^{-1}, 1:1-interactions will be the main contribution to G(c).

4.2.3 KINETICS OF REACTIONS IN MODERATELY CONCENTRATED SOLUTIONS OF HYDROTROPES

In the higher molality range from 0.3 mol kg^{-1} up to 1.5 mol kg^{-1}, kinetic data for hydrolysis in the presence of **4.2d** and **4.2e** indicate strong self-association of the hydrotropes, most probably even cooperative self-association, as indicated by the markedly non-linear, almost sigmoidal plots of $\ln[k(m_c)/k(m_c=0)]$ vs. m_c. This sigmoidal-like pattern is not observed for the shorter-chain benzenesulfonates **4.2a-c** and the other hydrotropes. For example, in the case of sodium 4-methylbenzenesulfonate, an archetypal hydrotrope, $\ln[k(m_c)/k(m_c=0)]$ is linearly dependent on hydrotrope molality, the deviation being towards higher values of

$\ln[k(m_c)/k(m_c=0)]$ at higher molalities. This pattern is generally observed for non-associating cosolutes.

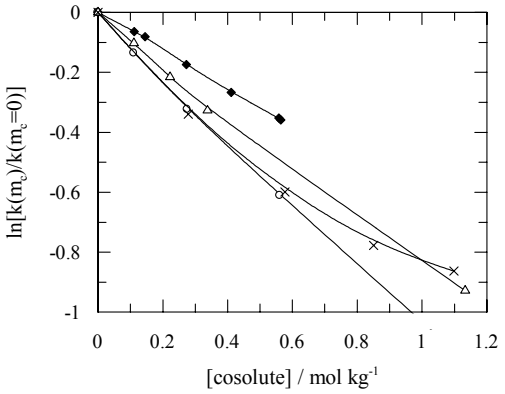

Figure 4.5: The effect of different non-alkylated hydrotropes on the hydrolysis of **4.1**.Hydrotropes: **4.2a** (o), **4.4** (x), **4.5a** (♦) and **4.5b** (Δ).

Unfortunately, the interpretation of the observed plots of $\ln[k(m_c)/k(m_c=0)]$ as a function of hydrotrope molality is hampered by the difference in interpretation of deviations from linearity according to the equations in Chapters 1 and 2. According to Equation (1.9), a linear plot of $\ln[k(m_c)/k(m_c=0)]$ versus molality indicates the prevalence of 1:1-interactions in the corresponding molality range. Deviations to higher values of $\ln[k(m_c)/k(m_c=0)]$ at higher molalities then signify a tendency to (weakly) self-associate. This self-association effectively reduces the interactions between cosolute and hydrolytic probe if the shielding of potential interaction sites occurs without the dimer (or higher aggregates) having a stronger rate-retarding effect than the monomer. According to Equation 2.1, however, curves of $\ln[k(m_c)/k(m_c=0)]$ as a function of molality are non-linear for 1:1-interactions. According to this equation, linearity actually is a result of weak cosolute self-association.

For the non-alkylated hydrotropes, plots of $\ln[k(m_c)/k(m_c=0)]$ versus molality are linear or deviate towards higher values of $\ln[k(m_c)/k(m_c=0)]$ at higher molality. This result not only excludes the possibility of cooperative self-association in this molality range, it also indicates that K_{ass} (for non-cooperative association between the hydrotropes) is small, most probably significantly smaller than 1 kg mol^{-1}, as we assumed on the basis of the kinetic data obtained for dilute solutions (*vide supra*). The linearity of plots of $\ln[k(m_c)/k(m_c=0)]$ vs. molality up to high molalities therefore indicates that high molalities of hydrotropes are achievable in aqueous solution, without significant association or phase separation. The fact that $K_{ec} > K_{ass}$ corroborates the conclusion that interactions with uncharged molecules are not hindered by charge repulsion and that interaction between apolar non-ionic

solubilisates and ionic hydrotropes is much stronger than interactions between hydrotropic molecules. Consequently, if the hydrophobic moiety of the hydrotrope is made less hydrophobic, for example by introduction of a hydroxy-substituent, a strong decrease in hydrotropic activity is observed.[56]

The lack of strong self-association results in the presence of many "single hydrophobic binding sites", facilitating the dissolution of apolar molecules. Therefore, solubilising effects of hydrotropes are normally larger than those of surfactants. We also note that these single hydrophobic binding sites can participate in rather strong hydrophobic interactions with apolar solutes, making hydrotropes different from typical salting-in solutes.

The transition from weak association to cooperative association is apparent from a marked change in the molality dependence of $\ln[k(m_c)/k(m_c=0)]$. Weak association is accompanied by higher values of $\ln[k(m_c)/k(m_c=0)]$ than expected on the basis of linear behaviour at higher cosolute molalities. Cooperative association, however, is accompanied by sigmoidal plots of $\ln[k(m_c)/k(m_c=0)]$ against molality.[62] First, the slope of plots of $\ln[k(m_c)/k(m_c=0)]$ vs. m_c becomes more negative, a pattern attributed to stronger cooperative binding of **4.1** to small self-associated clusters of added cosolute molecules. A levelling off at higher molalities is the result of the substrate being almost completely bound. For **4.2d** and **4.2e**, the hydrophobic moieties are large enough for hydrophobic interactions to overcome the electrostatic repulsion. As a consequence, small and weakly organised clusters are formed. For both hydrotropic molecules and hydrolytic probe, it now becomes possible to interact favourably with more than one hydrophobic moiety and cooperative binding starts to take place. In fact, **4.2d** and **4.2e** are the link between hydrotropes and surfactants.

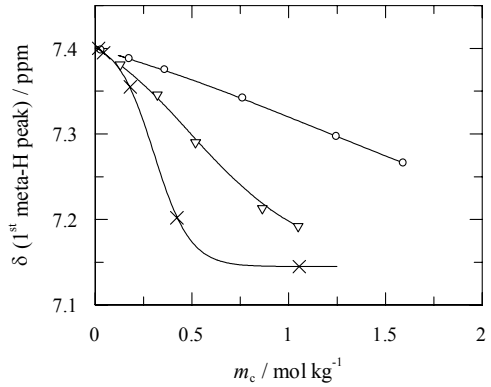

Figure 4.6: Chemical shift of the meta protons in the aromatic ring of **4.2b** (o, +0.03 ppm), **4.2d** (∇) and **4.2e** (x). Molalities were calculated after correction for the density difference between H_2O and D_2O.

In accord with the kinetic data, **4.2d** and **4.2e** show a sigmoidal dependence of the chemical shift of the meta protons as a function of the molality (Figure 4.6), revealing a critical molality of association. The observed critical hydrophobic interaction molalities (CHIMs) are 0.5 molal and 0.25 molal for **4.2d** and **4.2e**, respectively, in accord with the molalities obtained from the kinetic experiments.

In addition to ionic hydrotropes, a few nonionic hydrotropes have been examined previously.[63] As nonionic molecules lack repulsive electrostatic interactions, they are more generally expected to show cooperative self-association at low molality. Indeed, *N*-cyclohexyl-2-pyrrolidinone **4.6** has been shown to have a rate retarding effect very similar to that observed for **4.2d** and **4.2e**.[52,64]

The absence of a clear CHIM for the studied hydrotropes is remarkable and in sharp contrast with solubilisation experiments.[9] One of the reasons for not observing a clear CHIM may be that the concentration of hydrolytic probe has been kept some 3 orders of a magnitude lower than the concentrations of dyes and drugs in typical solubilisation experiments.[65] Introducing relatively high concentrations of hydrophobic materials may well induce clustering of the hydrotrope monomers, even when clustering is not occurring in the absence of hydrophobic solubilisates. This conclusion is in accord with results of a study of Horvath-Szabo *et al.*[11] on the solubilisation of lecithin by sodium dimethylbenzensulfonate. They concluded that instead of cooperative self-association of sodium dimethylbenzensulfonate (SXS), "a cooperative interaction *between lecithin and SXS* is responsible for the phenomena". Similarly, Ueda[44] found that solubilisation at low concentrations of solubilisate occurs by one to one complexation, whereas at the higher solubility limits, one to one complexation was no longer sufficient to account for the increased solubilities of apolar compounds. Significantly, da Silva *et al.*[66] have shown that non-linear increases in solubilising power and other properties of hydrotrope solutions are not necessarily suggestive of any critical phenomenon.

4.3 CONCLUSIONS

In the present study, we have examined the effect of a series of charged hydrotropes on the water-catalysed hydrolysis of **4.1**. We find that typical hydrotropes stabilise the apolar substrates in aqueous solution by forming encounter complexes with equilibrium constants in the range between 1 kg mol^{-1} and 3 kg mol^{-1}. These equilibrium constants are in most cases larger than the equilibrium constants for self-association between hydrotrope monomers as a result of charge repulsion

between the latter. The balancing of favourable hydrophobic interaction and unfavourable charge repulsion results in the hydrotropes being soluble over a large molality range. The mode of action of a hydrotrope differs from the mode of action of a salting-in compound since a hydrotrope contains a hydrophobic moiety, albeit small, that is able to participate in relatively strong hydrophobic interaction with an uncharged apolar molecule. As soon as the hydrophobic moieties are large enough for the hydrophobic interaction to overcome the charge repulsion, cooperative self-association takes place, presumably producing highly dynamic and loose micellar-type aggregates.

4.4 EXPERIMENTAL

4.4.1 KINETIC EXPERIMENTS

Aqueous solutions were prepared by weight immediately before use. Water was distilled twice in an all-quartz distillation unit. Reactions were monitored at 25.0±0.1°C using appropriate wavelengths to avoid overlap with strong absorption bands of the cosolutes used. Reactions were followed for at least six half-lives using a Perkin-Elmer lambda 2, lambda 5 or lambda 12 spectrophotometer. Good to excellent pseudo-first-order kinetics were obtained, the error in the rate constants being 2% or less. Between 4 and 7 μl of a stock solution containing 1-benzoyl-3-phenyl-1,2,4-triazole **4.1** in cyanomethane were injected into about 2.7 ml of reaction medium in a 1.000 cm path length stoppered quartz cuvette. The resulting concentrations of hydrolytic probe were about 10^{-5} mol dm^{-3} or less. The pH of every solution was determined using a SENTRON ISFET pH probe and was adjusted to 3.9±0.3 using aqueous HCl. The pH was checked again at the end of each kinetic run and was found to be still well within the pH-range in which solely water-catalysed hydrolysis takes place.

4.4.2 MATERIALS

1-Benzoyl-3-phenyl-1,2,4-triazole,[67] sodium 4-*n*-butylbenzenesulfonate[68] and sodium 4-methoxybenzenesulfonate[69] were prepared according to literature procedures. *p*-Toluenesulfonic acid monohydrate, 4-ethylbenzenesulfonic acid, phenyltrimethylammonium bromide and benzyltrimethylammonium bromide were obtained from Aldrich, benzamidinium chloride was from Sigma, caesium hydroxide hydrate was from Acros and 4-*n*-propylbenzenesulfonyl chloride was from Lancaster

and all were used as received. Sodium 4-methylbenzenesulfonate and sodium 4-ethylbenzenesulfonate were prepared by neutralising the corresponding acid using a sodium hydroxide solution, followed by filtration and evaporation of the solvent. Caesium 4-methylbenzenesulfonate was prepared analogously using CsOH hydrate. All prepared salts were tested and found pure using ^{1}H-NMR and elemental analysis. All hydrotropes were stored in a desiccator over P_2O_5 or KOH. NMR spectra were recorded on Varian Gemini 200 (^{1}H: 200MHz) and VRX 300 (^{1}H: 300MHz) spectrometers, with HOD set to 4.79 ppm. In the determination of the molality dependence of the ^{1}H-NMR spectra of **4.2b**, **4.2d** and **4.2e**, methanol was added as a second reference. The signal of methanol did not shift with respect to the set signal of HOD.

Sodium 4-*n*-propylbenzenesulfonate (4.2d). 4-*n*-Propylbenzenesulfonyl chloride (15g, 65 mmol) was suspended in 1M aqueous NaOH and stirred vigorously for 2 days at 40°C. The resulting acidic solution was neutralised and the solvent evaporated, resulting in a 1:1 sodium 4-*n*-propylbenzenesulfonate/NaCl mixture (18.2 g, 65 mmol). The mixture was extracted continuously overnight in a Soxhlet apparatus using *n*-propanol. Only part of the 4-*n*-propylbenzenesulfonate was extracted to avoid contamination with NaCl. The absence of sodium chloride was confirmed using a silver nitrate precipitation test. ^{1}H-NMR (D_2O): δ (ppm): 0.88 (3H, $CH_2CH_2C\mathbf{H}_3$, t), 1.61 (2H, $CH_3C\mathbf{H}_2CH_2$, sextet), 2.64 (2H, $CH_3CH_2C\mathbf{H}_2$, t), 7.36 and 7.71 (4H, phenyl, AB-system); anal. calcd. for $C_9H_{11}SO_3Na$, %: C, 48.64; H, 4.99; S, 14.43; found %: C, 48.30; H, 4.84; S, 14.30.

4.5 ACKNOWLEDGEMENTS

Elemental analyses were performed by H. Draayer and J. Ebels of the analytical section of this department.

4.6 REFERENCES AND NOTES

(1) Buurma, N. J., Blandamer, M. J. and Engberts, J. B. F. N. *Adv. Synth. Catal.* **2002**, *344*, 413-420.

(2) Blandamer, M. J., Burgess, J., Engberts, J. B. F. N. and Blokzijl, W. *Annu. Rep. R. Soc. Chem. ,Sect. C* **1990**, 45-74.

(3) J. B. F. N. Engberts, M. J. Blandamer, *J. Phys. Org. Chem.*, **1998**, *11*, 841-846 and references cited therein.

(4) Friberg, S. E. *Curr. Opin. Colloid Interface Sci.* **1997**, *2*, 490-494.

(5) Balasubramanian, D. and Friberg, S. E. *in* "Surface and Colloid Science" (Matejevic, E., ed.), Vol. 15, p. 197-220. Plenum, New York, **1993**.

(6) Schobert, B. *Naturwissenschaften* **1977**, *64*, 386.

(7) Schobert, B. and Tschesche, H. *Biochim. Biophys. Acta* **1978**, *541*, 270-277.

(8) Mukerjee, P. *J. Pharm. Sci.* **1974**, *63*, 972-981.

(9) Balasubramanian, D., Srinivas, V., Gaikar, V. G. and Sharma, M. M. *J. Phys. Chem.* **1989**, *93*, 3865-3870.

(10) Balasubramanian *et al.* (reference 9) observed that the hydrotrope concentration at which the sudden rapid increase in solubility of a hydrophobic solubilisate occurs, coincides with a break in a plot of surface tension as a function of hydrotrope concentration. However, as pointed out by Da Silva *et al.* (reference 66), cooperative aggregation (*e.g.* micellisation) is accompanied by a break in a plot of surface tension as a function of the logarithm of concentration. Horvath-Szabo *et al.* (reference 11) showed that in a plot of surface tension as a function of the logarithm of hydrotrope activity, no break occurs at the activity at which the sudden increase in solubilisation occurs.

(11) Horvath-Szabo, G., Yin, Q. and Friberg, S. E. *J. Colloid Interface Sci.* **2001**, *236*, 52-59.

(12) Srinivas, V. and Balasubramanian, D. *Langmuir* **1998**, *14*, 6658-6661.

(13) Poochikian, G. K. and Cradock, J. C. *J. Pharm. Sci.* **1979**, *68*, 728-732.

(14) Flaim, T. and Friberg, S. E. *J. Colloid Interface Sci.* **1984**, *97*, 26-37.

(15) Friberg, S. E., Rananavare, S. B. and Osborne, D. W. *J. Colloid Interface Sci.* **1986** , *109*, 487-492.

(16) (a) Neuberg, C., *Biochem. Z.* 1916, 76, 107-176. (b) Neuberg, C., *J. Chem. Soc.* 1916, 110 (II), 555.

(17) McKee, R. H. *Ind. Eng. Chem.* **1946**, *38*, 382-384.

(18) Usage of sodium dimethylbenzenesulfonate (mixture of isomers) according to the National Toxicology Program (US).

(19) Kahdilkar, M. K., Gaikar, V. G. and Chitnavis, A. A. *Tetrahedron Lett.* **1995**, *36*, 8083-8086.

(20) Sadvilkar, V. G., Samant, S. D. and Gaikar, V. G. *J. Chem. Technol. Biotechnol.* **1995**, *62*, 405-410.
(21) Janakiraman, B. and Sharma, M. M. *Chem. Eng. Sci.* **1985**, *40*, 2156-2158.
(22) Chen, X. N. and Micheau, J. C. *J. Colloid Interface Sci.* **2002**, *249*, 172-179.
(23) Gupta, G. D., Jain, S. and Jain, N. K. *Pharmazie* **1997**, *52* , 709-712.
(24) Khalil, R. M. *Pharmazie* **1997**, *52*, 866-870.
(25) Gupta, G. D., Jain, S. and Jain, N. K. *Pharmazie* **1997**, *52* , 621-624.
(26) ElNahhas, S. A. *Pharmazie* **1997**, *52*, 624-627.
(27) Jain, N. K., Jain, S. and Singhai, A. K. *Pharmazie* **1997**, *52*, 942-946.
(28) Guo, R., Zhang, Q. Q., Qian, J. H. and Zou, A. H. *Colloids Surf. , A* **2002**, *196*, 223-234.
(29) Yu, W. L., Zou, A. H. and Guo, R. *Colloids Surf. , A* **2000**, *167*, 293-303.
(30) Tavare, N. S. and Colonia, E. J. *J. Chem. Eng. Data* **1997**, *42*, 631-635.
(31) Colonia, E. J., Dixit, A. B. and Tavare, N. S. *Ind. Eng. Chem. Res.* **1998**, *37*, 1956-1969.
(32) Marszall, L. *Langmuir* **1990**, *6*, 347-350.
(33) Gonzalez, G., Nassar, E. J. and Zaniquelli, M. E. D. *J. Colloid Interface Sci.* **2000** , *230*, 223-228.
(34) Horvath-Szabo, G. and Friberg, S. E. *Langmuir* **2001**, *17*, 278-287.
(35) Heldt, N., Zhao, J., Friberg, S. E., Zhang, Z., Slack, G. and Li, Y. *Tetrahedron* **2000**, *56*, 6985-6990.
(36) Friberg, S. E., Campbell, S., Fei, L., Yang, H. F., Patel, R. and Aikens, P. A. *Colloids Surf. , A* **1997**, *130*, 167-173.
(37) Mansur, C. R. E., Spinelli, L. S., Lucas, E. F. and Gonzalez, G. *Colloids Surf. , A* **1999**, *149*, 291-300.
(38) Mansur, C. R. E., Oliveira, C. M. F., Gonzalez, G. and Lucas, E. F. *J. Appl. Polym. Sci.* **1997**, *66*, 1767-1772.
(39) Mansur, C. R. E., Spinelli, L. S., Oliveira, C. M. F., Gonzalez, G. and Lucas, E. F. *J. Appl. Polym. Sci.* **1998**, *69*, 2459-2468.
(40) daSilva, R. C. and Loh, W. *J. Colloid Interface Sci.* **1998**, *202*, 385-390.
(41) Friberg, S. E., Brancewicz, C. and Morrison, D. S. *Langmuir* **1994**, *10*, 2945-2949.
(42) Horvath-Szabo, G., Masliyah, J. H. and Czarnecki, J. *J. Colloid Interface Sci.* **2001** , *242*, 247-254.
(43) Friberg, S. E., Fei, L., Campbell, S., Yang, H. F. and Lu, Y. C. *Colloids Surf. , A* **1997**, *127*, 233-239.
(44) S. Ueda, *Chem. Pharm. Bull.*, **1966**, *14*, 22-29; S. Ueda, *Chem. Pharm. Bull.*, **1966**, *14*, 29-38; S. Ueda, *Chem. Pharm. Bull.*, **1966**, *14*, 39-45.
(45) Streefland, L., Blandamer, M. J. and Engberts, J. B. F. N. *J. Phys. Chem.* **1995**, *99*, 5769-5771.

(46) Streefland, L., Blandamer, M. J. and Engberts, J. B. F. N. *J. Am. Chem. Soc.* **1996**, *118*, 9539-9544.

(47) Streefland, L., *Effects of overlap of hydration shells on noncovalent interactions in aqueous solution*, PhD Thesis, University of Groningen, **2000**. Available online: http://www.ub.rug.nl/eldoc/dis/science/e.streefland/

(48) Makhatadze, G. I. and Privalov, P. L. *Biophys. Chem.* **1994**, *50*, 285-291.

(49) Costas, M. and Kronberg, B. *Biophys. Chem.* **1998**, *74*, 83-87.

(50) Savage, J. J. and Wood, R. H. *J. Solution Chem.* **1976**, *5*, 733-750.

(51) Hol, P., Streefland, L., Blandamer, M. J. and Engberts, J. B. F. N. *J. Chem. Soc. , Perkin Trans. 2* **1997**, 485-488.

(52) Apperloo, J. J., Streefland, L., Engberts, J. B. F. N. and Blandamer, M. J. *J. Org. Chem.* **2000**, *65*, 411-418.

(53) Noordman, W. H., Blokzijl, W., Engberts, J. B. F. N. and Blandamer, M. J. *J. Org. Chem.* **1993**, *58*, 7111-7114.

(54) Buurma, N. J., Pastorello, L., Blandamer, M. J. and Engberts, J. B. F. N. *J. Am. Chem. Soc.* **2001**, *123*, 11848-11853.

(55) Bruice, T. C. and Lapinski, R. *J. Am. Chem. Soc.* **1958**, *80* , 2265-2267.

(56) Srinivas, V. and Balasubramanian, D. *Langmuir* **1995**, *11*, 2830-2833.

(57) Marcus, Y. "The Properties of Solvents" 1st edition, (Fogg, P. G. T., ed.). Wiley, Chichester, **1998**.

(58) Cubberley, M. S. and Iverson, B. L. *J. Am. Chem. Soc.* **2001**, *123*, 7560-7563.

(59) Bijma, K. and Engberts, J. B. F. N. *Langmuir* **1997**, *13*, 4843-4849.

(60) Manohar, C., Rao, U. R. K., Valaulikar, B. S. and Iyer, R. M. *J. Chem. Soc. , Chem. Commun.* **1986**, 379-381.

(61) Compositions were calculated iteratively. K_{ass} was set to 1 mol kg^{-1} for all association steps up to 20-merisation. Molalities of 20-mers were low enough to cut off the calculation for higher order aggregates.

(62) As pointed out by Mukerjee (reference 8), sigmoidal plots of solubilising effect versus concentration of solubilising agent are not necessarily indicative of cooperative self-aggregation of the solubilising agent. Likewise, sigmoidal curves of $\ln[k(m_c)/k(m_c=0)]$ as a function of molality m_c can be the result of stepwise association (Equation 2.7). For the present case, however, either the hydrotrope self-association or the binding of the hydrolytic probe to the hydrotrope assemblies (or both) should be unexpectedly high (in comparison with the 1:1-interaction) to reproduce the observed curves.

(63) Srinivas, V., Rodley, G. A., Ravikumar, K., Robinson, W. T., Turnbull, M. M. and Balasubramanian, D. *Langmuir* **1997**, *13*, 3235-3239.

(64) Mooijman, F. R. and Engberts, J. B. F. N. *J. Org. Chem.* **1989**, *54*, 3993-3995.

(65) See for example V. G. Gaikar, V. Latha, *Drug Dev. Ind. Pharm.*, **1997**, *23*, 309-312.

(66) da Silva, R. C., Spitzer, M., da Silva, L. H. M. and Loh, W. *Thermochim. Acta* **1999**, *328*, 161-167.

(67) a) Staab, H. A., Lüking, M. and Dürr, F. H. *Chem. Ber.* **1962**, *95*, 1275-1283. b) Karzijn, W., *The water- and hydroxide-ion catalyzed hydrolysis of 1-acyl-1,2,4-triazoles*, Ph.D. Thesis, University of Groningen, **1979**. c) Mooij, H. J., Engberts, J. B. F. N. and Charton, M. *Recl.Trav.Chim.Pays-Bas* **1988**, *107*, 185-189.

(68) Gray, F. W., Gerecht, J. F. and Krems, I. J. *J. Org. Chem.* **1955**, *20*, 511-524.

(69) Bruggink, A., Zwanenburg, B. and Engberts, J. B. F. N. *Tetrahedron* **1970**, *26*, 4995-5006.

Hydrolysis in Aqueous Solutions Containing Micelle Forming Surfactants[1]

*The nature of the rate retarding effects of cationic, anionic and nonionic micelles on the water-catalysed hydrolysis of 1-benzoyl-3-phenyl-1,2,4-triazole (**5.1**), p-methoxyphenyl dichloroethanoate (**5.2**) and a series of substituted 1-benzoyl-1,2,4-triazoles (**5.3a-f**) has been studied using kinetic methods. A comparison is drawn between medium effects in micellar solutions and in different model solutions. Two types of model solutions are used. Simple model solutions involved concentrated aqueous solutions of a small molecule resembling the surfactant headgroup. In this model the entire rate-retarding effect is attributed to interactions with the ionic headgroup. An improved model solution for alkyltrimethylammonium bromide micelles contains both salts, mimicking micellar headgroups, and 1-propanol, mimicking hydrophobic tails. The rate-retarding effect of micelles on the hydrolysis of **5.1**, **5.2** and **5.3a-f** is shown to be caused by the high concentration of headgroups and by the hydrophobic tails in the Stern region where **5.1**, **5.2** and **5.3a-f** bind to the micelle. The rate retarding effects found for different probes with different sensitivities for the interactions as they occur when the probe binds to the micelle, are reproduced by the new model solution comprising both salt and 1-propanol.*

5.1 Introduction

5.1.1 Micelles

Related to the hydrotropes discussed in Chapter 4 are micelle-forming surfactants. However, in contrast to hydrotropes, micelle-forming surfactants self-aggregate in a cooperative manner, forming stable but highly dynamic clusters above a critical concentration called the critical micelle concentration (cmc). Gruen has described a realistic model for a micelle (Figure 5.1).[2] This model involves a rather sharp interface between a dry[2,3] hydrophobic hydrocarbon core and a region filled with surfactant headgroups, part of the counter ions and water, *viz.* the Stern region. This model has been validated using molecular dynamics simulations[4,5] and is valid for both ionic and nonionic micelles.

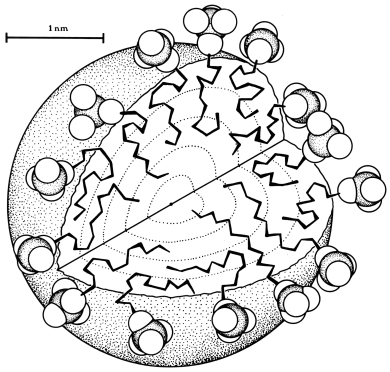

Figure 5.1: Picture of a micelle (taken from reference 2)

In micellar solutions, reactions can be both accelerated and inhibited compared to the reaction in water without added cosolutes.[6-8] Continuous interest developed in micellar catalysis of both organic and inorganic reactions. Remarkable success in enhancing reaction rates[9] by the introduction of catalytic moieties in surfactants has been achieved.[10] However, we limit our discussion to "medium effects" as they occur in solutions of unfunctionalised micelle-forming amphiphiles. The distinction between medium effects and surfactants equipped with catalytic moieties may not always be clear, as for example in the case of micelles with catalytic counterions.[11]

Until now, the exact mechanism of micellar acceleration and deceleration by medium effects has remained rather obscure as a good description of the micellar pseudophase (*vide infra*) is lacking. The aim of the present study was to investigate mechanistic aspects of micellar effects on pH-independent hydrolytic reactions and to develop a satisfactory description of the micellar pseudophase as a reaction medium.

A prerequisite for understanding the reaction medium offered by micelles is to know where the reaction is taking place. A micelle offers several binding sites for relatively apolar molecules. These include the hydrophobic core and hydrophobic binding sites located in the Stern region. The latter region is particularly flexible in binding molecules as it contains the highly hydrophilic surfactant headgroups and hydrophobic domains in part due to backfolding of the surfactant tails[2,4,5] as well as water molecules.

A number of techniques is suitable for the study of binding locations inside micelles. Typically, these methods include aromatic ring current effects which induce changes of (NMR) chemical shifts,[12-14] paramagnetic relaxation enhancement experiments,[15-17] fluorescence probing experiments[18] and fluorescence lifetime experiments.[19] From the results of numerous studies applying, among others, the

techniques mentioned above, it is commonly assumed that polar molecules preferably bind to micelles in the Stern region.[20-26] Moreover, it is also commonly assumed that, up to a critical concentration, aromatic molecules also bind in the Stern region.[12,27,28] However, for benzene the binding depends on surfactant structure with the preference for binding in the Stern region being higher for trimethylammonium headgroups (DTAB and CTAB) than for sulfate headgroups (SDS).[29] In combination with our results (*vide infra*), we contend that the reactions under study take place in the Stern region.

One of the key factors in the medium offered by the micellar Stern region is the concentration of headgroups and counterions. It has been estimated[30-32] that the concentration of headgroups in the Stern region lies in the range of 3 to 5 mol dm^{-3}, though recent work also suggested lower values.[33,34] The concentration of counterions is slightly less due to incomplete counterion binding, creating an electrically non-neutral environment.

In order to study the nature of the micellar Stern region, two approaches were followed. One approach involved kinetic measurements of the rates of the water-catalysed hydrolysis of activated amides and an activated ester in micelles and in solutions mimicking the local environment in the Stern region. The second approach involved spectroscopic studies employing the solvatochromic $E_T(30)$ micropolarity indicator.[35]

5.1.2 MICELLAR KINETICS AND THE PSEUDO-PHASE MODEL

The hydrolytic reactions that we used are the water-catalysed, pH-independent hydrolysis reactions (see Chapter 1) of 1-benzoyl-3-phenyl-1,2,4-triazole **5.1**, *p*-methoxyphenyl dichloroethanoate **5.2** and substituted 1-benzoyl-1,2,4-triazoles **5.3a-f** (Scheme 5.1).

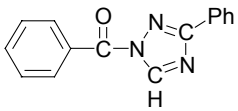

5.1

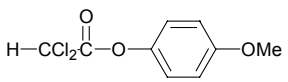

5.2

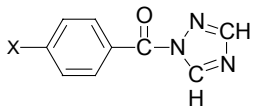

5.3a X=MeO, **b** X=Me, **c** X=H, **d** X=Cl, **e** X=CF_3O, **f** X=NO_2

Scheme 5.1

Kinetic data for reactions occurring in micellar solutions are generally analysed using the Menger–Portnoy equation[36] (Equation 5.1).

$$\left(k(m_c = 0) - k_{obsd}\right)^{-1} = \left(k(m_c = 0) - k_{mic}\right)^{-1} + \left(k(m_c = 0) - k_{mic}\right)^{-1} \cdot \left(\frac{N}{K_m}\right) \cdot \left([surf] - cmc\right)^{-1} \quad (5.1)$$

Here k_{obsd} is the observed rate constant at a surfactant concentration [surf], $k(m_c=0)$ is the rate constant in water without added cosolute (pH = 4.0) and k_{mic} is the rate constant under conditions of complete binding of the substrate to the micelles. N is the aggregation number of the micelle, K_m is the binding constant of the kinetic probe to the micelle, and cmc is the critical micelle concentration of the surfactant. This equation follows from an analysis in terms of the pseudophase model in which the micelle and bulk water are treated as if they were different phases. Equation 5.1 is the linearised form of Equation 5.2.[36]

$$k_{obsd} = \frac{k(m_c = 0) + k_{mic} \cdot K_m \cdot \left([surf] - cmc\right)/N}{1 + K_m \cdot \left([surf] - cmc\right)/N} \quad (5.2)$$

According to Equation 5.1, a plot of $(k(m_c=0)-k_{obs})^{-1}$ versus $([surf]-cmc)^{-1}$ yields $(k(m_c=0)-k_{mic})^{-1}$ as the intercept, and therefore k_{mic} can be calculated if $k(m_c=0)$ is known. From the intercept and the slope of the Menger–Portnoy plot, the micellar binding constant K_m can be calculated. Alternatively, Equation 5.2 can be used in a non-linear least-squares fitting procedure. In both treatments, $k(m_c=0)$ is set equal to the rate constant in water without added cosolute. However, the monomeric surfactant concentration in the bulk water phase equals the cmc so that there is a possibility that hydrophobic interactions between probe molecules and monomeric surfactant molecules could exert an effect on the rate of hydrolysis in bulk water. This has been shown[37] to occur for a surfactant with a cmc of 24.8 mmol dm^{-3}. For the present reactions, the minor decrease in rate constant before the cmc indicates that these effects are small. In addition, the cmc of the surfactants used here is (significantly) lower than 24.8 mmol dm^{-3}. Moreover, the Menger–Portnoy treatment is not particularly sensitive to the precise value of $k(m_c=0)$, because k_{mic} is determined from the intercept, *i.e.* mainly from the kinetic data at high surfactant concentrations. Furthermore, micellar rate constants for substrates bound to spherical micelles can be determined as long as the surfactant concentration is below the concentration at which wormlike micelles start to form.

A refinement of Equations 5.1 and 5.2 includes the possibility of different reaction domains within the micelle. The pseudo-phase model, only distinguishes

between a micellar phase and an aqueous phase. However, a three[38,39] (or multiple[40,41]) domain model can be explored in which, for example, the Stern region and the hydrophobic micellar core are treated as separate regions. Hydrolysis in the first domain, *i.e.* the core of the micelle, then occurs with a rate constant k_c, hydrolysis in the Stern region, a second domain, occurs with a rate constant k_s and the hydrolysis in bulk water, the third domain, has rate constant $k(m_c=0)$. In the limit of an infinite number of domains this model yields the "true" rate constant as the integral over the domains with their local rate constant of hydrolysis.

If we use the three domain model and assume that in the anhydrous, hydrophobic core no hydrolysis takes place (setting k_c to zero), k_{obsd} is given by Equation 5.3. (Note that here partition coefficients - concentration in one (pseudo) phase divided by concentration in another phase - and volumes are used instead of equilibrium constants and concentrations.)

$$k_{obsd} = \frac{k(m_c=0) + k_{mic} \cdot P_m \cdot \frac{V_m}{V_w}}{1 + P_m \cdot \frac{V_m}{V_w}} \tag{5.3}$$

Here, V_m, V_w, and P_m are the micellar volume, the bulk water volume and the partition coefficient of the hydrolytic probe over the micellar phase with respect to the water phase, respectively, This relation still resembles the ordinary Menger–Portnoy equation, but k_{mic} is now given by Equation 5.4.

$$k_{mic} = k_s \cdot \left\{ \frac{V_m \cdot P_m - V_c \cdot P_{ws} \cdot P_{sc}}{V_m \cdot P_m} \right\} = k_s \cdot \left\{ \frac{V_s \cdot P_{ws}}{V_m \cdot P_m} \right\} \tag{5.4}$$

Here, V_c is the micellar core volume, P_{ws} is the water–Stern region partition coefficient, P_{sc} the partition coefficient for the Stern region–core equilibrium and V_s is the Stern region volume. It turns out that the micellar rate constant is, under the above conditions, given by the rate constant for the hydrolysis in the Stern region multiplied by a factor which represents the fraction of the total amount of micellar-bound probe that resides in the Stern region.

In addition to the determination of the micellar rate constants and the micellar binding constants K_m, as outlined above, transition state pseudo-equilibrium constants K^{TS} can be determined.[42,43] Transition state pseudo-equilibrium constants K^{TS} are the hypothetical binding contants of the activated complex to the micellar pseudophase. For the system under study, K^{TS} is given by Equation 5.5.

$$K^{TS} = \frac{k_{mic} \cdot K_m}{k(m_c=0)} = \frac{k_{mic}^3 \cdot [H_2O]_{mic}^2 \cdot K_m}{k_w^3 \cdot [H_2O]_w^2} \quad (5.5)$$

In Equation 5.5, k_w^3 and k_{mic}^3 are the third-order rate constants (rate of reaction of probe P: $d[P]/dt = k_x^3 \cdot [P] \cdot [H_2O]_x^2$) in the aqueous and the micellar pseudophase, respectively, $[H_2O]_w$ the water concentration in bulk water and $[H_2O]_m$ the water concentration in the Stern region.

5.1.3 KINETIC STUDIES OF MICELLAR SYSTEMS

Reactions and reaction product distributions have previously been used to investigate micellar properties. Kinetic studies aimed at identifying the noncovalent interactions determining micellar catalysis and inhibition by medium effects have been performed on purely micellar solutions[6,7,32,37,44-48] but also on, *e.g.*, mixtures of both polymers and surfactants[49,50] to study the effect of bound polymer on micellar inhibition. In particular, the work involving the arenediazonium probe by Romsted's group is applicable and can be used to determine the concentrations of a wide range of reactive (towards arenediazonium) compounds.[33,34,51-54] In another kinetic study, the sensitivity of hydrolysis reactions towards the charge of the micelle's Stern region has been exploited in order to estimate the relative importance of hydrophobic and ionic interactions.[55,56] The polarity as a description of the medium offered by the micellar Stern region was also studied kinetically, *viz.* by a Hammett-type analysis yielding Hammett ρ values.[57] In addition, a discussion of the effects that determine the rate of hydrolysis of phenyl chloroformate in different micellar systems has been published recently.[58]

The kinetic approach used in the present study is less common. We compare the rate of reaction of a hydrolytic probe in the micelle with the rate of reactions in a model solution. Aqueous model solutions have been used before in order to estimate the polarity and water content of the micellar Stern region.[59] However, only binary mixtures containing either a salt or a polar non-ionic molecule have been used, thus modelling only one type of interaction. Here, it is shown that the Stern region can be accurately modelled in different ways depending on the sensitivity of the probe. The most elaborate model containing both salt, mimicking ionic interactions, and 1-propanol, mimicking hydrophobic interactions, separates the effect of the ionic headgroups and of the hydrophobic tails and accurately reproduces the behaviour of all tested probes.

5.2 RESULTS AND DISCUSSION

5.2.1 MICELLAR RATE CONSTANTS FOR HYDROLYSIS OF 1-BENZOYL-3-PHENYL-1,2,4-TRIAZOLE AND P-METHOXYPHENYL 2,2-DICHLOROETHANOATE, A MODEL SYSTEM FOR THE STERN REGION

In the present study, the following surfactants were used: cetyltrimethylammonium bromide (CTAB), dodecyltrimethylammonium bromide (DTAB), dodecyltrimethylammonium chloride (CTACl), sodium dodecylsulfate (SDS) and dodecylheptaoxyethylene glycol ether ($C_{12}E_7$). (Pseudo)-first-order rate constants for hydrolysis of **5.1** and **5.2** have been determined at a range of surfactant concentrations below and above the cmc; representative examples of the observed rate constants as a function of surfactant concentration are given in Figure 5.2.

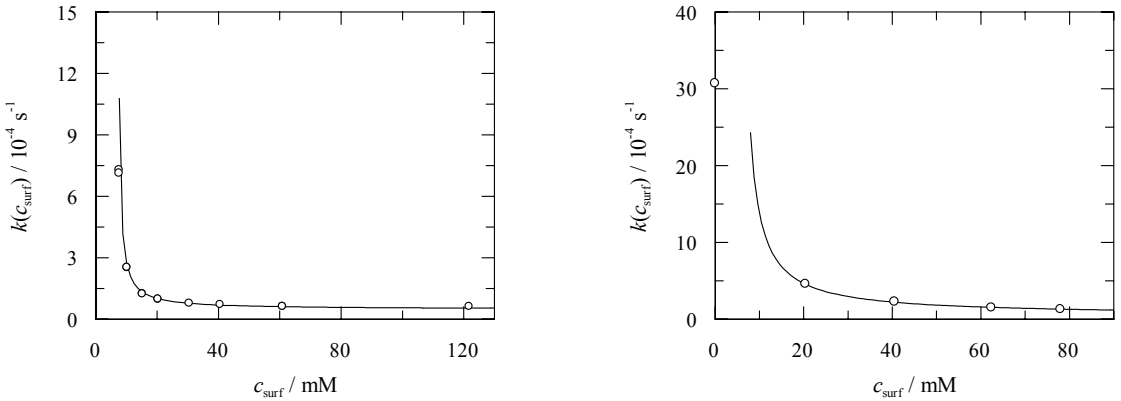

Figure 5.2: Representative examples of the hydrolysis rate constants for **5.1** and **5.2** as a function of surfactant concentration at 298.15K. *Left*: **5.1** in SDS and *Right*: **5.2** in SDS. Lines are fits to Equation 5.2.

According to Figure 5.2, rates decrease with increasing surfactant concentration. For every probe–micelle combination, the rate constant for hydrolysis of the probe bound to the micelle, k_{mic}, was determined, using the "conventional two domain" Menger–Portnoy equation. Results for **5.1** and **5.2** as well as the micellar $E_T(30)$ values, indicating the micropolarity in the micellar pseudophase, are summarised in Table 5.1.

Table 5.1: Micellar rate constants[a] and $E_T(30)$ values for different micelle-probe combinations at 298.15K.

	k_{mic} / 10^{-5} s^{-1}		
	5.1	**5.2**	$E_T(30)$ / kcal mol^{-1}
CTAB	6.7±0.8	1.6±0.5	53.5
DTAB	12.6±0.5	n.d.	53
CTACl	14.5±1.5	n.d.	n.d.
SDS	4.8±0.9	4.7±1.8	57
SDS[b]	2.4±0.2	n.d.	n.d.
$C_{12}E_7$	5.8±0.3	0.6±0.4	n.d

[(a)] Rate constants in water without added cosolute are $k_{\mathbf{5.1}}(m_c=0)$: (125.5±1.5) × 10^{-5} s^{-1}, $k_{\mathbf{5.2}}(m_c=0)$: (307±6) × 10^{-5} s^{-1} and $E_T(30)$: 63.1 kcal mol^{-1}. [(b)] In the presence of 0.5 mol dm^{-3} of NaCl.

From the same curve-fits, the micellar binding constants K_m were determined. Micellar binding constants, together with transition state pseudo-equilibrium constants as determined from Equation 5.5 are given in Table 5.2.

Table 5.2: Micellar binding constants[a] and transition state pseudo-equilibrium constants for different micelle-probe combinations at 298.15K.

	K_m / 10^4 dm^3 mol^{-1}		K^{TS} / 10^3 dm^3 mol^{-1}	
	5.1	**5.2**	**5.1**	**5.2**
CTAB	7±2	11±2	3.7±1.2	0.6±0.2
SDS	11±1	3.1±0.3	4.2±0.9	0.5±0.2
$C_{12}E_7$	11±1	5.2±0.4	5.1±0.6	0.1±0.07

[(a)] In calculating the binding constant, the following aggregation numbers were used: N_{CTAB}=110, N_{SDS}=64 and N_{C12E7}=100.

According to Table 5.1, the hydrolysis of **5.1** and **5.2** is not completely inhibited upon binding to the micelles ($k_{mic}\neq0$). Therefore the reaction has to take place in a relatively "wet" region of the micelle. Since the hydrocarbon core of micelles has been shown to be virtually dry,[2-5] the hydrolyses take place in the Stern region.[60] This conclusion is strengthened by the fact that addition of salt to the micellar solution, leading to increased counterion binding, causes a further decrease in hydrolysis rate. Increased counterion binding not only affects the Stern region by

the increased concentration of counterions but also by increasing the chain packing efficiency as a result of more effectively shielded electrostatic repulsion between the headgroups. Moreover, the hydrolytic probes are slightly polar aromatic molecules, hence the Stern region is expected to be the most favourable binding site (*vide supra*).

In line with the notion that polar probe molecules bind to the Stern region, the order of micellar reaction rates for **5.1** can be accounted for by simple electrostatics.[61] First, the negative charge developed on the carbonyl moiety during the activation process will be stabilised by the net positive charge of the Stern region of CTAB-micelles. The formation of negative charge will be disfavoured by the negative charge at the surface region of the SDS-micelles. The positive charge evolving on the water molecule that acts as a general base is dispersed into other water molecules.[61] These electrostatic effects are relatively small as in all cases hydrolysis is considerably retarded, but they still show up as small differences in the observed rate constants for the fully micellar-bound hydrolytic probe. The rate constant for the nonionic micelle, in the case of **5.1** is between those for the anionic and cationic micelles, in accord with this idea. The difference in hydrophobic character of the binding site of the hydrolytic probe molecules resulting from the difference in surfactant tail length hardly seems to influence the kinetics.

The order of rate constants of **5.2** in different surfactant solutions cannot be explained in terms of the Stern region electrolyte effects. In this case, the order is opposite to what would be expected on the basis of simple electrostatics. Apparently, the difference in influence of the hydrophobic chains is more pronounced for **5.2** than for **5.1**. It has been observed before[62] that the hydrolysis of **5.2** is more sensitive to hydrophobic interactions than the hydrolysis of **5.1** and is more strongly retarded by hydrophobic cosolutes. Even in micellar solutions, the influence of the hydrophobic tails on the rate of reaction is smaller for **5.1** than for **5.2**. A similar difference in behaviour as described above for **5.1** and **5.2** has previously been used to estimate the importance of hydrophobic and electrostatic interactions for reactions occurring inside micelles.[55]

The rate decrease in the micellar solutions relative to the reaction in bulk water can be caused by several effects. The water activity decreases. The substrate is stabilised by hydrophobic interactions at the micellar surface, whereas the transition state is destabilised (or less stabilised). The kinetic probe molecule can also be stabilised by interactions with the surfactant headgroups.[63] Orientation of the hydrolytic probe in the Stern region may be unfavourable, *i.e.* with the reactive

ester functionality lying closer to the micellar core. This, however, is not expected as previous work on hydrolysis of micellar bound probes yielded no evidence for specific probe orientation.[64,65] Finally, it has been demonstrated by molecular dynamics simulations[66] that the rate of reaction critically depends on the water configuration around the amide functionality. In the Stern region, the surfactant molecules, particularly the headgroups, will probably reduce chances for finding water molecules in the positions needed for the hydrolysis reaction as a result of the conformational requirements on the water molecules in the hydration shells of the headgroups. This effect will be most pronounced in the case of the ionic micelles. All the aforementioned effects might be either increased or attenuated by the electrostatic effects mentioned before.

An analysis based on the transition state pseudo-equilibrium approach,[42,43] as used before in micellar catalysis and inhibition,[40,41,67] yields insight into the stabilisation of the activated complex, as compared to the initial state. In the ideal case of reactants undergoing exactly the same reaction but having different micellar binding constants because of increasing hydrophobic tail length, K^{TS} varies linearly with K_m with a slope of 1.[68] Unfortunately, as can be seen from Equation 5.5, the difference in water activity between bulk water and water as bound to the micelle in this analysis also determines K^{TS}/K_m. This means that, in the system under study, the activated complex is stabilised to a much lesser extent than the initial state by binding to the micelle or the water activity in the Stern region is considerably lower than that in bulk water, or, a combination of these two effects occurs.

As a model system for the Stern region of the micelle, a concentrated solution of a model solute was used. These solutes were chosen on the basis of their resemblance to the micellar headgroup.[19,32,69] For both CTAB and DTAB, tetramethylammonium bromide (TMAB) was chosen. For SDS, sodium monomethylsulfate (NMS) was used. As a model for $C_{12}E_7$, both tetra- and heptaethylene glycol (TEG and HEG) were used.[70] The effect of incomplete counterion binding, leading to a net charge of the micellar Stern region, cannot be mimicked by these concentrated solutions. Plots of the rate constants for the two probes as a function of model-solute concentration are given in Figure 5.3.

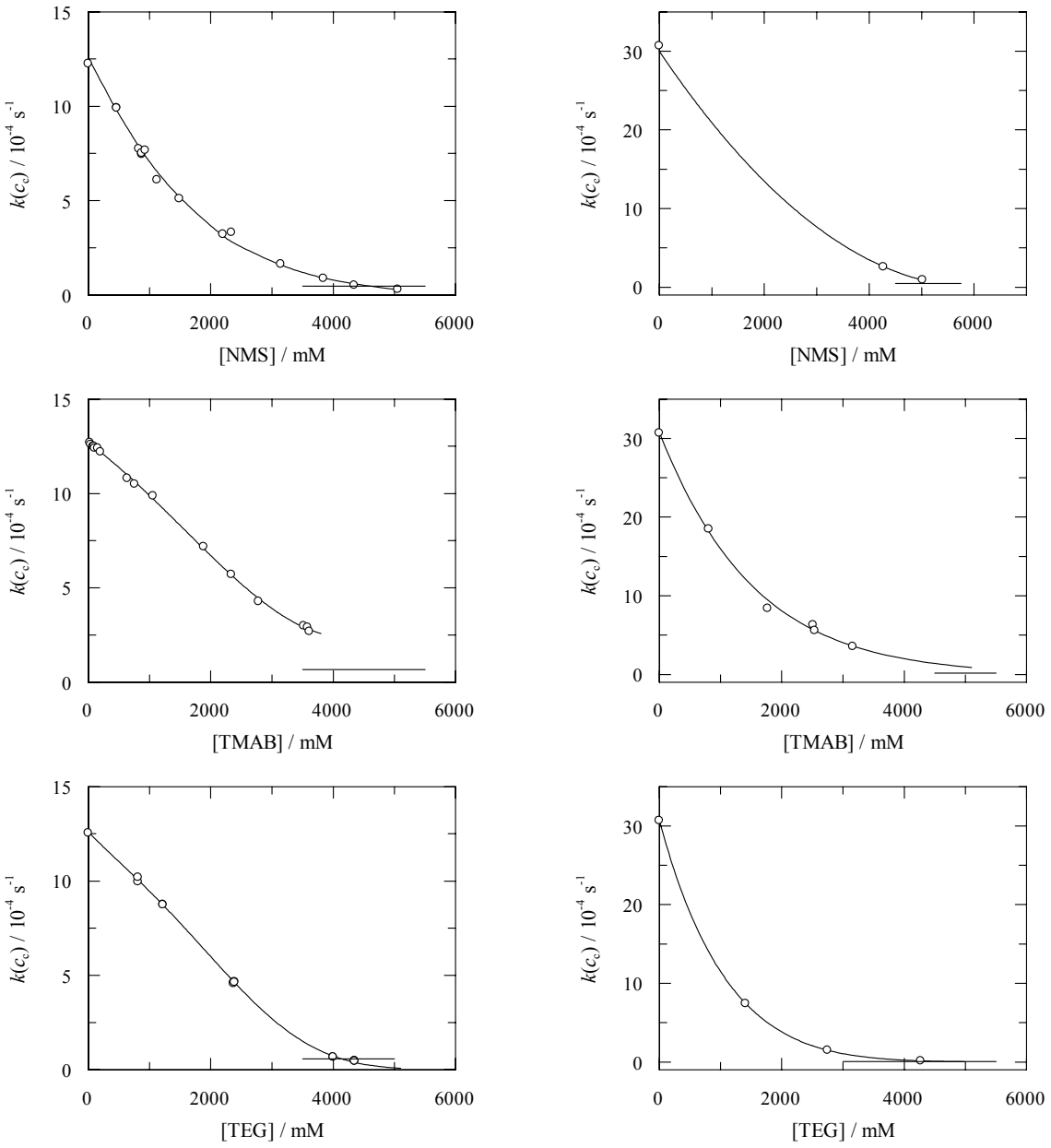

Figure 5.3: Matching and near-matching of the rate constants at 298.15K. Horizontal lines indicate micellar rate constants. *Upper left*: **5.1** in NMS/SDS *Upper right*: **5.2** in NMS/SDS *Middle left*: **5.1** in TMAB/CTAB *Middle right*: **5.2** in TMAB/CTAB *Bottom left*: **5.1** in TEG/$C_{12}E_7$ *Bottom right*: **5.2** in TEG/$C_{12}E_7$. Please note that the vertical scales for kinetics involving **5.2** start at –1.

The model compounds, lacking the hydrophobic chains, decelerate the reaction, indicating that hydrophobic interactions are not the only interactions decelerating the water-catalysed hydrolysis reactions. Interestingly, the micellar rate constant matches (for **5.1**) or nearly matches (for **5.2**) the rate constant for hydrolysis in the model compound solutions at rather high concentrations. The matching for **5.1** occurs at a 4.3 mol dm^{-3} aqueous solution of NMS for the SDS micelles, at 4.2 mol

dm^{-3} TEG for $C_{12}E_7$ micelles and around 5 mol dm^{-3} (from extrapolation, at least >4.2 mol dm^{-3}) for CTAB micelles.

The headgroup concentration in the Stern region can be estimated. From known micellar and molecular dimensions, an educated guess can be made of the volume of the micellar Stern region.[71] Together with the aggregation number and counterion binding,[72] the headgroup concentration in the Stern region can be calculated. These concentrations are given in Table 5.4.

Table 5.3: Calculated[a] and experimental salt concentrations in the micellar Stern region.

	[Headgroup] / mol dm^{-3}		
	calculated	kinetics	$E_T(30)$
SDS	2.7-5.4	4.3	17
CTAB	2.9-5.7	>4.2	10
DTAB	2.6-5.3	>4.1	10
$C_{12}E_7$	7-10[b]	16.8	
	15-18[c]		

(a) The following parameters were used in the estimation of headgroup concentrations in the Stern region: SDS: l_c=16.7 Å, d_{Stern}=3.7-6.5 Å, N=64, β=0.65; CTAB: l_c=21.7 Å, d_{Stern}=4.0-6.6 Å, N=110, β=0.8; DTAB: l_c=16.7 Å, d_{Stern}=4.0-6.6 Å, N=60, β=0.75; $C_{12}E_7$: l_c=16.7 Å, d_{Stern}=3.6 Å, N=64-100. See reference 72. (b) Monomer concentration of the completely stretched ethylene glycol chain. (c) Monomer concentration of a backfolded ethylene glycol chain.

The calculated concentrations can be compared to the electrolyte concentrations for which the substrate hydrolyses with the same rate constant as under conditions of 100% binding to the micelles (k_{mic}). The fact that the salt concentrations, as they are deduced from the kinetic experiments, match the calculated salt concentrations so closely, can be regarded as evidence that for **5.1** and **5.2**, an important part of the rate inhibition is a salt effect.[73,74] Hence, differences in stabilisation of the initial state and the activated complex by hydrophobic interaction with surfactant tails are not the only rate-retarding effects. The hydrolysis reactions of **5.1** and **5.2** are able to respond strongly to hydrophobic interactions as has been demonstrated convincingly for a range of hydrophobic co-solutes.[62,75-78] Depending on the relative importance of hydrophobic interactions for the rate retardations, the salt

concentrations at which the match in rate constants occurs still denote an upper limit for the Stern region headgroup concentration.

Remarkably, the seven ethylene glycol units of the $C_{12}E_7$ surfactant headgroup have a similar effect on the hydrolysis of both probes as the ionic headgroups of the other surfactants used in this study.[79] When kinetic data obtained for the micellar solutions are compared with those for tetraethylene glycol solutions,[70] no match in rate constant occurs until an ethylene glycol monomeric unit concentration of 16 mol dm^{-3}, suggesting that the concentration of ethylene glycol units in the Stern region has a similar value. A calculation of the Stern region concentration of ethylene glycol headgroup units suggests a value of 8 mol dm^{-3} in the case that the ethylene glycol chain is fully extended. The discrepancy by a factor of two can be explained by taking into account back folding or meandering of the heptaethylene glycol units of the surfactant molecules, as has been observed in other studies.[3,80]

The decreased water activity in the Stern region of SDS, estimated by others[81] to be about 0.6, coincides with the decreased water-concentration in the model compound solutions corresponding to the Stern region, *viz.* around 33 mol dm^{-3} (vs. 55.5M for pure water). This means that only a deceleration factor of three (the reaction is bimolecular in water) can be attributed to the decreased water activity. The rest of the deceleration has to be attributed to reaction-specific requirements on probe and water configuration[66] not being met as a result of the presence of surfactant headgroups or model compound molecules forcing the water molecules into certain configurations. For CTAB, the water concentration in the Stern region has been estimated to be 45 mol dm^{-3},[33,34] (from an extrapolated density of 1.17 g cm^{-3} for a hypothetical 4.3 mol dm^{-3} aqueous solution of TMAB, the water concentration is estimated to be approximately 28 mol dm^{-3}) meaning that almost the entire rate deceleration is caused by restricted motion (lower activity coefficient) of the water molecules as found in the Stern region.

This effect is different for the ethylene glycol solutions. Here the concentration of water in solution for the matching solutions is so low (approx. 15 mol dm^{-3}) that a large part of the deceleration, *viz.* a factor of 13.4, can be directly attributed to the reduced availability of water molecules in the solution, without invoking reduced mobility of the water molecules. Alternatively, the water concentration in the Stern region can be estimated to be approximately 48 mol dm^{-3}, from the hydration number of ethylene glycol moieties of three.[54,72] However, creating a solution that is 48 mol dm^{-3} in water and 16 mol dm^{-3} in ethylene glycol is impossible. Therefore the hydration of the ethylene glycol units varies over the Stern region with the

innermost ethylene glycol units, close to the hydrophobic core and presumably also to the binding location of the hydrolytic probe, least hydrated. In the case of the ionic solutions, water molecules are present, but are now much more restricted in their movements as a result of stronger interactions with the ions.

In order to check the generality of the results obtained with the kinetic probes, a second type of probe was employed, *viz.* the solvatochromic $E_T(30)$ probe. This dye indicator is regarded as one of the most useful polarity indicators.[35,82] One of the reasons for this is the marked sensitivity of the visible absorption spectrum to small changes in the medium surrounding the betaine dye.

Table 5.4: $E_T(30)$ values of salt solutions at 298.15K.

[TMAB] / mM	$E_T(30)$ / kcal mol^{-1}	[NMS] / mM	$E_T(30)$ / kcal mol^{-1}
995	61.8	1989	63.8
2185	61.2	4248	62.6
3178	60.3		
3686	59.5		

The $E_T(30)$-probe shows completely different behaviour from that of the hydrolytic probes (Tables 5.1, 5.3 and 5.4). Comparison of the $E_T(30)$ value of micellar solutions with those for the same model compound solutions (Table 5.4) as used in the kinetic experiments, shows that matching occurs in a completely different region of model compound concentration (Table 5.3). Assuming that the $E_T(30)$ probe also binds in the Stern region, in terms of the solvatochromic comparison, the micellar Stern region does not resemble a 4–5 mol dm^{-3} model compound solution. Hence, the spectroscopic probe is sensitive to and/or experiencing other types of interactions than the kinetic probes **5.1** and **5.2**.[83]

The overall way the Stern region manifests itself turns out to be the result of a subtle interplay between the interactions a probe molecule (*e.g.* a hydrolytic probe or a solvatochromic probe) can have with both the hydrophobic tails and with the headgroups and water molecules present in the Stern region and how sensitive the measured property is to those interactions. This, of course, can be expected for a region that constitutes a concentrated aqueous solution of surfactant headgroups and counter-ions next to the hydrophobic micellar core. Interestingly, different probes may have different sensitivity towards interactions with the headgroups and interactions with the alkyl tails.

5.2.2 AN EXTENDED MODEL OF THE MICELLAR STERN REGION

As indicated above, different probes may have different sensitivities towards interaction with the ionic headgroups or the hydrophobic tails. The extreme example of this sofar being the $E_T(30)$ probe, the behaviour of which cannot be accounted for solely on the basis of a concentrated salt solution. The fact that the hydrolysis of phenyl chloromethanoate is not nearly as much retarded in salt solutions as it is in micellar solutions provides another example.[58] Yet another indication is the failure of **5.2** to show a relation between the charge of the Stern region and the rate-retarding effect, as also observed by others for the hydrolysis of 4-nitrophenyl 2,2-dichloropropanoate.[55] If we accept the $E_T(30)$ probe as a good micropolarity indicator, this indicates that the micropolarity of the micellar Stern region is considerably lower than expected on the basis of the concentrated salt solutions used as a Stern region mimic so far. Another indication of the polarity of a reaction medium can be obtained from Hammett plots.[84-86] The sensitivity of the rate of reaction towards electron donating and electron withdrawing abilities of substituents (as quantified by their Hammett σ-values) depends on the medium in which the reaction is performed. A Hammett-type analysis has been performed for the micellar Stern region before,[57] the main conclusion from that study was that the micellar Stern region is more apolar than water. We have chosen the hydrolysis of a series of substituted 1-benzoyl-1,2,4-triazoles **5.3a-f** (Scheme 5.1), occurring via the mechanism as described in Chapter 1, in the presence of micelles of DTAB and CTAB for detailed analysis. The rate constants in water without added cosolutes, $k_p(m_c=0)$,[87] together with the Hammett substituent constants[88] are summarised in Table 5.5.

Table 5.5: Overview of the hydrolysis rate constants of 1-benzoyl-1,2,4-triazoles **5.3a-f** at 298.15K.

probe	σ_p	$k_p(m_c=0)$ / 10^{-4} s^{-1}
5.3a	-0.28	4.1
5.3b	-0.14	9.4
5.3c	+0.00	21.2
5.3d	+0.24	36.0
5.3e	+0.32	43.1
5.3f	+0.81	278

According to Table 5.5, the rate of hydrolysis increases with increasing electron-withdrawing ability of the para-substituent, as expected for a reaction in which a (partial) negative charge develops going towards the activated complex. The hydrolysis of all of these probes is retarded in solutions containing micelles of CTAB and DTAB (examples given in Figure 5.4).

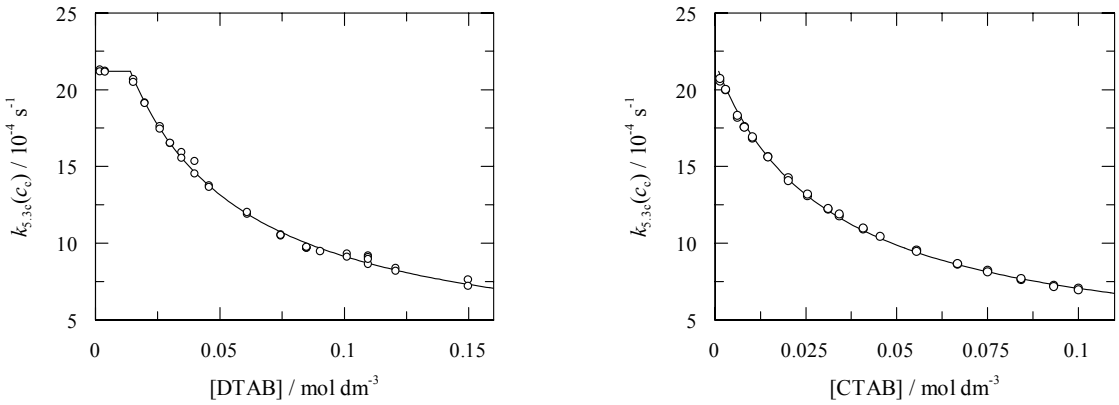

Figure 5.4: Rate constants of hydrolysis of **5.3c** at 298.15K in solutions containing *Left*: DTAB micelles and *Right*: CTAB micelles.

From a non-linear least-squares fit to Equation 5.2, micellar rate constants for hydrolysis and micellar binding constants were determined (Table 5.6).

Table 5.6: Overview of micellar rate constants of hydrolysis and micellar binding constants of 1-benzoyl-1,2,4-triazoles **5.3a-f** at 298.15K.

	$k_{p,CTAB}$ / 10^{-4} s^{-1}	$k_{p,DTAB}$ / 10^{-4} s^{-1}	$K_{p,CTAB}$[b] / 10^3 dm^3 mol^{-1}	$K_{p,DTAB}$[c] / 10^3 dm^3 mol^{-1}
5.3a	0.34±0.03	0.25±0.04	9.3±0.3	3.1±0.2
5.3b	0.78±0.08	0.70±0.06	10.3±0.4	3.4±0.1
5.3c	2.5±0.2	2.4±0.3	3.44±0.07	1.5±0.1
5.3d	5.4±0.2	6.67±0.10	13.9±0.4	4.2± 0.1
5.3e	7.0±0.1	8.4±0.2	21.0±0.3	6.0±0.1
5.3f	67±3	74±12	6.4±0.3	1.4±0.2

[a] Cmc's set to 0.9mM and 14.0mM for CTAB and DTAB, respectively. These are the average values of the cmc's determined from initial curve-fitting with unrestricted cmc's. [b] Based on an aggregation number of 110.[72] [c] Based on an aggregation number of 70.[72]

According to Table 5.6, there is no appreciable trend in the micellar binding constants of **5.3a-f** with substituent constant. However, micellar binding constants for CTAB on average are about three times the corresponding micellar binding constant for DTAB. For comparison of the rate retarding effects on the hydrolysis of the individual hydrolytic probes, the relative rate constants of hydrolysis in aqueous solutions of DTAB and CTAB and in water without added cosolutes and the natural logarithms of the relative rate constants are given in Table 5.7.

Table 5.7: Natural logarithms of the relative rate constants of hydrolysis of **5.3a-f** taking place in micelles of DTAB and CTAB at 298.15K.

	CTAB		DTAB	
	$k_{p,mic}/k_p(m_c=0)$	$\ln(k_{p,mic}/k_p(m_c=0))$	$k_{p,mic}/k_p(m_c=0)$	$\ln(k_{p,mic}/k_p(m_c=0))$
5.3a	0.08	-2.5±0.1	0.06	-2.8±0.2
5.3b	0.08	-2.5±0.1	0.07	-2.6±0.1
5.3c	0.12	-2.14±0.06	0.12	-2.1±0.3
5.3d	0.15	-1.90±0.04	0.19	-1.68±0.02
5.3e	0.16	-1.82±0.02	0.20	-1.63±0.02
5.3f	0.24	-1.42±0.03	0.27	-1.3±0.2

For most probes, micelles of CTAB retard hydrolysis more than micelles of DTAB, which intuitively is in line with the higher micellar binding constants for **5.3a-f** and the longer alkyl tail on the surfactant both suggesting the possibility to engage in stronger hydrophobic interactions. However, according to Table 5.7, micelles of DTAB retard the hydrolysis of **5.3a** and **5.3b** more compared with micelles of CTAB. This is remarkable, as the binding constant to micelles of DTAB is considerably lower than to micelles of CTAB (Table 5.6). Apart from this unexpected stronger rate-retarding effect by DTAB, a second point that emerges is that there is a trend in the values of $\ln(k_{p,mic}/k_p(m_c=0))$ to increase (decrease in absolute value) with increasing σ_p.

In the previous section, the micellar Stern region was modelled using only a salt resembling the surfactant headgroups.[89] Just like other studies in which the micellar medium was modelled using only a single characteristic (*vide supra*), the model was not always successful. In the next series of experiments, we attempt to improve the model that only takes the ionic interactions into account by adding a compound mimicking the interactions with the alkyl tails of the surfactants. 1-Propanol was used as added cosolute because it is the highest linear alcohol completely miscible with water at 298.15K. Therefore an attempt was made to find solutions containing appropriate molalities of TMAB and 1-propanol in order to mimick the ionic and hydrophobic interactions in the micellar Stern regions of DTAB and CTAB micelles. In order to find such a solution, the effects of the ionic headgroups and alkyl tails as mimicked by TMAB and 1-propanol, respectively, have to be distinguished. Ideally, trends in sensitivity towards the presence of these two compounds should be different within the series of hydrolytic probes used. Therefore, the rate-retarding effects of TMAB and 1-propanol were determined in the ranges from 0 up to (at most) 5 mol kg^{-1} and from 0 up to 3.6 mol kg^{-1}, respectively (Table 5.8).

Table 5.8: Rate-retarding effects of 1-propanol and TMAB on the hydrolysis of substituted 1-benzoyl-1,2,4-triazoles **5.3a-f** at 298.15K.

	$\frac{\partial \ln\{k_p(m_{1\text{-propanol}})/k_p(m_c=0)\}}{\partial m_{1\text{-propanol}}}$ / 10^{-1} kg mol^{-1}	$\frac{\partial \ln\{k_p(m_{TMAB})/k_p(m_c=0)\}}{\partial m_{TMAB}}$ / 10^{-1} kg mol^{-1}
5.3a	-2.36±0.05	-3.06±0.15
5.3b	-2.32±0.06	-2.40±0.07
5.3c	-2.01±0.05	-2.58±0.06
5.3d	-1.51±0.03	-2.59±0.07
5.3e	-1.31±0.03	-2.26±0.02
5.3f	-0.58±0.02	-2.40±0.07

According to Table 5.8, the necessary difference in sensitivity trends indeed exists. Whereas the effect of TMAB on the hydrolysis of **5.3a-f** is nearly constant, the rate-retarding effect of 1-propanol varies dramatically with the Hammett substituent constant (Figure 5.5).

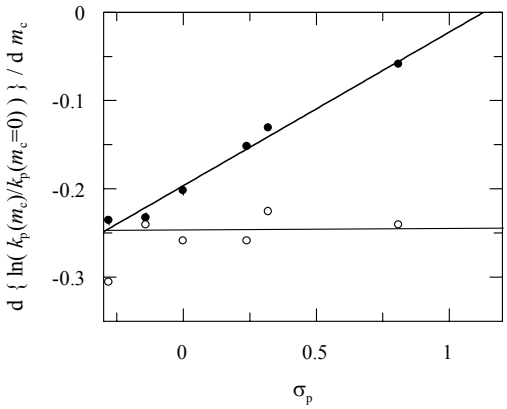

Figure 5.5: Plot of the rate retarding effects of 1-propanol (•) and TMAB (o) on the hydrolysis of probes **5.3a-f** at 298.15K.

This difference in behaviour allows the calculation of the individual molalities of the headgroup mimic and the tail mimic for a solution mimicking the micellar Stern region. Therefore, these molalities reflect the relative importance of the ionic interactions and the hydrophobic interactions in the Stern region. A quantitative description is obtained of their relative importance. The determination can be carried out both graphically and mathematically. For the graphical solution, it is noted that the rate-retarding effect of 1-propanol decreases roughly linearly with

substituent parameter. Hence, there is a hypothetical hydrolytic probe with a (hypothetical) substituent, the hydrolysis of which is not retarded by 1-propanol. This hypothetical substituent has a σ_p of about 1.13.[90]

A plot of $\ln(k_{p,mic}/k_p(m_c=0))$ as a function of σ_p can be divided into two parts, *viz.* a part where the rate retardation is caused by hydrophobic interactions and a part where the rate retardation is caused by the interactions with the ionic headgroups (Figure 5.6).

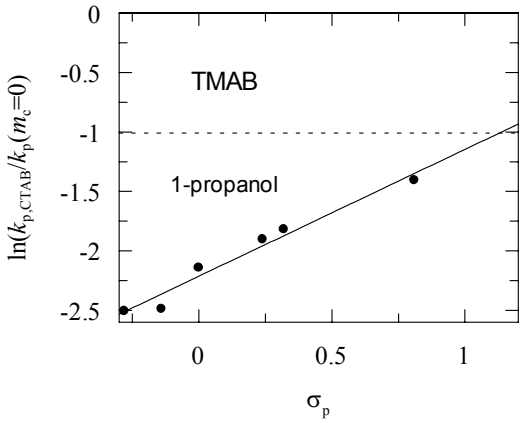

Figure 5.6: Plot of the rate-retarding effects of CTAB micelles on hydrolytic probes **5.3a-f** at 298.15K. Dotted line indicates the division between rate-retarding effects attributed to interactions with ionic surfactant headgroups as modelled by TMAB (upper section) and the rate-retarding effects attributed to interactions with the surfactants' alkyl tails as modelled by 1-propanol (lower section). Note that the dotted and the solid lines cross at σ_p=1.13.

From Figure 5.6, the average rate-retarding effect of TMAB on the hydrolysis reactions and the approximate slope of a plot of the rate-retarding effect of 1-propanol as a function of substituent parameter, the solution resembling the micellar Stern region of a CTAB micelle is estimated to be 4 mol kg^{-1} in TMAB and 6 mol kg^{-1} in 1-propanol.

A more elegant solution, however, is provided by mathematics. Using the equations as set up in Chapter 1, the rate-retarding effect as found in an aqueous solution containing 1-propanol and TMAB can be described as a summation of the individual effects caused by added TMAB and 1-propanol. Again, assuming that the environment in which the probe binds to the micelle can be modelled by an aqueous solution of TMAB and 1-propanol, Equation 5.6 is obtained.

$$\frac{\partial \ln\left[\frac{k_{\mathrm{p}}(m_{\text{1-propanol}})}{k_{\mathrm{p}}(m_c=0)}\right]}{\partial m_{\text{1-propanol}}} \cdot m_{\text{1-propanol}} + \frac{\partial \ln\left[\frac{k_{\mathrm{p}}(m_{\mathrm{TMAB}})}{k_{\mathrm{p}}(m_c=0)}\right]}{\partial m_{\mathrm{TMAB}}} \cdot m_{\mathrm{TMAB}} = \ln\left[\frac{k_{\mathrm{p,mic}}}{k_{\mathrm{p}}(m_c=0)}\right] \tag{5.6}$$

Equation 5.6 can be rewritten in the form of Equation 5.7.

$$a_{\mathrm{p,1\text{-}propanol}} \cdot m_{\text{1-propanol}} + a_{\mathrm{p,TMAB}} \cdot m_{\mathrm{TMAB}} = c_{\mathrm{p}} \tag{5.7}$$

Herein is $a_{\mathrm{p,1\text{-}propanol}}$ the derivative of the natural logarithm of the relative rate constant with respect to molality of 1-propanol, $a_{\mathrm{p,TMAB}}$ the same derivative with respect to the molality of TMAB and c_{p} is the natural logarithm of the the relative micellar rate constant. For a model solution consistently describing the micellar Stern region, this equation should hold for all surfactant/probe combinations. For a given surfactant, there is a model solution of $m_{\text{1-propanol}}$ mol kg^{-1} in 1-propanol and m_{TMAB} mol kg^{-1} in TMAB in which the hydrolysis reactions of *all* hydrolytic probes **5.3a-f** are retarded to the same extent as in the micelle. Hence, for every surfactant there is a set of linear equations given by Equation 5.7. In its extended form, this gives an equation of the form given in Equation 5.8 for every surfactant.[91]

$$\begin{bmatrix} a_{\text{MeO, 1-propanol}} & a_{\text{MeO, TMAB}} \\ a_{\text{Me, 1-propanol}} & a_{\text{Me, TMAB}} \\ a_{\text{H, 1-propanol}} & a_{\text{H, TMAB}} \\ a_{\text{Cl, 1-propanol}} & a_{\text{Cl, TMAB}} \\ a_{\text{F}_3\text{CO, 1-propanol}} & a_{\text{F}_3\text{CO, TMAB}} \\ a_{\text{NO}_2\text{, 1-propanol}} & a_{\text{NO}_2\text{, TMAB}} \end{bmatrix} \cdot \begin{bmatrix} m_{\text{1-propanol}} \\ m_{\mathrm{TMAB}} \end{bmatrix} = \begin{bmatrix} \mathrm{c}_{\mathrm{MeO}} \\ \mathrm{c}_{\mathrm{Me}} \\ \mathrm{c}_{\mathrm{H}} \\ \mathrm{c}_{\mathrm{Cl}} \\ \mathrm{c}_{\mathrm{F_3CO}} \\ \mathrm{c}_{\mathrm{NO_2}} \end{bmatrix} \tag{5.8}$$

Overdetermined (not exact) matrix systems of the form given in Equation 5.8 can be solved (finding the least-squares solution vector m_{c}) using singular value decomposition.[92,93] The entries in the vector c_{p} and the matrix $a_{\mathrm{p,c}}$ are given in Tables 5.7 and 5.8, respectively. Applying the singular value decomposition method, a calculated model solution mimicking the micellar Stern region of a CTAB micelle is decribed in Table 5.9. These numbers decribe the “first-order solution” (1OS).

Table 5.9: Molalities and concentrations[a] of 1-propanol and TMAB in first-order solutions for binding sites in micelles of DTAB and CTAB.

	DTAB		CTAB	
	m_c / mol kg^{-1}	c_c / mol dm^{-3}	m_c / mol kg^{-1}	c_c / mol dm^{-3}
1-propanol	9.3±0.9	5.1	5.0±0.5	2.6
TMAB	1.5±0.6	0.8	4.9±0.3	2.6
water		30		29

(a) Concentrations were calculated using the (experimentally determined) densities of the first-order solutions at 298.15K for CTAB of 1.079 g cm^{-3} and for DTAB of 0.975 g cm^{-3}

The salt concentrations in Table 5.9 are lower than those in the concentrated salt solutions described in the previous section, where the salt was taken as the only origin of rate retardation. Still, the salt concentrations match the calculated concentration ranges as given in Table 5.3, but now at the lower side of the calculated range. In fact, the value of 2.6 mol dm^{-3} is in reasonable agreement with the concentration of bromide anions (1.6 mol dm^{-3}) as determined by the Romsted arenediazonium probe.[69] Assuming a counterion binding of 0.8, this corresponds to a concentration of ionic headgroups of 2.0 mol dm^{-3}. The rate constants for hydrolysis[94] and the $E_T(30)$-value were determined in the solution mimicking CTAB made according to Table 5.9. The results are summarised in Table 5.10.

Table 5.10: Comparison of the first-order solution and the micellar system for CTAB at 298.15K.

	$k_{p,mic}$ / 10^{-4} s^{-1}	$k_{p,1OS}$ / 10^{-4} s^{-1}	$k_{p,1OS}^{calc}$ / 10^{-4} s^{-1} [a]	$\ln(k_{p,mic}/k_{p,1OS})$
5.3a	0.34±0.03	0.54±0.04	0.28	-0.463
5.3b	0.78±0.08	1.45±0.03	0.92	-0.620
5.3c	2.5±0.2	3.71±0.24	2.21	-0.399
5.3d	5.4±0.2	8.0±0.1	4.76	-0.402
5.3e	7.0±0.1	10.28±0.07	7.41	-0.386
5.3f	67±3	77.7±5.6	64.6	-0.132
$E_T(30)$	(53.5)[b]	(55.8)[b]		

(a) Calculated using Equation 5.8. (b) $E_T(30)$-values in kcal mol^{-1}.

According to Table 5.10, the rate constants for hydrolysis of all the individual probes in the model solution are only slightly higher than those in the CTAB Stern region. This is attributed to the fact that the hydrolysis data for **5.3a-f** in binary aqueous solutions of TMAB or 1-propanol have been extrapolated to rather high concentrations. In addition, the final solution is a ternary solution. A further encouraging observation is that the experimental $E_T(30)$-value found in the mimicking solution is in far better agreement with the micellar values than the model solution containing only TMAB. As a further test of the reliability of these predicted molalities, we calculated the expected micellar (CTAB) rate constant of hydrolysis for **5.1**. Using the molalities (and concentrations) determined here, together with the *G*(c)-value of 1-propanol for the hydrolysis of **5.1** determined previously[95] and the molarity dependence of the hydrolysis of **5.1** in aqueous solutions containing TMAB (Figure 5.3), the natural logarithm of the relative rate constant of the hydrolysis of **5.1** in CTAB micelles is expected to be -2.17±0.24, corresponding to a micellar rate constant of 1.4±0.4 10^{-4} s^{-1}. Experimentally, a micellar rate constant of 0.67±0.08 10^{-4} s^{-1} is found (Table 5.1). Similarly, the natural logarithm of the relative rate constant of the hydrolysis of **5.1** in DTAB micelles is expected to be -2.46±0.24. This corresponds to a micellar rate constant of 1.1±0.3 10^{-4} s^{-1}, in good agreement with the experimental micellar rate constant of 1.26±0.05 10^{-4} s^{-1} (Table 5.1).

Returning to the results with the $E_T(30)$-probe, apparently, the $E_T(30)$-value is more sensitive towards hydrophobic interactions than towards ionic interactions, as was already mentioned above.

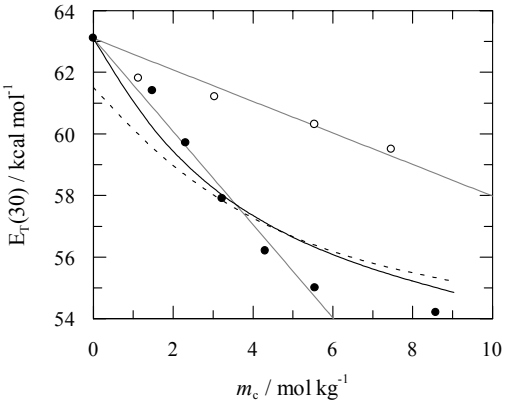

Figure 5.7: Plot of the $E_T(30)$-value as a function of molality of aqueous solutions containing TMAB (o) or 1-propanol; experimental data (•), fit (solid line) according to reference 96 and polynomial description of experimental data (dotted line) according to reference 97. Gray lines are linear fits, forced through the $E_T(30)$-value of water.

According to Figure 5.7, the $E_T(30)$-value is indeed more sensitive towards interactions with 1-propanol, mimicking hydrophobic interactions, than towards TMAB, mimicking ionic interactions (slopes of –1.51 and –0.51, respectively). Note that **5.1** and the $E_T(30)$ probe are the only probes tested here that are more sensitive towards hydrophobic interactions than towards ionic interactions. Despite the apparent lack of agreement about the actual $E_T(30)$-values of aqueous solutions of 1-propanol (Figure 5.7), the relatively high sensitivity of the $E_T(30)$ probe towards hydrophobic interactions provides a possibility for a quick test of the nature of the micellar Stern region; using the $E_T(30)$ probe for the interactions with the alkyl tails and **5.3e** for the interactions with the ionic headgroups.[98] This results in a 2×2 matrix with one row strongly dependent on TMAB molality and one row mainly dependent on 1-propanol molality. However, the $E_T(30)$-value of a micelle has been shown to be ambiguous as $E_T(30)$ is not always independent of micelle concentration.[59,99] Hence, the number that is thus obtained will be primarily indicative.

The determination of the composition of a hypothetical solution mimicking the micellar Stern region yields valuable insight into the nature of the micellar Stern region. The present results (Table 5.9) suggest that DTAB micelles offer binding sites that, as a reaction medium, are more hydrophobic in nature than those in CTAB. At the same time, the hydrolytic probes seem to experience weaker interactions with the ionic headgroups. This difference in reaction medium indicates that binding-sites in micelles of DTAB are deeper inside the micelle than binding sites in CTAB micelles. This in turn suggests that micelles of DTAB possess more open structures than micelles of CTAB, which is an intuitively correct conclusion.

Using the results obtained in the preceding analysis, we can describe the micellar binding and micellar inhibition together in a single scheme (Scheme 5.2, different contributions not drawn to scale).

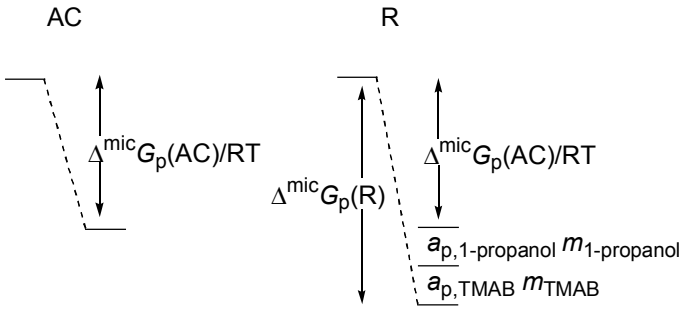

Scheme 5.2

Both reactant (R) and activated complex (AC) bind to the micelle (Table 5.2). However, R binds to the micelle much more strongly than AC, causing the rate retardation. It is useful to divide the Gibbs energy of binding of R to the micelle into a "dynamic" part, causing rate effects, and a "passive" part, not causing rate effects (*cf*. a related division into passive and dynamic interactions in reference 100). Using Equation 5.8, the dynamic part has been divided into rate-retarding effects caused by interactions with ionic groups (as quantified by $a_{p,TMAB}{\cdot}m_{TMAB}$, the rate-retarding effect per mol kg^{-1} caused by TMAB multiplied by the molality of TMAB) and effects caused by interactions with hydrophobic groups (as quantified by $a_{p,1\text{-propanol}}{\cdot}m_{1\text{-propanol}}$).[101] The individual contributions of hydrophobic interactions and ionic interactions to the passive part of the binding Gibbs energy of R cannot be determined using the kinetic methods described here, as the passive part of the Gibbs energy is not related to rate effects. Hence, a complete quantification of the relative importance of the interactions binding R to the micelle is not feasible. Directly related to this, for probes for which the dynamic part of the Gibbs energy of binding to the micelle is the same (*i.e.* probes with the same kinetic sensitivity towards hydrophobic and ionic interactions, but for which the passive part is different) a linear relation between K_m and K^{TS} with a slope of 1 is logically expected. Such a linear relation indeed is found for probes of which only the hydrophobicity is increased by elongating an alkyl chain remote from the reaction center.[68] Similarly, the reason for the absence of a relation between rate-retarding effect, micellar binding constant and hydrophobicity of the surfactants constituting the micelle as found for some hydrolytic probes and DTAB or CTAB micelles, stems from different passive contributions to the Gibbs energy of binding to the micelle.

The present analysis, separating the contributions of hydrophobic and ionic interactions, uses the differences in rate-retarding effects caused by hydrophobic interactions and ionic interactions. However, other effects causing differences in rate-retarding effects have not been included in the present model and hence

cannot be singled out. Two of these effects influencing the differences in rate-retarding effects on different probes are easily identifiable and their source, effect and importance can be estimated. First, different hydrolytic probes could bind in different areas of the micelle and therefore experience different interactions. A possible trend in rate effects accompanying these variable binding locations is not accounted for in the present analysis. Hence, if the trend in rate effects caused by changing binding locations is comparable (or opposite) to those found for the hydrophobic (or ionic) interactions, this trend will incorrectly (and unnoticed) end up in the calculated molalities of 1-propanol and TMAB describing the micellar Stern region. However, the kinetic probes used in this study are very similar and any difference in rate effect caused by a difference in binding locations is expected to be of minimal importance. Second, the electrostatic non-neutrality of the micellar Stern region can (de)stabilise charges developing in the activated complex. In the present case, the partial negative charge on AC will be stabilised by the effectively cationic Stern region, thereby increasing the rate of reaction. The overall importance of the stabilising effect of the cationic medium depends on other factors (de)stabilising the partial negative charge; *e.g.* (de)stabilisation by substituent effects. Hence, different probes can be differently stabilised by the cationic nature of the micellar Stern region, resulting in another trend in rate effects that is not accounted for in the present analysis. The substituent-dependent stabilisation of the partial anionic charge in the activated complex by the cationic medium offered by the micellar Stern region follows a trend comparable with the trend in sensitivity towards hydrophobic interactions. Therefore, the effect of the electrostatic charge of the micellar Stern region will influence the calculated relative importance of hydrophobic and ionic interactions. It is difficult to estimate the importance of this effect from the difference in rate retarding effects observed for **5.1** in micelles of different charge (Table 5.1) as the numbers reported there include specific effects of the headgroups structure. A series of test reactions in which no charge is developed upon going to the activated complex might shed light on the importance of the micellar charge. From the previous discussion, it is also clear that whether the effect of the electrostatic non-neutrality of the micellar Stern region will be observed[55] is strongly dependent on the importance of the other interactions; trends in electrostatic effects will only be observed as long as variations in salt and hydrophobic effects do not overwhelm them.

Notwithstanding the fact that conclusions about the micellar binding sites can be drawn from the first-order solution, it would be useful to have a real solution

accurately reproducing rate constants in the micellar Stern region.[102] Especially in the study of bimolecular reactions occurring in the Stern region, it is often difficult to determine independently binding constants of both reactants and the micellar rate constant. We therefore extended the model for CTAB further to be able to make a solution that includes the non-linear rate-retarding effects at high molalities of TMAB and 1-propanol. In order to do this, we determined these rate-retarding effects at high molality in much the same way as was done at low molality. Instead of taking the rate constants in water without added cosolute as reference points, now the rate constants at the 1OS, $k_p(m_{TMAB}=4.85, m_{1\text{-propanol}}=5.00)$, for brevity denoted as $k_p(1OS)$, were taken as reference points. Rate constants of hydrolysis for the hydrolytic probes in the presence of high molalities of TMAB and 1-propanol, $k_p(m_{TMAB}, m_{1\text{-propanol}})$, were determined around the 1OS (*cf.* p. 21) molalities of 4.85 mol kg^{-1} TMAB and 5.00 mol kg^{-1} 1-propanol.

Plotting $\ln[k_p(m_{TMAB}, m_{1\text{-propanol}})/k_p(1OS)]$ as a function of molality around the 1OS molalities does not yield linear plots as was found at low concentration (Figure 5.8).

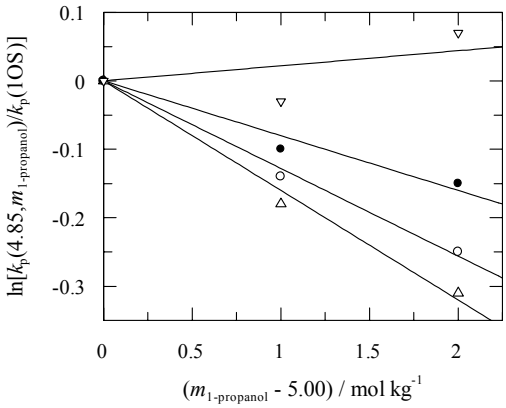

Figure 5.8: Representative examples of the rate-retarding effect of (additional) added 1-propanol on the hydrolysis of **5.3a** (o), **5.3b** (Δ), **5.3d** (•) and **5.3f** (∇) at 298.15K, using the 1OS as a reference point.

Despite the deviations from linearity of the rate retardations, we used a linear fit, forced through the 1OS reference point, to these numbers to obtain $\delta\ln[k_p(4.85, m_{1\text{-propanol}})/k_p(1OS)]/\delta m_{1\text{-propanol}}$ (denoted $a^{1OS}_{p,1\text{-propanol}}$). For the dependence on m_{TMAB}, only one additional data point (for every probe) was determined as an indication of $\delta\ln[k_p(m_{TMAB}, 5.00)/k_p(1OS)]/\delta m_{TMAB}$ (denoted $a^{1OS}_{p,TMAB}$). The resulting slopes are given in Table 5.11.

Table 5.11: Rate-retarding effects of 1-propanol and TMAB on the hydrolysis of substituted 1-benzoyl-1,2,4-triazoles **5.3a-f** at 298.15K for molalities around the 1OS.

	$a^{1OS}_{p,1\text{-propanol}}$ / 10^{-1} kg mol^{-1}	$a^{1OS}_{p,TMAB}$ / 10^{-1} kg mol^{-1}
5.3a	-1.28 ± 0.05	-1.31[a]
5.3b	-1.60 ± 0.08	-1.91
5.3c	-1.48 ± 0.12	-2.25
5.3d	-0.80 ± 0.08	-1.80
5.3e	-0.78 ± 0.05	-2.23
5.3f	+0.22 ± 0.19	-1.86

[(a)] The error has been set to 0.1 10^{-1} kg mol^{-1} for all entries in this column.

Using these numbers, an improved estimate of the molalities making a model solution accurately reproducing the micellar rate constants can be determined starting from the first-order solution. The improved solution takes into account the non-linearity of the rate-retarding effects at high molalities of TMAB and 1-propanol. Solving Equation 5.7 with $c_p=\ln(k_{p,mic}/k_p(1OS))$ (the residual of the first-order model solution) and with $a_{p,1\text{-propanol}}$ and $a_{p,TMAB}$ set to $a^{1OS}_{p,1\text{-propanol}}$ and $a^{1OS}_{p,TMAB}$ (Table 5.11), respectively, yields a correction term for the first-order solution. This correction terms equals +2.7±0.9 mol kg^{-1} for 1-propanol and +0.8±0.4 mol kg^{-1} for TMAB. Therefore the "second-order solution" should contain 7.7±0.9 mol kg^{-1} 1-propanol and 5.7±0.4 mol kg^{-1} TMAB. We have tested this second-order solution using the "quick test" described above. The rate constant for hydrolysis of **5.3e** equals 7.6 10^{-4} s^{-1}, in good agreement with the micellar value of (7.0±0.1) 10^{-4} s^{-1}, the $E_T(30)$-value equals 54.4±0.2 kcal mol^{-1}, in reasonable agreement with the micellar value of 53.5 kcal mol^{-1} (90% of the decrease in excitation energy accounted for). In addition, the rate constant for hydrolysis of **5.1** in the second-order solution was found to be (9.5±0.5) 10^{-5} s^{-1}, in reasonable agreement with the micellar value of (6.7±0.8) 10^{-5} s^{-1} (88% of the increase in Gibbs energy of activation accounted for). We therefore contend that reasonable estimates of micellar rate constants and even micropolarity as determined using the $E_T(30)$ probe can be obtained using the present model solution for CTAB.[103] Importantly, the results suggest that this can also be done for reactions and properties that were not included in the construction of the model. To our knowledge this renders the present model the first to be able to reproduce a diverse range of medium controlled

micellar properties and it indicates that the effects that were not included in the analysis (*vide supra)* play a minor role in the rate effects. In addition, the present model is not limited to alkyltrimethylammonium bromide surfactants and comparable model solutions can also be determined for other surfactants, provided the salt mimicking the micellar headgroups is chosen appropriately. The availability of solutions mimicking the micellar Stern region is especially useful for determining the factors underlying micellar catalysis or inhibition of bimolecular (or higher molecularity) reactions.

5.3 CONCLUSIONS

From the match in the CTAB and SDS micellar rate constant with the rate constant in a concentrated headgroup-model compound solution, we contend that salt effects play an important role in the micellar retardation of the hydrolysis of **5.1** and **5.2**. The hydrophobic substrate is bound in the Stern region of the micelle. However, this salt effect includes the effect of the hydrophobic moieties in the surfactant headgroup. For nonionic $C_{12}E_7$ micelles, the term 'salt effect' denotes the effect of the oligoethylene glycol moieties in the $C_{12}E_7$ headgroup, even though these are not ionic. We conclude that the Stern region can be regarded as a separate phase with a high surfactant headgroup and counterion concentration. The failure of concentrated salt solutions in reproducing other (especially polarity-related) properties of the micellar Stern region indicated the necessity to expand our model solution mimicking the Stern region in such a way that rate-retarding hydrophobic interactions are also correctly taken into account. For DTAB and CTAB, this has been done by modelling the micellar Stern region using an aqueous solution containing both 1-propanol, mimicking hydrophobic surfactant tails, and TMAB, mimicking ionic surfactant headgroups. The molalities of TMAB and 1-propanol in these solutions can be determined graphically and mathematically, using singular value decomposition. There are two "types" of model solutions, *viz*. first-order and second-order solutions. First-order solutions are determined from the rate-retarding effects of 1-propanol and TMAB at intermediate molalities, and indicate the relative importance of ionic and hydrophobic groups in the micellar Stern region. Second-order solutions can be derived from first-order solutions and take into account the non-linear rate retardations at high molalities of cosolutes. Second-order solutions

can be used to obtain estimates of micellar rate constants for reactions of which the micellar rate constants cannot be determined directly.

5.4 EXPERIMENTAL

SDS was obtained from BDH Chemicals, CTAB and TMAB[104] from Merck or Aldrich and DTAB from Sigma. $C_{12}E_7$ was from Nikko Chemicals Co., 1-benzoyl-3-phenyl-1,2,4-triazole **5.1**, p-methoxyphenyl dichloroethanoate **5.2** and substituted 1-benzoyl-1,2,4-triazoles **5.3a-f** were synthesised according to literature procedures.[105] The $E_T(30)$-probe was kindly provided by Prof. Chr. Reichardt. Sodium monomethylsulfate was synthesised by hydrolysis of dimethyl sulfate and subsequent neutralisation with NaOH. Tetraethylene glycol was obtained from Merck Schuchardt. Micellar solutions were 1×10^{-4} mol dm^{-3} in HCl, model compound solutions were acidified to pH 4 to achieve conditions for pH-independent hydrolysis. The pH of solutions was checked using either a ROSS Semi-micro combination pH electrode or a SENTRON ISFET pH probe. All solutions were made in water that was distilled twice in an all-quartz apparatus. Surfactants and salts were dried before use. If solutions were made volumetrically, the mass of all components of the solutions was determined in order to know both solute and solvent concentration, if model solutions were made by weight, the density was determined using a Mettler Toledo DA-100M density meter. Reactions were followed at 273 nm (for **5.1**), 288 nm (for **5.2**) and at 260, 262, 252, 262, 253 and 262 nm for **5.3a-f**, respectively, at 298.15±0.2K for at least six half-lives using a Perkin-Elmer λ2, λ5 or λ12 spectrophotometer. Good to excellent pseudo-first-order kinetics were obtained, the error in the rate constants being 2% or less for the micellar solutions and the dilute solutions, but up to 10% for the concentrated solutions.

The probes were injected as 2–5 μl of a stock solution of **5.1** or **5.2** or 6 μl of a stock solution of **5.3a-f** in cyanomethane into a 1 cm quartz cuvette of ca. 2.5 ml yielding a total probe concentration during the reaction of ca. 10^{-5} mol dm^{-3}. These concentrations were chosen in order to have absorbance changes not larger than 0.6. Kinetics of hydrolysis of **5.1** and **5.2** in concentrated model compound solutions were checked for salting out of the hydrolytic probes by performing a number of experiments with different probe concentrations to exclude possible effects due to rate-determining dissolution of the probe.

The measurements involving the $E_T(30)$-probe were performed at pH 11, using a Perkin-Elmer λ2-spectrophotometer. The $E_T(30)$ probe was injected as <6 μl of a stock solution of the solvatochromic probe in EtOH.

The singular value decomposition method was used as implemented in Mathcad 2001 Professional by Mathsoft Inc.

5.5 ACKNOWLEDGEMENTS

Paola Serena, Marie Jetta den Otter and Dr. Ana Martin Herranz are gratefully acknowledged for their contributions to the work described in this Chapter.

5.6 REFERENCES AND NOTES

(1) Part of this chapter has been published: Buurma, N. J., Herranz, A. M. and Engberts, J. B. F. N. *J. Chem. Soc. , Perkin Trans. 2* **1999**, 113-119.

(2) Gruen, D. W. R. *Prog. Colloid Polym. Sci.* **1985**, *70*, 6-16.

(3) Clemett, C. J. *J. Chem. Soc. A* **1970**, 2251-2254.

(4) Böcker, J., Brickmann, J. and Bopp, P. *J. Phys. Chem.* **1994**, *98*, 712-717.

(5) Shelley, J., Watanabe, K. and Klein, M. L. *Int. J. Quantum Chem. : Quantum Biol. Symp.* **1990**, *17*, 103-117.

(6) Bunton, C. A. *Catal. Rev. -Sci. Eng.* **1979**, *20*, 1-56.

(7) Berezin, I. V., Martinek, K. and Yatsimirskii, A. K. *Russ. Chem. Rev.* **1973**, *42*, 787-802.

(8) Engberts, J. B. F. N. *Pure Appl. Chem.* **1992**, *64*, 1653-1660.

(9) The difference between reaction rates and reaction rate constants should be noted. Due to compartmentalisation, concentrations of reactants inside micelles can be higher so that notwithstanding lower reaction rate constants, reaction rates can still be higher than observed in bulk water.

(10) Examples of surfactants equipped with catalytically active headgroups can be found among others in: Sirieix, J., de Viguerie, N., Riviere, M. and Lattes, A. *New J. Chem.* **1999**, *23*, 103-109; Ghosh, K. K., Pandey, A. and Roy, S. *J. Phys. Org. Chem.* **1999**, *12*, 493-498; Tagaki, W., Chigira, M., Amada, T. and Yano, Y. *J. Chem. Soc. , Chem. Commun.* **1972**, 219-220.

(11) For a particularly effective example of catalytically active counterions, see: Otto, S., Engberts, J. B. F. N. and Kwak, J. C. T. *J. Am. Chem. Soc.* **1998**, *120*, 9517-9525.

(12) Eriksson, J. C. and Gillberg, G. *Acta Chem. Scand.* **1966**, *20*, 2019.

(13) Bunton, C. A. and Cowell, C. P. *J. Colloid Interface Sci.* **1988**, *122*, 154-162.

(14) Ulmius, J., Lindman, B., Lindblom, G. and Drakenberg, T. *J. Colloid Interface Sci.* **1978**, *65*, 88.

(15) Gao, Z. S., Wasylishen, R. E. and Kwak, J. C. T. *J. Phys. Chem.* **1989**, *93*, 2190-2192.

(16) Fox, K. K., Robb, I. D. and Smith, R. *J. Chem. Soc. , Faraday Trans. 1* **1972**, 445-449.

(17) Jagannathan, N. R., Venkateswaran, K., Herring, F. G., Patey, G. N. and Walker, D. C. *J. Phys. Chem.* **1987**, *91*, 4553-4555.

(18) Almgren, M., Grieser, F. and Thomas, J. K. *J. Am. Chem. Soc.* **1979**, *101*, 279-291.

(19) Cang, H., Brace, D. D. and Fayer, M. D. *J. Phys. Chem. B* **2001**, *105*, 10007-10015.

(20) Abuin, E. and Lissi, E. *J. Colloid Interface Sci.* **1986**, *112*, 178.

(21) Yoshino, A., Yoshida, T., Okabayashi, H., Kamaya, H. and Ueda, I. *J. Colloid Interface Sci.* **1998**, *198*, 319-322.

(22) Menger, F. M. *Acc. Chem. Res.* **1979**, *12*, 111-117.
(23) Mukerjee, P., Cardinal, J. R. and Desai, N. R. *in* "Micellisation, Solubilisation and Microemulsions" (Mittal, K. L., ed.), Vol. 1, p. 241. Plenum, New York, **1977**.
(24) Russell, J. C. and Whitten, D. G. *J. Am. Chem. Soc.* **1982**, *104*, 5937-5942.
(25) Bunton, C. A., Romsted, L. S. and Smith, H. J. *J. Org. Chem.* **1978**, *43*, 4299-4303.
(26) Vitha, M. F., Dallas, A. J. and Carr, P. W. *J. Phys. Chem.* **1996**, *100*, 5050-5062.
(27) Fendler, J. H. and Patterson, L. K. *J. Phys. Chem.* **1971**, *75*, 3907.
(28) Fendler, J. H. and Patterson, L. K. *J. Phys. Chem.* **1970**, *74*, 4608-4609.
(29) Hawrylak, B. E. and Marangoni, D. G. *Can. J. Chem* **1999**, *77*, 1241-1244.
(30) Bunton, C. A., Nome, F., Quina, F. H. and Romsted, L. S. *Acc. Chem. Res.* **1991**, *24*, 357-364.
(31) Mukerjee, P. *J. Phys. Chem.* **1962**, *66*, 943-945.
(32) Menger, F. M., Yoshinaga, H., Venkatasubban, K. S. and Das, A. R. *J. Org. Chem.* **1981**, *46*, 415-419.
(33) Chaudhuri, A. and Romsted, L. S. *J. Am. Chem. Soc.* **1991**, *113*, 5052-5053.
(34) Chaudhuri, A., Loughlin, J. A., Romsted, L. S. and Yao, J. H. *J. Am. Chem. Soc.* **1993**, *115*, 8351-8361.
(35) Reichardt, C. "Solvents and Solvent Effects in Organic Chemistry" 2nd edition VCH, Weinheim, **1988**.
(36) Menger, F. M. and Portnoy, C. E. *J. Am. Chem. Soc.* **1967**, *89*, 4698-4703.
(37) Marconi, D. M. O., Frescura, V. L. A., Zanette, D., Nome, F. and Bunton, C. A. *J. Phys. Chem.* **1994**, *98*, 12415-12419.
(38) Minero, C., Pramauro, E. and Pelizzetti, E. *Langmuir* **1988**, *4*, 101-105.
(39) Da Rocha Pereira, R., Zanette, D. and Nome, F. *J. Phys. Chem.* **1990**, *94*, 356-361.
(40) Davies, D. M., Gillitt, N. D. and Paradis, P. M. *J. Chem. Soc. , Perkin Trans. 2* **1996**, 659-666.
(41) Davies, D. M. and Foggo, S. J. *J. Chem. Soc. , Perkin Trans. 2* **1998**, 247-251.
(42) Kurz, J. L. *J. Am. Chem. Soc.* **1963**, *85*, 987-991.
(43) Kraut, J. *Science* **1988**, *242*, 533-540.
(44) Rupert, L. A. M. and Engberts, J. B. F. N. *J. Org. Chem.* **1982**, *47*, 5015-5017.
(45) Fadnavis, N. W. and Engberts, J. B. F. N. *J. Org. Chem.* **1982**, *47*, 152-154.
(46) Bunton, C. A. and Robinson, L. *J. Am. Chem. Soc.* **1968**, *90* , 5972-5979.
(47) Bunton, C. A. and Robinson, L. *J. Org. Chem.* **1969**, *34*, 780-785.
(48) Bunton, C. A., Mhala, M. M. and Moffatt, J. R. *J. Phys. Chem.* **1989**, *93*, 7851-7856.
(49) Fadnavis, N. W. and Engberts, J. B. F. N. *J. Am. Chem. Soc.* **1984**, *106*, 2636-2640.
(50) Fadnavis, N. W., Van den Berg, H. J. and Engberts, J. B. F. N. *J. Org. Chem.* **1985**, *50*, 48-52.
(51) Keiper, J., Romsted, L. S., Yao, J. and Soldi, V. *Colloids Surf. , A* **2001**, *176*, 53-67.

(52) Chaudhuri, A., Romsted, L. S. and Yao, J. H. *J. Am. Chem. Soc.* **1993**, *115*, 8362-8367.

(53) Yao, J. H. and Romsted, L. S. *J. Am. Chem. Soc.* **1994**, *116* , 11779-11786.

(54) Romsted, L. S. and Yao, J. H. *Langmuir* **1996**, *12*, 2425-2432.

(55) El Seoud, O. A., Ruasse, M. F. and Possidonio, S. *J. Phys. Org. Chem.* **2001**, *14*, 526-532.

(56) In our opinion, the conclusion of reference 55 that the rate-retarding effect brought about by the micelles is not a salt effect is unwarranted. The conclusion has been based on activation parameters of the reaction occurring in the micelle. However, these activation parameters will include effects of the thermodynamics of micellisation changing with temperature.

(57) Brinchi, L., Di Profio, P., Germani, R., Savelli, G., Spreti, N. and Bunton, C. A. *Eur. J. Org. Chem.* **2000**, 3849-3854.

(58) Munoz, M., Rodriguez, A., Graciani, M. D. and Moya, M. L. *Int. J. Chem. Kinet.* **2002**, *34*, 445-451.

(59) Tada, E. B., Novaki, L. P. and El Seoud, O. A. *Langmuir* **2001**, *17*, 652-658.

(60) It should be noted that, in view of the multiple domain model suggested above, the hydrolysis in the micellar media can also be explained in another way—*i.e.*, a weakly retarded hydrolysis of the micellar-bound probe molecules that reside in the Stern region can be combined with completely inhibited hydrolysis of the probe molecules bound in the micellar core. This could also result in a significantly reduced overall micellar rate constant for the hydrolysis.

(61) Al-Lohedan, H., Bunton, C. A. and Mhala, M. M. *J. Am. Chem. Soc.* **1982**, *104*, 6654-6660.

(62) Kerstholt, R. P. V., Engberts, J. B. F. N. and Blandamer, M. J. *J. Chem. Soc. , Perkin Trans. 2* **1993**, 49-51.

(63) The observation that the rate of hydrolysis of **5.1** is constant up to higher kinetic probe concentrations in a 1.6 mol dm^{-3} solution of TMAB than in pure water, suggests that the alkyltrimethylammonium group is able to solubilise the hydrolytic probe.

(64) Witte, F. M. and Engberts, J. B. F. N. *J. Org. Chem.* **1985**, *50*, 4130-4134.

(65) Van de Langkruis, G. B. and Engberts, J. B. F. N. *J. Org. Chem.* **1984**, *49*, 4152-4157.

(66) Lensink, M. F., Mavri, J. and Berendsen, H. J. C. *J. Comput. Chem.* **1999**, *20*, 886-895.

(67) Tee, O. S. and Fedortchenko, A. A. *Can. J. Chem* **1997**, *75*, 1434-1438.

(68) Tee, O. S. and Yazbeck, O. J. *Can. J. Chem* **2000**, *78*, 1100-1108.

(69) Soldi, V., Keiper, J., Romsted, L. S., Cuccovia, I. M. and Chaimovich, H. *Langmuir* **2000**, *16*, 59-71.

(70) For the nonionic surfactant, initially both tetraethylene glycol and heptaethylene glycol solutions in water were used as models for the Stern region. As heptaethylene glycol gave the same results as tetraethylene glycol, eventually tetraethylene glycol was chosen as it was available in the purest form.

(71) Stigter, D. *J. Phys. Chem.* **1964**, *68*, 3603-3611.

(72) van Os, N. M.; Haak, J. R.; Rupert, L. A. M. "Physico-Chemical Properties of Selected Anionic, Cationic and Nonionic Surfactants" Elsevier, Amsterdam, **1993**.

(73) In these salt effects, all possible interactions with the headgroup mimic are included. It is worth mentioning, however, that compounds such as TMAB or TMACl possess hydrophobic hydration shells as has been shown by a neutron diffraction study (Finney, J. L., Soper, A. K. and Turner, J. Z. *Pure Appl. Chem.* **1993**, *65*, 2521-2526 and Turner, J. Z., Soper, A. K. and Finney, J. L. *J. Chem. Phys.* **1995**, *102*, 5438-5443). This means that the molecule is probably involved in hydrophobic interactions as well. These hydrophobic interactions are, in the current definition, included in the salt effect.

(74) Curiously, it has been shown (Lopez, P., Sanchez, F., Moya, M. L. and Jimenez, R. *J. Chem. Soc., Faraday Trans.* **1996**, *92*, 3381-3384) that rate effects on reactions occurring in the aqueous phase of micellar solutions can be explained by a salt effect as well. In this case, the rate effect is explained by modelling complete micelles by single ions, thus creating a diluted solution of high valent ions.

(75) Streefland, L., Blandamer, M. J. and Engberts, J. B. F. N. *J. Phys. Chem.* **1995**, *99*, 5769-5771.

(76) Noordman, W. H., Blokzijl, W., Engberts, J. B. F. N. and Blandamer, M. J. *J. Org. Chem.* **1993**, *58*, 7111-7114.

(77) Apperloo, J. J., Streefland, L., Engberts, J. B. F. N. and Blandamer, M. J. *J. Org. Chem.* **2000**, *65*, 411-418.

(78) Hol, P., Streefland, L., Blandamer, M. J. and Engberts, J. B. F. N. *J. Chem. Soc. , Perkin Trans. 2* **1997**, 485-488.

(79) For the nonionic compound, the term salt effect is rather misplaced, as oligoethyleneglycol is not ionic, but the term is used for convenience.

(80) Nilsson, P. G., Wennerström, H. and Lindman, B. *J. Phys. Chem.* **1983**, *87*, 1377-1385.

(81) Angeli, A. D., Cipiciani, A., Germani, R., Savelli, G., Cerichelli, G. and Bunton, C. A. *J. Colloid Interface Sci.* **1988**, *121*, 42-48.

(82) Reichardt, C. *Chem. Rev.* **1994**, *94*, 2319-2358.

(83) Considering the fact that, compared to a micelle, the $E_T(30)$ solvatochromic probe is a huge dipolar molecule, a perturbation of the micellar structure upon binding of this molecule could be anticipated.

(84) Hammett, L. P. *Chem. Rev.* **1935**, *17*, 125-136.

(85) Hammett, L. P. *J. Am. Chem. Soc.* **1937**, *59*, 96-103.

(86) Maskill, H. "The Physical Basis of Organic Chemistry" Oxford University Press, Oxford, **1985**.

(87) The subscript p indicates the probe.

(88) Exner, O. *in* "Correlation Analysis in Chemistry" (Chapman, N. B., Shorter, J., eds.), Chapter 10, p. 439-540. Plenum, London, **1978**.

(89) The correlation between Hammett ρ-values as found for concentrated aqueous solutions of TMAB with the micellar ρ-value is as bad as the correlation between $E_T(30)$-values in concentrated salt solutions and the micellar $E_T(30)$-values.

(90) Substituents with a σ_p-value of approximately 1.13 exist, however, their structure does not suggest great stability in aqueous solution. Intriguingly, the existence of substituents with a substituent constant higher than 1.13, *e.g.* N_2^+ with a substituent constant of approximately 2 (see reference 88), seems to suggest that rate accelerations by added 1-propanol could occur.

(91) For the mathematical solution, a difference in trends of rate-retarding effects with Hammett substituent constant as given in Figure 5.5 is not necessary. In fact, it is not even necessary that the observed effect is a rate retardation; any parameter varying with molality of 1-propanol or TMAB can be used (approximately linear variations provide the easiest equations). In principle, mimics for other micellar properties, apart from hydrophobic and ionic interactions, if any, could be added as well.

(92) Atkinson, K. E. "An Introduction to Numerical Analysis" 2nd edition Wiley, New York, **1988**.

(93) Press, W. H.; Flannery, B. P.; Teukolsky, S. A.; Vetterling, W. T. "Numerical Recipes in Pascal" Cambridge University Press, Cambridge, **2002**.

(94) The 1-propanolysis of **5.3a-f** is expected to make a negligible contribution to the observed rate constants. However, the possibility has to be kept in mind.

(95) Blokzijl, W., Engberts, J. B. F. N. and Blandamer, M. J. *J. Am. Chem. Soc.* **1990**, *112*, 1197-1201.

(96) Skwierczynski, R. D. and Connors, K. A. *J. Chem. Soc. , Perkin Trans. 2* **1994**, 467-472.

(97) Tada, E. B., Novaki, L. P. and El Seoud, O. A. *J. Phys. Org. Chem.* **2000**, *13*, 679-687.

(98) The word "quick" is relevant here. Activated amide **5.3f** reacts quickest (following the reaction for 6 half-lifes corresponds to 10 minutes in the case of CTAB). The hydrolytic probes that "provide the sensitivity" towards hydrophobic interactions, most notably **5.3a**, take at least 22 hours (6 half-lifes in first order model solution, for a truly matching solution, this time is approximately doubled) to react. Using the $E_T(30)$ probe for determining the effect of hydrophobic interactions therefore results

in an enormous gain of time. In practice, it is more convenient to use **5.3e** instead of **5.3f** to "provide the sensitivity" towards ionic interactions as it takes approximately 100 minutes (in the case of CTAB) to follow the reaction for 6 half-lifes. The additional time provides the opportunity for better homogenisation of the probe through the aqueous model solutions.

(99) Novaki, L. P. and El Seoud, O. A. *Langmuir* **2000**, *16*, 35-41.

(100) Kirby, A. J. *Angew. Chem. , Int. Ed. Engl.* **1996**, *35*, 707-724.

(101) The hydrophobic and ionic contributions to the rate-retarding effect include the effect of the surfactant headgroups and tails on water concentration and reactivity in the Stern region (Equation 5.5).

(102) Despite having applied the current approach to micellar solutions only, we feel that that it should equally apply to vesicular solutions.

(103) More optimisation steps (yielding third and higher order solutions) could be performed. Considering the fact that both the $E_T(30)$ value and the rate constant of hydrolysis of **5.1** were too high and that both probes are more sensitive to hydrophobic interactions than to ionic interactions (unlike any of the probes **5.3a-f** for which the model solution has been optimised), it is likely that the final model solution would contain a slightly higher molality of 1-propanol.

(104) As rather high molalities of TMAB and 1-propanol are required in the model solutions, they should be of high purity. We obtained good results using 98+% TMAB obtained from Aldrich.

(105) a) Staab, H. A., Lüking, M. and Dürr, F. H. *Chem. Ber.* **1962**, *95*, 1275-1283. b) Karzijn, W., *The water- and hydroxide-ion catalyzed hydrolysis of 1-acyl-1,2,4-triazoles*, Ph.D. Thesis, University of Groningen, **1979**. c) Mooij, H. J., Engberts, J. B. F. N. and Charton, M. *Recl.Trav.Chim.Pays-Bas* **1988**, *107*, 185-189.

Hydrolysis of Activated Amides Around the Temperature of Maximum Density of Water – Isochoric Conditions[1]

*At temperatures above and below the temperature of maximum density, TMD, for water at ambient pressure, pairs of temperatures exist at which the molar volumes of water are equal. First-order rate constants for the pH-independent, water-catalysed hydrolysis of 1-benzoyl-1,2,4-triazole (**6.1**) in very dilute aqueous solution at pairs of temperatures at which the solutions are isochoric do not show unique features. Taken together with previously published kinetic data, we conclude that special significance in the context of rates of chemical reaction in aqueous solutions should not be attached to the isochoric condition.*

6.1 INTRODUCTION

6.1.1 THE ISOCHORIC CONDITION AND THE TEMPERATURE OF MAXIMUM DENSITY OF WATER

In 1935 Evans and Polanyi[2] suggested that isochoric activation parameters for chemical reaction in aqueous solutions might be more mechanistically informative than conventional isobaric activation parameters; *i.e.* $[\delta\ln(k)/\delta T]_V$ rather than $[\delta\ln(k)/\delta T]_p$ where k is the rate constant for a spontaneous chemical reaction. They argued as follows: "Especial difficulty arises in solution, from the interaction between solvent and solute, which depends strongly on temperature. This effect would be to some extent eliminated by measuring the temperature coefficients at constant volume, instead of the current method of constant pressure." They continued: "… which would eliminate the influence of thermal expansion of the solvent …". Hence, isochoric enthalpies of activation can be envisaged to be more directly related to the temperature dependence of the reaction and therefore to the molecular details of the reaction under study without inclusion of the effect of temperature on the solvent. This proposal sparked enormous interest in several subject areas including ionic transport[3] and chemical equilibria[4] in solution.

With reference to chemical reactions in dilute aqueous solution, the isochoric (using "constant solvent molar volume" V_m as definition of the isochoric condition, *vide infra*) standard enthalpy of activation $\Delta^{\neq}H^0_{V_m}$ is related to the isobaric standard

enthalpy of activation $\Delta^{\neq}H_p^0$ at temperature T and the standard volume of activation $\Delta^{\neq}V_T^0$ via Equation 6.1 where α_{p1}^* and κ_{T1}^* are the isobaric expansibility and isothermal compressibility, respectively, of water, Π_{int} is the internal pressure of water.

$$\Delta^{\neq}H_{V_m}^0 = \Delta^{\neq}H_p^0 - T\cdot[\alpha_{p1}^*/\kappa_{T1}^*]\cdot\Delta^{\neq}V_T^0 = \Delta^{\neq}H_p^0 - \left(\Pi_{\text{int}} + p\right)\cdot\Delta^{\neq}V_T^0 \qquad (6.1)$$

Baliga and Whalley[5] noted that the dependence of $\Delta^{\neq}U_V^0$, a quantity related to $\Delta^{\neq}H_{V_m}^0$, on solvent mixture composition is less complicated than that of $\Delta^{\neq}H_p^0$ for solvolysis of benzyl chloride in ethanol + water mixtures at 298.125 K. A similar pattern was reported by Baliga and Whalley[6] for the hydrolysis of 2-chloro-2-methylpropane in the same mixture at 273.15 K. Nevertheless, the significance of isochoric parameters in the context of both kinetic[7] and equilibrium parameters[8] has been extensively debated.[9-11]

Much of the debate centred on the isochoric condition and the answer to the question 'what [is the] volume [that] is held constant?'.[8] With reference to Equation 6.1, α_{p1}^* and κ_{T1}^* depend on temperature. Then the volume identified by subscript V_{m} on $\Delta^{\neq}H_{V_m}^0$ is dependent on temperature, rendering $\Delta^{\neq}H_{V_m}^0$ a local (in p and T) quantity. Also, even if $\Delta^{\neq}H_p^0$ is independent of temperature, $\Delta^{\neq}H_{V_m}^0$ is clearly not. Further, the molar volumes of binary liquid mixtures (compositions in mole fractions) at fixed T and p (*cf.* kinetic data in reference 6) depend on composition so that within the context of $\Delta^{\neq}H_{V_m}^0$, the volume identified by subscript V_{m} is not constant across a range of solvent mixtures.

In 1985, Haak *et al.*[7] reported kinetic data for the neutral hydrolysis of two 1-acyl-1,2,4–triazoles in binary aqueous mixtures. In their comments, Haak *et al.*[7] noted that at either side of the TMD of water there are pairs of temperatures where the molar volumes of water at ambient pressure are equal. Hence, rates of reaction for chemical reaction in dilute aqueous solution at such temperatures would yield pairs of isochoric rate constants. The suggestion was not taken up.

However, another controversy had arisen concerning chemical reactions in aqueous solutions at low temperatures. Hills and Viana[12] reported that rate constants for hydrolysis of benzyl chloride in very dilute aqueous solutions increased with an increase in temperature above the TMD of water and, significantly, increased with a decrease in temperature below the TMD. Albery and

Curran[13] were unable to confirm the pattern in rate constants reported by Hills and Viana.[12]

Here, we report that rate constants for the hydrolysis of 1-benzoyl-1,2,4-triazole (**6.1**) in aqueous solution increase gradually as the temperature increases from below to above the TMD and that this is the normal pattern.

Having established the gradual increase in rate constant for hydrolysis of **6.1** around the TMD, the suggestion made by Haak *et al.*,[7] concerning rates of reaction at pairs of temperatures for which the solvent molar volume is constant was taken up. For this study to be meaningful, the studied reaction had to satisfy at least three criteria;

(i) the rate of the chemical reaction can be precisely measured;

(ii) the mechanism of reaction is well understood, and

(iii) the rate of reaction is quite sensitive to temperature.

These three criteria are satisfied by the spontaneous first-order hydrolysis of 1-benzoyl-1,2,4-triazole (**6.1**) in aqueous solution. The mechanism of hydrolysis involves water-catalysed nucleophilic attack at the carbonyl group (Chapter 1 and the reaction scheme in reference 14).

The dependence of rate constants on temperature near the TMD of water is examined in terms of the dependence of the molar volume V_m of water on temperature. Considering that a small amount of cyanomethane is introduced in the reaction medium, we did not use the data reported by Kell and Whalley[15] and summarised by Kell[16,17] but assumed a quadratic dependence of molar volume with temperature around the TMD as shifted by the presence of cyanomethane. It is shown that the actual choice of TMD is not important.

We show that the 'isochoric condition' does not reveal novel features concerning the hydrolysis reaction in aqueous solution. We draw attention to published kinetic data which support our conclusion but which, in the debate over isochoric kinetics, were overlooked.

6.2. RESULTS AND DISCUSSION

6.2.1 HYDROLYSIS OF 1-BENZOYL-1,2,4-TRIAZOLE AROUND THE TMD

First-order rate constants for the hydrolysis of **6.1** in aqueous solution were determined at 12 temperatures between 276.15 and 278.15K using a UV/Vis setup that had been specifically improved for monitoring reactions at stable low temperatures without condensation of water vapour (Table 6.1).

Table 6.1: (Pseudo-) first-order rate constants for hydrolysis of **6.1a** between 276.15 and 278.15K.[a]

T / K	k / 10^{-4} s^{-1}
276.15	3.91
276.25	3.92 / 3.93 / 3.95
276.45	3.93 / 3.96 / 3.97
276.65	4.04
276.95	4.11
277.05	4.16 / 4.26
277.25	4.20 / 4.22 / 4.25
277.35	4.29
277.45	4.29 / 4.32
277.65	4.37
277.85	4.51
278.15	4.59

[a] The first order rate constant at 298.15K is 21.2 ·10^{-4} s^{-1} from previous work (Chapter 5 and reference 14).

At three temperatures, *viz*. 276.25, 276.45 and 277.25K, rate constants have been determined in triplicate. From the percentage-wise deviations from the individual average rate constants at each of these three temperatures, the standard deviation in the rate constants was determined to be 0.42%. From here on, the error in the rate constants has been taken to be 1.5 times the standard deviation.

We plotted both k and the molar volume of pure water, $V_{m,1}$, as given by Kell,[16] as a function of temperature (Figure 6.1). Please note that the molar volume and hence the concentration of water in pure water changes by less than 10ppm. Therefore, the temperature-induced change in concentration of water will not make a

detectable contribution to the change in observed (pseudo-) first-order rate constants.

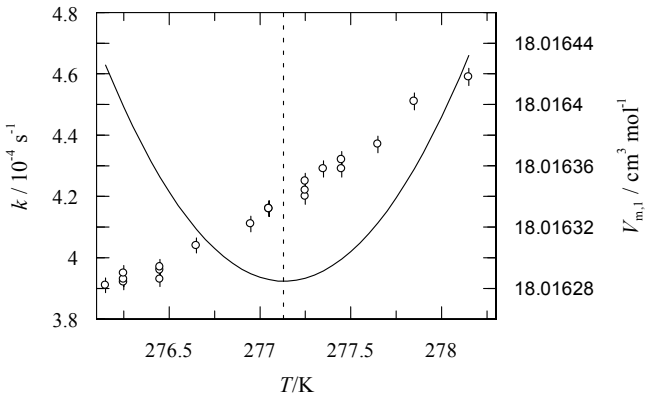

Figure 6.1: Plot of k as a function of T for the hydrolysis of **6.1** between 276.15 and 278.15K (o, *left axis*) and $V_{m,1}$ as a function of T in the same temperature interval (-, *right axis*). Dotted line indicates the TMD.

As evident from Figure 6.1, pairs of rate constants exist on both sides of the TMD for which the molar volume of water is constant. Hence, sets of rate constants have been determined under isochoric conditions.

It has to be noted that the actual TMD of the solutions in which the rate constants of hydrolysis have been determined is slightly lower than the TMD of pure water. This lowering of the TMD is caused by the introduction of cyanomethane in the reaction medium upon injecting the stock solution containing **6.1**. In a typical experiment, 6±2 μl of a stock solution in cyanomethane is injected in 2.75 ml of water, resulting in a 0.126±0.042 mole% aqueous solution of cyanomethane. This leads to a lowering of the TMD[18] by 0.28±0.09K to a TMD of 276.85±0.09K. In the following, we assume that the molar volume of the water/cyanomethane solution, $V_{m,1,2}$ varies quadratically with temperature around the TMD.[19]

Plotting $\ln(k/T)$ against T^{-1} produces a satisfactory linear Eyring plot (Figure 6.2) without an apparent break around the TMD.

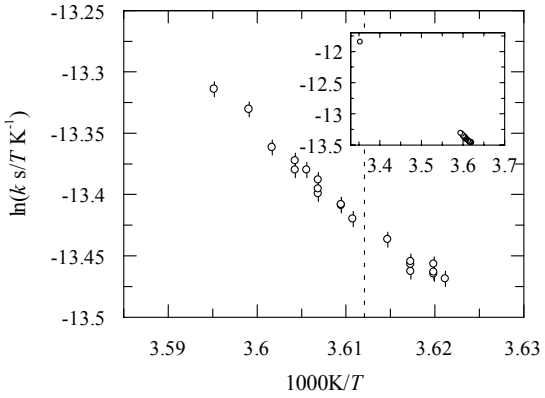

Figure 6.2: Plot of ln(k s/T K^{-1}) as a function of T^{-1} K for the hydrolysis of **6.1** between 276.15 and 278.15K. *Inset*: The same data, including 298.15K. Dotted line indicates the TMD.

The results are analysed using the Clark-Glew equation (Equation 6.2).[20,21]

$$\ln\left(\frac{k}{T}\right) = \ln\left(\frac{k(\theta)}{\theta}\right) + \left\{\frac{\Delta^{\neq}H_p(\theta)}{R}\right\}\cdot\left\{\frac{1}{\theta}-\frac{1}{T}\right\} + \left\{\frac{\Delta^{\neq}C_p(\theta)}{R}\right\}\cdot\left\{\frac{\theta}{T}-1+\ln\left(\frac{T}{\theta}\right)\right\}+\ldots \qquad (6.2)$$

The Clarke-Glew equation describes the isobaric dependence of rate constants on temperature around a chosen reference temperature θ in terms of a series of thermodynamic parameters. The series can be extended by one thermodynamic parameter at a time until the statistical significance of the next derived thermodynamic parameter is unacceptable. Here, we have chosen the TMD of the aqueous solution of cyanomethane, *viz.* 276.85K, as reference temperature. The results of the analysis are summarised in Table 6.2.

Table 6.2: Activation parameters of the hydrolysis of **6.1** in terms of the Clarke-Glew equation using 2 or 3 terms.

	parameters	excl. k(298.15K)	incl. k(298.15K)
2 terms	$k(\theta)$ / 10^{-4} s^{-1}	4.106±0.006	4.106±0.006
	$\Delta^{\neq}H_p(\theta)$ / kJ mol^{-1}	49.8±1.6	50.4±0.6
3 terms	$k(\theta)$ / 10^{-4} s^{-1}	4.093±0.007	4.107±0.006
	$\Delta^{\neq}H_p(\theta)$ / kJ mol^{-1}	47.0±1.4	49.2±1.6
	$\Delta^{\neq}C_p(\theta)$/ J K^{-1}mol^{-1}	(1.66±0.47) 10^4	(1.1±1.8) 10^2

From Table 6.2, we conclude that $\Delta^{\neq}C_p(\theta)$ is not statistically significant for the present data set ($\Delta^{\neq}C_p(\theta)$ determined without k(298.15K) is unrealistically large and has a considerable error margin, both as a result of the small temperature range whereas the value determined including k(298.15K) is mainly dictated by k(298.15K)). Hence, we conclude that $k(\theta)$ equals (4.106±0.006) 10^{-4} s^{-1} and $\Delta^{\neq}H_p(\theta)$ equals 49.8±1.6 kJ mol^{-1}, in close agreement with the literature value[14] at 298.15K of 47.2 kJ mol^{-1} (determined between 293.15 and 313.15K). This indicates that the isobaric standard enthalpy of activation is almost constant down to temperatures around the TMD of water. This is in contrast with the observation by Hills and Viana[12] that "… at one atmosphere the rate constant [for hydrolysis of benzyl chloride in water] as a function of temperature passes through a minimum at or near 4°C …".[22]

According to Figure 6.1, pairs of temperatures exist at which the molar volume of water is constant. Using a TMD of 276.85K and assuming the molar volume of the water/cyanomethane mixture to be a quadratic function of temperature around the TMD, we can plot the rate constant of hydrolysis as a function of (T-TMD)^2; Figure 6.3.

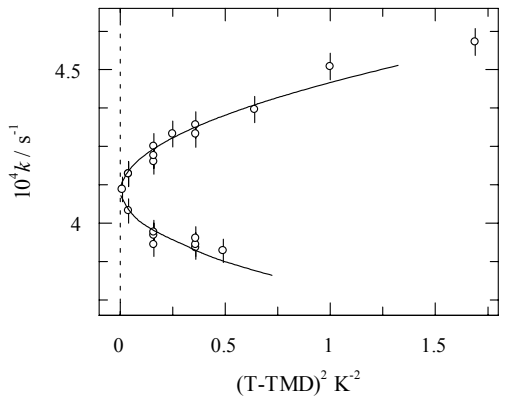

Figure 6.3: Plot of k as a function of (T-TMD)^2, as proportional to the molar volume of the water/cyanomethane mixture, for the hydrolysis of **6.1** between 276.15 and 278.15K. Solid lines are calculated rate constants using Equation 6.2, $k(\theta)$=4.106 10^{-4} s^{-1} and $\Delta^{\neq}H_p(\theta)$=49.8 kJ mol^{-1}.

According to Figure 6.3, activation parameters at constant molar volume of the solvent can be determined by taking the rate constants at different temperatures that correspond to the same solvent molar volume. The significance of the question 'What volume is held constant?' is emphasised by Figure 6.3, which shows that

despite the fact that isochoric sets of rate constants can be determined, the volume held constant is actually different for each set of isochoric rate constants. Essentially this is the case if isochoric activation parameters are determined at different temperatures and/or different solvent compositions. For three sets of data points, isochoric activation parameters can be determined directly. From the fit to Equation 6.2 and the assumption that $V_{m,1,2}$ varies quadratically with temperature around the TMD, isochoric activation parameters around the TMD can be determined *for different solvent molar volumes*! New results do not follow from the use of Equation 6.2 combined with the notion that at pairs of temperatures on both sides of the TMD the molar volume of the water/cyanomethane mixture is identical. Considering that ln(k/T) varies linearly with (T/K)$^{-1}$ around the TMD, and that the isochoric sets of rate constants are on the isobaric plot, the actual temperature interval taken for the calculation of $\Delta^{\neq}H_{\mathrm{p}}^{\circ}$ is irrelevant and a value of 49.8 kJ mol^{-1} is consistently found. The equality of $\Delta^{\neq}H_{V_m}^{0}$ and $\Delta^{\neq}H_{p}^{0}$ can be readily understood from the fact that the term $T\cdot\alpha_{p1}^{*}/\kappa_{T1}^{*}$ in the temperature interval between 276.15 and 278.15K does not exceed 84 bar (8.4 10^{6} N m^{-2}). Hence, assuming an isothermal volume of activation, $\Delta^{\neq}V_T^{\circ}$, of approximately -20 10^{-6} m^{3} mol^{-1} as determined for structurally similar activated amides at 298.15K,[7] the second term on the left-hand-side of Equation 6.1 contributes less than +168 N m mol^{-1} or +0.168 kJ mol^{-1}. In fact, $\left(d\ln V_1^{*}/dT\right)_p$ (*cf.* α_{p1}^{*}) by definition equals 0 K^{-1} between isochoric points on both sides of the TMD, further clarifying the link between isobaric and isochoric enthalpies of activation around the TMD. In general, for T limiting to the TMD, it can be shown that the isobaric and isochoric enthalpy of activation are identical (Equation 6.3).

$$\lim_{T\to\mathrm{TMD}}\left(\Delta^{\neq}H_V^{0}\right)=\lim_{\substack{T\to\mathrm{TMD}\\ \alpha_{p1}^{*}\to 0}}\left(\Delta^{\neq}H_p^{0}-T\cdot[\alpha_{p1}^{*}/\kappa_{T1}^{*}]\cdot\Delta^{\neq}V_T^{0}\right)=\lim_{T\to\mathrm{TMD}}\left(\Delta^{\neq}H_p^{0}\right) \qquad (6.3)$$

The above results are in line with kinetic results, obtained even before the Hills and Viana paper by Moelwyn-Hughes, Robertson and Sugamori.[23] The latter determined the rate constants for hydrolysis of 2-methyl-2-chloropropane between 0 and 20°C at 1°C intervals in water without added cosolutes. Fitting their dataset to Equation 6.2, using θ=TMD=277.13K, yields the activation parameters as summarised in Table 6.3 (Figure 6.4).

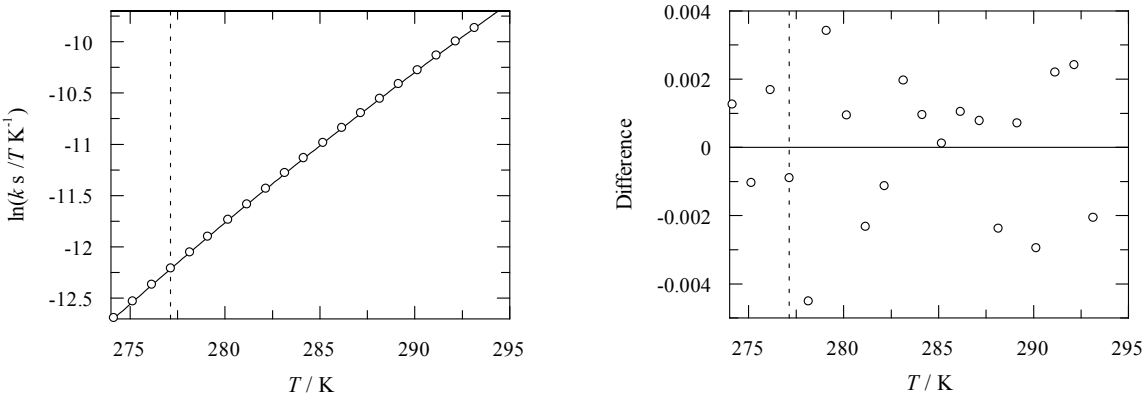

Figure 6.4: Plots of $\ln(k/T)$ for the hydrolysis of 2-methyl-2-chloropropane between 274.15 and 293.16K. *Left*: $\ln(k/T)$ as a function of (T/K), solid line indicates fit to Equation 6.2. *Right*: Residual as a function of T/K. Dotted lines indicate TMD. Data from reference 23.

Table 6.3: Activation parameters of the hydrolysis of benzyl chloride in terms of the Clarke-Glew equation using 3 terms.

$k(\theta)$ / 10^{-3} s^{-1}	1.3735±0.0010
$\Delta^{\neq}H_p(\theta)$ / kJ mol^{-1}	101.6±0.2
$\Delta^{\neq}C_p(\theta)$ / J K^{-1}mol^{-1}	(-3.3±0.3) 10^2

The activation parameters are identical to those obtained by Moelwyn-Hughes, Robertson and Sugamori and, important for the present study, there is no indication of deviating behaviour at low temperatures (Figure 6.4). In addition, rate constants for hydrolysis reactions of numerous substrates have been determined down to temperatures below the TMD of water, in particular in the Robertson group. However, no atypical behaviour was observed, neither crossing the TMD of H_2O,[24-31] nor crossing the TMD of D_2O.[25-27,31,32] In combination with the present dataset and in light of the failure of Albery and Curran to reproduce the patterns observed by Hills and Viana,[13] there is no reason to believe that isobaric enthalpies of activation below the TMD are consistently different from those above the TMD.

6.2.2 THE SIGNIFICANCE OF ISOCHORIC ACTIVATION PARAMETERS

Now we return to the question of the significance of isochoric activation parameters. As cited before, Evans and Polanyi[2] expected that the effect of temperature on solvent-solute interactions could be "*to some extent* eliminated" by working under isochoric conditions as that "would eliminate the influence of thermal expansion of

the solvent". From this suggestion, the isochoric condition as defined as "constant solvent molar volume" seems the most natural choice. However, care has to be taken in interpreting the isochoric activation parameters obtained using this definition for a number of reasons. First, under isochoric conditions, increasing temperature must be accompanied by an increase in pressure (for positive α_{p1}^{*} and κ_{T1}^{*}). Whereas the intermolecular distances in the solvent remain the same, "eliminating the influence of thermal expansion", the internal energy of the solvent does not. With the changing internal energy of the solvent, the solvent changes. Especially in the case of water, with increasing temperature more and more directionally sensitive hydrogen bonds are broken despite the pressure increase keeping the molar volume of water the same. Hence, the interactions between solvent and solute will change as well. Whereas this effect might be small for solvents largely interacting through London dispersion interactions, which are normally more sensitive to distance than direction, for water it is expected to be significant. Second, as argued before, on the basis of the temperature dependence of V_1^{*}, $\alpha_{p,1}^{*}$ and $\kappa_{T,1}^{*}$, the isochoric condition is a local condition. Therefore, isochoric activation parameters as calculated at different temperatures are not isochoric with respect to each other. In other words, at different temperatures, the molar volume that is (mathematically) held constant is the molar volume of the solvent corresponding to that particular temperature and (in most cases) standard pressure. Third, the fact that isochoric activation parameters have been determined in solvent mixtures provides intriguing complexities. As argued above, $V_{\mathrm{m},1,2}$, $\alpha_{p,1,2}$ and $\kappa_{T,1,2}$ for solvent mixtures are dependent on composition. By the same line of argument as before for the temperature dependence of V_1^{*}, $\alpha_{p,1}^{*}$ and $\kappa_{T,1}^{*}$, isochoric activation parameters determined at individual solvent mixture compositions are not isochoric with respect to each other. In fact, if one is interested in intermolecular interactions in aqueous solution, it can be argued that it is the partial molar volume of water that should be held constant and not the total solvent molar volume (as is effectively done by using the isobaric expansibilities and isothermal compressibilities of the solvent mixture together with Equation 6.1).

Bearing in mind the issues mentioned above, a truly isochoric condition is readily available around the TMD of water. It has been shown that isochoric activation parameters can be determined using the fact that sets of temperatures exist at which the molar volume of water is equal. Datasets like these can even be

expanded by the application of pressure as the application of pressure results in a shifted plot of solvent molar as a function of temperature (Figure 6.5) leading to a complete range of temperatures corresponding to isochoric conditions.

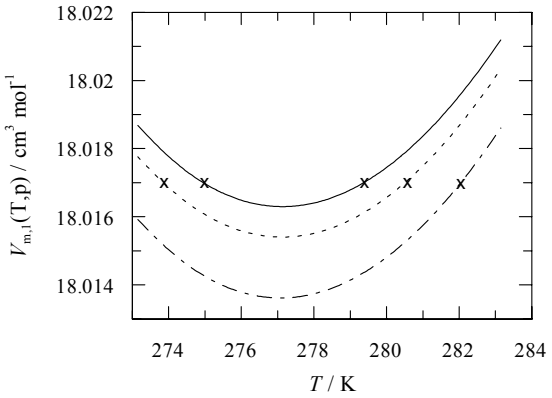

Figure 6.5: Plots of $V_{m,1}$ for water between 273.15 and 283.15K at pressures of 1 bar (solid line), 2 bar (dotted line) and 4 bar (dot-dash line). Crosses indicate isochoric conditions. Data from references 15 and 16.

Figure 6.5 shows that even at moderate (*i.e.* experimentally non-problematic) pressures, a range of temperatures of at least 10K around the TMD satisfying isochoric conditions can be easily achieved.[33]

From Equation 6.3 and from the experimental results, however, it follows that for T limiting to TMD, the isobaric and isochoric enthalpy of activation are equal. Therefore, using the natural isochoric conditions around the TMD to determine the isochoric enthalpy of activation does not yield additional insight.

6.3 CONCLUSIONS

Rate constants for hydrolysis of **6.1** have been determined between 276.15 and 278.15K. No atypical effects were found crossing the temperature of maximum density and neither were unusual effects found in a number of datasets available from literature. Isochoric activation parameters around the TMD of water have been determined at different solvent molar volumes. The isochoric activation parameters are equal to the corresponding isobaric activation parameters. We conclude that care has to be taken in interpreting isochoric activation parameters as they are only locally defined. These comments do not, of course, detract from the importance of the original proposal by Evans and Polanyi.[2] We simply suggest that in many cases

where isochoric activation parameters have been reported, the proper meaning of the term 'isochoric' has not been recognised.

6.4 EXPERIMENTAL

6.4.1 KINETIC EXPERIMENTS

The hydrolysis reactions were followed using a Shimadzu Diode-array spectrophotometer, absorbances being recorded between 200 and 400 nm. The cell compartment of the spectrophotometer was thermostatted to a preset temperature using a Haake thermostatting unit equipped with a Pt100 electrode for direct control of the temperature of the cell block of the spectrophotometer. The temperature was checked and found to deviate by not more than 0.05 K from the preset temperature using a copper/constantin thermocouple during the kinetic experiments. Experience showed that control of temperature was improved by using ethanol rather than water as a bath liquid. We attribute the problems with using water to the formation of ice in the refrigeration unit.

A quartz cuvette, path length 1 cm, contained approx. 2.75 cm^3 of water of which the pH had been adjusted to 3.8 ±0.3 using HCl(aq). The cuvette was fitted with a stopper which had two small holes. The cuvette was thermostatted overnight. The cell compartment was sealed with cling film so that the air flow in the spectrophotometer did not effect the temperature of the cell compartment. The cell compartment was continually flushed with dry pre-cooled air.

The cell compartment was fitted with a hole in the cover through which wires and tubing could be led into the sealed cell compartment. Through this hole 1.5 cm^3 of solution in the sample cell was withdrawn. Between 4 and 8 μl of a stock solution containing 5 mg of 1-benzoyl-1,2,4-triazole in 1 cm^3 cyanomethane was injected into the cuvette. The solution in the cuvette was withdrawn and re-injected several times. Finally, the solution was injected into the cuvette very slowly in order to prevent the formation of air bubbles. After the reaction had been initiated, the temperature of the cell was monitored. Only after the temperature had returned to the required temperature were data points recorded of absorbance and time. During a given kinetic run the absorbances were measured during a brief exposure (1 second of exposure per minute) of the cell to the incident uv-visible beam of light. Poor kinetic data resulted if the solution was subjected to continuous radiation.

6.4.2 MATERIALS

1-Benzoyl-1,2,4-triazole was synthesised according to published procedures.[34] Water was distilled twice from an all-quartz distillation unit.

6.5 REFERENCES AND NOTES

(1) Part of this chapter is to be published: Blandamer, M. J., Buurma, N. J., Engberts, J. B. F. N. and Reis, J.C.R. in press.

(2) Evans, M. G. and Polanyi, M. *Trans. Faraday Soc.* **1935**, *31*, 875-894.

(3) Hills, G. J., Ovenden, P. J. and Whitehouse, D. R. *Discuss. Faraday Soc.* **1965**, *39*, 207-215.

(4) Lown, D. A., Thirsk, H. R. and Lord Wynne-Jones *Trans. Faraday Soc.* **1970**, *66*, 51-73.

(5) Baliga, B. T. and Whalley, E. *J. Phys. Chem.* **1967**, *71*, 1166-1167.

(6) Baliga, B. T. and Whalley, E. *Can. J. Chem.* **1970**, *48*, 528-536.

(7) Haak, J. R., Engberts, J. B. F. N. and Blandamer, M. J. *J. Am. Chem. Soc.* **1985**, *107*, 6031-6035.

(8) Blandamer, M. J., Burgess, J. and Clark, B. *J. Chem. Soc. , Faraday Trans. 1* **1984**, *80*, 3359-3363.

(9) Wright, P. G. *J. Chem. Soc. , Faraday Trans. 1* **1986**, *82*, 2557-2564.

(10) Albuquerque, L. M. P. C. and Reis, J. C. R. *J. Chem. Soc. , Faraday Trans. 1* **1989**, *85*, 207-222.

(11) Whalley, E. *J. Chem. Soc. , Faraday Trans. 1* **1987**, *83*, 2901-2903.

(12) Hills, G. and Viana, C. A. N. *Nature* **1971**, *229*, 194-195.

(13) Albery, W. J. and Curran, J. S. *J. Chem. Soc. , Chem. Commun.* **1972**, 425-426.

(14) Karzijn, W. and Engberts, J. B. F. N. *Tetrahedron Lett.* **1978**, 1787-1790.

(15) Kell, G. S. and Whalley, E. *Phil. Trans. Roy. Soc.* **1965**, *258a*, 565-614.

(16) Kell, G. S. *J. Chem. Eng. Data* **1967**, *12*, 66-69.

(17) Note that volumes in references 15 and 16 are given both in cc (cm^3) and ml, the latter being derived from the 1901 liter. The conversion between the 1901 liter and the present liter (equal to 1 dm^3) is given by: 1 ml. = 1.000028 cm^3.

(18) Wada, G. and Umeda, S. *Bull. Chem. Soc. Jpn.* **1962**, *35*, 1797-1801.

(19) It turns out that the actual choice of the TMD for the present study is irrelevant. No differences emerge upon analysing the data around either a TMD set to 276.85K or set to 277.13K. In fact, both choices can be equally well defended.

(20) Clarke, E. C. W. and Glew, D. N. *Trans. Faraday Soc.* **1966**, *62*, 539.

(21) Blandamer, M. J. "Chemical Equilibria in Solution" 1st edition Ellis Horwood, Chichester, **1992**.

(22) If $\Delta^{\neq}H(\theta)$ is determined independently below and above the TMD, the following numbers are found: For θ=TMD=276.85: $k(\theta)$=(4.06±0.03) 10^{-4} s^{-1} (below TMD), (4.08±0.02) 10^{-4} s^{-1} (above TMD) and (4.10±0.01) 10^{-4} s^{-1} (above TMD, incl. 298.15K); $\Delta^{\neq}H(\theta)$=32.2±8.2 kJ mol^{-1} (below TMD), 57.4±2.6 kJ mol^{-1} (above TMD) and 50.7±0.6 kJ mol^{-1} (above TMD, incl. 298.15K). For θ=TMD=277.13: $k(\theta)$=(4.17±0.02) 10^{-4} s^{-1}

(below TMD), (4.18±0.02) 10^{-4} s^{-1} (above TMD) and (4.20± 0.01) 10^{-4} s^{-1} (above TMD, incl. 298.15K); $\Delta^{\neq}H(\theta)$=42.6±3.2 kJ mol^{-1} (below TMD), 58.8±4.0 kJ mol^{-1} (above TMD) and 50.6±0.6 kJ mol^{-1} (above TMD, incl. 298.15K). Considering the strongly different results upon changing the exact value of the TMD (276.85 or 277.13K) or depending on whether or not the rate constant at 298.15K is included, we contend that the apparent difference in $\Delta^{\neq}H$ (θ) is caused by the individual data sets being too small. Admittedly, this can be ameliorated by extending the dataset.

(23) Moelwyn-Hughes, E. A., Robertson, R. E. and Sugamori, S. *J. Chem. Soc.* **1965**, 1965-1971.

(24) Ko, E. C. F. and Robertson, R. E. *Can. J. Chem.* **1973**, *51*, 597-603.

(25) Robertson, R. E., Rossall, B. and Redmond, W. A. *Can. J. Chem.* **1971**, *49*, 3665-3670.

(26) Rossall, B. and Robertson, R. E. *Can. J. Chem.* **1975**, *53*, 869-877.

(27) Ko, E. C. F. and Robertson, R. E. *J. Am. Chem. Soc.* **1972**, *94*, 573-575.

(28) Blandamer, M. J., Golinkin, H. S. and Robertson, R. E. *J. Am. Chem. Soc.* **1969**, *91*, 2678-2683.

(29) Ko, E. C. F. and Robertson, R. E. *Can. J. Chem.* **1972**, *50*, 434-437.

(30) Ko, E. C. F. and Robertson, R. E. *Can. J. Chem.* **1972**, *50*, 946-951.

(31) Robertson, R. E., Rossall, B., Sugamori, S. E. and Treindl, L. *Can. J. Chem.* **1969**, *47*, 4199-4206.

(32) Rossall, B. and Robertson, R. E. *Can. J. Chem.* **1971**, *49*, 1451-1455.

(33) It has to be noted that despite the fact that Figure 6.5 contains data points on a line indicating the isochoric condition, isochoric activation parameters as calculated for the individual datapoints are different as the $T\alpha_p/\kappa_T$ terms varies around the TMD. This once more stresses the local character of calculated isochoric activation parameters.

(34) a) Staab, H. A., Lüking, M. and Dürr, F. H. *Chem. Ber.* **1962**, *95*, 1275-1283. b) Karzijn, W., *The water- and hydroxide-ion catalyzed hydrolysis of 1-acyl-1,2,4-triazoles*, Ph.D. Thesis, University of Groningen, **1979**. c) Mooij, H. J., Engberts, J. B. F. N. and Charton, M. *Recl.Trav.Chim.Pays-Bas* **1988**, *107*, 185-189.

Epilogue

In the final chapter of this thesis, the obtained results are briefly discussed and incentives for future research are given.

7.1 Introduction

This chapter summarises the results described in this thesis and their relation with some of the interesting properties of water as a solvent. The work described in this thesis has also led to new questions concerning aqueous solutions. These questions are discussed and suggestions for further research are made.

7.2 Goals, Achievements and Incentives for Future Research

7.2.1 Water, hydrophobic hydration and hydrophobic interactions

Chapter 1 offers an overview of contemporary *opinions and facts*[1] in the field of water chemistry. In the liquid, water molecules engage in a strong and structured yet highly dynamic H-bond network, making the properties of the liquid frequently surprising. Increasingly detailed knowledge and understanding are gained of the reasons for water's surprising liquid properties. Nevertheless, its properties as a solvent, being an intricate result of the liquid properties, are still far from understood. Hence, whereas general agreement exists on the average structure of hydration shells formed around small apolar solutes, detailed quantitative explanations of the observed thermodynamic parameters of transfer of apolar solutes into water are lacking. This situation is complicated by the fact that not all apolar solutes have similar properties in aqueous solution. Hydrophobic hydration of small convex apolar molecules differs from hydrophobic hydration of large convex and concave molecules because water is unable to retain its hydrogen-bond network near extended flat apolar surfaces. As a result, transfer parameters for large and/or concave solutes usually differ from those for small apolar solutes. In addition, the presence of polar groups near apolar groups can lead to mutual disturbance of hydration shells.[2] Possibly even worse than the situation for

hydrophobic hydration (*i.e.* solute-water interactions) is the situation for hydrophobic interactions (*i.e.* solute-solute interactions). Apart from differences resulting from different shape, size and the vicinity of hydrophilic groups, the nature of interactions between apolar solutes can also differ in different concentration ranges. In concentrated solutions, hydrophobic interactions differ from those in dilute solutions because hydrophobic interactions are not the sole reason why molecules cluster. Often, concentrations of solutes are high enough to cause the individual solute molecules to be (necessarily) in contact, so that the size of the solute molecules in comparison[3] to the size of water molecules is an important "driving force" in the "aggregation process". In the study of pure *pairwise hydrophobic interactions*, this effect of size and concentration should be taken into account. Moreover, with increasing concentration of (apolar) solute, the entropy of mixing that drives the dissolution process diminishes. At a certain concentration, the mixing entropy no longer cancels the unfavourable Gibbs energy of transfer and *bulk hydrophobic interactions* result in phase separation. In summary, in (experimental) studies of hydrophobic interactions, pure hydrophobic effects caused only by loss of hydrophobic hydration are rare. Therefore, an important improvement would be to distinguish between hydrophobic effects occurring for differently sized and shaped solutes as well as between those occurring in different concentration ranges so that comparisons with different experiments and with computational results can be made. In conjunction with the above, the biological cell is not a dilute solution[4,5] and the solutes differ significantly from the hydrophobic compounds commonly studied.

7.2.2 ENCOUNTER COMPLEXES

In Chapter 2, the rate-retarding effects of cosolutes on the hydrolysis of activated esters and amides are examined. The rate-retarding effects increase with increasing hydrophobicity of both hydrolytic probe and cosolute, indicating the importance of hydrophobic effects.[6] The observed rate-retarding effects can be described using both a molecular model and a thermodynamic model. According to the molecular model, rate retardations are caused by the formation of encounter complexes between hydrolytic probe and cosolute, quantified by equilibrium constants of encounter complex formation K_{ec}, in which hydrolysis of the hydrolytic probe is largely inhibited. In the thermodynamic description, rate retardations are caused by initial state stabilisation as quantified by G(c)-values. The thermodynamic parameters for encounter complex formation by the hydrolytic probe correspond to

the stabilisation of the initial state of the hydrolysis reaction. In fact encounter complex formation causes the lowering of the chemical potential of the initial state, and stabilisation of the encounter complexes by hydrophobic interactions leads to a concomitant further stabilisation of the initial state.

Hydrophobic stabilisation of encounter complexes relative to randomly formed encounter complexes has been quantified.[7] This analysis provides an experimental quantification of pairwise hydrophobic interactions, which can be used in understanding and optimisation of catalysts for use in aqueous solutions.

Despite the direct link between K_{ec} and $G(c)$ in dilute solution, the importance of higher order terms (in cosolute) in the models differs. This difference is a result of the different definitions of 1:1-interactions. In the thermodynamic description, concurrent interaction of a hydrolytic probe molecule with two cosolute molecules can be counted as two individual 1:1-interactions irrespective of whether the cosolute molecules are "dimerised" or not, as long as interactions with both individual cosolute molecules are equal to the interaction with one single cosolute molecule. In the molecular model, however, the interaction with a "dimer" can only be accounted for by stronger binding to this dimer.[8] This also indicates one of the drawbacks of the molecular model, *viz.* that quantification of the self-interaction of the cosolute is required in a model including higher-order interactions. Such quantification may, however, be independently obtained from the excess thermodynamic properties of solutions.[9-11]

The importance of cosolute binding remote from a reaction center, where it lowers the Gibbs energy of both initial and transition state of the reaction to the same extent, can be determined from transfer parameters for stable (in water) mimics of the more hydrophobic hydrolytic probes. Possibly, transfer parameters can also be determined for the hydrolytic probes themselves using two-phase kinetic experiments.[12] In the case of a hydrolytic probe and an inert cosolute, encounter complexes remote from the reaction center do not affect the rate constant because the complexes stabilise both initial and transition state to the same extent. In bimolecular reactions, *e.g.* in the Diels-Alder reaction, hydrophobic interactions between apolar groups in the reactants remote from the reaction center lead to an increase in reaction-rate constant as only the transition state is stabilised.[13]

A remaining challenge with respect to 1:1-hydrophobic interactions is the development of systems providing chiral recognition purely by hydrophobic interactions. Intrinsically, hydrophobic interactions are not directionally sensitive. In nature, chiral recognition is caused by more directionally-sensitive polar

interactions and hydrogen bonds between, for example, enzyme and substrate. These polar interactions together with the hydrophobic interaction lead to binding. In 1:1-interactions unaided by orientation-directing polar interactions, only steric interactions can cause hydrophobic interactions to lead to chiral recognition. Previous studies showed that the chiral hydrolytic probes (+)- and (-)-1-(2-phenyl-2-methylethanoyl)-1,2,4-triazole[14] in aqueous solutions containing small chiral cosolutes (+)- and (-)-2-butanol show no evidence of chiral recognition in pairwise interactions.[15] Therefore, more bulky chiral hydrolytic probes 1-((1*R*,2*S*,5*R*)-2-(2-isopropyl-5-methyl-cyclohexyloxy)ethanoyl)-1,2,4-triazole (menthoxyacetyl-1,2,4-triazole, **7.1**) and 4-nitrophenyl 2-((1*R*,2*S*,5*R*)-2-isopropyl-5-methyl-cyclohexyl-oxy)ethanoate (*p*-nitrophenyl menthoxyethanoate, **7.2**) were synthesised (Scheme 7.1).[16]

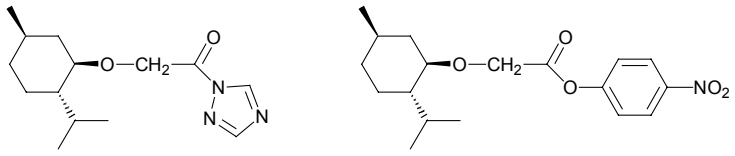

7.1 **7.2**

Scheme 7.1

Preliminary studies indicate that the (water-catalysed) hydrolysis of **7.1** can be followed at wavelengths below 240 nm and that the rate constant of hydrolysis of **7.1** at pH 3.6 is 6.8 10^{-2} s^{-1}. Unfortunately, hydrolysis of **7.2**, which can be followed at higher wavelengths because of the formation of 4-nitrophenol(ate), is *very* slow. Considering the unfavourable range of wavelengths in which the hydrolysis of **7.1** can be monitored, it is essential to use a cosolute that does not absorb in the UV-region between 210 nm (spectrophotometer limit) and 240 nm. A cosolute meeting this prerequisite is (1*R*,2*S*,5*R*)-2-isopropyl-5-methyl-cyclohexylsulfate (menthyl sulfate), which is synthesised from menthol and chlorosulfonic acid. Together, these chiral hydrolytic probes and chiral cosolutes presumably form a relatively easily accessible system for the study of chiral recognition in pairwise hydrophobic interactions

7.2.3 NUCLEOPHILIC SUBSTITUTION

In Chapter 3, the reaction pathways of hydrolytic probes are explored. A wide range of pathways (including general-base catalysis, nucleophilic substitution and general-base catalysed nucleophilic substitution) is available to the activated amide (and presumably also to the activated esters) if basic cosolutes are added. Knowledge of these reaction pathways and quantification of their contributions to the observed rate constants are prerequisites for the interpretation of rate effects exerted by added cosolutes. In particular, rate effects caused by particular α-amino acids measured previously[2] are mainly caused by nucleophilic substitution. The reactivity of 3-phenyl-1-benzoyl-1,2,4-triazole parallels that of *p*-nitrophenyl ethanoate (*p*NPA), enabling the construction of a linear free energy relationship (LFER). As extensive reactivity data is available for *p*NPA, this LFER can be used to predict the rate effects of basic functional groups in the added cosolutes on hydrolysis (or better: reaction) of 3-phenyl-1-benzoyl-1,2,4-triazole.

Chapter 3 also provides a clear example that reactions not normally carried out in aqueous solution, because of hydrolysis occurring as a side reaction, are nevertheless possible in water if carried out appropriately. This example involves the reaction of 3-phenyl-1-benzoyl-1,2,4-triazole with amines. Despite the fact that 3-phenyl-1-benzoyl-1,2,4-triazole is sensitive to hydrolysis, reaction with amines is fast enough for the amide to be the only product.

One of the most complicated cosolutes used in the study of reactions of the hydrolytic probes in this thesis is aspartame (Scheme 7.2). Aspartame is a strong nucleophile towards 3-phenyl-1-benzoyl-1,2,4-triazole, showing intramolecular general-base catalysed nucleophilic substitution as a consequence of two basic functional groups. The reactivity of aspartame in aqueous solution is presumably enhanced even further by the presence of the aromatic ring leading to hydrophobic stabilisation of the initial encounter complex between 3-phenyl-1-benzoyl-1,2,4-triazole and aspartame as an intermediate in the overall reaction.

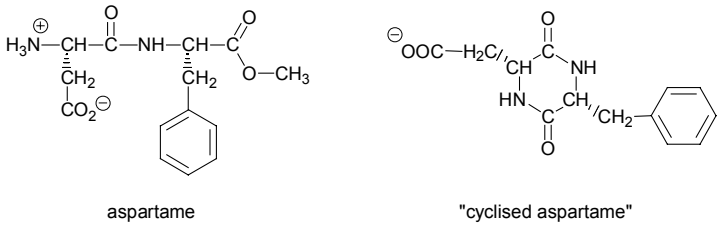

aspartame "cyclised aspartame"

Scheme 7.2

However, aspartame can also be cyclised *via* an intramolecular nucleophilic substitution,[17] forming a cyclic dipeptide or diketopiperazine ("cyclised aspartame", Scheme 7.2). The cyclic dipeptide thus formed offers both a hydrophobic binding site and a group that can act as a general base. It would be interesting to test this molecule as a small enzyme mimic.[18,19]

7.2.4 HYDROTROPES

Both the solubilising effect of charged hydrotropes and their aggregation state in aqueous solution are discussed in Chapter 4. Hydrotropes with charged hydrophilic groups are present in high concentrations without significant self-aggregation because their like charges repel. Only sodium 4-n-butylbenzensulfonate and sodium 4-n-propylbenzenesulfonate show signs of cooperative self-association. These two compounds form the transition between hydrotropes and micelle-forming surfactants. Whereas hydrotropes themselves do not aggregate cooperatively, presumably the presence of high concentrations of solubilisate (as typically used in solubilisation studies) eventually leads to cooperative aggregation of the hydrotrope and the solubilisate. This solubilisate-induced cooperative aggregation can be quite solubilisate-selective, identifying the importance of the solubilisate in cooperative solubilising effects. Related to this cooperative aggregation, it would be interesting to investigate the maximum concentrations of hydrotropes and/or solubilisate for which water retains its beneficial effects on, for example, Diels-Alder reactions.

The solubilising behaviour of hydrotropes is caused by weak hydrophobic binding between solubilisate and hydrotrope. Aggregation between solubilisate and solubiliser creates the possibility of combining the roles of hydrotrope and catalyst into one molecule.

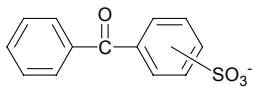

Scheme 7.3

Benzophenone sulfonate (Scheme 7.3) is strikingly similar to the hydrotropes used in the work described in Chapter 4. Currently, it is used as a photosensitiser in photochemistry in aqueous solutions[20,21] and it may actually combine the roles of hydrotrope and catalyst. It would be interesting to examine a possible link between quantum yield and hydrophobicity of both sensitiser and substrate.

Upon addition of 4-methylbenzenesulfinate (originally chosen as a hydrotrope with a higher charge density on the ionic group than the sulfonates) as a cosolute in the reaction of 1-benzoyl-3-phenyl-1,2,4-triazole, an as yet unexplained rate-increasing effect was observed. Upon decreasing the pH, the rate of reaction increased. The pK_a of 4-methylbenzenesulfinic acid is 1.45±0.10, determined from using UV/vis spectroscopy (Figure 7.1).[22]

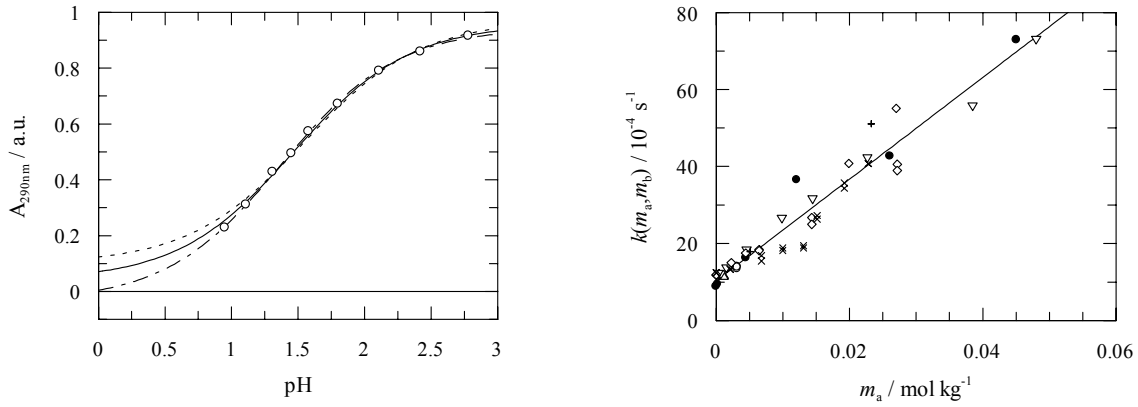

Figure 7.1: *Left:* Absorption of 4-methylbenzenesulfinic acid/4-methylbenzenesulfinate at 290 nm as a function of pH. Fits are sigmoids with end points 0.04 (absorption of cuvet filled with water, solid line), 0.1 (dotted line), -0.035 (final absorption unrestricted in fit, dot-dash line) *Right:* Rate constants $k(m_a,m_b)$ (or k_{obsd}-k_{H^+}·[H$^+$]) for the reaction of 1-benzoyl-3-phenyl-1,2,4-triazole in the presence of 4-methylbenzenesulfinic acid and sodium 4-methylbenzenesulfonate (m_a+m_b= 0.03 (x), 0.06(◊), 0.17 (▽), 0.28 (Δ), 0.40 (•), 0.61 (o), and 0.85 (+) mol kg^{-1}) as a function of molality of 4-methylbenzenesulfinic acid m_a.

Rate constants $k(m_a,m_b)$ are linear with molality of the protonated form, m_a, suggesting that 4-methylbenzenesulfinic acid either catalyses a reaction (not necessarily the hydrolysis reaction) or reacts efficiently with 1-benzoyl-3-phenyl-1,2,4-triazole in a 1:1 stoichiometry. A linear fit of $k(m_a,m_b)$ to m_a yields a second-order rate constant, (1.32±0.05) 10^{-1} kg mol^{-1} s^{-1}, significantly higher than the second-order rate constant, 0.32 10^{-1} dm^3 mol^{-1} s^{-1}, for specific-acid catalysis (at low concentrations, molalities and molarities are effectively equal).

7.2.5 THE MICELLAR STERN REGION AS A REACTION MEDIUM

Medium effects on the hydrolysis reactions of activated esters and amides exerted by micelles have been divided into contributions by ionic and hydrophobic effects. The micellar Stern region, where the hydrolytic probes bind to micelles, offers a reaction medium consisting of a concentrated solution of surfactant headgroups

and hydrophobic interaction sites. A solution mimicking the micellar Stern region incorporating both ionic and hydrophobic effects was prepared using both salt and alcohol. This model is more representative of interactions occurring in the micellar Stern region than models containing solely either a salt or a hydrophobic solute. As a result, the solution also reproduces micellar medium effects on probes that have not been used in the development of the mimicking solution. Despite the fact that the present approach has been used only for micellar solutions, it should also be valid for aqueous solutions containing vesicles.

Inclusion of medium effects of both ionic and hydrophobic groups results in a satisfactory description of the micellar Stern region. However, several effects are still not taken into account. These effects include the charge of the Stern region resulting from incomplete counterion binding and the fact that different probes can bind at different locations inside the micelle. These effects may be further investigated by including probes that are not sensitive to surface charge in the analysis. In fact, the analysis advanced in Chapter 5 poses neither a limit on the number of probes, nor on the number of "properties" investigated. A further important characteristic of the micellar Stern region is the local pH[23] which can be calculated from the bulk pH and the micellar surface charge using the Poisson-Boltzmann equation.[24]

Apart from satisfying a fundamental interest into the properties of the micellar Stern region as a reaction medium, detailed understanding of these effects facilitates the design of micelles that act as catalysts. The present method of mimicking solutions also provides a useful alternative for the determination of second-order rate constants inside micellar aggregates as these rate constants are notoriously difficult to obtain from kinetic data for bimolecular processes in surfactant aggregates.[25]

7.2.6 TEMPERATURE OF MAXIMUM DENSITY

In Chapter 6, the hydrolysis of 1-benzoyl-1,2,4-triazole around the temperature of maximum density (TMD) of water is discussed. Rate constants of hydrolysis around the TMD show no unique features, in accord with other studies but contrary to a previous claim by Hills and Viana.[26] The latter authors reputed that the rate constants for hydrolysis of 2-chloro-2-methylpropane in aqueous solution increase with both increase in temperature above the TMD and with decrease in temperature below the TMD. The importance of the TMD in kinetic studies stems from the fact that it provides the possibility of obtaining rate constants of reactions at pairs of

temperatures for which the molar volume of the solvent is constant.[27] From these rate constants, isochoric activation parameters can be calculated (this procedure can also be used for D_2O, which is experimentally easier because of the higher TMD of D_2O). As noted in Chapter 6, isochoric activation parameters around the TMD do not differ from isobaric activation parameters indicating that special significance should not be attached to the isochoric condition for solvolysis in aqueous solution.

7.3 GENERAL CONCLUSIONS

Organic reactions in aqueous solutions have been studied in the presence of a variety of different cosolutes, forming a range of different aggregation structures in aqueous solution. Different interactions and aggregation structures lead to different rate effects on hydrolysis reactions. However, common to all effects is that hydrophobic interactions form (one of) the driving forces of all pairwise interactions and aggregation processes encountered in the research described in this thesis. Our results show that, based upon the present knowledge regarding the solvent properties of water, cosolute effects on aqueous organic reactions can now be understood in some qualitative detail.

7.4 REFERENCES AND NOTES

(1) Blokzijl, W. and Engberts, J. B. F. N. *Angew. Chem. , Int. Ed. Engl.* **1993**, *32*, 1545-1579.

(2) Streefland, L., *Effects of overlap of hydration shells on noncovalent interactions in aqueous solution*, PhD Thesis, University of Groningen, **2000**. Available online: http://www.ub.rug.nl/eldoc/dis/science/e.streefland/

(3) The actual definition of the size of molecules (Meyer, A. Y. *Chem. Soc. Rev.* **1986**, *15*, 449-474) is not important, as the 'size driven aggregation process' is governed by the *relative* size of the solute molecule compared to water molecules.

(4) Ellis, R. J. *Trends Biochem. Sci.* **2001**, *26*, 597-604.

(5) Ball, P. *Cell. Mol. Biol.* **2001**, *47*, 717-720.

(6) As perfluorinated compounds have even less interaction with water than "normal" apolar solutes, hydrophobic interactions between perfluorinated compounds could be even stronger than "normal" hydrophobic interactions.

(7) The Gibbs energy of random encounter complex formation can be described in several ways. Hence, the quantification of hydrophobic stabilisation of these encounter complexes is still somewhat arbitrary.

(8) As briefly discussed in Chapter 2, comparison of Equations 2.7 and 2.9, shows that linearity of plots of $\ln\{k\ (m_c)/k(m_c=0)\}$ with m_c indicates a connection between the equilibrium constants K'_{ecc} (defined including self-association of the cosolute) and K_{ec}; *viz.* K'_{ecc} should equal $\frac{1}{2}\cdot K_{ec}^2$. Significantly, K_{ecc}' should vary quadratically with K_{ec}, indicating that Gibbs energies of encounter complex formation involving a "cosolute dimer" differs from encounter complex formation involving "monomeric" cosolutes by a factor of 2. This seems reasonable for both contributions to the Gibbs energy of encounter complex formation (Equation 2.5), *viz.* the hydrophobic stabilisation of the encounter complex and the Gibbs energy (entropy) of random encounter complex formation.

(9) Perron, G. and Desnoyers, J. E. *J. Chem. Thermodyn.* **1981**, *13*, 1105-1121.

(10) Kirkwood, J. G. and Buff, F. P. *J. Chem. Phys.* **1951**, *19*, 774-777.

(11) Newman, K. E. *Chem. Soc. Rev.* **1994**, *1994*, 31-40.

(12) The rate constant of hydrolysis in, for example, an aqueous ethanol solution can be determined directly. Kinetic analysis of a hydrolysis reaction in a two-phase system containing an aqueous phase and an octanol phase then provides a partition coefficient. This procedure is, however, experimentally difficult.

(13) Meijer, A., Otto, S. and Engberts, J. B. F. N. *J. Org. Chem.* **1998**, *63*, 8989-8994.

(14) This chiral hydrolytic probe has the unfortunate disadvantage that chirality is lost upon deprotonation on the 2-position of the ethanoyl group.

(15) Wessels, F.E., unpublished results.

(16) Both the (1R,2S,5R)- and the (1S,2R,5S)-isomer of 1-(2-(2-isopropyl-5-methyl-cyclohexyloxy)ethanoyl) chloride are commercially available.

(17) Skwierczynski, R. D. and Connors, K. A. *Pharm. Res.* **1993**, *10*, 1174-1180.

(18) "Polyaspartame" (the product of intermolecular nucleophilic substitution) could have similar effects as those anticipated for "cyclic aspartame".

(19) Another cyclic dipeptide, *cyclo*[(*R*)-His-(*R*)-Phe], is a known catalyst for the enantioselective formation of cyanohydrins from aldehydes and HCN (Oku, J. and Inoue, S. *J. Chem. Soc. , Chem. Commun.* **1981**, 229-230).

(20) Ramsay, G. C. and Cohen, S. G. *J. Am. Chem. Soc.* **1971**, *93* , 1166-1171.

(21) Ricci, A., Personal Communication.

(22) The end point of the titration cannot be determined accurately as a consequence of the limited solubility of 4-methylbenzenesulfinic acid in water.

(23) For a bulk pH of 4.0, the pH in the micellar Stern region is approximately 6.5. Preliminary experiments using **5.3e** indicate that hydroxide-catalysed hydrolysis contributes less than 5% to the rate constant of hydrolysis of **5.3e** in the second-order solution at pH 6.5. This suggests that, for the system studied in Chapter 5, hydroxide-catalysed hydrolysis is not an important factor.

(24) Fernandez, M. S. and Fromherz, P. *J. Phys. Chem.* **1977**, *81* , 1755-1761.

(25) Rispens, T. and Engberts, J. B. F. N. *J. Org. Chem.* **2002**, *67*, 7369-7377.

(26) Hills, G. and Viana, C. A. N. *Nature* **1971**, *229*, 194-195.

(27) Performing similar measurements under pressure provides an opportunity to determine isochoric activation parameters from more than 2 data points for a series of molar volumes.

Water, a Unique Medium for Organic Reactions

Water is an exceptional solvent in many respects. On a molecular scale, water as a liquid is unlike most other liquids; it is strongly self-interacting and structured yet highly dynamic. These properties give water its characteristic behaviour as a liquid but also as a solvent. The remarkable behaviour as a solvent (together with its reactivity) has caused water to have a reputation as a bad solvent for organic reactions. Interestingly, however, some of the characteristic properties of water can be highly beneficial for organic reactivity and hence a thorough understanding of these properties as a solvent will undoubtedly change the "hydrophobicity of organic chemists". Admittedly, certain reactions will never be possible in aqueous solutions, but still, water can be used as a solvent for far more reactions than currently is the case. Apart from being a chemically interesting solvent, water provides a cheap (both in cost price and in ecotax) alternative for organic solvents, making it environmentally and economically interesting as well. It was with the aim of clarifying water's behaviour in aqueous reactivity and thereby advancing it as a viable alternative solvent for organic chemistry that the work described in this thesis been performed.

An overview of present knowledge and understanding of the (characteristic) properties of water both as a liquid and as a solvent has been given in Chapter 1. This Chapter also describes (the mechanism of) the water-catalysed hydrolysis reactions of activated esters and amides that have been used to study organic reactivity in aqueous solutions. The activated esters and amides used in the studies described in this thesis are *p*-methoxyphenyl 2,2-dichloroalkanoates and substituted 1-benzoyl-1,2,4-triazoles, all of these hydrolytic probes hydrolyse within several hours. The thermodynamic analysis developed previously for reactions occurring in (aqueous) solution is summarised and the effects of clustering of solutes in (aqueous) solution as well as their aggregate morphology are briefly discussed.

In Chapter 2, the pH-independent hydrolysis reactions of four activated esters and two activated amides of varying hydrophobicity have been studied in dilute aqueous solution as a function of the molality of added cosolutes ethanol, 1-propanol and 1-butanol. Rate constants for the neutral hydrolysis decrease with increasing cosolute molality. These kinetic medium effects respond to both the hydrophobicity of the ester and of the monohydric alcohol, indicating the

importance of hydrophobic interactions in these rate effects. The kinetic data are analysed using both an existing thermodynamic model and a molecular/kinetic model. According to the kinetic model a hydrophobically-stabilised encounter complex between the hydrolytic probe molecule and a cosolute molecule is formed with equilibrium constants K_{ec}, often smaller than unity. In such an encounter complex, the cosolute blocks the reaction center of the hydrolytic ester or amide from attack by water and the hydrolysis reaction is largely inhibited. In fact, formation of these encounter complexes leads to a dominant initial-state stabilisation as described by the thermodynamic model. Decreases in both apparent enthalpies and entropies of activation for these hydrolysis reactions upon addition of the monohydric alcohols correspond to unfavourable enthalpies and favourable entropies of complexation, confirming that the encounter complexes are stabilised by hydrophobic interactions. The results provide a quantification of hydrophobic interactions and indicate their additivity. In addition, Chapter 2 shows that two seemingly different descriptions of the rate-retarding effects are, in fact, closely linked.

The analysis advanced in Chapter 2 describes the rate effects caused by *inert* cosolutes. However, cosolutes often contain one or more functional groups that could be *reactive*. Chapter 3 describes reaction pathways observed for an activated amide (1-benzoyl-3-phenyl-1,2,4-triazole) in aqueous solution containing general bases of varying basicity. The observed reaction mechanism changes from general-base catalysed hydrolysis to nucleophilic substitution and general-base catalysed nucleophilic substitution with increasing basicity of the added cosolute. The mechanism and the rate constants vary in a predictable way, with the changes paralleling those for reactions of *p*-nitrophenyl ethanoate. Apart from the changes in mechanism with changing basicity, a slight tendency is also observed for more hydrophobic general bases to show higher reactivity with the hydrophobic probe, an effect expected to be typical for water as a solvent. Aspartame, having two basic functional groups as well as an aromatic ring available for hydrophobic interactions, is an exceptionally effective nucleophile. The nucleophilicity of this molecule is possibly enhanced because nucleophilic substitution is subject to intramolecular general-base catalysis and, in addition, the encounter complex formed as part of the activation process is stabilised by hydrophobic interactions. A general conclusion from Chapter 3 is that unexpected rate effects can only be rationalised provided that the detailed reaction mechanisms are understood in

sufficient detail. For cosolutes carrying basic functional groups, this is now the case.

Chapter 4 deals with the effect of added hydrotropes on hydrolysis reactions of 1-benzoyl-3-phenyl-1,2,4-triazole. Hydrotropes typically contain a hydrophilic and a strongly hydrophobic moiety and act as strong solubilisers of apolar solutes in water but do not form micelles. In our kinetic experiments, most hydrotropes induce strong rate-retarding effects, indicative of strong interactions with the hydrolytic probe and often involving remarkably strong hydrophobic interactions between aromatic moieties. Despite showing strong interactions with the hydrolytic probe, most hydrotropes show neither spectroscopic (^{1}H NMR) nor kinetic evidence for cooperative self-aggregation in the molality range studied, *i.e.* from 0 to 1.4 mol kg^{-1}. Cooperative self-aggregation of the hydrotrope molecules is absent because the hydrophobic moieties are too small for hydrophobic interactions to overcome electrostatic repulsion. It is exactly this lack of aggregation that results in a high availability of hydrophobic binding sites for *uncharged* apolar compounds, thereby accounting for the high solubilising power of hydrotropes. The hydrotropes with the longest alkyl tails, however, *viz.* sodium 4-*n*-propylbenzenesulfonate and sodium 4-*n*-butylbenzenesulfonate do show cooperative self-association and provide the link between hydrotropes and micelle-forming surfactants, the subject of Chapter 5.

Kinetic effects exerted by this next category of compounds, the cationic, anionic and nonionic micelle-forming surfactants, is discussed in Chapter 5. Typically, micelles can be treated as a pseudophase with properties rather different from bulk water. A comparison is drawn between medium effects inside the micelles and in different model solutions. Two types of model solutions are used. Simple model solutions involve concentrated aqueous solutions of a small molecule resembling the surfactant headgroup. In this model the entire rate-retarding effect is attributed to interactions with the (ionic) headgroup. An improved model solution for alkyltrimethylammonium bromide micelles is developed, using a series of hydrolytic probes (*p*-substituted 1-benzoyl-1,2,4-triazoles) showing different sensitivities towards ionic and hydrophobic interactions. These ionic and hydrophobic effects can be mathematically (or graphically) separated. Such improved model solutions contain both a salt mimicking the micellar headgroups, and 1-propanol, mimicking hydrophobic tails. The rate-retarding effects of micelles on the hydrolysis of the series of hydrolytic probes described in Chapter 5 can be rationalised by assuming that they are caused by the high concentration of headgroups and by the hydrophobic tails in the Stern region. Not only the rate-retarding effects found for

the probes used to determine the contributions of ionic and hydrophobic effects are reproduced by the model solution comprising both salt and 1-propanol. The micellar effects on the hydrolysis reaction of a different probe and on the $E_T(30)$ values, both not included in the design of the mimicking solution, are also reproduced rather well. The availability of such model solutions that are able to mimic the (reaction) medium presented by the micellar Stern region is of importance for an understanding of micellar effects on reactions and other processes. In addition, the present approach is not restricted to the micellar Stern region, nor is the (mathematical) procedure restricted to the separation of rate effects caused by only two properties (here ionic and hydrophobic interactions), raising the possibility of including more properties in the mimicking solution.

Chapter 6 is different from the other Chapters in that it does not deal with effects of added cosolutes on the hydrolysis reactions of activated esters or amides but rather with isochoric conditions (constant volume) in respect to the temperature of maximum density of water (TMD). At temperatures above and below the TMD, pairs of temperatures exist at which the molar volumes of water are equal. Hence, without the application of pressure (used to keep constant the molar volumes of solvents without a TMD) water offers sets of temperatures for which the isochoric condition holds. First-order rate constants for hydrolysis of 1-benzoyl-1,2,4-triazole in very dilute aqueous solution at such isochoric pairs of temperatures do not show unique features, contrary to a previous claim. Taken together with previously published kinetic data for hydrolysis reactions that were monitored both below and above the TMD of water, we conclude that special significance in the context of rates of chemical reaction in aqueous solutions should not be attached to the isochoric condition.

Finally, in Chapter 7 of this thesis, the results described in Chapters 2 to 6 are put into perspective and incentives for future research are given.

Water, een Uniek Medium voor Organische Reacties

Water is in vele opzichten een bijzonder oplosmiddel. Moleculair gezien is de vloeistof water sterk verschillend van de meeste andere vloeistoffen: de watermoleculen vertonen sterke interactie met elkaar en vormen een gestructureerd, maar ook zeer dynamisch netwerk. Deze eigenschappen geven water haar bijzondere eigenschappen zowel als vloeistof als als oplosmiddel. Deze bijzondere eigenschappen (samen met de reactiviteit van water) hebben water de reputatie van een slecht oplosmiddel voor organische reacties opgeleverd. Toch kunnen juist de bijzondere eigenschappen van water zeer gunstig zijn voor organische reactiviteit en het valt dan ook te verwachten dat een goed begrip van de eigenschappen van water als oplosmiddel de "hydrofobiciteit" van organisch chemici zal doen verminderen. Hoewel bepaalde reacties wel nooit mogelijk zullen zijn in waterige oplossingen, kan water voor veel meer organische reacties gebruikt worden dan waarvoor het nu gebruikt wordt. Behalve dat water interessant is vanuit een chemisch en ecologisch oogpunt, is het ook een goedkoop (wat betreft aanschafprijs en milieubelastingen) alternatief voor de tegenwoordig in gebruik zijnde organische oplosmiddelen. Het werk beschreven in dit proefschrift is verricht met het doel om het gedrag van water met betrekking tot reacties in water verder op te helderen.

In hoofdstuk 1 wordt een overzicht gegeven van de eigenschappen van water als vloeistof en als oplosmiddel. Dit hoofdstuk beschrijft verder (het mechanisme van) de hydrolysereacties van geactiveerde esters en amiden die zijn bestudeerd in de studie van organische reactiviteit in water. De gebruikte geactiveerde esters en amiden zijn *p*-methoxyfenyl 2,2-dichlooralkanoaten en gesubstitueerde 1-benzoyl-1,2,4-triazolen. Deze verbindingen ondergaan volledige hydrolyse in enige minuten tot enkele uren. Bovendien wordt in hoofdstuk 1 een samenvatting gegegeven van de reeds eerder ontwikkelde thermodynamische analyse van de (vertragende) effecten van toegevoegde niet-reactieve stoffen op reacties in (waterige) oplossing. Ook het effect van het clusteren van moleculen en de morfologie van de gevormde clusters wordt kort besproken.

In hoofdstuk 2 is de watergekatalyseerde hydrolyse bestudeerd van vier geactiveerde esters en twee geactiveerde amiden, alle met varierende hydrofobiciteit. De hydrolyse werd gevolgd in verdunde waterige oplossingen als functie van de molaliteit van toegevoegd ethanol, 1-propanol en 1-butanol. Reactiesnelheidsconstanten voor hydrolyse nemen af met toenemende molaliteit van

de toegevoegde alcohol. Deze kinetische medium effecten zijn zowel afhankelijk van de hydrofobiciteit van de ester als van de hydrofobiciteit van het toegevoegde alcohol. De gevonden kinetische data zijn geanalyseerd met behulp van zowel een bestaand thermodynamisch als een moleculair/kinetisch model. Volgens het kinetische model worden "ontmoetingscomplexen" gevormd tussen de hydrolysegevoelige stof en moleculen van de toegevoegde alcohol. Deze ontmoetingscomplexen worden gestabiliseerd door hydrofobe interacties. De evenwichtsconstante voor de vorming van deze ontmoetingscomplexen, K_{ec}, is vaak kleiner dan 1. In deze ontmoetingscomplexen schermt de toegevoegde stof (de cosolute) het reactiecentrum van de hydrolysegevoelige ester af voor aanval door water en dientengevolge wordt de hydrolyse vrijwel volledig verhinderd. De vorming van deze ontmoetingscomplexen resulteert in een stabilisering van de begintoestand van de reactie, zoals ook beschreven door het bestaande thermodynamische model. De afname in zowel de enthalpie als de entropie van activering voor deze hydrolysereacties bij toenemende cosolutemolaliteit komen voort uit de positieve enthalpie en de positieve entropie van de vorming van de ontmoetingscomplexen. Dit patroon bevestigt dat de ontmoetingscomplexen worden gestabiliseerd door hydrofobe interacties. De verkregen resultaten kwantificeren hydrofobe interacties en geven aan dat ze additief zijn. Bovendien wordt duidelijk dat twee, op het eerste gezicht verschillende, beschrijvingen van de vertragende effecten sterk gerelateerd zijn.

De analyse die wordt beschreven in Hoofdstuk 2 geldt voor reactiesnelheidseffecten uitgeoefend door niet-reactieve toegevoegde stoffen. Toegevoegde stoffen hebben echter vaak functionele groepen die reactief t.o.v. de substraten kunnen zijn. Hoofdstuk 3 beschrijft de veranderingen in het mechanisme van de reactie van een geactiveerd amide in waterige oplossingen die algemene Brönsted basen met verschillende basiciteit bevatten. Met toenemende basiciteit van de toegevoegde stof verandert het reactiemechanisme van algemeen basegekatalyseerde hydrolyse in nucleofiele substitutie en uiteindelijk zelfs in algemeen basegekatalyseerde nucleofiele substitutie. Het mechanisme verandert op een voorspelbare manier waarbij de veranderingen in mechanisme parallel lopen aan die voor de reacties van *p*-nitrofenylethanoaat. Behalve deze verandering in reactiemechanisme is er ook een lichte tendens dat meer hydrofobe algemene basen een verhoogde reactiviteit te vertonen, zoals men zou verwachten voor water als oplosmiddel. Een bijzonder complexe solute, aspartaam, heeft twee basische groepen en een hydrofobe aromatische ring en blijkt een zeer effectief nucleofiel. De

nucleofiliciteit van dit molecuul is mogelijkerwijs versterkt als gevolg van intramoleculaire algemene basekatalyse en het feit dat het ontmoetingscomplex dat tot reactie leidt, gestabiliseerd wordt door hydrofobe interacties. Een algemene conclusie uit hoofdstuk 3 is dat onverwachte reactiesnelheden slechts verklaard kunnen worden wanneer mogelijke reactiemechanismen voldoende nauwkeurig in kaart zijn gebracht. Voor toegevoegde stoffen met basische groepen is dit nu het geval.

Hoofdstuk 4 behandelt het effect van hydrotropen op watergekatalyseerde hydrolysereacties. Typische hydrotropen hebben een (geladen) hydrofiele en een sterk hydrofobe groep en ze functioneren als effectieve hulpstoffen bij het oplossen van apolaire stoffen in water. Ze vormen echter geen micellen. Het merendeel van de gebruikte hydrotropen veroorzaakt sterk vertragende effecten die aangeven dat er sterke interacties zijn met de hydrolysegevoelige teststof en verder dat interacties tussen aromatische groepen bijzonder sterk zijn in water. Ondanks de sterke interacties tussen hydrotropen en de hydrofobe testmoleculen, vertonen de meeste hydrotropen noch spectroscopisch (^{1}H NMR) noch kinetisch enig teken van coöperatieve zelfaggregatie in het onderzochte molaliteitsgebied (0 tot 1.4 mol kg^{-1}). Coöperatieve zelfaggregatie is afwezig omdat de hydrofobe groepen te klein zijn om de elektrostatische repulsie tussen de geladen hydrofiele groepen te overwinnen. Juist omdat de hydrotropen niet aggregeren zijn er veel hydrofobe bindingsplaatsen vrij beschikbaar in oplossing voor interactie met ongeladen apolaire stoffen. Dit verklaart waarom hydrotropen zo effectief zijn in het verhogen van de oplosbaarheid van andere stoffen. De hydrotropen met de langste alkylstaarten vormen echter een uitzondering; natrium 4-*n*-propylbenzeensulfonaat en natrium 4-*n*-butylbenzeen-sulfonaat vertonen beide coöperatieve zelfaggregatie en zij vormen de overgang tussen hydrotropen en micelvormende surfactanten, het onderwerp van hoofdstuk 5.

Het effect van kationische, anionische en niet-ionische micelvormende surfactanten wordt besproken in hoofdstuk 5. Micellen kunnen in kinetisch analyses beschouwd worden als een aparte fase (pseudofase) met eigenschappen die sterk verschillen van de eigenschappen van water. De mediumeffecten op reacties die plaatsvinden in micellen worden vergeleken met die van modelsystemen. Twee verschillende modelsystemen zijn gebruikt. Het eenvoudigste model behelst een geconcentreerde waterige oplossing van een klein molecuul dat lijkt op de kopgroep van het surfactant. In dit modelsysteem wordt het totale effect van de micel toegeschreven aan de (ionische) kopgroep. Een verbeterd model voor micellen

gevormd door het surfactant alkyltrimethylammoniumbromide is ontwikkeld met behulp van een reeks gesubstitueerd hydrolysegevoelige teststoffen die verschillend gevoelig zijn voor electrostatische en hydrofobe interacties. De ionische en hydrofobe effecten kunnen nu grafisch of wiskundig onderscheiden worden. Dit modelsysteem bevat zowel een zout dat model staat voor de geladen kopgroepen, als 1-propanol, dat model staat voor de hydrofobe staarten. In het hoofdstuk wordt aangetoond dat het vertragende effect van micellen op de hydrolyse van de serie hydrolysegevoelige teststoffen veroorzaakt wordt door zowel de hoge kopgroepconcentratie als door de hydrofobe staarten in de Sternlaag van de micel. Ook de micellaire effecten op de hydrolyse van een ander hydrolysegevoelig molecuul alsook de micellaire $E_T(30)$-waarde (beide niet gebruikt in het bepalen van de samenstelling van de modeloplossing) worden naar behoren gereproduceerd. De beschikbaarheid van zulke modeloplossingen die de micellaire Sternlaag als reactiemedium reproduceren is van belang voor een goed begrip van micellaire effecten op reacties en andere processen. Bovendien is de huidige methode niet beperkt tot de micellaire Sternlaag, noch is de (wiskundige) procedure beperkt tot het opsplitsen in slechts twee eigenschappen (zoals hier in elektrostatische en hydrofobe interacties) zodat de mogelijkheid bestaat om een modelsysteem te ontwikkelen dat nog meer eigenschappen van de micellaire Sternlaag reproduceert.

Hoofdstuk 6 verschilt van de andere hoofdstukken in de zin dat het niet de effecten van toegevoegde stoffen op de hydrolyse van geactiveerde esters en amiden behandelt, maar isochore omstandigheden (constant volume) in het temperatuur-gebied rond de temperatuur van maximale dichtheid van water (TMD). Er bestaan paren van temperaturen boven en onder de TMD waarbij het molaire volume van water identiek is. Water biedt dus, zonder het gebruik van variatie van de druk (zoals gebruikt om het volume van oplosmiddelen zonder TMD constant te houden) paren van temperaturen waarvoor aan de isochore conditie voldaan wordt. Eerste-orde reactiesnelheidsconstanten in zeer verdunde oplossingen gemeten bij zulke paren van temperaturen vertonen geen afwijkend gedrag. Samen met eerder gepubliceerde kinetische data voor hydrolysereacties die zowel boven als onder de TMD gevolgd zijn, leidt dit tot de conclusie dat er geen bijzondere betekenis verbonden dient te worden aan de isochore conditie.

Tot slot worden de verkregen resultaten in hoofdstuk 7 van dit proefschrift in perspectief geplaatst en worden suggesties gedaan voor toekomstig onderzoek.